Report

Finch, J. W.; Hall, R. L.; Rosier, P. T. W.; Clark, D. B.; Stratford, C.; Davies, H. N.; Marsh, T. J.; Roberts, J. M.; Riche, A.; Christian, D.. 2004 *The hydrological impacts of energy crop production in the UK. Final report.* London, UK, Department of Trade and Industry, 151pp. (CEH Project Number: C01937)

THE HYDROLOGICAL IMPACTS OF ENERGY CROP PRODUCTION IN THE UK

FINAL REPORT

J W Finch, R L Hall, P T W Rosier, D B Clark, C Stratford,
H N Davies, T J Marsh and J M Roberts

A Riche and D Christian (Rothamsted Research)

Agreement number B/CR/000783/00/00

EXECUTIVE SUMMARY

This report describes the work carried out between March 2002 and January 2004 under ETSU Contract number B/CR/000783/00/00 by the Centre for Ecology and Hydrology, Wallingford. It also describes the results of measurements made by Rothamsted Research staff under a sub-contract.
The objectives of this work are:

1. To determine the effects on water availability at the catchment and sub-catchment scale, of production of energy crops, across England and Wales.
2. To indicate areas where the crops will be most productive, which will be largely determined by water availability.

The two objectives have been met by a programme of field measurements, to provide parameter values for a numerical model and data to test the predictions of the model, and a numerical model that produced predictions of the water use of the current land cover and four energy crops: willow short rotation coppice, poplar short rotation coppice, *Miscanthus* and switchgrass, for a wet, a dry and a typical year. A demonstration GIS has been produced which shows how the predictions can be made use of in catchment management.

Measurements

The purpose of the measurements was to provide values for parameters used by numerical models and data against which the predictions of the model could be tested. Values for some parameters were available from the literature or previous studies

A previous study had made measurements on poplar short rotation coppices (SRC) and so field measurements took place on willow SRC at Roves Farm (Wiltshire) and *Miscanthus* and switchgrass in experimental plots at Rothamsted and Woburn (Bedfordshire) and a field of *Miscanthus* near Richard's Castle (Herefordshire).

Willow SRC

Measurements of the stomatal conductance were made in order to develop a relationship between the stomatal conductance and the atmospheric drivers on evaporative demand. These measurements were compatible with a published relationship.

The evaporative flux of the willow SRC was measured using the eddy correlation technique, applied to data obtained from a sonic anemometer, and provided data for model testing. This was also the purpose of sap flow gauges which were used to quantify the transpiration of individual stools. These data were scaled up to the full canopy on the basis of measurements of the number of stools and the leaf area.

The enhanced evaporation at the edges of plantations was investigated using the transpiration data and measurements of the soil water content in the top 10 cm. The results showed that the effect was only significant at the extreme edge of the coppice and is the result of the larger leaf area occurring at the edge. A simple relationship has been developed to capture this effect.

Miscanthus and switchgrass

Measurements of the stomatal conductance enabled a model of the variation of the stomatal conductance of the switchgrass as a result of the atmospheric drivers to be calibrated.

Measurements of the interception by switchgrass were made during two seasons. These data were used to quantify the canopy capacity and relate it to the leaf area index. Measurements of the changes in the soil water with depth under both *Miscanthus* and switchgrass were made to enable the numerical model to be

tested. For the same purpose, measurements were made of the evaporative flux from *Miscanthus* at the site near Richard's Castle.

Numerical modelling

The numerical model used was based on the Met. Office Surface Energy Scheme (MOSES) which is physically based and provides a comprehensive description of the exchanges of energy, water and carbon at the land surface.

The data collected on this project were used to give values for the parameters that determine the model's description of the energy and water balances. The results of running the model to predict the water use of the energy crops were tested against measurements of soil water content and evaporation made in this project. The values of the parameters for the carbon balance of the MOSES were determined by calibrating the model against the measured canopy height and leaf area index.

An analysis of the rainfall data for England and Wales enabled the choice of dry, wet and typical years to be made, *viz*: 1976, 1988 and 1982 respectively. The analysis also demonstrated that the water year (the period running from the beginning of October in the previous year to the end of September in the year) was appropriate, given the importance of the amount of the soil water stored in the period prior to the growing season.

The MOSES model was run on grid cells of 1 km^2. The fractions of existing land cover classes (broadleaf woodland, needliferous woodland, grassland, shrubs, tilled land, urban, bare soil and water) were determined by aggregating the 25 classes of the Land Cover Map 2000 to eight MOSES classes and then calculating the fractions in each model grid cell.

The soil hydraulic properties were obtained using the Hydrology Of Soil Types (HOST) as the basis. The dominant HOST class of each 1 km^2 was used. The properties were obtained by producing the average texture of the soil series within a HOST class and then using pedo-transfer models to calculate the properties.

The daily meteorological driving variables were obtained from the Met Office as values on a 1600 km^2 grid. These were interpolated to the model grid using a bilinear algorithm. A further refinement was made to the values of air temperature by allowing for the altitude of the grid cell using the standard lapse rate. The greater spatial variability of the rainfall was handled by using a data set of monthly totals on a 1 km^2 grid, which were disaggregated to daily values using the data from the 1600 km^2 grid.

There is no simple answer to whether energy crops will use more water than the existing land cover. It is a function of a number factors that include: the current type of the land cover; the specific energy crop, the amount of rainfall and the hydraulic properties of the soils. This was investigated in two ways: monthly time series for eight grid cells, to investigate the detailed temporal variability, and spatial distributions for water years with typical high and low rainfall, to investigate the spatial variability.

Monthly time series

The model was run on eight selected grid cells, representative of a range of climatological, soil and land cover conditions, to generate monthly times series, covering the period 1971 to 2000, of the predicted water use of each of the four energy crops, the change in water use from the existing land cover and the indicative yield. These time series allow the seasonal and inter-annual variability to be assessed. The results show that poplar SRC has a much higher transpiration rate than the other energy crops. This is due to the stomata having little response to high atmospheric evaporative demand. The effect of soils with low soil water storage in reducing indicative yield is reflected in the results. The three year harvesting cycle,

assumed for the SRC, is apparent in the results and shows an increase in water use in successive years. The switchgrass and *Miscanthus* show an annual pattern that reflects the seasons but, there is a shorter growing season than for other land cover types because the threshold temperature, below which photosynthesis ceases, is higher

Spatial distribution

The predicted spatial distributions of the water use, change in water use and the indicative yield are presented as 39 maps which show: the predicted annual water use for the current land cover and the four energy crops, the change in annual water use if the current land cover were replaced with one of the energy crops and the indicative yield, all for water years with typical, high and low rainfall.

The results show that, when soil water is plentiful, poplar SRC uses considerably more water that the current land cover or any of the other energy crops and also has significantly higher indicative yields. In areas of low rainfall, the rapid rate of transpiration early in the year rapidly depletes the soil water store with a result that growth is restricted in the later part of the year so that a low indicative yield is obtained. The conclusion is that the varieties of poplar SRC that the model was calibrated for are probably only viable in areas of high rainfall. Willow SRC has a higher water use than the existing land cover in most situations. This is mainly because it is specified in the model as having a greater rooting depth than the other land cover types, with the exception of broadleaf woodland and so is less affected by soil water stress.

Miscanthus and switchgrass are predicted to have a lower water use than the existing land cover in most areas. This is because the canopy develops later in the year, due to these grasses being specified to have a higher threshold temperature below which photosynthesis ceases, with the result that the period when the transpiration occurs is shorter and occurs during the summer months. In addition, they have a higher water efficiency than the other land cover types because they use the C_4 photosynthetic pathway. To some extent, these factors are offset by the rooting depth, which is intermediate between the existing woodlands and grasses. However, it is acknowledged that measurements through at least one full year would be needed to confirm this prediction.

Demonstration GIS

Software for a simple demonstration GIS has been written which, for a 60×60 km area of the head waters of the river Severn, allows the user to explore the possible impact of energy crop plantations on the water losses within a catchment.

Conclusions

- The effect of enhanced evaporation at the edges of SRC plantations is localised and so will have the greatest impact on small plantations. For plantation greater than 10 ha the effect is certainly comparable or less than other factors, e.g. the nature of the soil.
- More measurements are needed on poplar SRC varieties to determine whether the high water use is a consistent feature and, if not, the model should be run using the new information.
- Additional measurements are needed on the energy grasses in order to reduce the uncertainty arising from the model parameter values.
- For the same rainfall and soils, the water use of the energy grasses is likely to be less or comparable to that of the existing land cover where it is grass or tilled land and less if the existing land cover is woodland or heathland.
- In the final year of the three year cropping cycle, the water use of SRC is likely to be greater than the existing land cover if it is grass or tilled land and comparable or greater if it is woodland or heathland. However, in the first year it is likely to be less than existing land cover types.

- The results for poplar SRC show a very high water use. These results should be interpreted with caution as it is likely that varieties could be or are available that would have lower water use. In which case the water use is likely to be comparable to that of willow SRC.
- In areas of high annual average rainfall (greater than around 800 mm), the nature of the soil has little impact on the water use of the energy crops, or the existing land cover. However, in other areas, the soil hydraulic properties, particularly the ability to store water that can then be used by the plants for transpiration, can be important because of the higher transpiration rates of the energy crops.
- When the rooting depth of the energy crop is deeper than the existing land cover, there is the possibility that, after a period of drought, the soil water deficits will be greater resulting in a reduction in recharge and/or runoff in the following winter.
- During years with above average rainfall, when the transpiration rates are not constrained by soil water, the energy crops tend to use more water, than the existing land cover, mainly due to the higher interception losses.
- The predicted indicative yield from the energy crops is a function of air temperature and the amount of sunshine. The energy grasses are predicted to be more sensitive to these factors than the SRC and so show a more marked trend of decreasing indicative yield with increasing latitude and altitude.
- There are strong indications that, in areas of low annual average rainfall (less than about 700 mm), the indicative yields of all the energy crops are reduced by soil water stress.

.

CONTENTS

LIST OF FIGURES

LIST OF PLATES

LIST OF TABLES

1. Introduction

Over the last decade there has been steady progress in the development of energy crops across the UK, with increasing areas of land planted with Short Rotation Coppice, especially willow. Other crops, in particular certain grasses, are potential energy crops and have been the subject of research for several years and are now approaching the stage that commercial plantation is starting, e.g. *Miscanthus.* In many respects energy crops are thought to be environmentally beneficial, most importantly in providing a fuel that, when used to replace fossil fuels, would reduce CO_2 emissions to the atmosphere, but also in providing habitats and ecosystems that support increased biodiversity. However, concomitant with the rapid growth that characterises and qualifies particular plants as energy crops, is high water use. This has been shown in several studies on trees grown as Short Rotation Coppice (SRC), e.g. willow and poplar species (Hall *et al*., 1996), and also in a few studies on energy grasses (e.g. Beale *et al*., 1999). Although the water use with irrigation of *Miscanthus* is similar to the water use by SRC, it has higher water use efficiency so that the production of dry matter is substantially larger. For this and other, agronomic reasons they are seen as a potentially very useful source of biomass energy. Bullard (1999) estimates that the UK would need energy crops to be grown on in excess of 110 000 ha (assuming a yield of 18 tonne ha^{-1}) if 5% of energy generation is to be produced from energy crops.

Nevertheless, if biomass conversion is to make a significant contribution to the national energy supply, large areas will need to be planted around purpose-built power stations. Careful consideration must be given to the location and scale of these plantations if adverse impacts on the water resources are to be avoided. This is particularly true in the south east of the country where high population density and small differences between the precipitation and the evaporation, i.e. low effective precipitation, make southern England particularly sensitive to any reduction in groundwater recharge or river flow.

It is the purpose of this project to provide tools to help water resource managers, and growers select the appropriate crop, and plantation scale for a particular location. The tools will predict the likely effects on catchment and sub-catchment water use and river flows and the likely indicative yields that can be expected.

1.1 Project Objectives

This report describes the work carried out between March 2002 and January 2004 under ETSU Contract number B/CR/000783/00/00 by the Centre for Ecology and Hydrology, Wallingford. It also describes the results of measurements made by staff from Rothamsted Research under a sub-contract.
The objectives of this work are:

1. To determine the effects on water availability at the catchment and sub-catchment scale, of production of energy crops, across England and Wales.
2. To indicate areas where the crops will be most productive, which will be largely determined by water availability.

These have been achieved through a combination of measurements and the application of validated models, in conjunction with a GIS, to allow the change in water use accompanying the replacement of existing land cover with energy crops to be calculated.

1.2 Project outline

The project consists of three work packages summarised below:

1.2.1 Work package 1

'*Models for water use of energy crops grown in the UK'*

Although not mentioned in the title, this work package contains a significant field work component required to provide the data essential for developing, running and testing the models. This fieldwork component focussed on measurements at Roves Farm, on willow SRC, and at Rothamsted, Woburn and Richard's Castle on the energy grasses *Miscanthus* and switchgrass (*Panicum virgatum*). The measurements and the results are described in Section 3.

The model development work undertaken is described in Section 4. The Met. Office Surface Exchange Scheme (MOSES) is the model that has been used as the basis for this work.

1.2.2 Work package 2

'Sub-catchment level modelling of hydrological impacts of energy crop production in the UK'

The model developed as part of Work Package 1, has been used in conjunction with gridded sets of the driving data. These data comprise rainfall, climate, soils, land cover, and elevation for England and Wales at a range of resolutions. Some of these data have been transformed to grids at different spatial (and temporal) resolutions and some variables have been determined from others; e.g. in the weather driving data, sunshine hours have been used to derive radiation values.

Once the appropriate driving variables have been calculated they have been used with the model to calculate the water use of a selected energy crop at a selected location. Monthly coverages of the virtual additional abstraction for each of the energy crops have been produced for a typical, a wet and a dry year. These will be required for accurate assessment of the resource balance in sub-catchments and the Water Resource Management Units (WRMU) of the EA Catchment Abstraction Management Strategy (CAMS).

Other output products from this project include:

- hard-copy maps of additional abstraction for England and Wales;
- a demonstration GIS data set, supplied on CD, operational within a restricted 60 km by 60 km area of the country and hydrological data, e.g. run off, and drainage on a restricted area of 60 km by 60 km;
- VisualBasic program to extract data from the system.

An operational system for the whole of England and Wales is the likely extension of this project but is not within its current scope.

1.2.3 Work package 3

Production of guidelines for siting individual plantations

Although numbered third, this work package was the first to be addressed and was completed in September 2002, with publication of Guidelines:

Grasses for energy production – hydrological guidelines URN 03/882

SRC for energy production – hydrological guidelines URN 03/883

2. Process models of plant water use

This chapter provides a brief introduction to the concepts underlying the model used in this project.

The water use of plants is dominated by the amount of water that they transpire, i.e. which is evaporated from the leaves through the stomata. The amount of water taken up in the biomass is, by comparison, negligible. In addition the intercepted rainfall on the surface of the leaves that evaporates directly back into the atmosphere is also a loss. Numerical models of plant water use are commonly based on the water balance, which is:

$$P = E_a + I + Q_o + Q_i + \Delta S$$

where:

P	precipitation (mm)
Ea	actual evaporation (mm)
I	canopy interception loss (mm)
Q_o	surface runoff and interflow (mm)
Q_i	soil water drainage (mm)
ΔS	change in soil water (mm)

A significant part of such models is the component used to predict the evaporation losses which, in turn, involves consideration of the energy balance of the land surface.

2.1 The energy balance

The energy balance at the land surface takes the form:

$$R_n = \lambda E + H - G$$

The net radiation, R_n, is the net input radiation at the surface, i.e. the difference between the downward and reflected solar radiation, plus the difference between the downward long-wave (thermal) and upward long-wave radiation (that emitted from the land surface).

The latent heat flux, λE, is the energy used to convert water from the liquid phase, in the soil and vegetation, into the gaseous phase. It is the product of the mass of water evaporated, E, with the latent heat of vaporisation of water, λ.

A portion of the radiant energy input to the earth's surface is not used for evaporation but warms the atmosphere in contact with the ground and which then moves upward. It is referred to as 'sensible' heat flux, H, because it changes air temperature, a property of the air that can be easily measured.

The soil heat flux, G, is the heat conduction into the soil. It varies on both a diurnal and annual cycle. With dense vegetation, little radiation reaches the ground and heat storage can often be neglected.

2.2 A process based model of evaporation

The Penman-Monteith evaporation model (Monteith, 1965) has gained wide acceptance for estimating evaporation for operational hydrology because it combines a physically based approach with a pragmatic requirement for data. It is at the heart of the Met. Office Surface Energy Scheme (MOSES) that is used in this project. It is sometimes referred to as a 'big-leaf' model as it assumes that the overall effect of the

whole canopy on the energy fluxes above the canopy can be approximated by assuming that all the elements that make up the vegetation are exposed to the same microclimate. It assumes that all the energy available for evaporation is accessible by the plant canopy, and water vapour diffuses first out of the leaves, through the stomata, against the surface resistance, r_s, and then out into the atmosphere above against the aerodynamic resistance, r_a. Meanwhile, the sensible heat, which arises outside rather than inside the leaves, only has to diffuse upward against the aerodynamic resistance. These resistances are parameters that must be specified for each vegetation type but are independent of the soil type and climate. The aerodynamic resistance is generally taken as a function of the vegetation height, see below. The surface resistance is a function of the type and number per unit leaf area, which is defined as the stomatal resistance (or its inverse, the stomatal conductance, g_s) and is specific to any particular plant type. The stomatal resistance can then be scaled up to the surface resistance by multiplying it by the leaf area index (LAI) or, in the case of plants with stomata on both sides of their leaves, twice the LAI. The leaf area index is defined as the one sided green leaf area per unit ground area.

The Penman-Monteith model can be expressed as:

$$\lambda E = \frac{\Delta(R_n - G) + 86.4\rho c_p \dfrac{(e_a - e_d)}{r_a}}{\Delta + \gamma\left(1 + \dfrac{r_s}{r_a}\right)}$$

where:

E	evaporation (kg m^{-2} d^{-1})
G	soil heat flux (MJ m^{-2} d^{-1})
Rn	net radiation flux density at the surface (MJ m^{-2} d^{-1})
c_p	specific heat of moist air (kJ kg^{-1} $^oC^{-1}$)
e_a	saturation vapour pressure (kPa)
e_d	saturation vapour pressure computed at dew point (kPa)
r_a	aerodynamic resistance (s m^{-1})
r_s	bulk surface resistance of the vegetation canopy (s m^{-1})
Δ	slope of the saturation vapour pressure curve (kPa $^oC^{-1}$)
λ	latent heat of vaporisation (MJ kg^{-1})
γ	psychrometric constant (kPa $^oC^{-1}$)
ρ	atmospheric density (kg m^{-3})

the aerodynamic resistance is calculated as:

$$r_a = \frac{\ln\left(\dfrac{z_h - d}{z_{om}}\right)\ln\left(\dfrac{z_h - d}{z_{oh}}\right)}{k^2 U_z}$$

where:

U_z	mean wind speed at height z (m s^{-1})
d	zero plane displacement of wind profile (m)
k	von Karman constant
z_h	height of air temperature and humidity measurements (m)
z_m	height of wind speed measurement (m)
z_{oh}	roughness parameter for heat and water vapour (m)
z_{om}	roughness parameter for momentum (m)

d is taken to be $2/3h_c$, where h_c is the mean vegetation height. The roughness lengths used are often calculated in the way of Monteith and Unsworth (1990):

$$z_{om} = 0.123h_c$$

$$z_{oh} = 0.1z_{om}$$

Several terms are used in describing different evaporation rates. One of these involves the concept of a reference crop. It is defined as an idealised grass crop with a fixed crop height of 0.12 m and a surface resistance of 70 s m^{-1}. It is implicit in this definition that the evaporation is not limited by the availability of soil water. The evaporation from the reference crop is termed the reference transpiration (Cain, 1998). A term often found in the literature is potential evaporation. Unfortunately, this term has been applied to a variety of conditions with the result that there is no clear definition. In general, it can be taken that the term potential evaporation refers to evaporation rates for a specific land surface (e.g. open water, coniferous woodland etc.), a given evaporation model and that the evaporation rate is not limited by the availability of soil water. Thus, it is important to understand the context in which this term is used. Finally, the terms evaporation or actual evaporation are taken as the 'true' evaporation from a given land surface and thus may be limited by soil water availability.

2.3 Interception loss

The amount of rainfall actually reaching the ground surface, and thus infiltrating into the soil, is largely dependant upon the nature and the density of the vegetation cover. This cover intercepts part of the falling rain and temporarily stores it on its surface, from where the water is either evaporated back into the atmosphere, interception loss, or falls to the ground, both directly and as flow down the stem or trunk. The remainder of the falling rain misses the vegetation canopy and falls directly on the soil (free throughfall). The maximum amount of water that can be stored on the surface of the vegetation is called the canopy capacity.

Interception by the canopy is normally greatest at the beginning of a storm because the dry surfaces of the vegetation prevent a large proportion of the rainfall from reaching the ground. As the leaves become wetter, the weight of water eventually overcomes the surface tension by which it is held and further additions from rainfall are almost entirely offset by water droplets falling from the edges of leaves. Even during rainfall, a significant amount of water may be lost by evaporation from the leaf surfaces with the result that there is some further retention of water to make good this evaporation loss. During prolonged rainfall, the interception loss may be closely related to the rate of evaporation so that meteorological factors affecting the latter become significant. Some or all of the energy available for evaporating water will be used to evaporate the intercepted water on the vegetation's leaves and stems and so is not available for evaporating the water within the leaves, i.e. transpiration is reduced. The rate of evaporation of the intercepted water is faster, for the same meteorological conditions, than the evaporation of water from within the leaves because the water vapour does not have to diffuse out of the stomata, i.e. the surface resistance is zero. Whilst rain is falling, the net radiation tends to be low due to the presence of clouds and hence the wind speed becomes the significant factor. Thus interception losses are higher from trees than short, uniform vegetation, such as grass or crops, because the trees have a greater surface roughness.

2.4 Soil water

The amount of water, in the soil, which is available to the plants can be a significant limitation on the water use. Infiltration is the process of water entry into a soil from rainfall. Soil water movement is the process of water flow from one point to another within the soil. The two processes cannot be separated as the rate of infiltration is controlled by the rate of soil water movement below the surface and the soil water movement continues after an infiltration event, as the infiltrated water is redistributed. The soil water movement also controls the supply of water for plant uptake and for evaporation at the soil surface. The soil properties affecting soil water movement are the hydraulic conductivity and the water-retention characteristics. These soil hydraulic properties are closely related to the soils physical properties such as particle-size and morphology.

The water-retention characteristic of the soil describe the soil's ability to store and release water and is defined as the relationship between the soil water content and the matric potential (soil suction). Matric potential is a measure of the energy status of water in the soil and is a component of total soil water potential that includes gravitational and osmotic potentials.

The hydraulic conductivity is a measure of the soil's ability to transmit water and depends upon both the properties of the soil and the water content. The hydraulic conductivity is a non-linear function of volumetric soil water content and varies with the soil texture. Surface runoff is generated either when the rainfall rate exceeds the hydraulic conductivity of the soil at the surface, rate exceedance, or when the soil nearest the surface becomes saturated, storage exceedance. Soil water drainage can be considered as being split into vertical and horizontal components, recharge and interflow. The relative proportions are a function of both the slope of the land surface and the difference in hydraulic conductivity between the soil and the underlying substrate. In the case of direct recharge of aquifers there is usually little difference in the hydraulic conductivities and so interflow is the minor component.

2.5 The link between soil water and evaporation from plants

Soil saturated by rain or irrigation first drains until the remaining water held by surface tension on the soil particles is in equilibrium with gravitational forces causing drainage. It is then defined as being at field capacity with a fractional water content of θ_f. The drying proceeds with little soil water restriction until the soil moisture falls to a critical value, θ_d, when the evaporation rate begins to fall. It continues to fall until a wilting point is reached, when the soil water content is θ_w, at which point the evaporation rate effectively ceases. These two soil water contents represent progression from the evaporation controlled by meteorological conditions to it being controlled by the soil. However the actual nature of the progression and the processes involved in evaporation at the wilting point are poorly understood. Soil moisture deficits are defined as relative to the soil water content at field capacity. However, it should be remembered that the field capacity is actually a point on the curve describing the water retention characteristics of a soil rather than a clear break when drainage ceases.

The amount of accessible soil water available to plants depends on their rooting depth, which can, of course, change as the vegetation grows.

Soil water models used for modelling the water balance often work in terms of soil water content. However, plants are more sensitive to soil water potential and some of the differences reported in the literature in the functions linking the soil water content to reducing the evaporation may be caused by the variability in the water retention characteristic of different soils. The actual mechanisms involved in the plant are complex and not fully understood. However, studies have shown that, in terms of modelling, a

simpler formulation is possible if it is assumed that there is a correspondence between the soil water content and the stomatal resistance, r_s. In models based on the Penman-Monteith model, to be strictly correct, the effect of soil water limiting evaporation should be applied to the stomatal or surface resistances, rather than as a factor applied to the potential evaporation of that plant type.

3. Experimental work

3.1 Introduction

The programme of field measurements was undertaken to provide the data required to allow various parameter values to be estimated for use in the models, and also provide evaporative flux data for future model validation. The parameters and data required are shown in Table 1.

During the growing season of 2002, measurements were made on willow SRC, *Miscanthus* and switchgrass. During 2003, measurements on *Miscanthus* and switchgrass have been made at Rothamsted (Hertfordshire), Woburn (Bedfordshire) and Richard's Castle (Herefordshire).

Table 1 The parameters and variables determined from field measurements

parameter or variable	units	derivation	required measurements	crop
surface conductance (g_S)	mmol m^2 s^{-1}	from stomatal conductance (g_s) scaled by leaf area (L)	g_s, L	willow SRC, *Miscanthus,* switchgrass
fractional soil water content (θ)	m^3 m^{-3}	measured directly	Surface Capacitance Insertion Probe or neutron probe	willow SRC, *Miscanthus,* switchgrass
evaporative flux (λE)	(W m^{-2}) or (mm day^{-1})	determined from measurements of heat flux and energy balance components	Solent eddy correlation device	willow SRC, *Miscanthus*
transpiration	(W m^{-2}) or (mm day^{-1})	determined from measurements of sap flow rates and leaf areas	sap flow gauges	willow SRC

3.2 Willow SRC

Measurements have been made during the summer and autumn of 2002 on willow SRC growing at Roves Farm, (Ordnance Survey Nat. Grid Ref. 420941,188975), Sevenhampton, Wiltshire. Roves Farm[1] is a mixed farm of 154 ha with relatively large plantations of willow SRC (ca.16.5 ha in total) set in a topography of low relief on the edge of the Vale of the White Horse. Soils are primarily clays or clay loams, with alluvial clay along stretches of the river Cole, a tributary of the Thames.

This location was chosen for the measurements because the large blocks of SRC make it possible to use the eddy correlation method for measuring directly evaporation from the crop, and because the farm's proximity to CEH, Wallingford makes frequent visits within the project budget possible. The purpose of the measurements on the willow is to provide:

i. estimates of parameters (e.g. stomatal conductance, leaf area index, stem height) for use in the MOSES model;

[1] Further information about the farm can be found on the internet (see for example: http://www.rovesfarm.co.uk/)

ii. estimates of the evaporative fluxes from the SRC for testing the MOSES model;
iii. information on the magnitude and range of any enhancement of evaporation at the coppice edge.

Of these three the least is known about the edge effect (item iii); there are some published parameter values in the literature for willow SRC (item i) that can be used in models based on the Penman-Monteith equation (Monteith, 1965) to give estimates of evaporative fluxes (item ii): indeed we have used these parameter values in this report to provide estimates of a reference transpiration rate for willow.

If there is enhanced evaporation from tall vegetation at plantation edges it is believed to be through various mechanisms, including greater radiation input, greater exposure to the wind, and increased leaf area. It is not known how large the effect is nor how rapidly it reduces with distance into a plantation.

3.2.1 Site description

Instruments were installed in the northern sub-block (block 2; see Figure 1) of a 6.9 ha block of SRC planted in 1994/95 on a slight (c. 2%) north-facing slope. The soil type at this location is of two types. In the north-western part, including the site we selected for the edge study (see below), the soil is a deep calcareous clay with limestone within 1.2 m; soil within the remainder of the block varies between clay and loam to heavy loam over clay.

Block 2 comprised nine varieties of willow (viz. Jorrun, Q83, Bowles Hybrid, Dasyclados, Jorr, ST2481/55, Germany, Orm and Ulv) planted in double rows of the same variety aligned east-west. The average spacing is about 1.25 m between rows of different varieties, and 0.8 m between rows of the same variety, with stools separated in the rows by 0.8 m. The height of the canopy top ranged from about 6 to 9 m depending upon variety. The western edge of this block was chosen for the edge-effect study and the central 21 rows surveyed. These rows included all the varieties except for Jorr, but only three, Dasyclados, Bowles Hybrid and Orm were instrumented. A 10 m-high instrument tower was sited about 50 m in from the eastern edge of the same block to provide a platform for the eddy correlation equipment and an automatic weather station (AWS).

3.2.2 Measurements

With the exception of the long term collection of the weather data, the basic, ancillary data, viz. plant physiological and biometrical measurements on three varieties of willow, and the water content of the top 10 cm of soil under the SRC, were collected on particular field trips. For the two main investigative programmes, measuring evaporative fluxes over the SRC, and sap flow rates as part of the edge effect study, equipment was installed and the measurements automatically collected over a period of weeks.
At the time of installation of the equipment tower in early June, it was clear that there was significant beetle damage. The severity of the damage varied between varieties and some, e.g. Jorunn, were worse than others. The varieties used in the study were not so badly affected as others. As the summer progressed the severity of the beetle damage on the willow at Roves Farm remained the same despite the crop not being sprayed.

3.2.2.1 Weather

An AWS recording incoming solar radiation, net radiation, air temperature and humidity, wind speed and rainfall was mounted on the instrument tower. The AWS was at a height of about 10.5 m above the ground. The weather variables were logged at 10 s intervals by a Campbell logger (Model CR10, Campbell Scientific Ltd, Loughborough) and ten-minute averages and sums stored. Data collection continued throughout the summer and autumn until 8 January 2003.

A summary of the weather recorded by the AWS is tabulated in Table 2. In addition, daily values of the weather variables derived from the AWS data that have been used in the Penman-Monteith equation to estimate the mean daily potential transpiration from willow SRC using published parameter values (Lindroth, 1993).

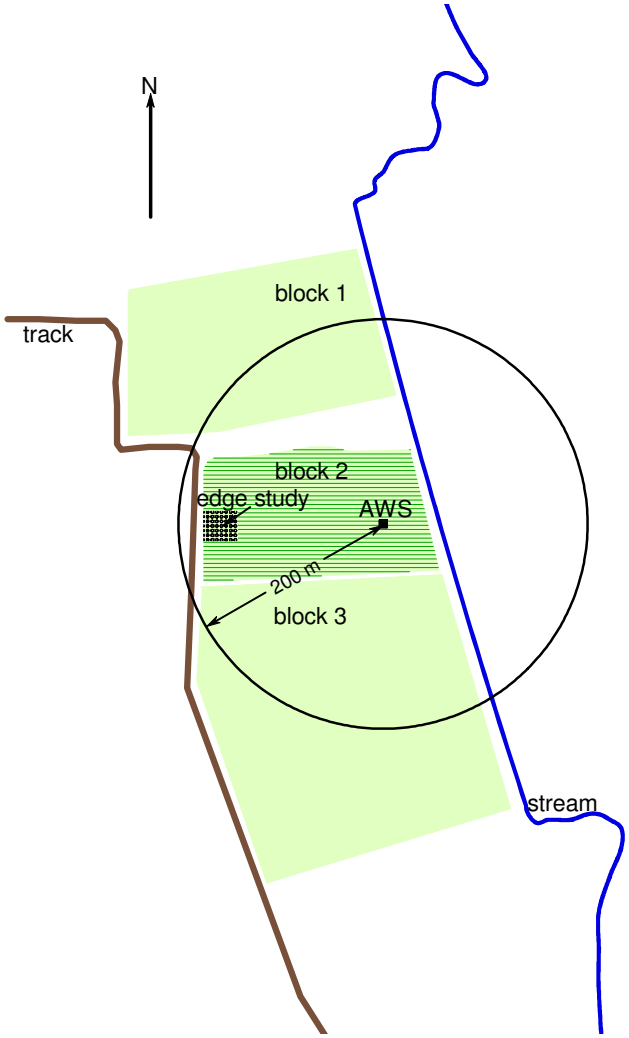

Figure 1 The position of instruments within a block of willow SRC and the alignment of the rows. The area of block 1 is c. 3 ha, and of blocks 2 and 3 together, c. 6.9 ha.

Table 2 Summary of the weather at Roves Farm during the growing and dormant seasons recorded by the automatic weather station. Measurements during the growing season were made between 6 June 2002 and 30 September 2002 (unshaded rows), and measurements during the dormant season (shaded rows) were from 1 October 2002 to 8 January 2003. The transpiration is that estimated for willow SRC using the weather data together with literature-based values for the resistance parameters. It provides a reference indicating the evaporative demand of the atmosphere.

variable	minimum	maximum	mean	s.d.	total
solar rad. (MJ m^{-2})					1722.9
					332.7
air temp. (°C)	1.6	28.6	14.8	3.8	
	-6.2	19.4	7.5	4.2	
humidity deficit (g kg^{-1})	0	11.54	2.18	2.21	
		5.0	0.58	0.73	
wind speed (m s^{-1})	0	6.8	1.8	1.1	
	0	9.8	2.4	1.5	
rainfall (mm)					246.8
					460.6
transpiration (mm day^{-1})	0.32	5.14	2.52	0.94	
	0.02	2.04	0.59	0.47	

3.2.2.2 Stem and leaf surveys

Information on the distribution of stem diameter was required for estimating the leaf areas of stools using a stratified sampling method. To provide the information a survey of stem diameters at one metre above the ground (d_{100}) from 467 stools in a block of 21 rows by about 22 stools in the area designated for the edge study was made on 25 April 2002. The diameters of all stems greater than 6 mm were recorded. These data were subsequently used to determine representative stems for sap flow measurements (see below). The information on the distributions of both stem diameters and leaf areas was needed for:

- estimating the leaf area index (the single-sided leaf area per unit ground area) of the coppice for use in the MOSES model (Section 4);
- scaling measurements of stomatal conductance to give the surface conductance, again required in the MOSES model;
- scaling measurements of the stem sap flow (Section 3.2.3.2) to provide estimates of transpiration rates.

The distributions of stem cross-sectional areas, calculated from the diameters at 1 m, for the three varieties that we measured in the edge effect study are shown in Figure 2. These show that Dasyclados has the largest diameter stems, whereas the total stem cross-sectional area of Orm is distributed more evenly across smaller diameter stems. Bowles Hybrid at this site has a significantly smaller total cross-sectional area with more small diameter stems. These survey results therefore indicate that transpiration rates from Bowles Hybrid are likely to be less than from the other varieties.

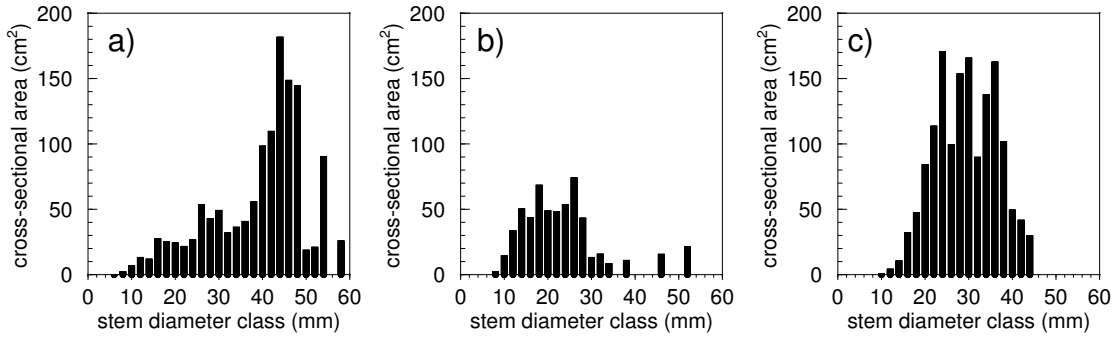

Figure 2 The distribution of stem cross-sectional area by diameter class for a) Dasyclados, b) Bowles Hybrid and c) Orm

Leaf samples from each of the three varieties were collected during the summer. However because of the time-consuming nature of this work no attempt was made to monitor the variation of leaf area through the summer. All the leaves were collected from stems, representative of the diameter classes that contributed significantly to the total stem cross-sectional area of the stools were selected at the edge, and within the coppice. These stems were mostly those which had been gauged for the sap flow measurements. On return to Wallingford the leaves were stored in a freezer until analysis.

An investigation of the optimum sub-sample size was carried out to establish the best compromise between time taken to measure the leaf area of the sub-sample and accuracy of results. Sub samples of 30%, 20% and 10% were taken from the same well mixed bulk sample, and their leaf area measured and compared with the area of the whole sample. This was carried out on both a large and a small sample. The results indicated that although a 10% sub sample was acceptable for the larger sample, considerable variation occurred when the same method was used for the smaller sample. As a result, it was decided that a sub sample of approximately 15 g should be used regardless of the bulk sample size.

When ready for analysis, the frozen samples were laid out on a plastic tray to defrost. When fully defrosted, the sample was well mixed, bits of twig and bark removed and the leaves weighed. A 15 g to 18 g sub-sample was taken and then weighed accurately. The leaf area of the sub-sample was measured using a leaf area meter (Model 3100, LI-COR Inc. Lincoln, USA). Dead leaves and pieces of leaves were then removed from the sub sample, which was then passed through the area meter again. These results were used to calculate leaf area of both the whole sample and the portion of the whole sample that was live at the time of sampling.

The values of the live leaf areas were plotted against cross-sectional areas of the sampled stems and the relationship between the two determined by linear regression with the intercept at zero, giving an equation of the form $L = aC_{100,}$ where L is the leaf area, a is the regression slope parameter, and C_{100}, is the stem cross-sectional are at 1 m. Two different values of a were needed for each variety: one for the two stools nearest the edge (zone 1) and one for the other stools (zone 2). This was because at the coppice edge the stems develop more leaves to maximise the capture of sunlight. Also in some varieties (e.g. Dasyclados) the growth habit of the stools at the plantation edge is different; the stems tend to grow more horizontally. Values of the regression slope parameter, a, for the different varieties are given in Table 3. For Orm and Dasyclados the parameter values are, statistically, significantly different. We used these relationships to estimate the leaf area and leaf area indices of all the surveyed stools. No leaf samples were collected from the Bowles Hybrid in zone 1, and so the value of a for zone 1, was estimated using the values that were available. We assumed that the mean of the ratio between the values of a for the two zones of the other two varieties could be used for the Bowles Hybrid to calculate a for zone 1 from the value for zone 2, that was available.

The variation of the stem cross-sectional area, and the stool leaf area, with distance from the western edge of the plantation for the three varieties used in the edge-effect study are shown in Figure 3 and Figure 4.

Table 3 The slope parameter relating the leaf area (m^2) to the stem cross sectional area (cm^2) at 1 m above the ground for stems of stools 1 and 2 from the edge (zone 1), and all other stems (zone 2).

variety	slope parameter	
	zone 1	zone 2
Dasyclados	0.178	0.078
Bowles Hybrid	0.308[2]	0.124
Orm	0.132	0.047

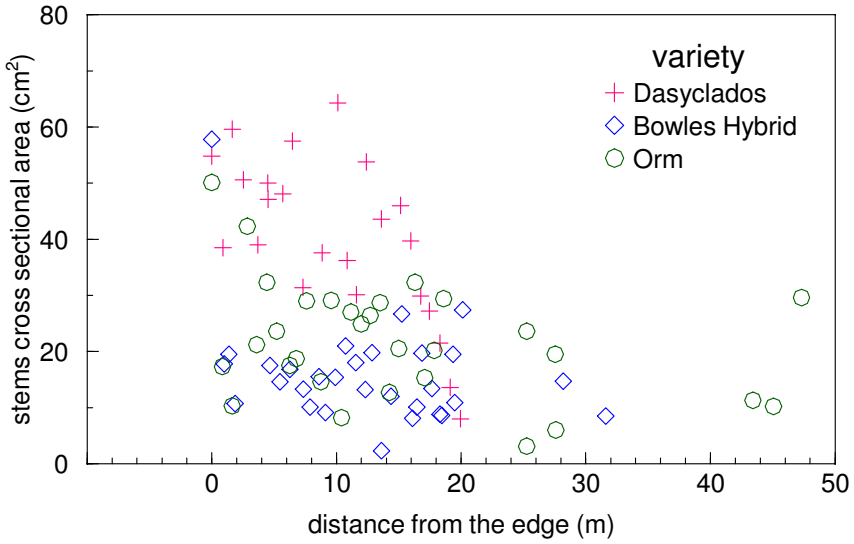

Figure 3 The variation of the summed stem cross-sectional area (at 30 cm from the stool base) for each measured stool of three varieties, with distance from the western edge of the coppice

[2] *The slope parameter for Bowles Hybrid zone 1 was not determined from regression as the other values were (see text)*

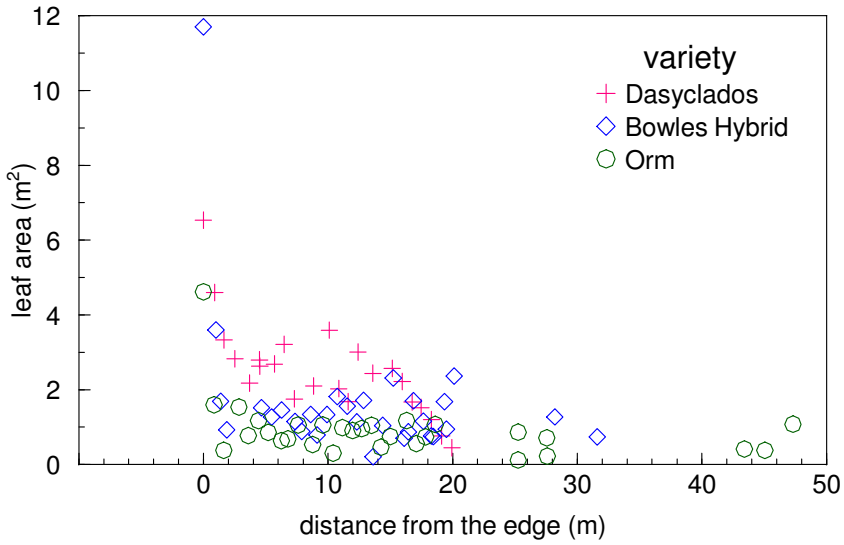

Figure 4 The variation of leaf area for each measured stool of three varieties, with distance from the western edge of the coppice

3.2.2.3 Soil water

An extensive survey of the soil water content in the top 10 cm was made in the spring (12 April 2002) for the block of 21 rows of willow and 5 m of adjacent grass track at approximately 1 m resolution using a Surface Capacitance Insertion Probe (SCIP). These data were interpolated to produce the map of surface volumetric water content (Figure 5) using plotting software. Three further sets of measurements (13 June, 22 August and 6 September 2002) were made for selected rows of the willow (and the track) to determine the extent of any changes in water content: The dates on which the different varieties and rows were sampled are shown in Table 4. The measurements were restricted to the top 10 cm for the pragmatic reason that to have carried out such detailed spatial measurements over the full soil profile would not have been feasible. However, the results are thought to reflect the patterns in the deeper layers because the root density decreases with depth and so the majority of roots lie near the surface. Thus the soil moisture deficits are greatest near the surface, except after rain. In addition SRC willows are shallower rooting than 'normal' trees.

The results of the SCIP surveys are shown in Figure 5 and 6. It is clear that, at the start of the growing season, the top 10 cm of soil under the coppice is drier than that under the grass on the track. Figure 5 also shows that, at the start of the season, the soil under the Dasyclados in rows 14 and 15 was drier than that under the other two varieties. Figure 6 shows that the soil dried more under the coppice than the grass, as the summer progressed. However these limited data do not provide evidence of enhanced water use at the edge of the coppice.

Table 4 Date on which SCIP measurements of the water contents of the top 10 cm of soil were made on stools of different willow varieties. A full survey of all varieties within the 21-row block was made on 12 April 2002.

date of measurements	rows (numbered from the south)	variety
12 April	1, 20, 21	Jorunn
	2, 3, 18, 19	Q83
	4, 5, 16, 17	Orm
	6, 7	Germany
	8, 9	Bowles Hybrid
	10, 11	ST2481/55
	12, 13	Ulv
	14, 15	Dasyclados
13 June	1, 20, 21	Jorunn
	2	Q83
	11	ST2481/55
22 August	4, 5	Orm
	8, 9	Bowles Hybrid
	14, 15	Dasyclados
6 September	4, 5	Orm

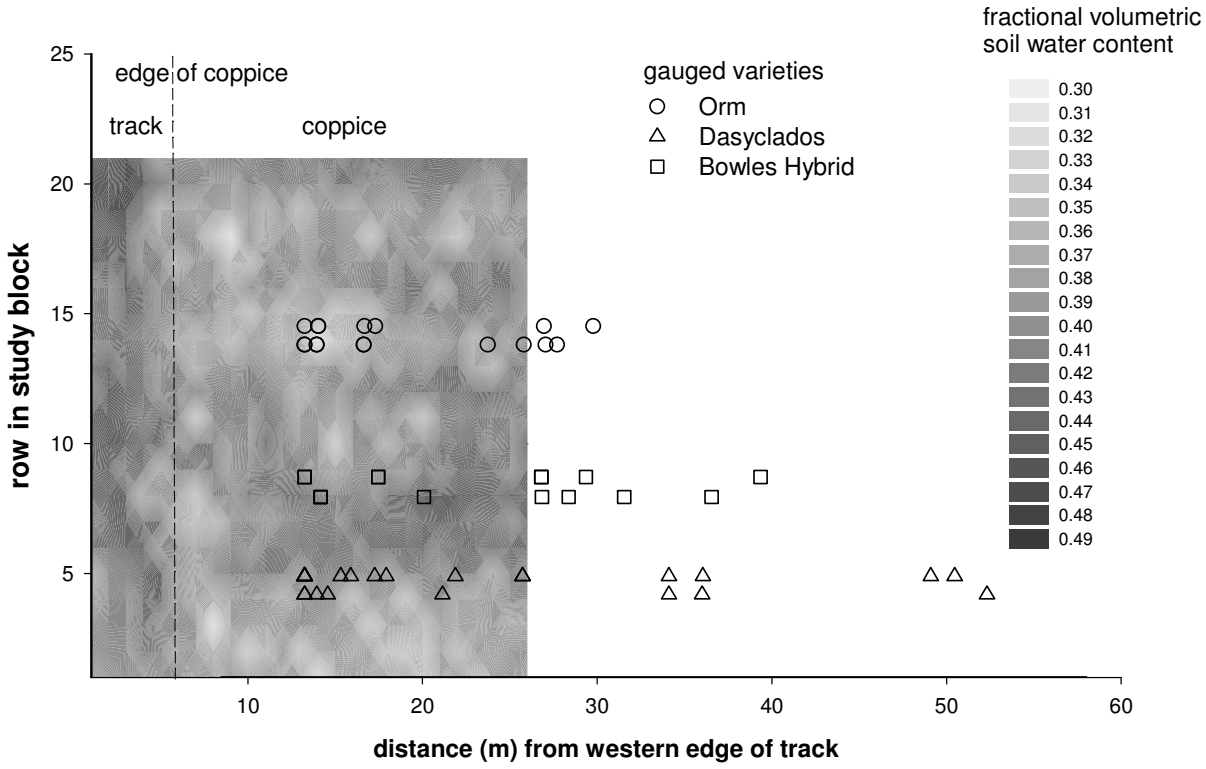

Figure 5 The fractional volumetric water content of the top 10 cm of soil measured on 12 April 2002. The positions of the stems used for measuring sapflow (Section 4.2.2.4) are also shown.

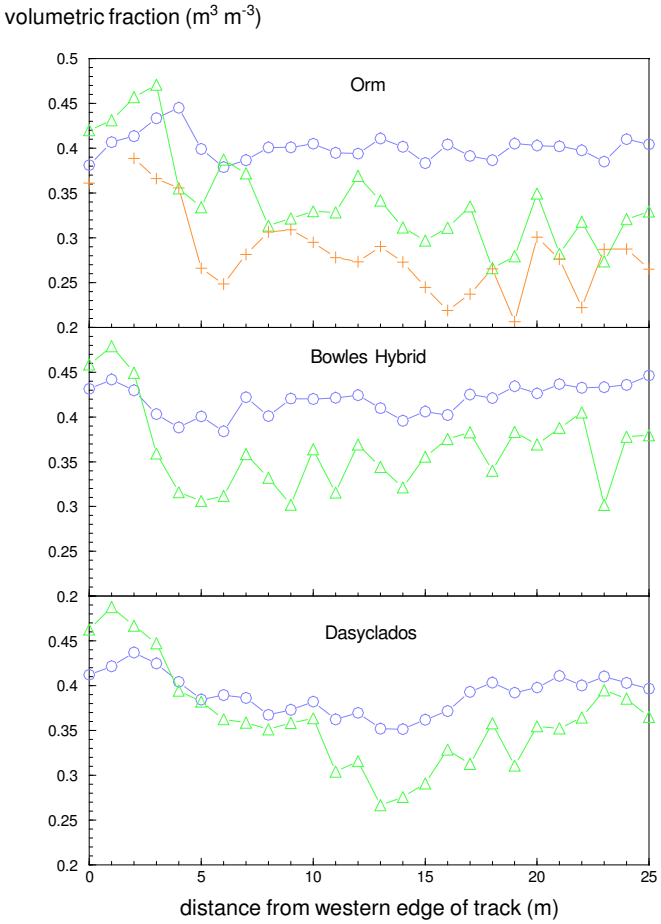

Figure 6 The variation in the volumetric water contents of the top 10 cm of soil under the grass track (0 to 5 m) and under the coppice (5 to 25 m). Circles are used to indicate readings taken on 12 April 2002, triangles indicate readings taken on 22 August, and crosses, readings taken on 6 September.

3.2.2.4 Stomatal conductance

Plants regulate the rate of water loss to the environment through the physiological control of the opening of their leaf stomatal pores. Stomatal conductance is a measure of the efficiency of the transfer of water vapour through the stomata in response to the humidity gradient between the interior of the leaves and the atmosphere. Stomatal conductance varies in response to environmental and physiological controls including, the dryness of the soil, the amount of light incident upon the leaf, air temperature and the ambient CO_2 concentration, the age of a leaf, and its position within the canopy.

Stomatal conductance measurements need to be made on a number of leaves at different levels in the canopy and over a range of climatic conditions throughout the growing season. For completeness, measurements are made over time periods of about an hour with about a gap of about one hour between runs. This ensures that measurements made at the start and at the end of the measurement hour are experiencing roughly the same climatic conditions. To ensure that the stomatal conductances obtained are representative of the canopy as a whole, measurements have to be made on a number of leaves at different levels within the canopy.

Unfortunately persistent intermittent mechanical and electronic problems with the porometer, used to measure the stomatal conductance, severely limited its availability for measurements during 2002. Measurements were taken on three occasions on the willow at Roves Farm.

Calibration was carried out according to the manufacturer's instructions. For every leaf sampled, the upper surface conductance was measured first, followed by the lower surface conductance. Two sampling runs were carried out on 23 May 2002 using the AWS tower to gain access to the different levels of the willow canopy. Unfortunately subsequent analysis of these data has shown that the porometer was malfunctioning and the data are unreliable and therefore have been discounted.

A further sampling run was carried out on 1 August 2002 and was designed to provide comparative measurements of the different varieties. This commenced at 13:32 GMT when 2 leaves from each of edge effect study rows 1 to 20, were measured at about 1.5 m giving 80 readings.

3.2.2.5 Edge effect study

The purpose of this study was to measure the size of any enhancement in transpiration at the edge of the coppice. It was therefore important that rows of the same variety were oriented perpendicular to the edge to be studied so that differences in transpiration arising from different varieties did not confound the measurements. This requirement limited the number of locations available for the edge study. Ideally an edge facing south-west, the direction of the prevailing wind would have provided the most occasions when wind-driven enhancement could be detected. However an edge with this orientation was not available and the east-west rows ruled out using a south-facing edge; a west-facing edge was therefore used. The edge was unshaded for much of the day.

Measurement of the transpiration rates involved measuring the rate of the sap flowing in the willow stems. This was measured using Dynagage™ Stem Heat Balance (SHB) sap-flow gauges (Dynamax, Houston, TX, USA). The Dynagage™ is an electronic instrument which can be installed on a stem in a few minutes and left in-situ for several weeks, providing automated measurements of sap flow. It operates using the heat balance principle: the difference between a measured amount of applied heat and the measured losses is the amount of heat, Q_f (W) dissipated by heating of the sap as it flows through the heated region. The gauge also measures the temperature increase of the sap, ΔT (K), so the rate of sap flow s (g s^{-1}) can be simply calculated as

$$s = \frac{Q_f}{c_s \Delta T}$$

where c_s (J g^{-1} K^{-1}) is the specific heat capacity of the sap (assumed equal to the value for water).
An estimate of the transpiration from each gauged stool on a ground area basis, T (mm day^{-1}), was calculated from the sap flow rate measured by each gauge using a scaling equation

$$T = \frac{sL^*}{L_i}$$

where s is the estimate of sap flow (kg day^{-1}), L_i is the leaf area of the gauged stem (either measured directly or calculated using the appropriate equation relating L to stem diameter) and L^* (m^2 m^{-2}) is the stool leaf area index. L^* was calculated as LA_g^{-1}, where L is the total leaf area (m^2), obtained by summing the L_i of all stems in the stool and A_g (m^2) is the mean ground area occupied by a stool of the particular variety.

There were three measurement campaigns (see Figure 7) spread over most of the summer on the three varieties, (Dasyclados, Bowles Hybrid and Orm). The campaigns were staggered so that there were periods when measurements were made on two varieties at the same time. These particular varieties were

chosen because they appeared to represent the range of enhancement in leaf area evident at the coppice edge in all varieties.

At the start of each measurement period, gauges were installed on a sample of stems at increasing distances from the plantation edge. The sample was chosen to be representative of the diameter classes that contributed significantly to the total stem cross-sectional area of the stools. To accommodate the variation in stem size, gauges of several different diameters were used, *viz.* 16 mm, 19 mm, 25 mm, 35 mm and 50 mm diameter. The gauges were positioned at different heights on the stems, but below the leaf canopy, taking advantage of the natural taper of the stems so that the limited range of gauge sizes could be used on a wider range of stem diameters. The stems of Bowles Hybrid were generally smaller than those of the other two varieties (see Figure 2) and so more of the smaller gauges were used on this variety.

Figure 7 The sap flow measurement campaigns during 2002

Conical shelters were designed, to prevent the ingress of rainwater running down the stems (see Plate 1). The shelters were formed from circles of heavy duty polythene wrapped around the stems, above each gauge. Electrical insulation tape was used to attach them to the stems and this joint was coated with waterproof grafting wax.

The signals from the gauges were recorded every 15 s and stored as ten-minute or 20-minute averages with an automatic data logger (model CR21X, Campbell Scientific, Shepshed, Leics.). The quality of all the data was checked graphically, before calculating the sap flow rates. Days with complete records of ten-minute values in further analysis were integrated to produce daily total sap flows (kg day^{-1} $stem^{-1}$)

To aid assessment of the magnitude of the edge effect on the transpiration rates, they were divided by the reference transpiration rate. Normalising the transpiration rates in this way removes variance in the data arising from the variation in the meteorological evaporative demand, and makes clearer any difference in transpiration rates with distance from the coppice edge and between the varieties.

3.2.2.6 Heat fluxes from the willow SRC

Direct measurements were made of the sensible heat flux from the SRC using an eddy correlation device (Solent R2A). The Solent was installed on the instrument tower at a height of 11.75 m above the ground, and where the height of the top of the SRC canopy was about 8 m. Data from the Solent were collected and stored on a Campbell 21X logger. Two net radiometers, in addition to the AWS net radiometer, fixed to the end of booms projecting from the top of the tower provided measurements of the net radiation. These and two soil heat flux plates detecting the soil heat flux were logged by a separate Campbell CR10 logger which recorded hourly averages.

The Solent measures the fluctuations in the air temperature and the vertical component of the wind speed, and from their product determines the net flux of sensible heat. This is used in conjunction with the measured net radiation and soil heat flux to calculate the latent heat flux (evaporation) from the energy balance.

Plate 1 The stem sap flow gauges in situ on an edge stool of Bowles Hybrid. The gauges are insulated from solar radiation by aluminium foil and protected from rain water by conical heavy-duty polythene shields

The evaporative fluxes measured by the device are the sum of the transpiration from any vegetation and evaporation from bare soil or any other wet surfaces (e.g. water bodies or wet roads). The sensors on the Solent are affected by the air passing by them so that the heat fluxes are those from the surface upwind of the device. The area of the surface, or footprint, changes according to the mean horizontal wind speed and atmospheric stability. So that the area is representative of the surface of interest (in this case the SRC) for as much time as possible, it is necessary to place the Solent so that the upwind distance or 'fetch' over the SRC is as large as possible in the direction of the prevailing wind. To achieve this, the tower on which we installed the Solent was erected about 50m in from the eastern end of the block. This ensured that in the direction of the prevailing wind there was a fetch of at least 200 m over willow SRC (see Figure 1), while allowing for some occasions when we might obtain useful data, under low wind speed sunny conditions that characterise unstable conditions, when the wind was from other directions. In the direction of the prevailing wind the land rose gradually so that the height difference between the sensors and the canopy top reduced by about1.5 m.

Delays by the manufacturer in repairing the Solent delayed the start to the measurement programme to late June. Afterwards, measurements continued through the summer with some data loss through battery failure (7 to 22 July 2002) and thermocouple breakages, possibly the result of bird activity.

3.2.3 Analysis and interpretation

3.2.3.1 Stomatal conductance

Because of the paucity of data resulting from the problems with the porometer, no information about the variation of stomatal conductance in response to environmental or physiological variables can be derived from the measurements. They do, however, provide an indication of typical magnitudes for the varieties that were measured (see Table 5).

Table 5 The stomatal conductance of eight willow varieties near midday on 1 August

Variety	No. of stools	Mean stomatal conductance (mmols m^{-2} s^{-1})	Standard Deviation
Jorunn	2	199.7	12.2
Q83	4	471.4	112.7
Orm	4	194.5	83.1
Germany	2	327.4	36.9
Bowles Hybrid	2	230.5	118.9
ST2481/55	2	177.7	17.5
Ulv	2	296.3	121.6
Dasyclados	2	330.1	32.7

It might be expected that in the afternoon at the edge of the coppice there would be little difference between conductances at the top of the canopy and those lower down. However there is a difference between the values recorded at the top of the canopy at the tower on 23 May and the values recorded at the coppice edge on 1 August for the Bowles Hybrid and ST2481/55. On reflection this is not surprising given the decrease in soil water over the sixty-day interval between the measurements and potential differences in the soil at the two locations, and also the ageing of the leaves over the summer.

Cienciala and Lindroth (1995a) made measurements of the LAI, gas flow and sap flow of short-rotation willow (*Salix Viminalis* L.) at a site in Sweden. They derived values of the stomatal conductance from these measurements (Cienciala and Lindroth, 1995b). From these values, plus measurements of the meteorological variables, they were able to formulate a model of the stomatal conductance per unit leaf area, g_s, (mmol m^{-2} s^{-1}) as a function of the global solar radiation and the vapour pressure deficit, δe (kPa):

$$g_s = \left(250 g_n + \frac{250 g_x R_g}{R_g + p_r} \right) f \delta e$$

where R_g is the downward global solar radiation (W m^{-2}), g_n is the fitted minimum stomatal conductance which occurs at night (25.75 mmol m^{-2} s^{-1}), g_x is a fitted parameter related to the minimum stomatal conductance (2.81 W m^{-2}), p_r is a fitted parameter related to the downward global solar radiation (847.2 W m^{-2}). $f\delta e$ is a function describing the response to vapour pressure deficit:

$$f\delta de = \frac{1}{1 + p_d \delta e}$$

where p_d is a fitted parameter related to the vapour pressure deficit (1.242 kPa).

The AWS at Roves Farm recorded the average downward global solar radiation for the ten minute period after 12:00 UST as 4857 and the vapour pressure deficit as 0.472. Putting these values into the model gives a value for the stomatal conductance of 178; whilst this is lower than the measurements made on this project, it is within the experimental error.

In the absence of more detailed measurements it was necessary to use the dependency of stomatal conductance on the environmental variables, reported by these authors, in the modelling work of this project.

3.2.3.2 Edge effect

To compare the stem sap flow rates (units of mass per unit time) measured by the heat balance gauges, requires that we normalise the rates by an appropriate scaling factor, e.g. leaf area or stem cross-sectional area, so as to compensate for the differences in stem size. The resulting values, which have units of velocity, are shown in Figure 8 to Figure 10.

Figure 8 compares the diurnal variation in sap flow in stems of Dasyclados and Bowles Hybrid at one metre into the coppice and the reference transpiration rate. This comparison shows that for these particular stems the rates of sap flow were greater in the Bowles Hybrid than the Dasyclados but that both follow the course of the transpiration rate predicted for a reference willow canopy.

Sap velocities from different stems have been averaged, for the three different willow varieties for time periods when the wind was blowing from different directions. These averages have been plotted against distance into the coppice from the western edge, as shown in Figure 9. Average values of sap velocity were also calculated for the morning and afternoon to see if there was any enhancement at the edge arsing from the more direct insolation in the afternoon (Figure 10). There appears to be no enhancement in sap flow at the edge of the coppice for any of the varieties or wind directions (Figure 9). Nor is there any enhancement arising from any additional direct insolation in the afternoon (Figure 10).

Transpiration rates were calculated from the daily sap flow rates using the ratio of the leaf areas of the gauged stems and leaf area indices of the stools. These daily transpiration values were divided by the reference transpiration rate, to remove the variation due to the weather, and then averaged over the whole measuring period and plotted against distance from the coppice edge (Figure 11). There is considerable variation in the transpiration rates and large error bars associated with some points. Some of this variation is what would be expected at any site due to the natural variability of the plants and the soil. Some of it is due to random instrumental errors. But at this site beetle infestation would also have contributed to reducing the accuracy of the results through systematically reducing the leaf area from that of unaffected plants, and also through introducing added variability between the leaf areas of different stems.

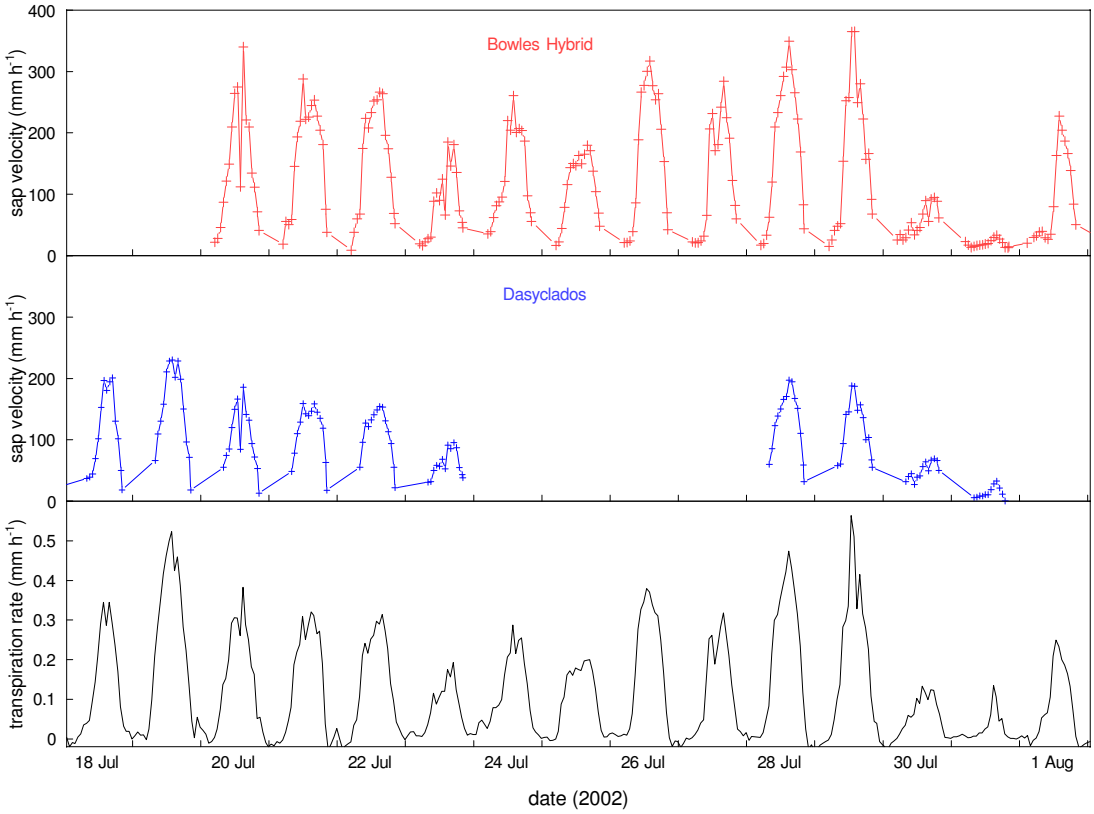

Figure 8 The sap velocity measured for two willow varieties using the stem heat balance method for different conditions of atmospheric demand as indicated by the reference transpiration rates

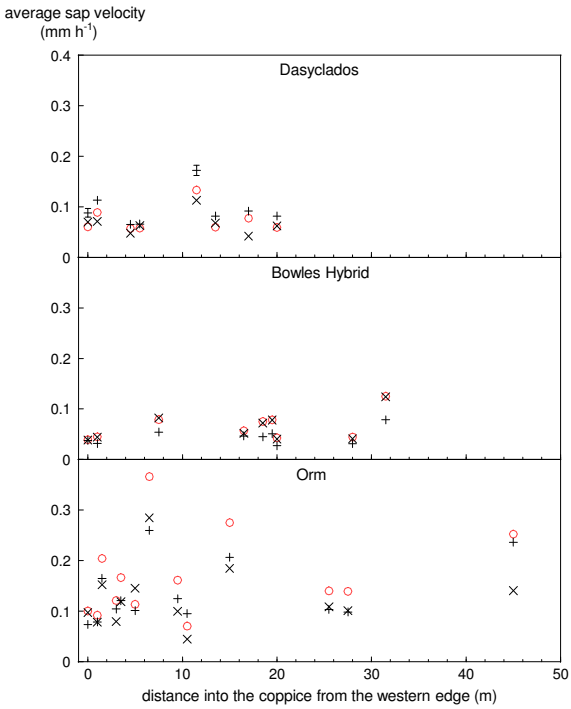

Figure 9 The variation of sap flow velocity for three different willow varieties with distance into the coppice from the western edge, for three different wind directions (westerly, indicated by x; easterly, indicated by +; and other directions indicated by ○)

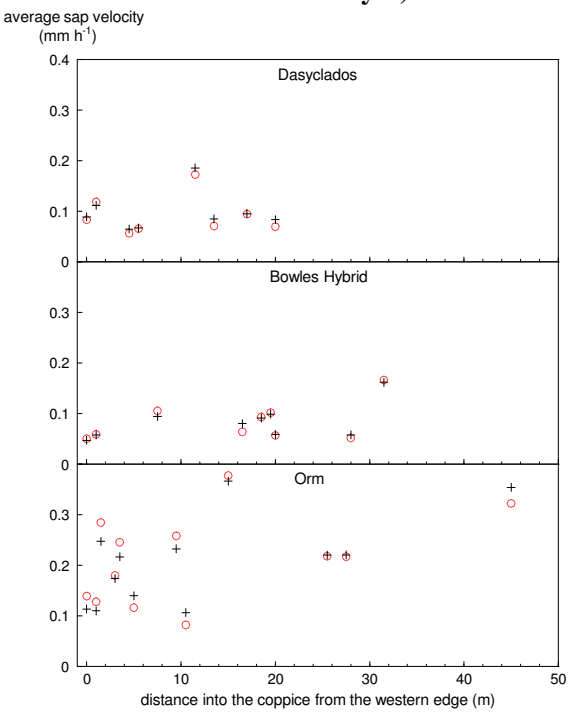

Figure 10 The variation of sap flow velocity for three different willow varieties with distance into the coppice from the western edge, during the morning (GMT) indicated by +, and during the afternoon, indicated by ○

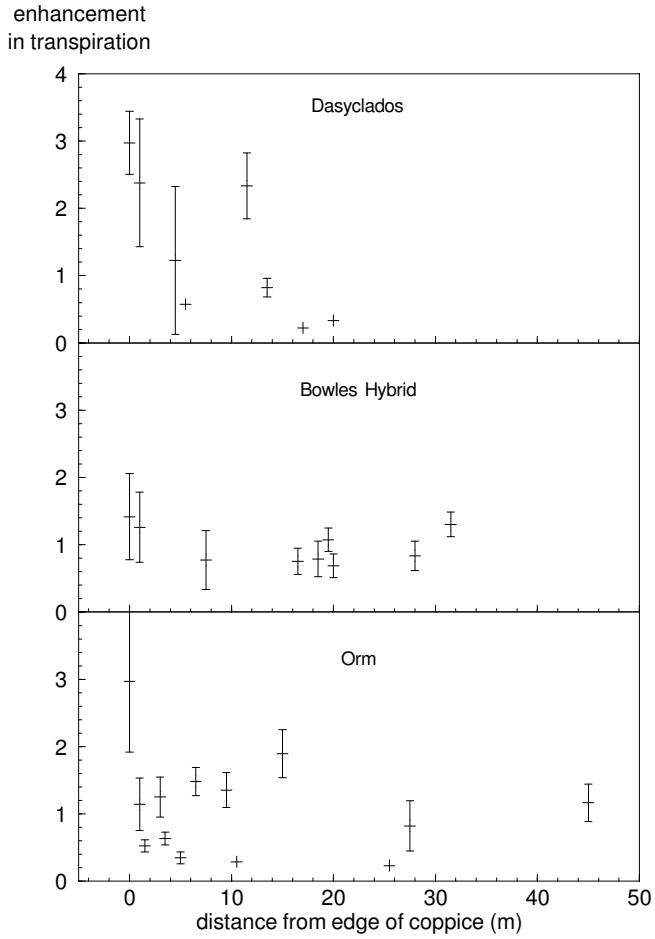

Figure 11 The variation of transpiration with distance into the coppice for the three varieties. Each of the points represents the mean daily transpiration over the period of measurements, relative to the mean daily reference transpiration rate for willow (see text), calculated using the weather variables recorded by the AWS. The error bars represent ± one standard deviation.

Despite the large variation the results indicate that there is an enhancement in transpiration only at the extreme edge of the coppice (no more than the first two stools) and that this enhancement is typically by a factor of two to three. This enhancement is not seen in the sap flow data, indicating that it is entirely due to the larger leaf area of the stools at the coppice edge.

With this new information on the edge effect, it is possible for the first time to make measurement-based estimates of the likely enhancement in evaporation that can be expected for different sized plantations. Such estimates are shown in Figure 12. These enhancement factors were calculated on the following assumptions: (i), that the within-row stool spacing is 0.8 m; (ii), that interception loss rates are affected to the same degree as transpiration rates; (iii), that the outermost stools evaporate at three times the reference rate and the next stools in at twice the reference rate; (iv) that the plantation area is approximately rectangular. The enhancement factor, F, is, for a plantation of area A m^2:

$$F = \frac{A + 9.6(A^{0.5} - 0.8) + 6.4(A^{0.5} - 2.4) - 6.4(A^{0.5} - 1.6)}{A}$$

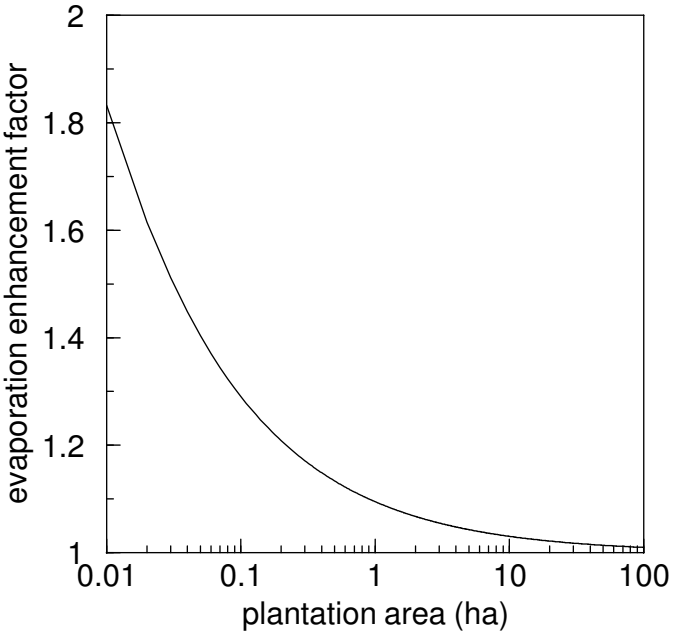

Figure 12 The evaporation enhancement factor for plantations of different sizes calculated on the basis of the edge effect measurements of transpiration

Because the edge effect is so limited in extent, only affecting the very edge of the plantations, the enhancement factor drops rapidly with increasing area, so that it is only 10% for plantations of 1 ha. Most commercial plantations are likely to be larger. However, if a large number of small plantations were established on a sub-catchment than it would be necessary to take this effect into account. It is simplest to make an adjustment for the enhancement in post-processing of the MOSES model outputs as part of the GIS system.

The daily transpiration values for the three varieties through the summer for gauged stems that were at least one metre from the edge of the coppice are shown in Figure 13. Unfortunately, sap flow data are missing between 12 and 16 July 2002, because of a memory module failure. They generally reflect the evaporative demand of the atmosphere, as indicated by the reference transpiration rate in the lower graph. Transpiration rates appear to be the same for the Bowles Hybrid and Dasyclados and close to the reference transpiration rates, whereas transpiration rates from the Orm appear to be higher, until the end of September. These apparently higher rates are also seen in the sap flow data (Figure 9 and Figure 10). We cannot be certain of the reason for these higher rates; the limited measurements of stomatal conductance do not provide an explanation since, if anything, they indicate lower conductances for Orm. It is possible that the available soil water was higher for these particular rows, or that it had developed a more extensive root system than the other varieties.

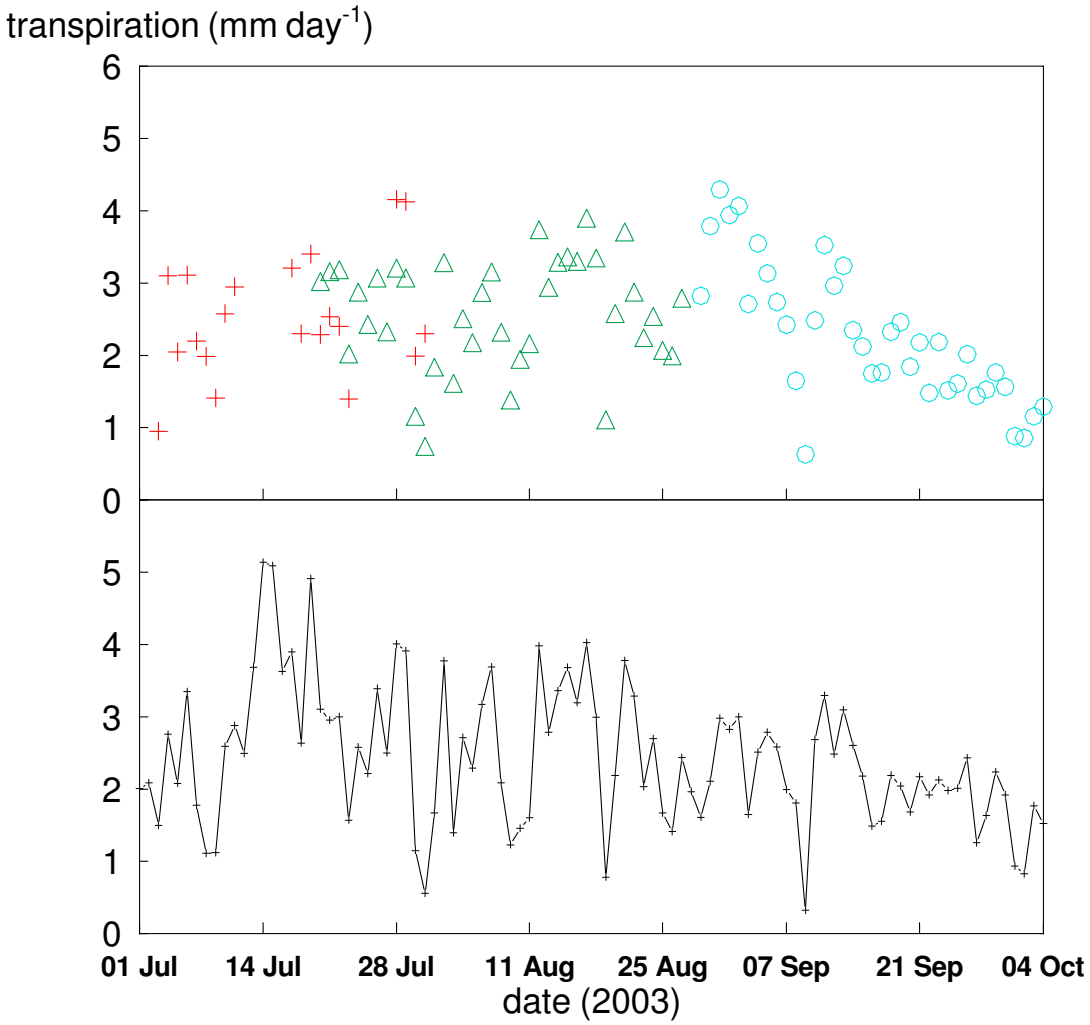

Figure 13 The mean daily transpiration for Dasyclados (+), Bowles Hybrid (Δ), and Orm (O) measured by the sap flow gauges through the summer on stems at least one metre from the coppice edge. For comparison the reference transpiration for willow, calculated using the weather data, and literature values for the resistance parameters, in shown in the lower graph.

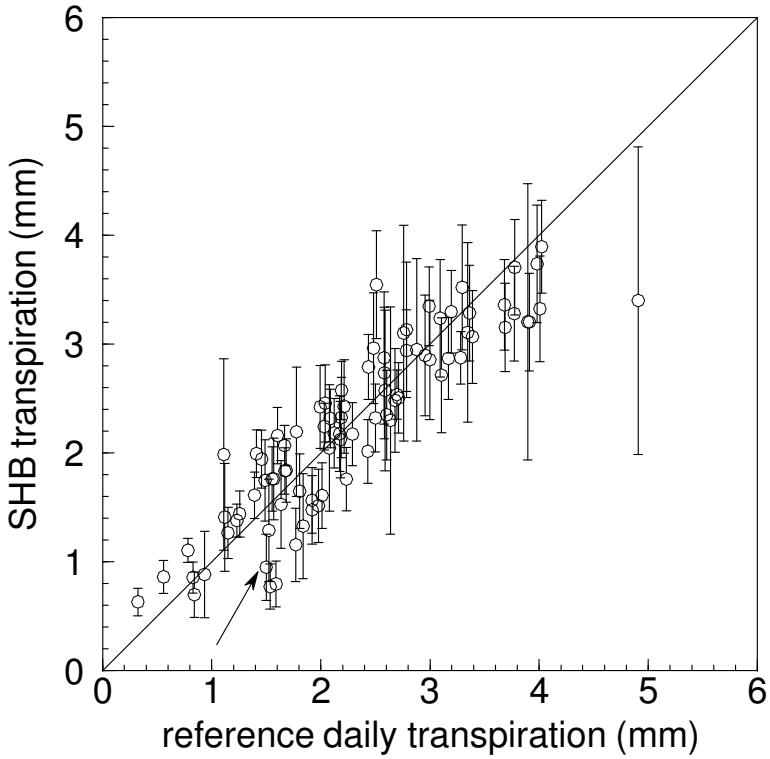

Figure 14 The daily transpiration measured by the sap flow gauges (averaged over all gauges at least one metre from the coppice edge) plotted against the reference transpiration rate. (The arrowed point is referred to in Section 3.2.3.3.)

The daily transpiration was calculated as the average of the daily transpiration rates from all the gauges which were at least one metre from the edge (i.e. stool number 3 and greater) and is plotted against the reference transpiration rate in Figure 14. The results indicate that there maybe a levelling off of the measured transpiration at the higher rates. If correct this would be quite reasonable, since a fixed value for the stomatal conductance was used in the calculation of the reference transpiration rate, whereas the stomata close with increasing humidity deficit, such as are likely on days of higher evaporative demand.

3.2.3.3 Evaporative fluxes measured with eddy correlation

Daily evaporative fluxes measured with the Solent are shown in Figure 15 and Figure 16, where they are compared with the mean daily transpiration (not including transpiration from the edge stools) measured by the sap flow gauges. Data are missing for the period 7 to 22 July as a result of battery failure. The fluxes measured on 1, 2 ,4 and 5 August are also not plotted as on these days the prevailing wind direction was such that the fluxes were not from the SRC.

The results are consistent with expectations in that generally, the evaporative fluxes measured by the Solent are slightly greater than the mean transpiration fluxes determined from the sap flow measurements. This is seen more clearly in Figure 16 where the two fluxes are plotted against each other. On 3 July the flux measured by the Solent is significantly higher than the SHB transpiration rate. It appears that the Solent flux is much higher than the reference transpiration rate, and Figure 14 (arrow) indicates that there is reasonable agreement between the reference and SHB rates.

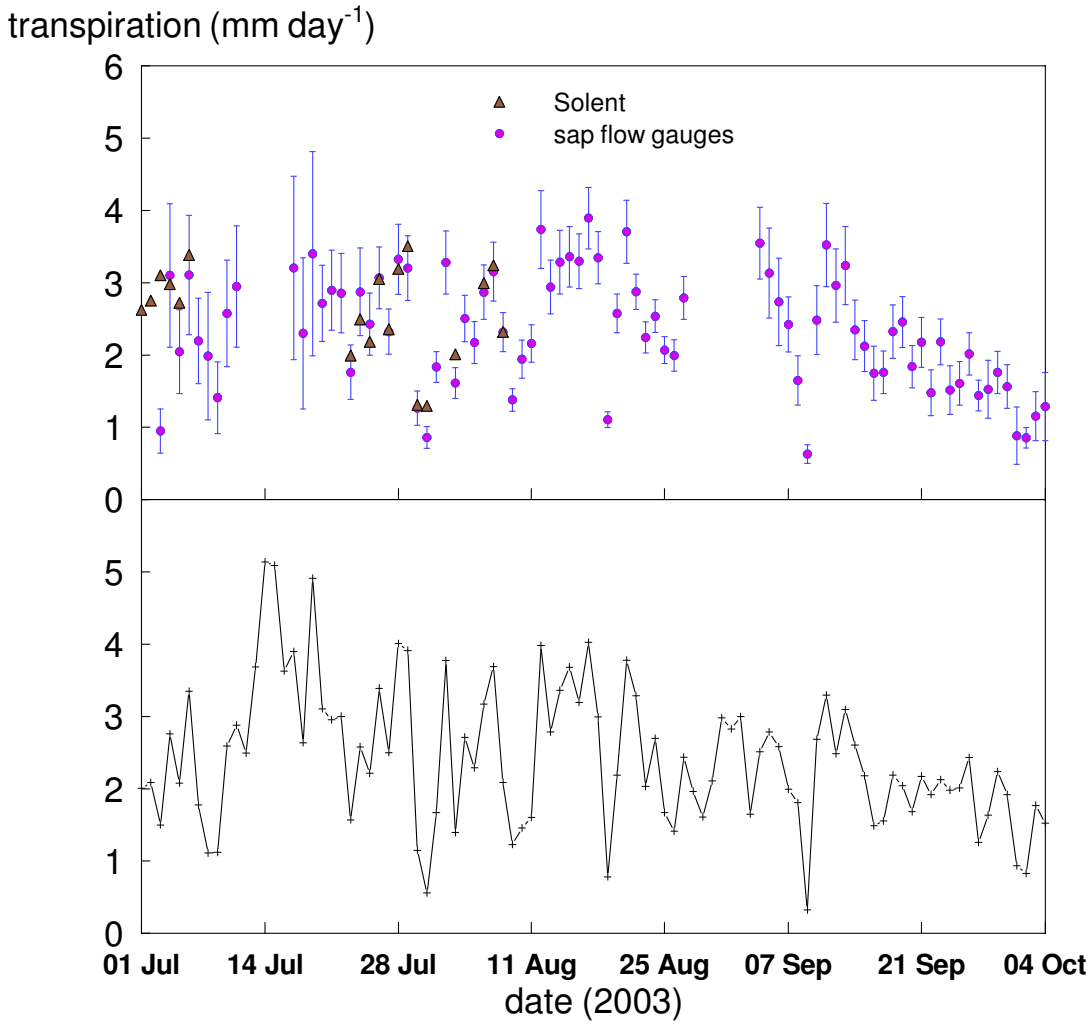

Figure 15 The mean daily transpiration (± one standard error) measured by the sap flow gauges through the summer, compared with the evaporative fluxes (transpiration plus evaporation from the soil) measured by the Solent eddy correlation device. The reference transpiration for willow calculated using the weather data, and literature values for the resistance parameters, is shown in the lower graph.

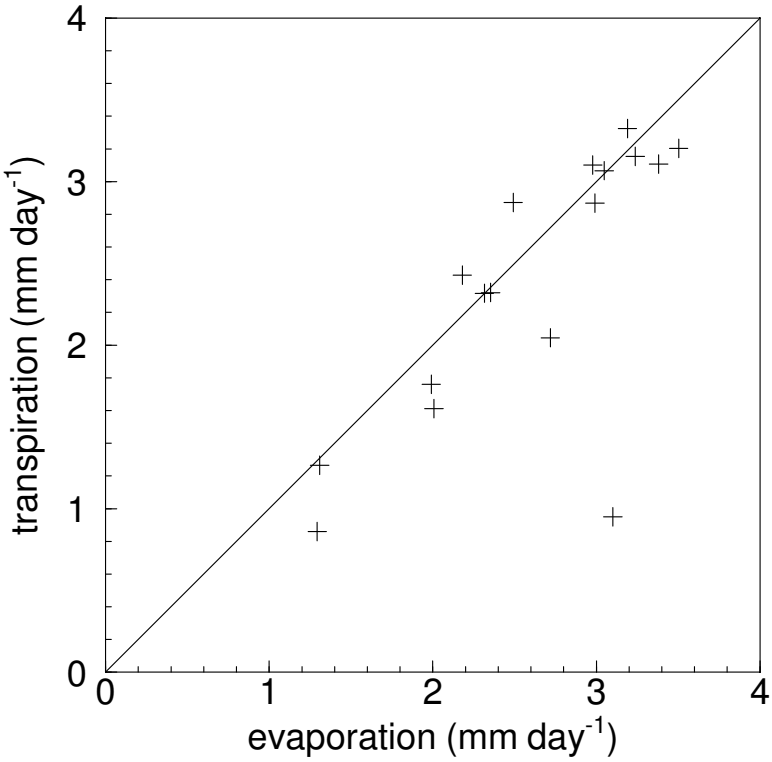

Figure 16 The mean daily transpiration measured by the sap flow gauges through the summer, plotted with the evaporative fluxes (transpiration plus evaporation from the soil) measured by the Solent eddy correlation device.

3.3 Miscanthus and switchgrass

Measurements were made at three locations, Rothamsted, Woburn and Richard's Castle. This was necessary as no single site was suited to the full set of measurements. The grasses at Rothamsted and Woburn are grown in experimental plots whilst at Richard's Castle *Miscanthus* is grown in a field (approximately 300 m long and 75 m wide with the long axis orientated south-south-west) making the scale suitable for eddy correlation measurements

3.3.1 Site descriptions

The soil at the Rothamsted (Ordnance Survey Nat. Grid Ref. 512500 213300) of the energy grass trial plots is a silty clay-loam over clay with flints (Batcombe series). There is no secondary drainage. Topsoil is about 20% clay. The site was in grassland until 1988 and then arable crops until switchgrass was planted in 1998. The average annual rainfall (1971-2000) is 704 mm

The site at Richard's Castle (Ordnance Survey Nat. Grid Ref. 350500 270370) is on soils of the Bromyard series. These are well drained reddish fine silty soils over the silty shales and siltstones of the Raglan Mudstone Formation.

At Woburn (Ordnance Survey Nat. Grid Ref.494800 233200), the soils are Evesham Series; clayey with low permeability subsoil.

3.3.2 Measurements

Regular measurements were made at Rothamsted, through the summer and autumn of 2002, of: the leaf area index of the grasses, the water contents of the soil (using a neutron probe) and the gross rainfall and net rainfall beneath switchgrass, the latter being repeated in 2003. Staff of Rothamsted Research, under a sub-contract, measured the leaf area and took the neutron probe readings. The gross and net rainfall data were collected on site visits by CEH staff and on one occasion stomatal conductance was measured.

During 2003, measurements of stomatal conductance were made on switchgrass at Woburn by CEH staff and soil moisture by Rothamsted Research staff.

Meteorological measurements were made at Richard's Castle using an AWS. Measurements of evaporation were made using a sonic anemometer and of soil moisture using a neutron probe.

3.3.2.1 Weather

An AWS recording incoming solar radiation, net radiation, air temperature and humidity, wind speed and rainfall was mounted on an instrument tower. The AWS was at a height of about 8 m above the ground. The weather variables were logged at 10 s intervals by a Campbell logger (Model CR10, Campbell Scientific Ltd, Loughborough) and hourly averages and sums stored. Measurements began on 10 July 2003 and ended on 6 November of the same year. A summary of the weather recorded by the AWS is given in Table 6.

Table 6 Summary of the weather at Richard's Castle recorded by the automatic weather station. Measurements during the growing season were made between 10 July and 6 November 2003.

variable	minimum	maximum	mean	s.d.	total
solar rad. (MJ m^{-2})					1768.6
air temp. (°C)	-2.2	31.2	13.7	5.6	
humidity deficit (g kg^{-1})	0	18.9	2.8	2.9	
wind speed (m s^{-1})	0	3.0	0.6	0.6	
rainfall (mm)					132.5

3.3.2.2 Leaf and stem areas

For *Miscanthus,* surface areas were calculated from 15 stems cut at random on each occasion. For the first date, 29 May 2002, the projected areas of the stems were measured using a planimeter and the surface areas calculated from the product of π and the planimeter reading. For subsequent dates the stem surface areas were calculated from the product of π, the stem length and the stem diameter at the mid-point.

For the switchgrass, two 50 cm lengths of row were sampled per occasion. The total, green and senesced areas were determined for the stems and leaves of switchgrass. For *Miscanthus*, only the total senesced area was determined.

The results (Figure 17 and 18) show that the leaf area of the grasses follow a similar pattern, increasing until mid-August and thereafter decreasing, whereas the development of the green stem areas differ between the grasses. In *Miscanthus* the green stem area increases until July and thereafter decreases as the stems senesce; whereas in switchgrass the green stem area continues to increase through the summer and does not start to senesce significantly until September (Figure 19).

The total (living and senesced) surface area indices of the grasses are compared in Figure 20 which clearly shows the larger indices attained by the switchgrass. Unlike the *Miscanthus* which peaks in August, the total surface area of the switchgrass continues to increase until the end of the summer.

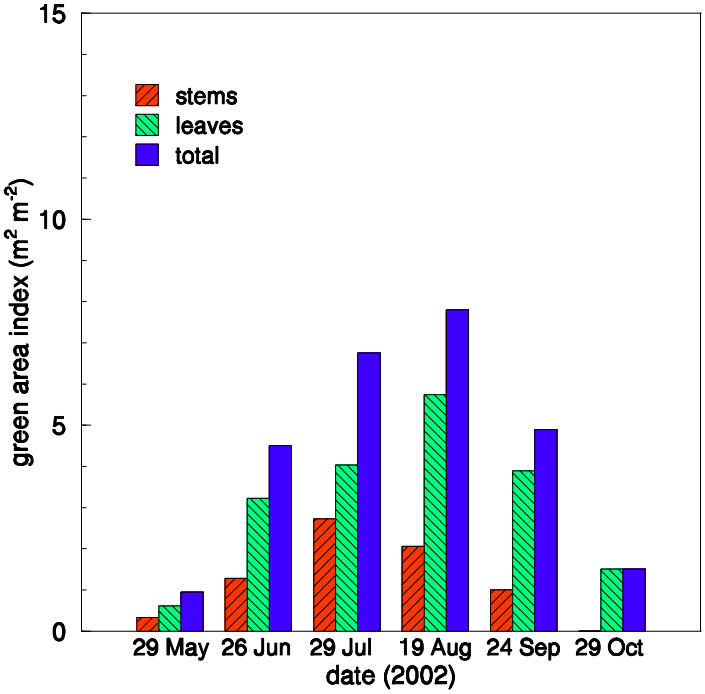

Figure 17 The variation through the summer of the green area index for leaves, stems and total surfaces for Miscanthus

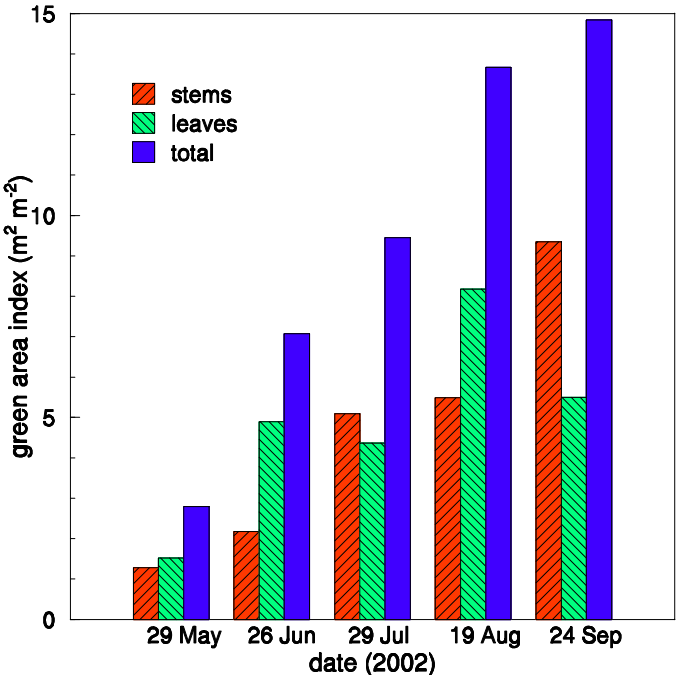

Figure 18 The variation through the summer of the green area index for leaves, stems and total surfaces for switchgrass

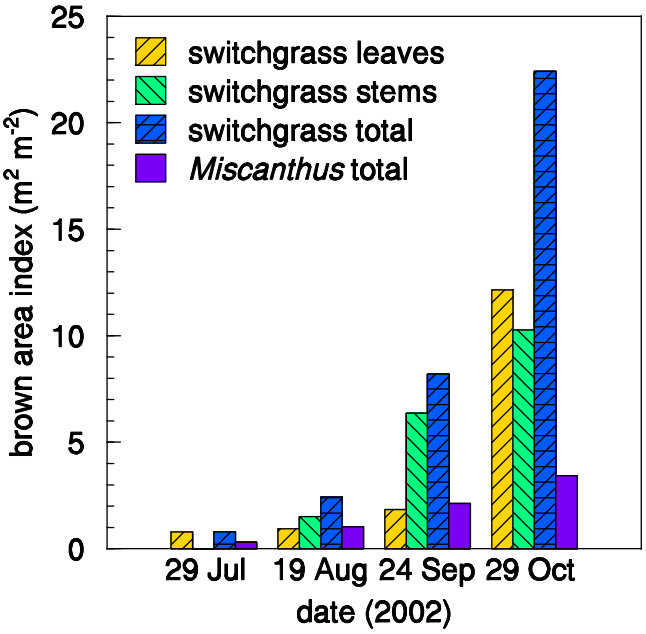

Figure 19 The variation through the summer of the brown (senesced) area index for leaves, stems and total surfaces for switchgrass and total surfaces only for Miscanthus

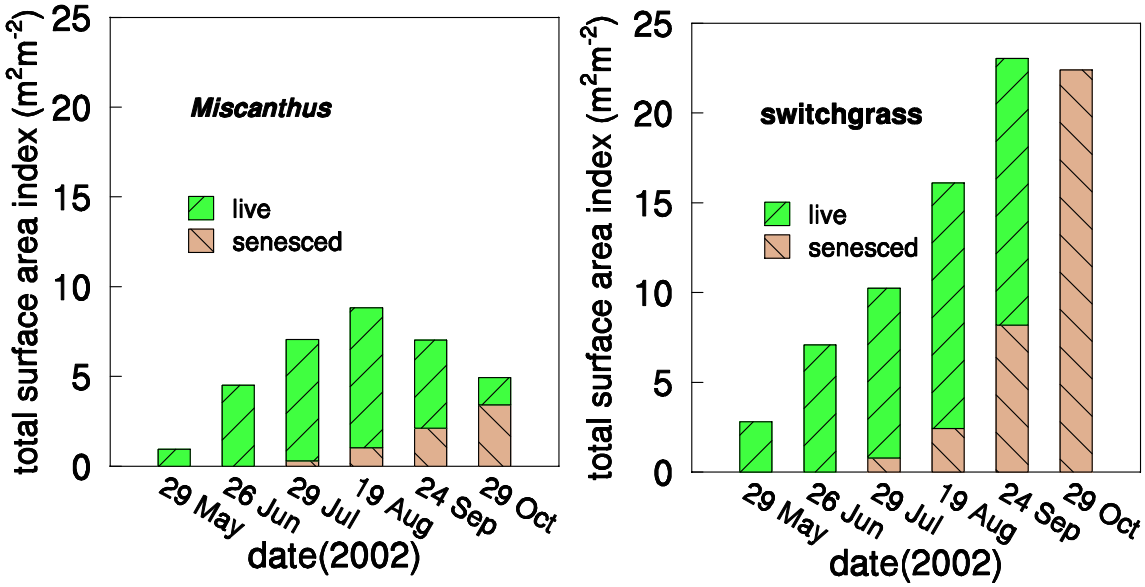

Figure 20 The total surface area index of Miscanthus and switchgrass through the summer

3.3.2.3 Interception loss

Interception loss, that portion of the precipitation that is intercepted by plants and evaporated directly back into the atmosphere without ever reaching the soil, is measured as the difference between the gross precipitation minus the precipitation collected beneath the vegetation.

At Rothamsted, during 2002, we designed and installed a gauge to collect the throughfall within one of the switchgrass plots. The final design, (see Figure 21), consisted of a main spur and eight branches made from standard 100 mm plastic guttering. The gauge occupied one half of the switchgrass plot and did not

prevent access being gained to either the soil moisture access tube or the soil water suction samplers. In addition to this gauge, two gauges in the form of funnels sealed with silicone sealant around the stems were installed in early July, on stems within the plot to sample that portion of the rainfall that flowed down the stems. One gauge enclosed four stems, the other enclosed eight. Installation of further stem-flow gauges had been planned but was prevented by the time taken on other adjustments needed to the throughfall gauge (see below). Rainfall was also recorded at the site automatically using a tipping bucket (0.1 mm per tip) raingauge logged with a miniature solid-state logger (TinyTag), with a 55-day capacity

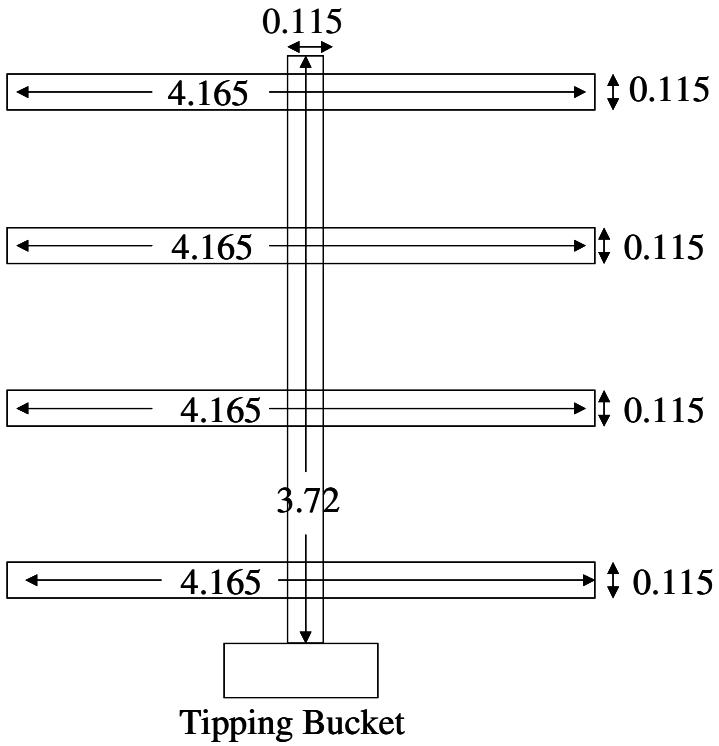

Figure 21 Schematic diagram of the through fall gauge in the switchgrass plot, during 2002. All dimensions are in metres.

The original gauge, constructed on 20 June 2002, had only four spurs making the operational area 2.34 m^2. However, to improve the accuracy of the through fall measurements four additional spurs were added on 27 June 2002 giving the through fall gauge a total area of 4.26 m^2. The guttering was held in place by brackets fixed to a supporting wooden frame. The main spur and the eight branches were constructed with a 5% slope. The slope would ensure that all water collected would be moved easily and quickly to the outlet where, the measuring device, a large tipping bucket flowmeter was located. The flowmeter was positioned at the edge of the plot so that the movement of the bucket would not be compromised by the switchgrass as it was either moved around by the wind or became lodged as a result of rain events bending and or breaking the stems.

The flow meter was calibrated dynamically and had an effective bucket volume of 1.291 litres. The calibration factor (mm per tip) for the through fall gauge was calculated from the bucket volume divided by the area and gave a value of 0.301 mm per tip. The pulses from a magnetically operated reed switch, closed on each tip of the bucket, were recorded at 5-minute intervals on an identical logger to that used with the raingauge.

With such a level site it was decided that the flow meter would be placed directly onto the ground rather than in a hole so that no drainage ditches would be needed and the water from the gauge would easily disperse over the surface. It was wrongly believed that the switchgrass would reach a height of 1.75 m and that the through fall gauge would be wholly contained within the crop and would not be exposed. However, Plate 2 shows that this was not the case.

Plate 2 One branch of the through fall gauge exposed in the switchgrass.

On 14 August we lowered the main spur and the eight branches of the gauge by approximately 35 cm. Care was taken during this process to minimise any damage to the switchgrass although inevitably some stems were damaged. Lowering the gauge also required that the tipping bucket flow meter was placed in a hole. The gradient of the site made it impracticable to provide drainage ditches to remove the water that had passed through the tipping bucket. Drainage would have to take place through the bottom of the hole that the bucket was placed in. To protect the tipping bucket from switchgrass that may lodge against it a protective shelter was built in late August 2002 (see Plate 3).

Plate 3 The protective screen built around the tipping bucket flow meter to prevent the switchgrass lodging against it.

After periods of heavy or prolonged rainfall the soil in the bottom of the hole became saturated and drainage was impaired. On occasions the hole filled with water impairing the action of the tipping bucket, reducing the number of recorded tips and erroneously indicating reduced net rainfall. Allowance has been made for this in the analysis of the data. Assuming that there was no drainage it is simple to calculate the

amount of rainfall that would cause the water to touch the tipping bucket, based on the area of the hole. By discarding any data collected, after this depth of rain (about 10 mm) has fallen during any one storm, we can allow for this flooding of the gauge; but of course at the cost of lost data.

During 2003 we designed a new system for measuring the interception losses of the switchgrass. This consisted of measuring the throughfall with two troughs feeding into tipping bucket raingauges (Plate 3), two sets of stemflow measurements also feeding into tipping bucket raingauges (plate 4), and a separate tipping bucket raingauge, outside the area of the plots, to measure the gross rainfall. All the raingauges were data logged using TinyTag single channel data loggers, which accumulated the number of tips per 5 minute interval. The two stem flow measurements consisted of 10 stems each. Each stem was surrounded by a small funnel, with the stem sealed so as to ensure no leakage. The outlets from the funnels were fed into a raingauge. The troughs, which were 0.115 m across, were elevated above the ground on metal supports and were at a height of 0.55 m at the end feeding into the raingauge and 0.75 m at the other, Figure 22.

Plate 4 The throughfall measurement system used on switchgrass at Rothamsted during 2003

Plate 5 The stemflow measurement system used on switchgrass at Rothamsted during 2003

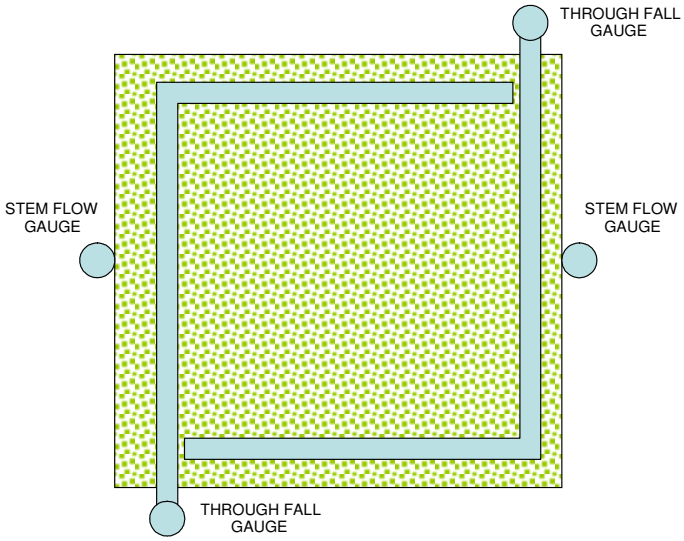

Figure 22 Schematic diagram of the interception measurements system used in a switchgrass plot at Rothamsted during 2003

3.3.2.4 Soil water

Soil moisture observations have been a part of the environmental measurement programme with respect to the energy crops at Rothamsted for a number of years. Soil moisture measurements can be used to determine the water use of a vegetation type if the lowest reading depth is beyond the rooting zone of the crop under investigation. They can also be used to determine if there are any differences between different vegetation types. For the 2002 measurement programme five tubes in each grass were chosen, tubes 8, 17, 27, 28 and 36 in the switchgrass tubes 2, 3, 4, 8 and 9 in the *Miscanthus*; see Figure 23 and Figure 24 for the location of the tubes and the dimensions of the plots.

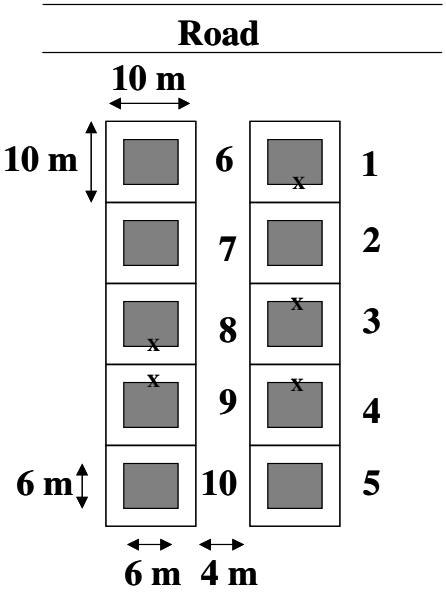

Figure 23 Schematic map of the *Miscanthus* plots showing the dimensions of the plots and the locations of the soil moisture access tubes (marked with an X)

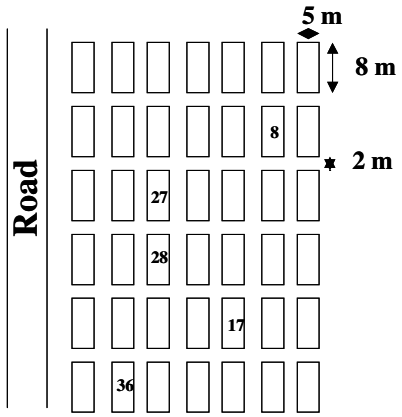

Figure 24 Schematic map of the switchgrass plots showing the dimensions of the plots and the locations of the individual soil moisture access tubes (marked with an X)

The first measurements were made on 26th April 2002 and continued, on an approximately fortnightly basis, until 7th November 2002. The reading protocol for each tube was that the first reading was made at

10 cm below the ground surface then at intervals of 10 cm to the bottom of the tube. Initially all ten tubes were read to 90 cm below the ground. However, it was clear from subsequent reading dates that the tubes were not deep enough to encompass the entire rooting zone as changes in the water content at the lowest reading depth could be seen. Consequently on 29 May two tubes, one in each species, were installed so that readings could be made down to 260 cm below the ground. To compensate for the deeper tubes it was agreed to stop taking readings in two of the tubes in each plot. Overall, however, the number of readings to be taken remained approximately the same.

During 2003, four neutron probe access tubes were installed in experimental plots at the Woburn field site. Two of the tubes were placed in plots of *Miscanthus*, one to a depth of 2.8 m and the other to 2.9 m, and two in plots of switchgrass, to a depth of 2.9 m. Readings began on 31st March 2003 and finished on 9th October 2003 and were taken at approximately fortnightly intervals by Rothamsted Research staff. The procedures used were identical to those used in 2002 at the Rothamsted site.

At Richard's Castle, a single neutron probe access tube was used. This was installed to a depth of 1.2 m. It was not possible to drive the access tube into the ground to a greater depth because bedrock had been encountered, which was confirmed by the soil samples recovered during the installation process. Readings began on 9th June 2003 and ceased on 17th November 2003 and were taken at intervals of around two weeks. The procedures used were the same as at the Woburn and Rothamsted sites.

Data were processed, at CEH Wallingford, using a Windows based processing system called SWIPS (**S**oil **W**ater **I**nformation **P**rocessing **S**ystem). SWIPS requires information, for each tube and each measurement depth within that tube, on the soil characteristics. It then converts the raw data into water content for each depth. Each depth is then multiplied by an appropriate layer factor to convert the water content value into mm of water for that particular depth. All the depths are then summed to obtain the total profile water content for that particular tube.

3.3.2.5 Stomatal conductance

Because of the problems with the porometer (see Section 3.2.2.4) we were only able to take readings on one occasion (18 September) on switchgrass during 2002. The strategy was to take readings at three levels within the canopy; the top, middle and the bottom, and to take those readings from a number of representative stems scattered throughout a switchgrass plot. The first set of measurements were made at 1100 GMT and was from 7 stems, the second set of measurements were made at 1300 GMT and was from 8 stems whilst the third run was made at 1500 GMT and was also from 8 stems. Stomata were found on both surfaces of the leaves and so those values have been summed to give a total leaf stomatal conductance. As expected the stomatal conductances decrease with depth into the canopy (Figure 25), reflecting the response of the stomata to the decreasing light levels that are found, as shading of the leaves increases.

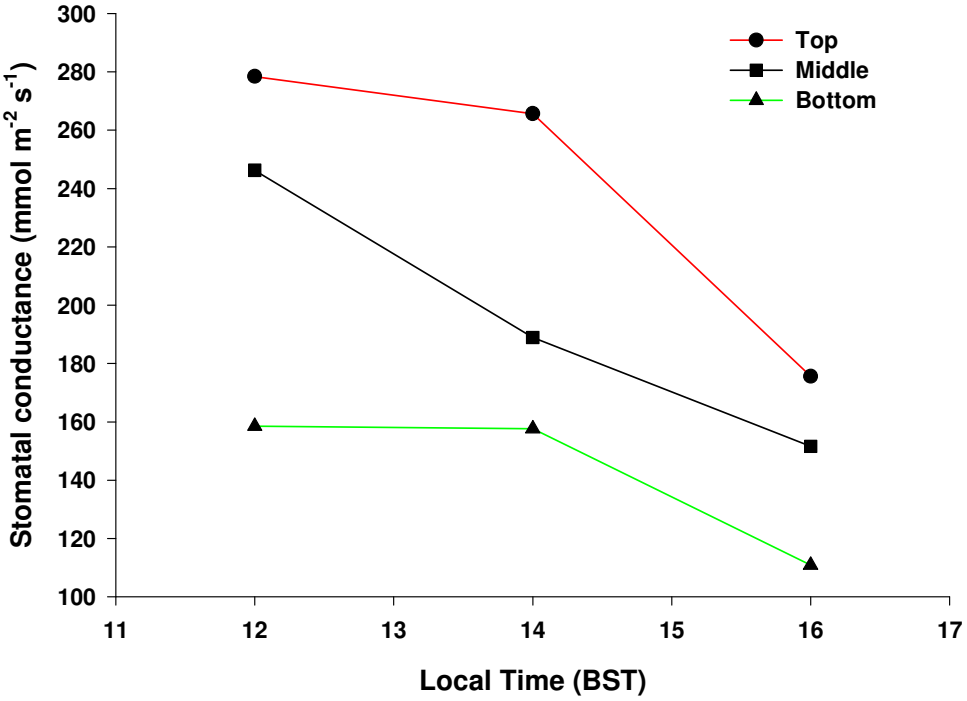

Figure 25 Variation in the leaf stomatal conductance for three layers in the switchgrass at Rothamsted during 2002.

During 2003, measurements were also made, but at a site near Woburn, on three days representing a range of conditions in terms of the atmospheric demand. The measurement procedure was identical to that used in 2002, except that no measurements were made on the lower leaves. As was found in 2002, the stomatal conductances of the middle leaves were less than those of the upper leaves, Figure 26.

3.3.2.6 Energy fluxes

Direct measurements were made of the sensible heat flux from *Miscanthus* at Richard's Castle using an eddy correlation device (Solent R2A). The Solent was installed on the instrument tower at a height of 8.5 m above the ground, Plate 6. (The height of the top of the canopy, at maximum development, was about 2.3 m.) Data from the Solent were collected and stored on a Campbell 21X logger. Two net radiometers, in addition to the AWS net radiometer, fixed to the end of booms projecting from the top of the tower provided measurements of the net radiation. These and two soil heat flux plates detecting the soil heat flux were logged by a separate Campbell CR10 logger which recorded hourly averages.

The Solent measures the fluctuations in the air temperature and the vertical component of the wind speed, and from their product determines the net flux of sensible heat. This is used in conjunction with the measured net radiation and soil heat flux to allow the latent heat flux (evaporation) to be determined from the energy balance.

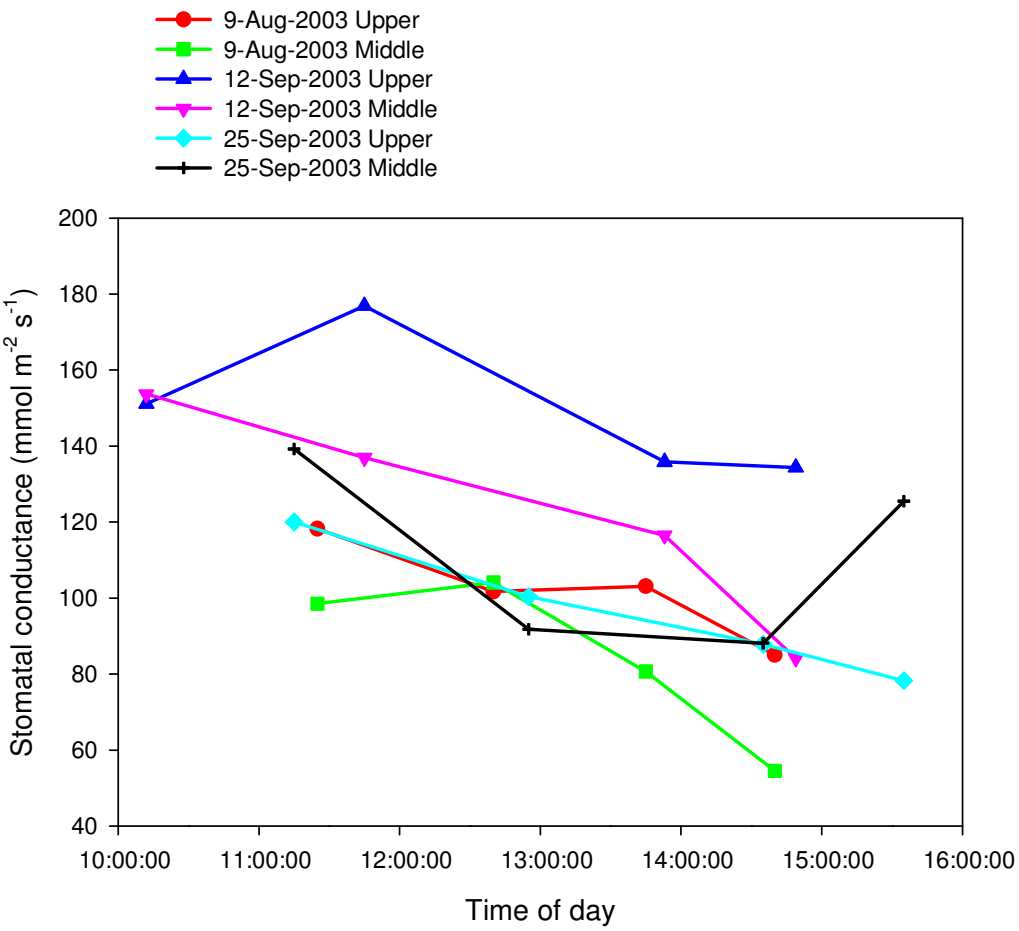

Figure 26 Stomatal conductances measured on switchgrass at Woburn during 2003

The evaporative fluxes measured by the device are the sum of the transpiration from any vegetation and evaporation from bare soil or any other wet surfaces (e.g. water bodies or wet roads). The sensors on the Solent are affected by the air passing by them so that the heat fluxes are those from the surface upwind of the device. The area of the surface, or footprint, changes according to the mean horizontal wind speed and atmospheric stability. So that the area is representative of the crop for as much time as possible, it is necessary to place the Solent so that the upwind distance or 'fetch' over the crop is as large as possible in the direction of the prevailing wind. To achieve this, the tower on which we installed the Solent was erected at the north-eastern corner of field, in the expectation that the prevailing winds would be from the south-west. This ensured that there was a fetch of at least 200 m over the *Miscanthus*.

Measurements began in mid August, when the canopy was fully developed, and continued throughout the summer, albeit with some data loss through battery failure.

Plate 6 The flux tower amongst the *Miscanthus* at Richard's Castle

3.3.3 Analysis and interpretation of the results

3.3.3.1 Interception loss in switchgrass

The stem flow measured by the two gauges indicated that stem flow is a very small component of the net rainfall. At the Rothamsted site, the stem flow recorded between July and October 2002 inclusive was always less than about 1% of the gross rainfall and so may be neglected without any significant loss of accuracy. The cumulative gross and net rainfall, with data ignored from storms exceeding 10 mm, are shown in Figure 27 and indicate that the interception loss (gross - net rainfall) over this period, was very high at 54% of the gross rainfall.

For modelling interception loss it is possible to use a simple regression relationship between gross (P), and net rainfall (N). Such a relationship has been derived from a plot of storm N against P (Figure 28a), where a storm is defined as a period of rain followed by at least three hours without rain, for the same data used

in Figure 27. The regression relationship is, $N = 0.507P - 0.114$ ($r^2 = 0.9556$). For more sophisticated modelling of the interception loss, such as that included in the MOSES model, it is necessary to derive a value for the canopy capacity, the amount of water retained by a saturated canopy. This can also be estimated by plotting the net rainfall against the gross rainfall, but using only data from storms that occurred when the grass canopy was at first dry. To select such storms from the data set, somewhat arbitrary criteria were used, viz. if the storm started between 1200 h and 1800 h GMT and was preceded by 8 hours without rain or for storms starting at any other times they were preceded by 20 hours without rain. The canopy capacity is then given by the absolute value of the intercept of a line that has near-unity slope plotted through the points of maximum net rainfall. For our data, once the storm selection criteria are applied there are only three relevant points (circled in Figure 28b) and the canopy capacity is 2 ± 1 mm. This figure is consistent with other vegetation capacity values, but less than would be expected from the very high interception loss indicated by the cumulative figures.

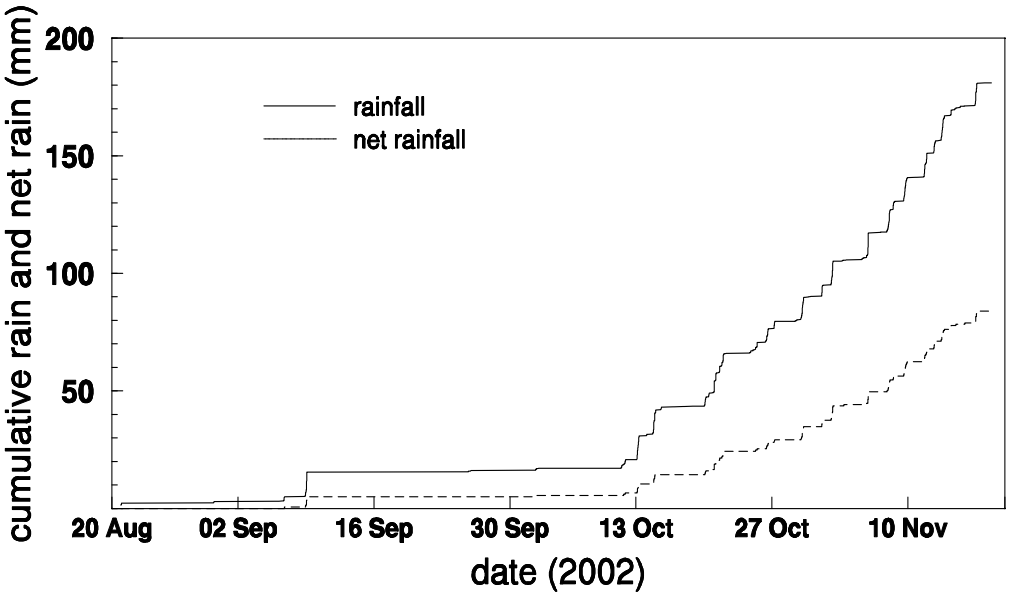

Figure 27 The cumulative gross and net rainfall beneath switchgrass recorded at the Rothamsted trials site, 2002

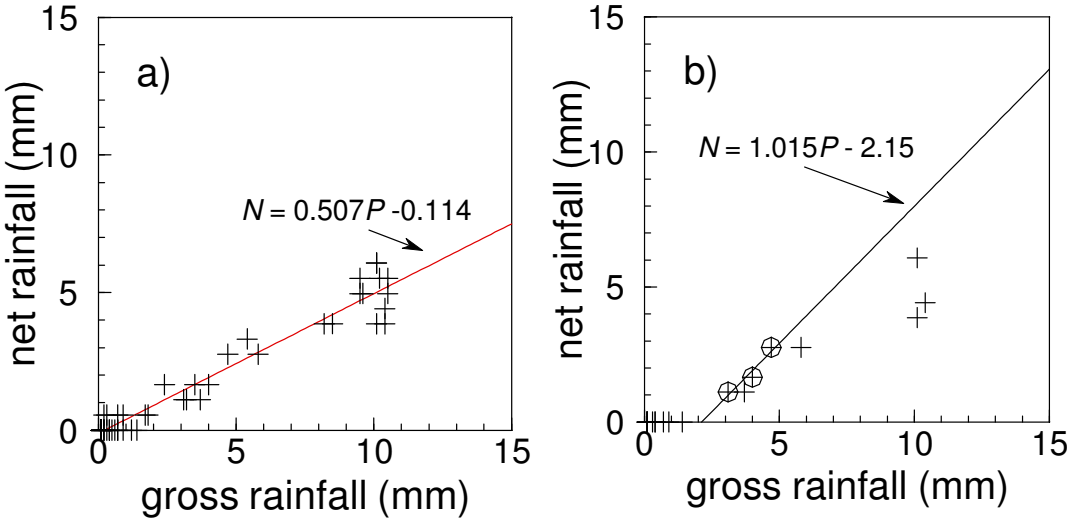

Figure 28 The relationship between storm gross and net rainfall beneath switchgrass measured at the Rothamsted trial site during the autumn of 2002. In a) all the storm data plotted in Figure 31 are shown and the equation of the regression line. In b) only those data are shown that conform to the criteria for a dry canopy at the start of the storms.

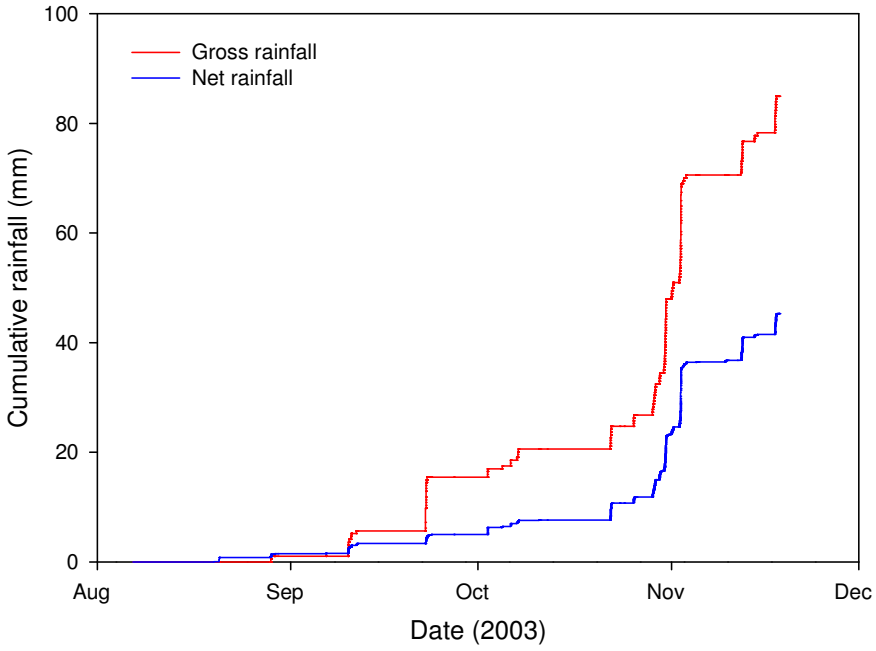

Figure 29 Cumulative gross and net rainfall beneath switchgrass measured at Rothamsted , 2003

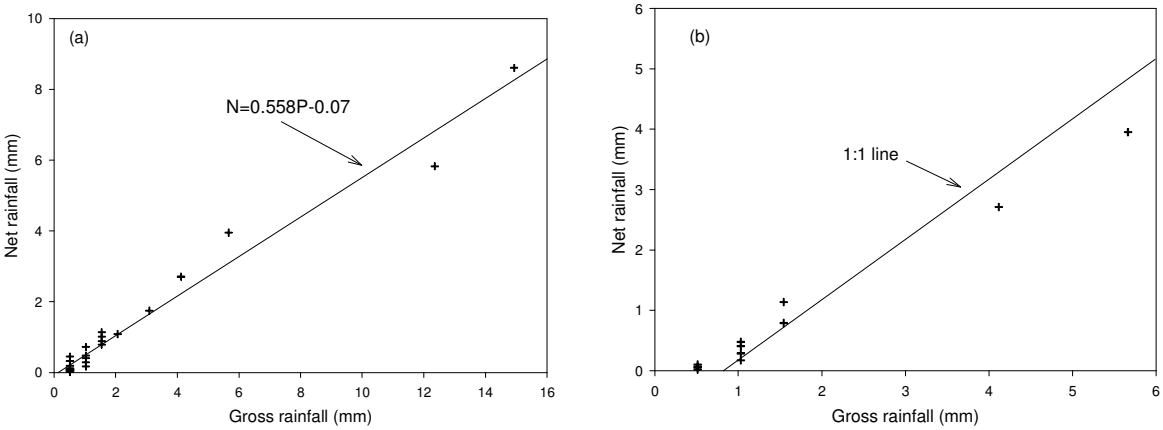

Figure 30 The relationship between storm gross and net rainfall beneath switchgrass measured at the Rothamsted trial site during the autumn of 2003. In a) all the storm data are plotted and the equation of the regression line. In b) only those data are shown that conform to the criteria for a dry canopy at the start of the storms.

The analysis of the data obtained in 2003 shows similar results. The stem flow measured was again negligible. The cumulative gross and net rainfall, Figure 29, show that interception losses were high and accounted for 47% of the gross rainfall.

A simple regression analysis between the storm gross and net rainfall gives a linear relationship N = 0.588P-0.070 (r^2=0.973), Figure 30. The coefficients of this relationship are very similar to those obtained for the data obtained in the previous year, suggesting that there is no significant difference in the measurements made despite using different measurements systems.

The canopy storage capacity was estimated using the same technique described above. Twelve events fulfilled the selection criteria, Figure 30 (b). The resulting estimate of the canopy capacity is 0.8 mm. This is based on 12 data points and so must be taken as a more reliable value than was obtained from the measurements made in 2002. However, it would appear to be towards the low range of values reported in the literature. Ward and Robinson (1999) give values, for a variety of vegetation types, which tend to be between 1 and 2 mm.

3.3.3.2 Soil water

Figure 31 shows all the soil water content profiles obtained, during 2002 at Rothamsted, from a tube in the Switchgrass. It can be clearly seen that most of the changes in the water content took place within the top 1 m. The water content at 0.1 m below the soil surface varies from 0.18 to nearly 0.45 whilst at 1 m it varies from 0.48 to 0.56. Below a depth of 1.3 m, changes in response to evaporative losses are not present.

Figure 32 shows the same information, but from one of the tubes in Miscanthus. A similar pattern is apparent, with the greatest changes in soil water content being near the surface, with a tendency to decrease with depth. However, changes in soil water content can be recognised down to a depth of 1.7 m. This is interpreted as the *Miscanthu*s having a greater rooting depth than the switchgrass.

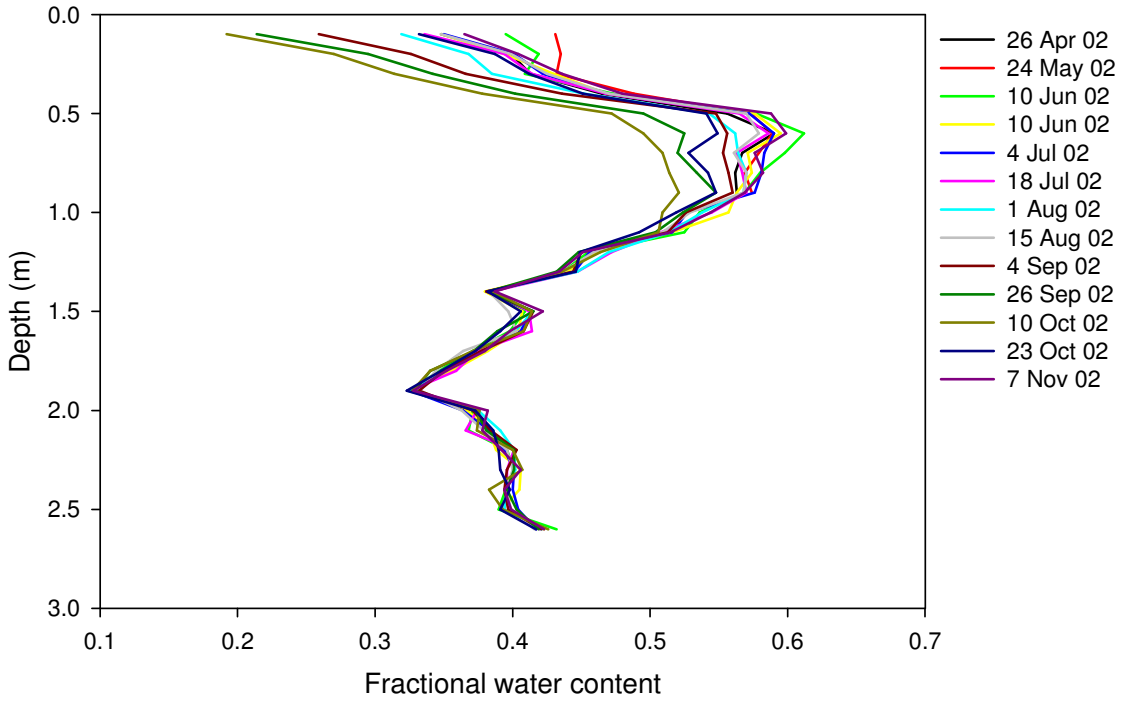

Figure 31 Profiles of the water content with depth for all the measurement dates for tube 28 in the Switchgrass at Rothamsted during 2002

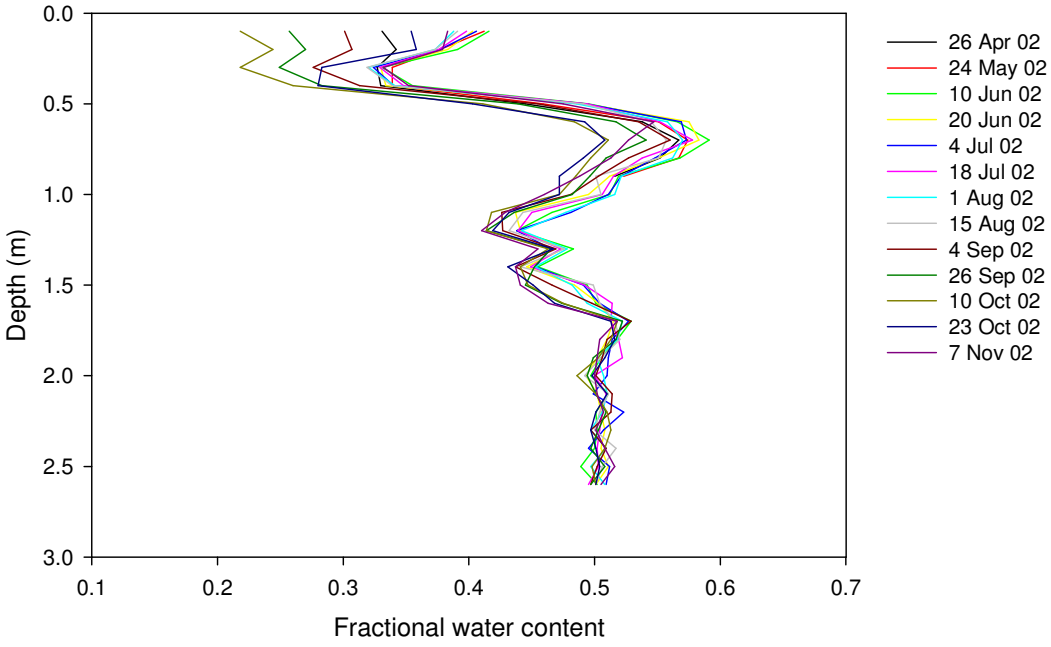

Figure 32 Profile of the water content with depth for all the measurement dates for a tube in the *Miscanthus* at Rothamsted during 2002

The effect of the greater rooting depth is evident when the changes in the total profile water content beneath the two types of grass are compared, Figure 33. The decrease in the soil water content tends to be faster beneath the *Miscanthus*, indicating a higher rate of evaporation. More rainfall is required to replenish the depleted soil water store beneath the *Miscanthus* and so, when readings ceased, the water contents still had not returned to those obtained when measurements began. In comparison, the switchgrass had essentially returned to those when measurements began. However, it is unlikely that the soil had returned to field capacity as, when measurements of the full profile began, it is probable that soil moisture deficits already existed.

Measurements made at Woburn during 2003 show similar features except where the depths from which water is extracted are concerned. The measured profiles beneath *Miscanthus* show changes down to a depth of around 1.7 m, Figure 34, whilst those below the switchgrass extend down to around 1.9 m, Figure 35. These apparent differences from the results obtained at Rothamsted probably reflect the different water contents in the two plots at Woburn. There appears to be a very porous layer between 1.1 and 1.7 m beneath the *Miscanthus*. This layer is absent beneath the switchgrass, whose roots have to penetrate deeper in order to obtain the water required. When the changes in the total profile water content beneath the two types of grasses are compared, Figure 36, it is clear that the Miscanthus is extracting more water than the switchgrass, albeit only slightly (5 mm). However, the profile shows a greater rate of change beneath the *Miscanthus* during June and July, indicating a higher rate of evaporation, as was observed in 2002. Given that the second half of the summer of 2003 was notable for the lack of rainfall, it is possible that the maximum deficits may reflect that the soils beneath the two types of grasses had similar available water contents.

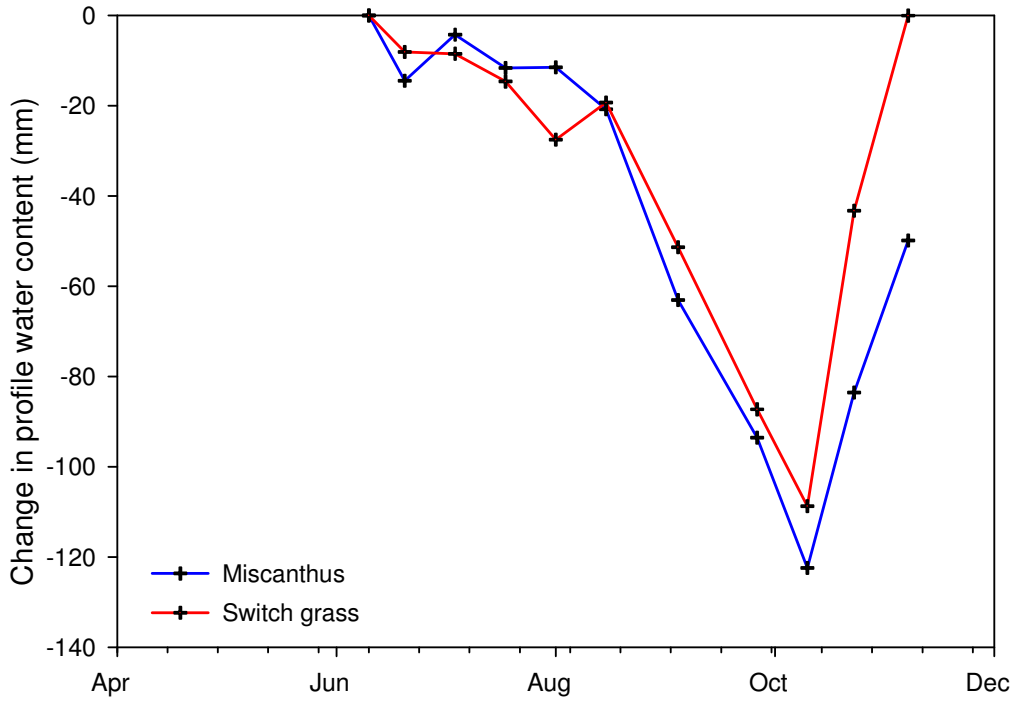

Figure 33 Time series of the departures from the wettest total profile water content for one tube in each of the Switchgrass and the *Miscanthus* at Rothamsted during 2002

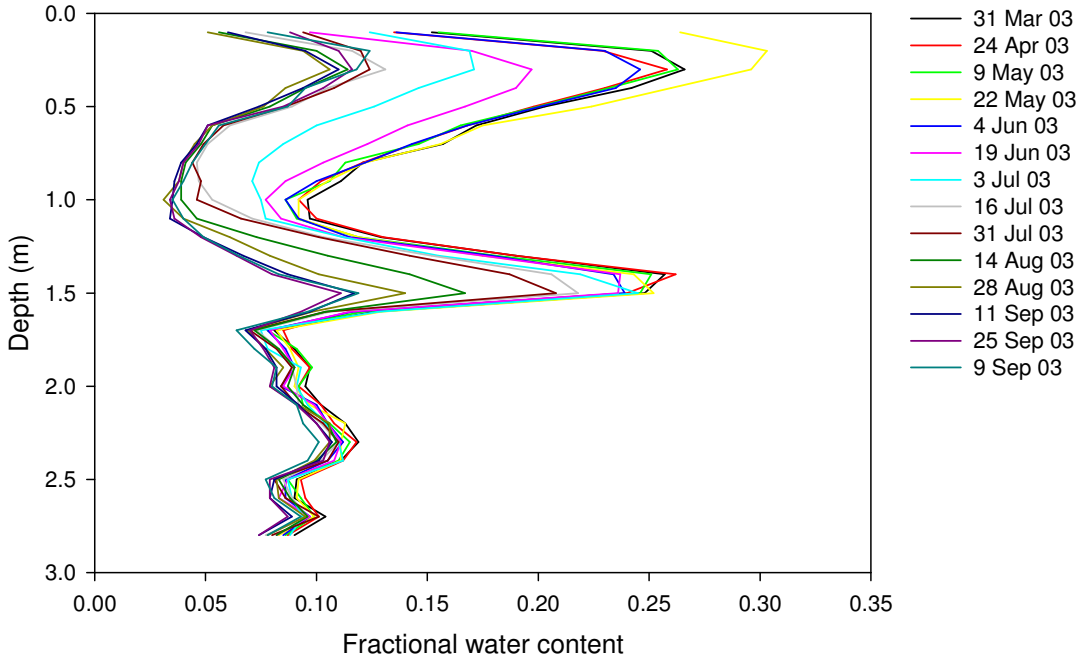

Figure 34 Profile of the water content with depth for all the measurement dates for a tube in the Miscanthus at Woburn during 2003

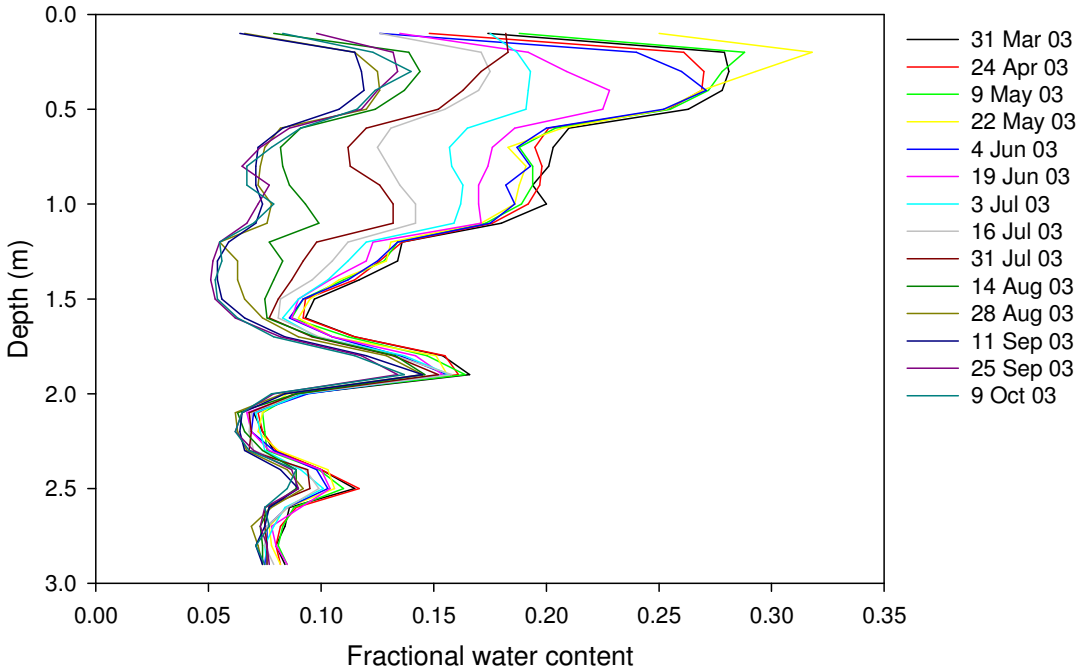

Figure 35 Profile of the water content with depth for all the measurement dates for a tube in the switchgrass at Woburn during 2003

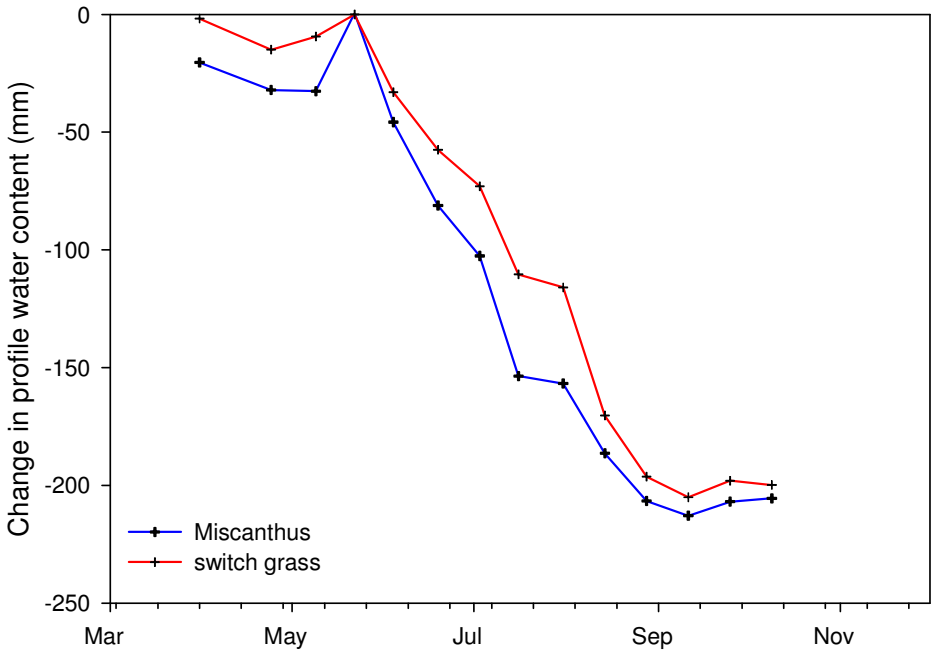

Figure 36 Time series of the departures from the wettest total profile water content for one tube in each of the Switchgrass and the Miscanthus at Woburn during 2003.

The hydraulic properties of the soil at Richard's Castle appear to be relatively uniform as there are no major changes in the soil water content with depth, observed in the earliest reading, when it is reasonable to assume that the soil is at or near field capacity, Figure 37. The soil water content profiles show a progressive drying out, increasing with depth through the summer. From mid-August, the water content at 1.2 m decreases, indicating that water is being extracted for evaporation from the soil deeper than the bottom of the access tube. Thus, the total change in water content was not observed. If the same rooting depth as was observed at Rothamsted and Woburn is assumed, then the measured soil water profile accounts for 87% of the maximum soil water deficit.

By the time that the measurements ceased, in mid-November, the soil water profile had still not returned to its initial conditions. This is particularly clear in the time series of the total soil water content, Figure 38. The soil water store was already being depleted when measurements began. High evaporation rates are implied by the rapid reduction in the soil water content through June, July and August. This period coincides with the maximum rate of growth of the *Miscanthus*. The small changes during September and October are deceptive because it was probably during this period that the *Miscanthus* was exploiting the water in soils beneath the access tube. The severity of the lack of the rainfall during the summer is clearly reflected in the time series as the soil water content during 2003 did not begin to recover until the end of October and, by mid-November had still not recovered to the levels recorded in June.

3.3.3.3 Evaporative fluxes measured with eddy correlation

An analysis of the wind directions recorded by the automatic weather station showed a pronounced mode at about 200° which coincides with the alignment of the long axis of the field, Figure 39. On this basis, only flux measurements obtained when the wind was in this direction have been included in the analysis. Unfortunately, this substantially reduces the number of observations available.

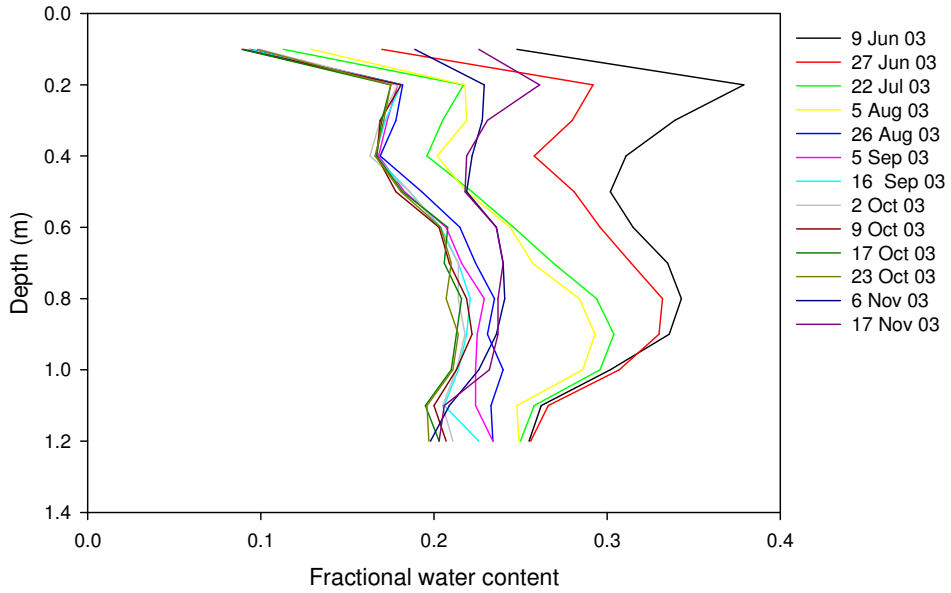

Figure 37 Soil water content profiles measured at Richard's Castle during 2003

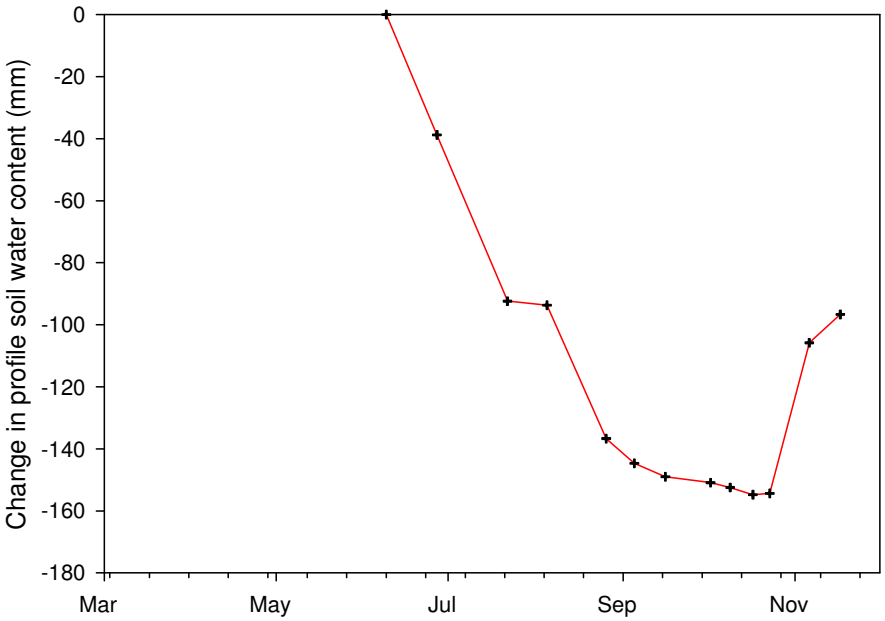

Figure 38 Total profile soil water content measured at Richard's Castle during 2003

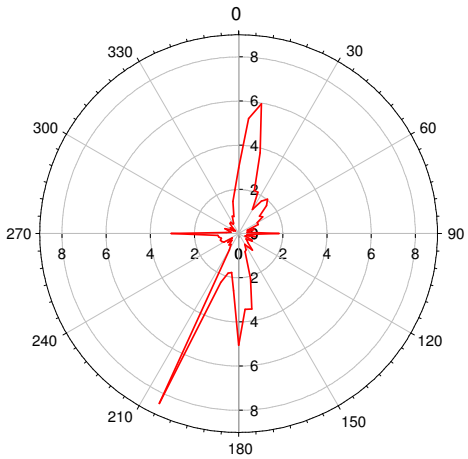

Figure 39 Wind directions observed at Richard's Castle

The measured energy fluxes, obtained from over the *Miscanthus*, show the decline in the net radiation from August to October, Figure 40; resulting from the reduction in the downward solar radiation due to the change in the solar declination angle. During August, the observations show the sensible heat flux exceeds the latent heat flux. This is illustrated more clearly if the evaporative ratio (the ratio of the latent heat flux to the net radiation) is plotted, Figure 41. There are two aspects to the variations in the evaporative ratio with time. The first is a diurnal fluctuation that is due to the stomata openings reducing in response to the atmospheric demand. The second is a long term change, due to the limited availability of soil water in August, that also causes the stomatal openings to be reduced.

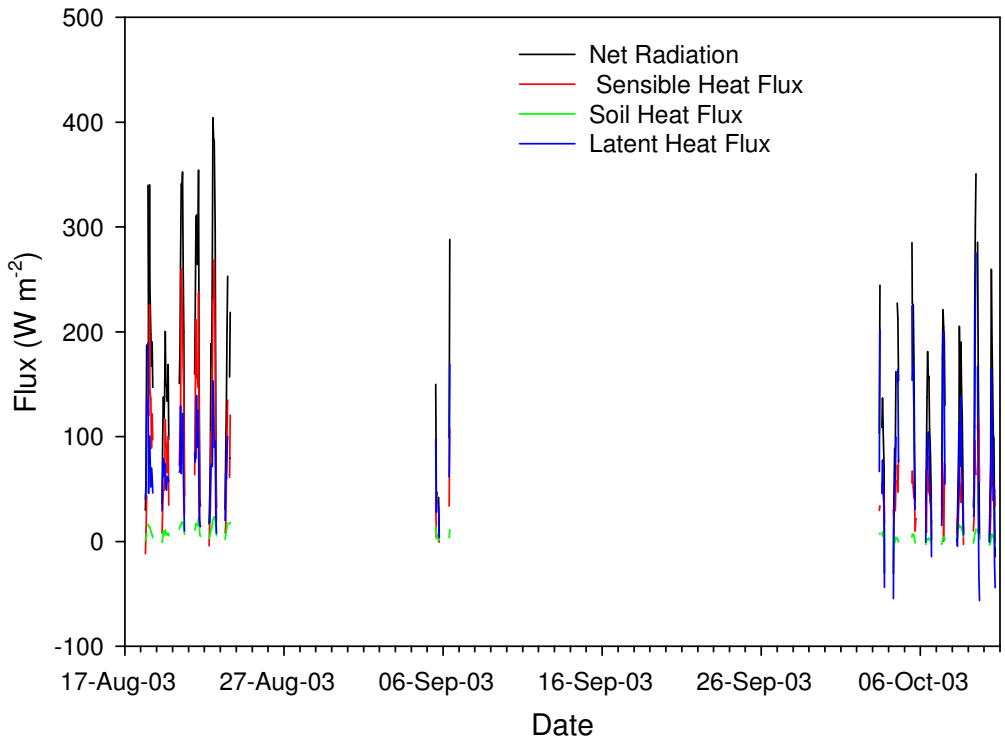

Figure 40 Fluxes measured over *Miscanthus* during daylight hours

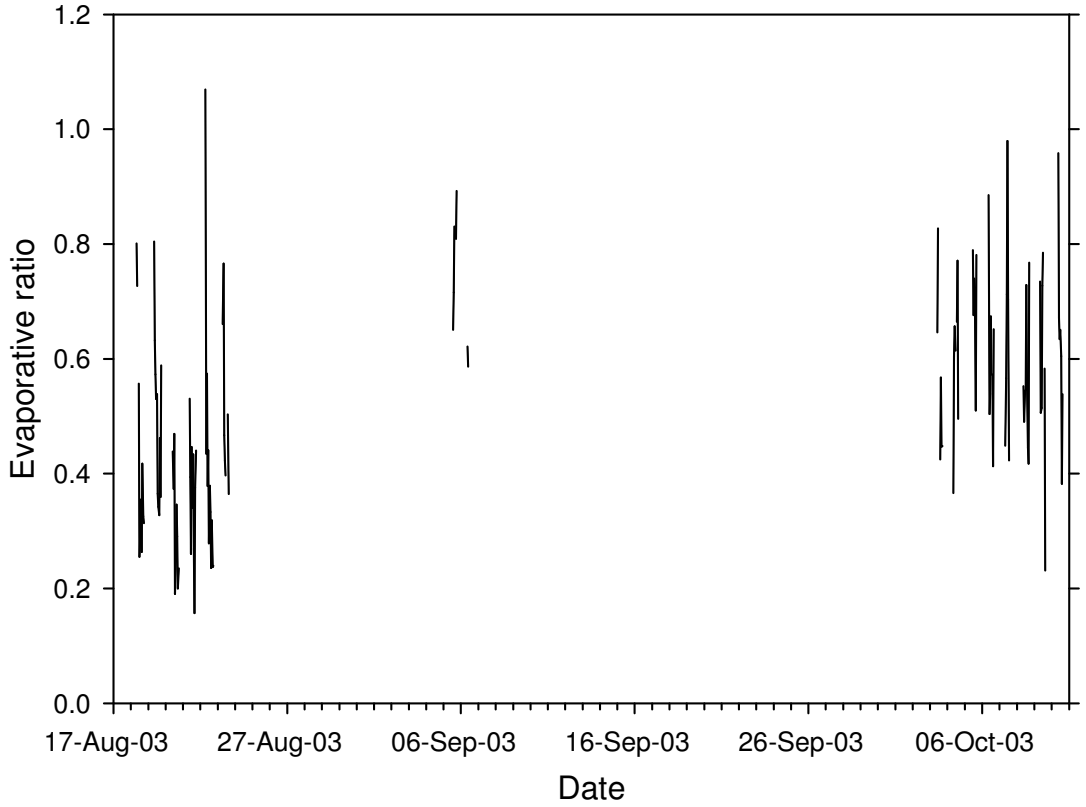

Figure 41 Evaporative ratio observed over *Miscanthus* during daylight hours

3.3.3.4 Stomatal conductance

The measurements of stomatal conductance have been used to calibrate the model of stomatal conductance used in the MOSES model. This sub-model is described by Harding *et al.* (2000) and relates the stomatal conductance, g_s, to the net photosynthesis (which contains an explicit dependence upon the soil water content), a_n, and the humidity deficit at the leaf surface, D_s.

$$g_s = \left(\frac{1.6}{1-F_0}\right)\frac{a_n}{(c_s - c_*)\left[1+\left(D_s/D_*\right)\left(F_0/(1-F_0)\right)\right]}$$

where c_s is the CO_2 concentration in the leaf surface and c_* is the CO_2 concentration at the photorespiration compensation point. F_0 and D_* are empirical factors. The net photosynthesis is calculated as:

$$a_n = \beta(1-\omega)0.5K^{\downarrow}$$

The factor of 0.5 is the proportion of the downward global solar radiation, $K^{\downarrow}$, that is in the photosynthetically active portion of the spectrum. The value of the reflection coefficient for the photosynthetically active radiation, ω, is taken as 0.17 for C_4 grasses. The value of the soil water stress function, β, ranges from 1, when the soil water content is greater than the critical soil water content, to 0, when it is at the soil water content at wilting point.

The soil water stress factor was estimated from the measured soil water contents, over the rooting depth, and the values of the soil water content at the critical and wilting points that had previously determined by Rothamsted Research staff for the experimental site. This allowed the empirical factors, F_0 and D_*, to be calibrated against the measured stomatal conductances, using the meteorological data from an automatic weather station maintained at Woburn by Rothamsted Research. The analysis gave values of 0.8 and 0.075 for F_0 and D_* respectively.

4. Numerical modelling

A numerical model has been used to predict the water use of the existing land cover and the four potential energy crops across England and Wales. In addition the biomass (which has been used to estimate the indicative yield) of the different crops has also been predicted using this model. The basis of the numerical model is the Met. Office Surface Energy Scheme (MOSES). This model was selected because it is physically based and provides a comprehensive land surface model describing the exchanges of energy, water and carbon at the land surface. The land surface of England and Wales has been represented as a series of 1 km^2 cells with the MOSES being run for each cell (ca 150000 cells). The choice of the size of the grid cells was a pragmatic decision taking into account factors such as: computational time, data availability, representation of the variability in the land surface and the meteorology.

The data requirements of MOSES fall into two categories: the driving data and the parameter values. The driving data are a continuous time series of meteorological variables: rainfall, downward solar and long-wave (thermal) radiation, wind speed, air temperature and humidity. The parameter values describe the characteristics of the specific soil and vegetation and do not vary with time.

The model has been run to predict outputs for three rainfall scenarios: typical, wet and dry years.

4.1 The MOSES model

Full descriptions of the model are given by Essery et al. (2001) and Cox (2001); both reports are available from http://www.met-office.gov.uk/research/hadleycentre/pubs/HCTN/. Only a brief resume of the model will be given here.

Transpiration is based upon a surface energy partition equation; splitting the available radiation into evaporative (latent heat) flux, sensible heat flux and soil heat flux. This equation is essentially an extended version of the Penman-Monteith equation (Monteith, 1965). Soil water movement is simulated using a four layer model, with vertical transfers described by the Richard's equation. For a given soil, the relationships between hydraulic conductivity, soil water content and soil water potential are those of Brooks and Corey (1964). Transpiration is not limited by the soil water content so long as the average amount in the root zone is above a critical value (that at a sol water potential 0f -33 kPa). As the soil water content diminishes, the transpiration rate is reduced until it ceases at a soil water content for a soil water potential of -1500 kPa. The reduction in transpiration is encompassed in MOSES by including it in as a component that represents the response of the stomatal resistance to environmental variables: net photosynthesis, atmospheric humidity and soil water content. Eight different types of land surface are represented in the model. These are water, soil, urban and five plant functional types: broadleaf tree, needliferous tree, C_3 grass, C_4 grass and shrub. These land surfaces capture differences in the way that key processes are represented, whilst differences within a land surface type, e.g. winter wheat and grass leys are both types of C_3 grass, are handled by different parameter values. Within a given model grid cell MOSES uses a tiled approach so that the different land surfaces are represented explicitly.

Runoff is calculated from both rate and storage exceedance in the upper portion of the soils. The Probability Distribution Model (PDM) of Moore (1985) is included to represent the variability in the soil water stores within a grid cell.

The carbon cycle component of the model, as used in this project, defines the soil carbon and the structure of the vegetation. The vegetation carbon fluxes are derived using the photosynthesis-stomatal resistance formulation; resulting in estimates of the net primary productivity which are then allocated to growth of the vegetation (leaf, wood and root biomass). Leaf phenology is included using air temperature and soil water content-dependent leaf turnover rates. The land surface parameters required for the calculation of the energy and water fluxes, e.g. vegetation height, albedo and leaf area index, are calculated as functions

of the biomass. Thus the carbon cycle is fully integrated with the calculation of the water and energy balances so that the feedbacks are represented. For example, soil water stress is a limiting factor on the uptake of carbon, i.e. growth, and so can reduce the development of the LAI. The reduced LAI will then result in reduced transpiration as it is used to scale the stomatal conductance up to the canopy conductance. The stomatal conductance is directly affected by soil water stress and so may further limit transpiration.

The energy and water exchanges are calculated at an hourly step, the leaf phenology at a daily step and the carbon allocation at a five day step.

The model predicts above ground carbon in tonnes, which has been converted to indicative yield in oven dried tonnes by multiplying by a factor of 2.2 which has been determined from measurements made at Rothamsted.

The energy crops are assumed to be harvested on the 31st December; annually in the case of the grasses and every third year for the short rotation coppice. The indicative yield of the SRC is taken as the above ground carbon, excluding the leaves. In the case of the grasses, the indicative yield includes the leaves, which is appropriate for winter harvesting but not necessarily for spring harvesting. In calculating the indicative yield, no allowance is made for losses during harvesting.

4.2 Driving data

4.2.1 Base line summary of 30 years weather data

Thirty years of daily weather data, for the period 1971 to 2000 inclusive, for the whole of England and Wales at a 40 km by 40 km resolution were purchased from the Met. Office. These data have been derived from the Met. Office weather station network for use in driving the MORECS model (Hough *et al.*, 1998). These data have been analysed to establish the mean, maximum and minimum annual and growing season (April to September) variables for the whole of England and Wales and for different regions. The five regions, north, south, east, west and the midlands are shown in Figure 42.

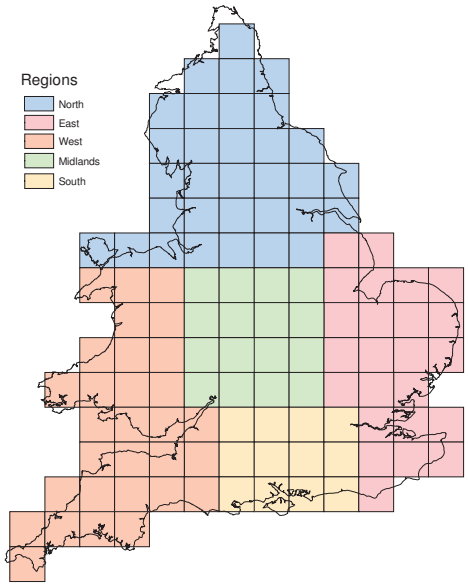

Figure 42 The regions used in the analysis of the weather driving data

Table 7 National weather statistics based on calendar years

year		vapour pressure (hPa)	windspeed (m s^{-1})	sunshine (hours)	rainfall (mm)
1971	9.5	10.4	4.7	4	802.7
1972	8.9	9.8	5	3.7	870.5
1973	9.3	10.2	4.7	4.1	758.2
1974	9.2	9.9	5.5	3.9	1008
1975	9.6	10.3	4.7	4.3	761.2
1976	9.7	10.2	4.6	4.3	807.3
1977	9.2	10.1	5.1	3.9	926.7
1978	9.1	10.1	4.7	3.7	876.7
1979	8.5	9.8	4.7	3.9	975.8
1980	9.1	10	4.7	3.8	978.8
1981	9	10.1	4.5	3.6	1002
1982	9.6	10.4	4.4	4	996
1983	9.7	10.4	4.5	3.9	884.6
1984	9.4	10.1	4.2	4.2	914.2
1985	8.6	9.8	4.3	3.9	904.1
1986	8.5	9.6	4.7	4.1	994.4
1987	8.8	9.9	3.9	3.8	935.4
1988	9.5	10.2	4.3	4	949.6
1989	10.3	10.4	4.2	4.8	830.6
1990	10.4	10.3	4.7	4.7	835.6
1991	9.3	10.1	4.2	3.9	790.9
1992	9.6	10.2	4.3	3.9	944.8
1993	9.2	9.9	4.2	3.8	976.8
1994	9.9	10.3	4.5	4.1	1013
1995	10.2	10.3	4.3	4.8	822.8
1996	8.9	9.4	4.3	4.3	744.2
1997	10.2	10.4	4.2	4.4	845.5
1998	10	10.3	4.5	3.9	1050
1999	10.2	10.5	4.2	4.4	1015
2000	9.9	10.4	4.3	4.1	1198

Table 8 Regional seasonal weather statistics, rainfall and temperature

region	season	min. rainfall (mm)	max. rainfall (mm)	wettest year	driest year	mean rainfall (mm)	min. temp. (°C)	max. temp. (°C)	warmest year	coolest year
east	dormant	223.3	570.8	2000	1973	373.9	5.4	7.9	1990	1985
east	growing	144.8	352.5	1987	1990	256.1	13.4	16.1	1976	1972
midl	dormant	255.8	611.2	2000	1973	424.5	5	7.4	1990	1985
midl	growing	170.9	402.2	1992	1990	286.1	12.9	15.6	1976	1972
north	dormant	433.8	820.7	2000	1973	619.3	4.5	6.8	1990	1979
north	growing	246.9	493.9	1985	1991	377.7	11.9	14.1	1976	1972
south	dormant	259.3	800.2	2000	1973	502.6	5.6	8	1990	1985
south	growing	149.2	438.2	1974	1990	287.8	13.2	16.2	1989	1972
west	dormant	527.6	1075	2000	1973	799.9	5.6	7.7	1990	1979
west	growing	263.4	564.9	1974	1989	409.9	12.2	14.9	1989	1972

Table 9 Regional seasonal weather statistics, wind and sunshine

region	season	min. windspeed ($m\ s^{-1}$)	max. windspeed ($m\ s^{-1}$)	windiest year	calmest year	min. sunshine (hours)	max. sunshine (hours)	sunniest year	dullest year
east	dormant	4.1	5.8	1974	1987	2.6	3.8	1990	1975
east	growing	3.5	4.9	1974	1989	5.4	8.1	1989	1987
midl	dormant	3.7	5.3	1974	1987	2.2	3.5	1995	1981
midl	growing	2.9	4.5	1974	1999	4.6	7.4	1989	1972
north	dormant	3.9	6.6	1974	1987	2.2	3.1	1995	1978
north	growing	3.5	5.4	1974	1999	4.6	6.8	1989	1978
south	dormant	3.9	4.9	1974	1973	2.6	3.8	1990	1981
south	growing	3.1	4.3	1974	1999	5.5	8.4	1989	1981
west	dormant	4.7	6.1	1977	1985	2.3	3.2	1990	1992
west	growing	3.6	5	1974	1999	4.9	7.3	1989	1981

Annual averages were calculated for the whole of England and Wales, of rainfall, vapour pressure, wind speed and sunshine hours (Table 7).

Regional averages (Tables 8 and 9) were also calculated for the dormant (defined as October to April) and growing (defined as May to September) seasons.

4.2.2 Spatial and temporal interpolation of the driving data

The MORECS gridded daily meteorological data set is at a 40 km resolution. but has been interpolated to a 1 km grid. This was achieved within ArcInfo GIS using a bilinear interpolation method. Figure 43 shows the MORECS 40 km air temperature data for the 26th July 1976. These data have been clipped to the coastline of England and Wales and interpolated to a 1km grid using the bilinear interpolation method (Figure 44). The air temperature had to be interpolated out to the coast where the MORECS grid does not cover the UK. To obtain a more accurate picture of temperature, altitude was taken into account by incorporating the CEH digital terrain model (DTM), to produce the final 1 km grid of air temperature for the 26 July 1976 (Figure 45).

In order to ensure that the high spatial variability of rainfall was represented in the modelling, a different approach was adopted for this variable. The basis data used was a 1 km resolution data set of monthly totals. These data were calculated, by CEH, using the data from raingauges held in the National River Flow Archive, using the procedures of BS 7843 (British Standards Institute, 1996) These data were disaggregated to daily values by using the MORECS daily data (which is at a 40 km resolution). Thus, for each 1 km grid cell, the daily value calculated was the 1 km monthly value multiplied by the daily fraction of the monthly total, for the same month and year, of the MORECS data.

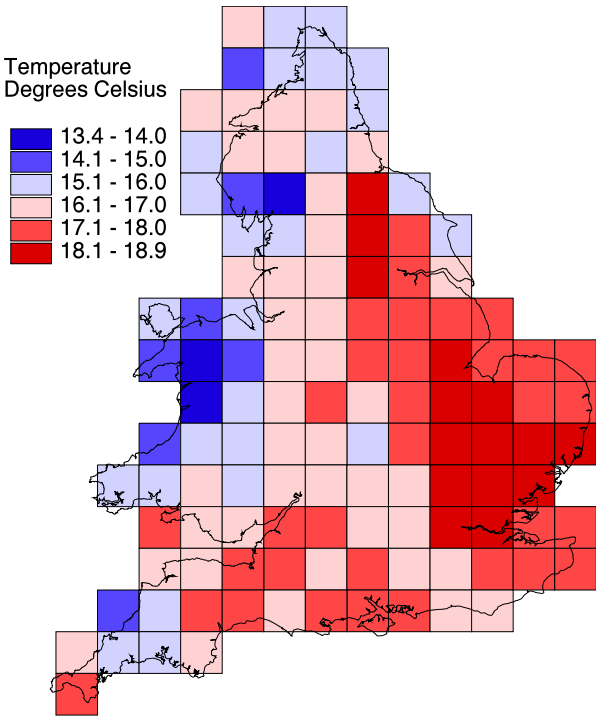

Figure 43 The MORECS gridded air temperature data for England and Wales for 26 July 1976

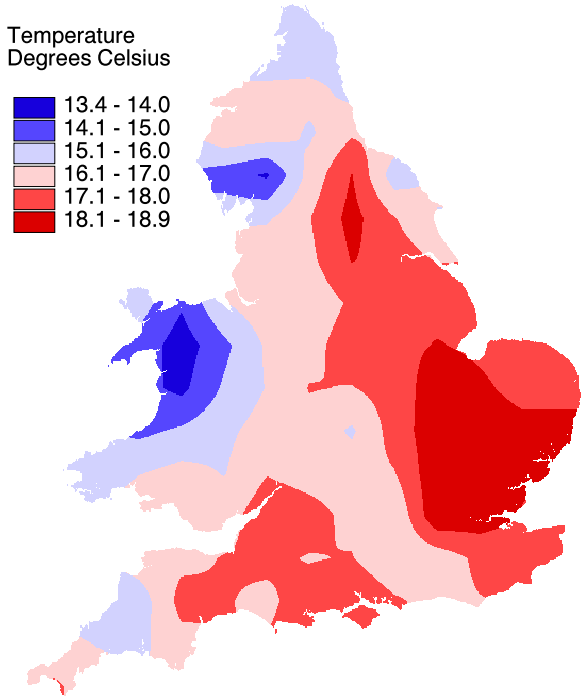

Figure 44 The MORECS data for 26 July 1976 clipped to the coastline and interpolated to a 1 km grid

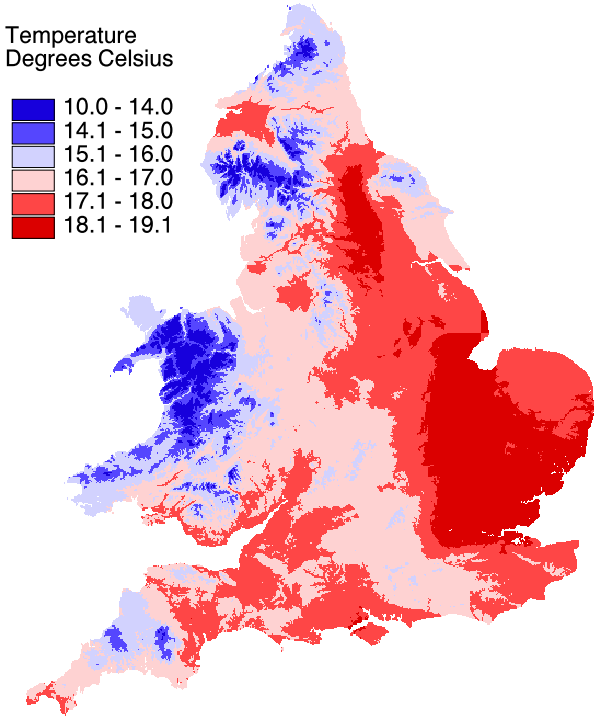

Figure 45 The 1 km gridded temperature data (26 July 1976) adjusted for altitude

4.3 Land surface parameters

4.3.1 Existing land cover

For the existing land cover, we have derived a 1 km resolution land cover data set, giving the fractions of the different land cover types within each grid cell, from the CEH 25m Land Cover Map 2000 (LCM2000). LCM2000 is derived from a computer classification of remotely sensed data obtained mainly from the Thematic Mapper sensor on the LANDSAT satellite. Details of LCM2000 can be found at: http://www.ceh.ac.uk/data/lcm/LCM2000.shtm.

The majority of the land cover of England and Wales is grass or tilled land with grass dominant in the west and tilled land dominant in the east, as shown in Figure 46 which shows the dominant land cover class in each 1 km grid cell. The relative scarcity of woodland is also demonstrated.

The LCM2000 data set classifies the land cover of the UK into 25 classes and so it was necessary to aggregate the classes into the 8 classes for use in the MOSES model. The reclassification used is given in Table 10.

The parameter values used have been the default set generally used with MOSES. These values have been established and tested in numerous studies and so may be considered to be the best estimates available. The exception is the crops; for which we have assumed a winter cereal with a harvesting date of 2nd September and an emergence date of 8th October. The maximum rooting depth, canopy height and leaf area index have values of 1.0, 1.0 and 6.5 respectively.

Table 10 Reclassification of the LCM2000 classes into MOSES land cover classes

MOSES land cover type	LCM 2000 classes
1 - broadleaved woodland	11
2 – needliferous woodland	21
3 – grassland and pasture (C_3 grass)	51, 52, 61, 71, 81, 111
5 – medium scale vegetation (shrubs)	91, 121, 101, 102, 151, 43
6 – crops (C_3 grass)	41, 42
7 – urban and suburban	171, 172
8 – inland water	212, 131
9 – soil and bare rocks	181, 191 ,161

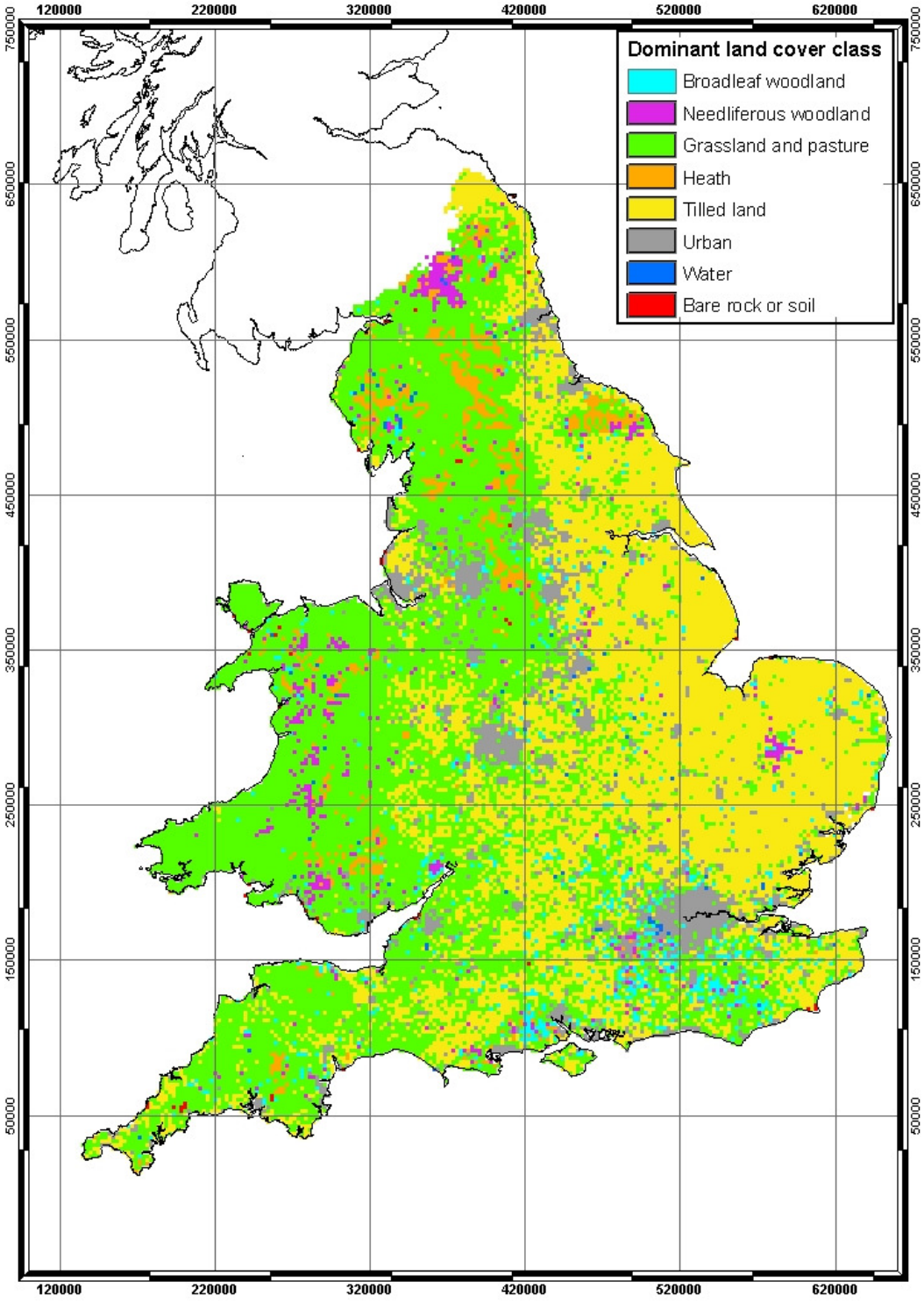

Figure 46 The dominant land cover class within each 1 km grid cell

4.3.2 Soils

For the soil data we have used the Hydrology Of Soil Types (HOST) data set by taking the dominant HOST soil type within each 1 km grid cell. The definitions of the HOST classes are given in Table 11. The HOST data set does not have the soil hydraulic and thermal properties required by the MOSES model. To produce the necessary values, we have used the National Soil Resource Institute's SEISMIC data set (http://www.silsoe.cranfield.ac.uk/nsri/services/seismic.htm). This data set gives a number of properties for the soil series of England and Wales. These properties include the HOST class and the texture measures (including the percentages of sand, silts and clays). Thus we were able to select all the soil series belonging to a HOST class and then calculate the average texture measures of these soils to produce a 'virtual' soil. The required hydraulic and thermal properties of these soils were then calculated from the texture measures using the methods of Saxton *et al*. (1986) and Hubrechts and Feyen (1996). The soil water content at which evaporation begins to be limited was calculated as that at a soil water potential of -33 M Pa. The resulting parameters are given in Table 12.

The HOST classification was designed as a means of aggregating the numerous soil series into groups which would have a similar hydrological response, i.e. it is the movement of water that is the dominant criteria. Thus it is not optimised for an application such as this when it is the ability of a soil to store water that is the important issue. Nevertheless, there is generally a very strong correlation between a soil's hydraulic conductivity and its ability to store water and so the classification is likely to reflect difference that affect the water use and indicative yield of the vegetation. A limitation of the data set is that it does not have information on the presence of a hard layer which might limit the rooting depth of the vegetation. This will influence the model predictions because, in reality plants on thin soils will have access to less water stored in the soils and so transpiration and growth will be limited during periods of low rainfall. However, this is possibly not a serious limitation as the areas where these soils occur also tend to be areas of high rainfall, reducing the probability of soil water stress occurring.

The spatial distribution of the soil classes is presented in Figure 47. In general, the deep and more porous/permeable soils are likely to occur in the east whilst the shallower, less porous soils occur in the west, reflecting the underlying geology. There is some correlation between the land use, Figure 46, and the soils because the underlying geology also has a strong effect on the topography and because the soil's suitability for a particular land use can be influenced by its hydraulic properties, e.g. poorly drained soils are less likely to be used for high value cereal crops.

Table 11 HOST soil classes (after Boorman et al., 1995)

<table>
<tr><th rowspan="2">SUBSTRATE HYDROGEOLOGY</th><th colspan="6">MINERAL SOILS</th><th colspan="2" rowspan="2">PEAT SOILS</th></tr>
<tr><th>ground-water or aquifer</th><th>No impermeable or gleyed layer within 100 cm</th><th colspan="2">Impermeable layer within 100 cm or gleyed layer at 40-100 cm</th><th colspan="2">gleyed layer within 40 cm</th></tr>
<tr><td>Weakly consolidated, microporous, by-pass flow uncommon (Chalk)</td><td rowspan="7">Normally present and at > 2 m</td><td>1</td><td colspan="2" rowspan="7">13</td><td colspan="2" rowspan="7">14</td><td colspan="2" rowspan="7">15</td></tr>
<tr><td>Weakly consolidated, microporous, by-pass flow uncommon (limestone)</td><td>2</td></tr>
<tr><td>Weakly consolidated, macroporous, by-pass flow uncommon</td><td>3</td></tr>
<tr><td>Strongly consolidated, non or slightly porous, by-pass flow common</td><td>4</td></tr>
<tr><td>Unconsolidated, macroporous, by-pass flow very uncommon</td><td>5</td></tr>
<tr><td>Unconsolidated, microporous, by-pass flow common</td><td>6</td></tr>
<tr><td>Unconsolidated, macroporous, by-pass flow very uncommon</td><td rowspan="2">Normally present and at ≤ 2 m</td><td colspan="3" rowspan="2">7</td><td>IK < 12.5</td><td>IK ≥ 12.5</td><td>drained</td><td>undrained</td></tr>
<tr><td>Unconsolidated, microporous, by-pass flow common</td><td colspan="3">8</td><td>9</td><td>10</td><td>11</td><td>12</td></tr>
<tr><td>slowly permeable</td><td rowspan="5">no significant groundwater or aquifer</td><td rowspan="2">16</td><td>IS > 7.5</td><td>IS ≤ 7.5</td><td colspan="2" rowspan="2">24</td><td colspan="2" rowspan="2">26</td></tr>
<tr><td>18</td><td>21</td></tr>
<tr><td>impermeable (hard)</td><td>17</td><td>19</td><td>22</td><td colspan="2"></td><td colspan="2">27</td></tr>
<tr><td>impermeable (soft)</td><td colspan="2"></td><td>20</td><td>23</td><td colspan="2">25</td><td colspan="2"></td></tr>
<tr><td>eroded peat</td><td colspan="4"></td><td colspan="2"></td><td colspan="2">28</td></tr>
<tr><td>raw peat</td><td colspan="4"></td><td colspan="2"></td><td colspan="2">29</td></tr>
</table>

IK used to index lateral saturated hydraulic conductivity
IS used to index soil water storage capacity

Table 12. MOSES soil parameters for HOST classes

HOST CLASS	exponent in the Brooks and Corey model	Saturated hydraulic conductivity (mm s^{-1})	Saturated soil water potential (m)	Fractional soil water content at which evaporation begins to be limited	Saturated fractional soil water content	Fractional soil water content at a soil water potential of -1500 kPa	Soil heat capacity (J K^{-1} m^{-3})	Dry soil thermal conductivity (W m^{-1} K^{-1})
1	5.95	1.36E-03	0.0598	0.2904	0.4887	0.1529	1.03E+06	0.5344
2	6.34	1.23E-03	0.0590	0.2845	0.4864	0.1559	9.37E+05	0.4941
3	5.04	8.52E-03	0.0307	0.1816	0.4050	0.0852	1.10E+06	0.3636
4	4.66	3.89E-03	0.0483	0.2496	0.4556	0.1101	9.64E+05	0.3719
5	5.35	6.58E-03	0.0342	0.1890	0.4150	0.0926	1.10E+06	0.3858
6	5.56	1.63E-03	0.0590	0.2872	0.4863	0.1446	1.10E+06	0.5483
7	5.43	6.90E-03	0.0331	0.1842	0.4119	0.0911	1.11E+06	0.3885
8	5.35	2.00E-03	0.0562	0.2742	0.4783	0.1343	1.08E+06	0.508
9	6.49	9.36E-04	0.0686	0.3504	0.5140	0.1946	1.00E+06	0.6222
10	5.43	3.02E-03	0.0474	0.2355	0.4532	0.1167	9.95E+05	0.4052
11	5.43	3.02E-03	0.0474	0.2355	0.4532	0.1167	9.95E+05	0.4052
12	5.64	2.48E-03	0.0497	0.2427	0.4597	0.1233	1.09E+06	0.4723
13	5.33	2.46E-03	0.0520	0.2549	0.4661	0.1246	1.03E+06	0.4533
14	4.69	2.57E-03	0.0579	0.2885	0.4833	0.1278	1.17E+06	0.5452
15	4.61	5.41E-03	0.0418	0.2287	0.4371	0.0998	9.36E+05	0.3196
16	5.76	1.81E-03	0.0549	0.2652	0.4747	0.1367	9.92E+05	0.4685
17	5.27	2.20E-03	0.0547	0.2678	0.4741	0.1299	9.86E+05	0.4482
18	5.50	1.53E-03	0.0616	0.3023	0.4938	0.1510	1.16E+06	0.6031
19	4.42	6.61E-03	0.0389	0.2242	0.4287	0.0946	9.46E+05	0.3057
20	7.35	7.53E-04	0.0726	0.3488	0.5254	0.2299	1.12E+06	0.7529
21	6.17	1.06E-03	0.0690	0.3518	0.5151	0.1896	1.12E+06	0.6742
22	5.49	3.02E-03	0.0471	0.2337	0.4522	0.1166	8.28E+05	0.3199
23	9.99	6.66E-04	0.0802	0.4126	0.5474	0.3218	1.05E+06	0.8807
24	6.39	9.75E-04	0.0667	0.3361	0.5086	0.1850	1.12E+06	0.6628
25	9.74	6.60E-04	0.0797	0.4074	0.5458	0.3142	1.11E+06	0.9008
26	6.11	1.08E-03	0.0683	0.3470	0.5132	0.1857	1.05E+06	0.6307
27	5.37	1.91E-03	0.0570	0.2780	0.4806	0.1366	4.70E+05	0.2091
29	5.37	1.91E-03	0.0570	0.2780	0.4806	0.1366	4.70E+05	0.2091

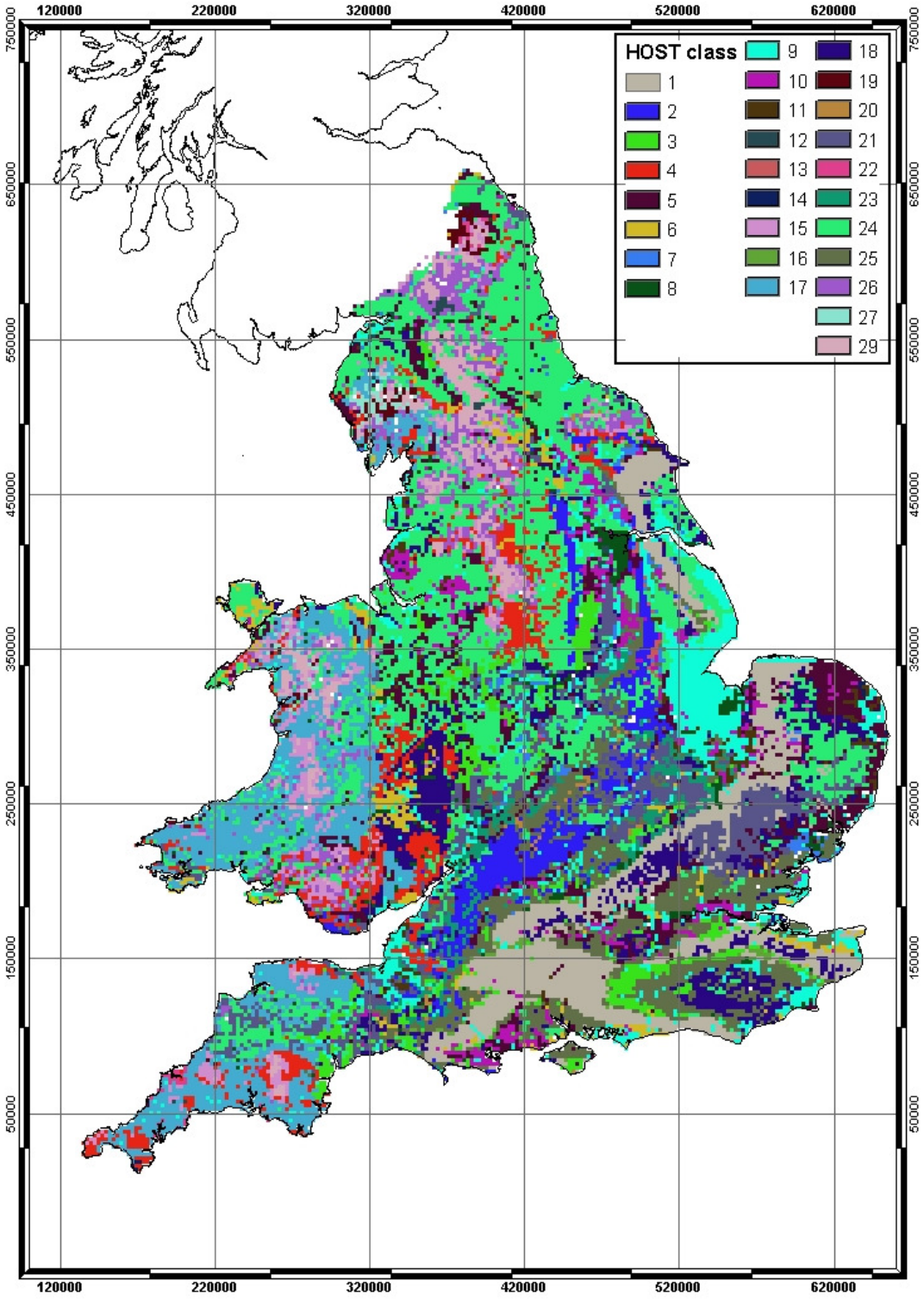

Figure 47 The spatial distribution of the HOST soil classes

4.4 Selection of typical, wet and dry years

In the UK, rainfall patterns tend to reflect the preferred tracks taken by Atlantic frontal systems. When, as for example in the summers of 1976, 1984 and 1995, these pass to the north, drought conditions can extend over much of the country. Conversely when persistent synoptic patterns cause the preferred route to be across southern Britain, much – but rarely all – of the country experiences a prolonged wet spell. It is unusual for drought severity or rainfall abundance not to exhibit substantial spatial and temporal variability; in particular rainfall patterns in the North-West commonly differ from those experienced in the South-East.

The calendar year is rather an arbitrary timeframe in hydrological and climatological terms and, commonly, it has limited utility in studies where the primary focus of interest is seasonal (including 'growing' season) or multi-seasonal in character. Often rainfall distribution within the year is very uneven and this can result in misleading perceptions of what constitutes a dry or wet 'year'. For instance, few recent years with notable spring/summer drought conditions (e.g. 1975, 1976, 1984, 1990, 1995) are associated with exceptionally low annual rainfall totals. None was as dry overall as 1973 but in that year the April-September period was somewhat wetter than average. Conversely, 2000 was the wettest year since 1872 for England and Wales, and all regions received well above average rainfall, but the summer (June-August) rainfall total was below average.

Clearly, a more refined characterisation of what 'wet' and 'dry' conditions are important for particular studies or applications is necessary before final selections of reference periods are made. Where water balances and/or soil moisture conditions are central to an investigation, the water-year is often a more effective baseline than the calendar year. Conventionally, the UK water-year runs from October to September; beginning and ending when river flows are modest and (at least in the lowlands) soil moisture deficits remain substantial. The following analyses are based on water-years and are considered to be more appropriate in circumstances where the growing season is influential.

The homogenised England and Wales rainfall series of the Climate Research Unit (now updated by Hadley Centre) has been used to identify the driest and wettest water years for the country as a whole. In order to index spatial variability, 1961-2000 gridded monthly rainfall assessments (derived by CEH Wallingford for the Environment Agency North-West, Thames and South West Regions) have been used.

As indicated above, a high degree of spatial correlation in regional rainfall deficiencies and surpluses is unusual but 1975/76 was outstandingly dry across almost all of England and Wales. In addition, rainfall was below average in all months of the water year with the exception of September. Therefore, 1976 has been adopted as the dry year.

The remarkably high England and Wales rainfall total water-year rainfall for 2000/01 reflects the outstandingly wet autumn, winter and early spring (the 8-months ending in April 2001 was the wettest 8-month sequence in the instrumented era) but the following May-August rainfall was below average. Therefore we have opted for 1987/88 as the wet year; because it was wet throughout England and Wales and the temporal distribution of the rainfall was much more even than in 2000/01.

For an average water-year 1981/82 has been chosen. Rainfall for England and Wales as a whole was very close to the long term average and regional departures were less than 5%; in addition the water-year contained no protracted very dry or very wet periods.

4.5 Calibration and testing of the MOSES model

Determining the values for the parameters of the MOSES model has been achieved by a combination of the analysis of the measurements made in this study and previous studies (notably Hall *et al*., 1996) and values reported in the literature. There are many parameters in the MOSES model but the key parameters that describe the vegetation, and which have been used in this study are:

k – the extinct coefficient for photosynthetically active radiation;
a_{ws} – woody biomass as a multiple of live stem biomass;
σ_l – specific density of leaf carbon (kg C m^{-2} leaf);
R_{pg} – growth respiration fraction;
D_c – critical specific humidity deficit (kg kg^{-1});
$n_l(0)$ – top-leaf nitrogen concentration (kg N (kg C)$^{-1}$);
F_0 – empirical constant in the stomatal conductance sub-model;
T_{off} – temperature below which leaves are dropped (K^{-1})
d_r – maximum rooting depth (m);
$\delta C_m/\delta\Lambda$ – rate of change of canopy capacity with Leaf Area Index.

The values used are given in Table 13

Table 13 Parameter values used for the energy crops

parameter	poplar SRC	willow SRC	*miscanthus*	switchgrass
k	0.3	0.3	0.3	0.3
a_{ws}	25.0	16.0	0.9	1.25
σ_l	0.02	0.02	0.05	0.05
R_{pg}	0.1	0.1	0.1	0.1
D_c	10.0	0.024	0.075	0.075
$n_l(0)$	0.04	0.04	0.03	0.03
F_0	0.875	0.65	0.8	0.8
T_{off}	278.15	278.15	280.15	280.15
d_r	3.0	3.0	1.7	1.3
$\delta C_m/\delta\Lambda$	0.5	0.2	0.2	0.15

4.5.1 Poplar SRC

The parameter values used are dominantly drawn from the report of Hall *et. al* (1996). Two could be used directly ($\delta C_m/\delta\Lambda$ and d_r). Those for the stomatal conductance model (D_c, and F_0) have been selected to simulate the results obtained by Hall *et. al* (1996) who found that the stomatal conductance poplar had very little response to the atmospheric variables such as humidity deficit. The remaining variables, which

mainly affect the growth of the vegetation, were obtained by doing model runs, driven by hourly meteorological data from the measurement site, and manually adjusting the parameter values until the reported maximum LAI and canopy height were reproduced. No data were available to test the final model parameterisation, however, the predicted development of the canopy height and LAI, using driving data from Roves Farm, are shown in Figure 48.

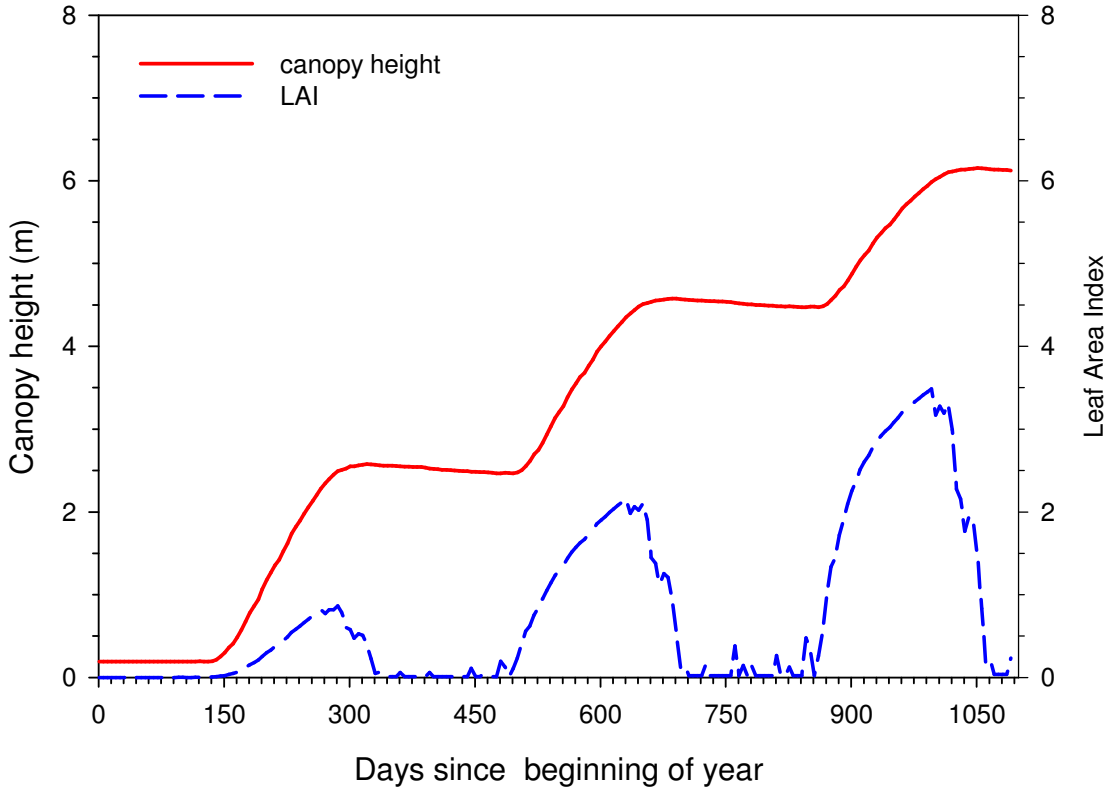

Figure 48 Predicted development of the canopy height and LAI of poplar SRC .

4.5.2 Willow SRC

The parameters values are derived from measurements made in this study, supplemented with information reported in the literature. The value for the change in canopy capacity with LAI ($\delta C_m/\delta \Lambda$) is taken from Itrix *et al.* (2001). The value of the parameters for the stomatal conductance sub-model (D_c, and F_0) were obtained by driving the model of Cienciala and Lindroth (1995b), see Section 3.2.3.1, with combinations of the global solar radiation and the vapour pressure deficit that represented conditions likely to be encountered in the UK. The MOSES stomatal conductance sub-model parameters were calibrated against the resulting data set by changing the parameter values until a minimum value for an objective function, the root mean square error, was obtained. The rooting depth, d_r, was obtained from Hall *et. al* (1996).

The ability of the MOSES model to simulate the water and energy fluxes, using these parameters values, has been testing by running the model with the simulation of the carbon cycle 'switched off'. The height and LAI of the vegetation were prescribed, using the values measured at the site. The soil hydraulic and thermal properties were derived from the texture measures given for the soil series in the SEISMIC database.

The predicted values of the net radiation and latent heat flux (evaporation) can be compared with those measured at the site for the period 26 June to 6 August 2002, Figure 49. Two error measures have been calculated to quantify the differences between the predicted and measured values. The root mean square error (RMSE) measures both systematic and random errors whilst the mean bias error (MBE) measures systematic errors. The error is defined as the measured minus the modelled. The MBE and RMSE for the predicted net radiation are 26 and 31 W m^{-2} whilst for the latent heat flux they are 18 and 35 W m^{-2} (corresponding to errors in the rate of evaporation of 0.64 and 1.1 mm day^{-1}). The positive MBE suggests that the model will under-estimate the evaporation rate, i.e. the water use. It should be noted that these represent the worse case since the data cover the period when evaporative losses are likely to be greatest and hence the errors are also at the maximum. During the winter months, the evaporation rate will be much lower, partly due to the reduction in the downward solar radiation, and partly due to the absence of leaves on the willows.

The variables discussed above dominantly describe the energy fluxes. The remainder, which mainly affect the growth of the vegetation, were obtained by doing model runs, driven by hourly meteorological data, and manually adjusting the parameter values until the measured maximum LAI and canopy height were reproduced. The time series, for a three year period, of the canopy height and LAI, predicted by the model are shown Figure 50.

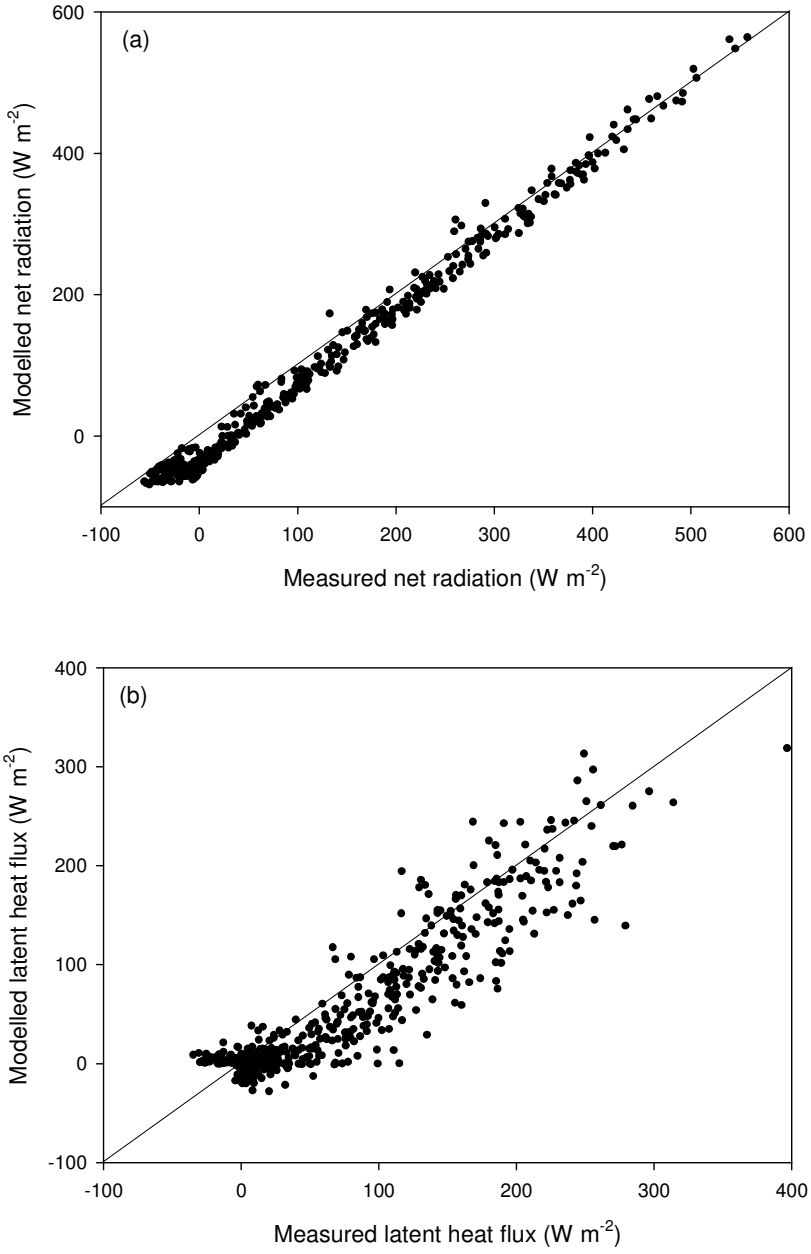

Figure 49 Comparison of measured and modelled values of (a) net radiation and (b) latent heat flux for willow SRC at Roves Farm.

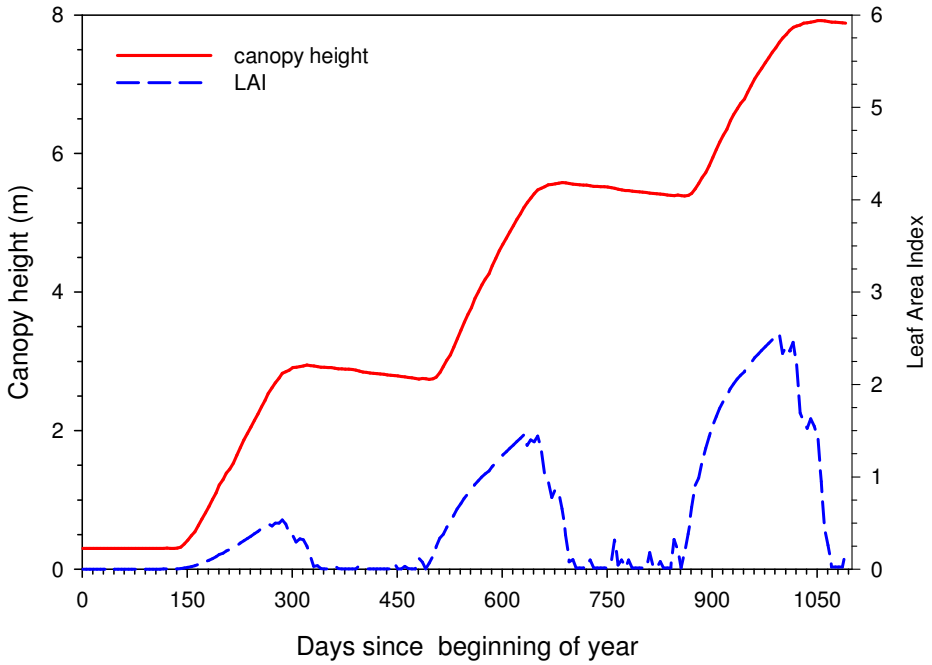

Figure 50 Predicted development of the canopy height and LAI of willow SRC

4.5.3 Miscanthus

The parameter values for *Miscanthus* have been mainly derived from measurements and modelling carried out in this project. The rooting depth was assumed to correspond to the maximum depth that soil water. The values of the parameter for the canopy capacity, $\delta C_m/\delta\Lambda$, was derived from the data presented by Riche and Christian (2001). In the absence of measurements or information from any other source, the values of the parameters (D_c, and F_0) for the stomatal conductance sub-model were assumed to be those used for switchgrass, i.e. it that there is no significant difference in the stomatal response between the two types of grass.

The ability of the MOSES model to simulate the water and energy fluxes, using these parameters values, has been testing by running the model with the simulation of the carbon cycle switched off. The height and LAI of the *Miscanthus* were prescribed, using the values measured at the site. The soil hydraulic and thermal properties were derived from the texture measures given for the soil series of the site in the SEISMIC database.

A comparison of the predicted values of the profile soil water content with the measured values, Figure 51, shows that there is very good agreement. This is encouraging as the soil water depletion is a good indicator the evaporative losses, i.e. the combination of the transpiration and interception from the evaporation and the evaporation from the soil.

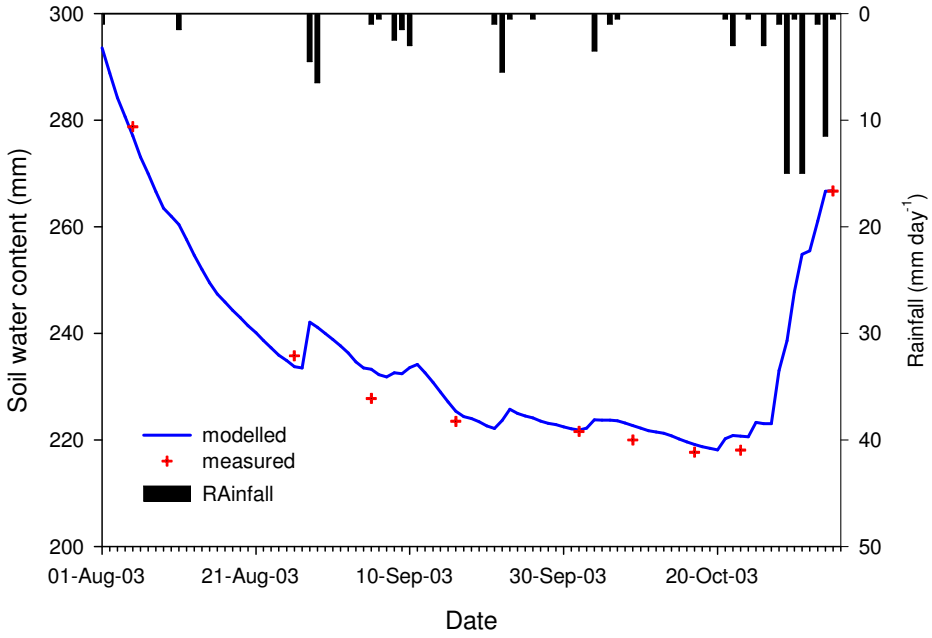

Figure 51 Measured and modelled soil water contents under *Miscanthus* at Richard's Castle

The predicted values of the net radiation and latent heat flux (evaporation) can be compared with those measured at the site for the period 15 August to 6 November 2003, Figure 52. The comparison shows a greater amount of scatter around the 1:1 line than with the simulation of the willow. This may be due to the vegetation canopy not being as continuous; there were gaps in the distribution of the *Miscanthus*. These gaps would have allowed the sunlight to penetrate further into the canopy; the amount varying according to the solar elevation and azimuth. The MBE and RMSE for the predicted net radiation are 30 and 49 W m^{-2} whilst for the latent heat flux they are 20 and 55 W m^{-2} (corresponding to errors in the rate of evaporation of 0.69 and 1.9 mm day^{-1}).

The variables discussed above dominantly describe the energy fluxes. The remainder, which mainly affect the growth of the vegetation, were obtained by doing model runs, driven by hourly meteorological data, and manually adjusting the parameter values until the measured maximum LAI and canopy height were reproduced. The time series, for a three year period, of the canopy height and LAI, predicted by the model are shown Figure 53.

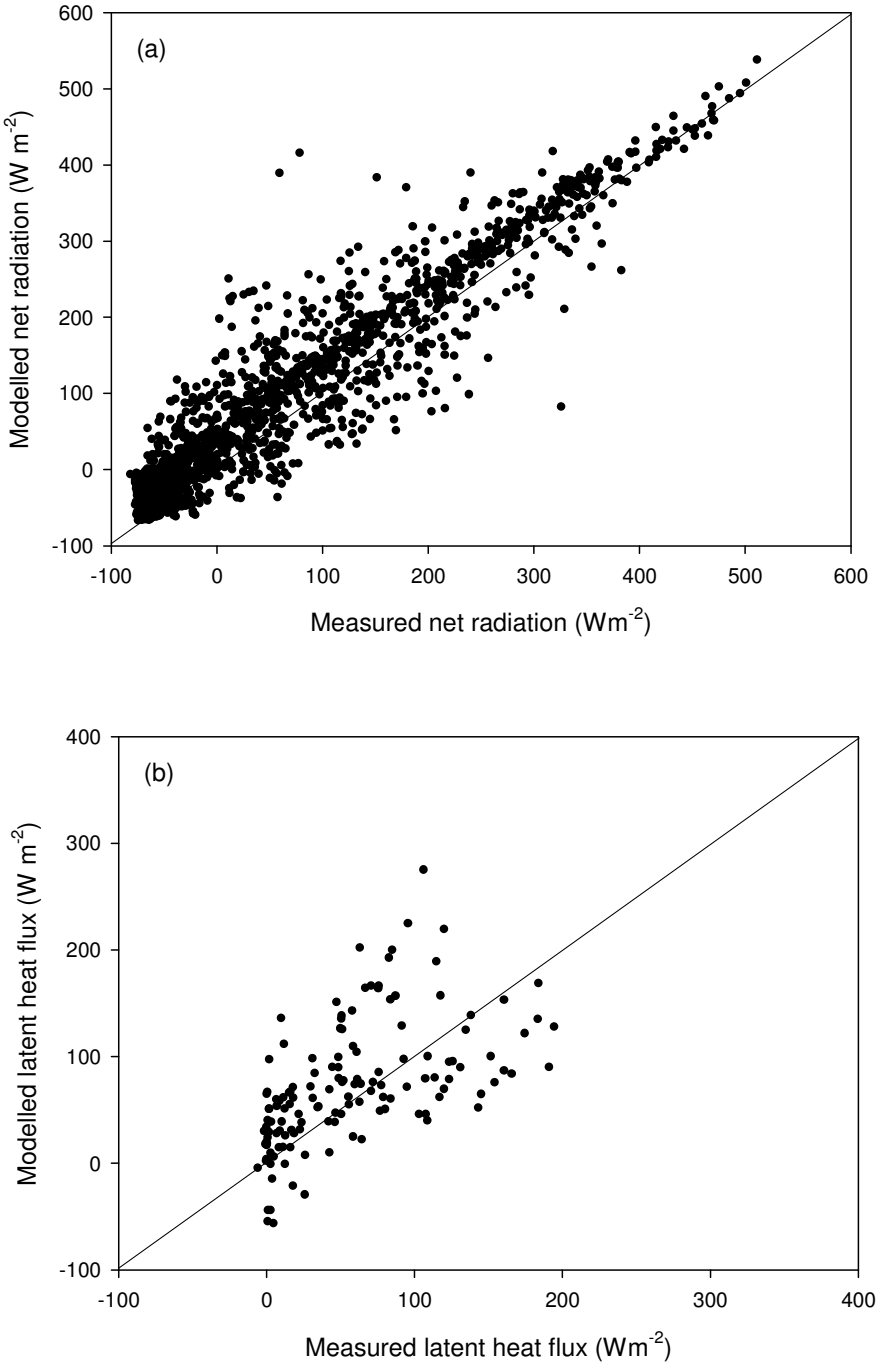

Figure 52 Modelled and measured net radiation and latent heat flux over *Miscanthus* at Richard Castle

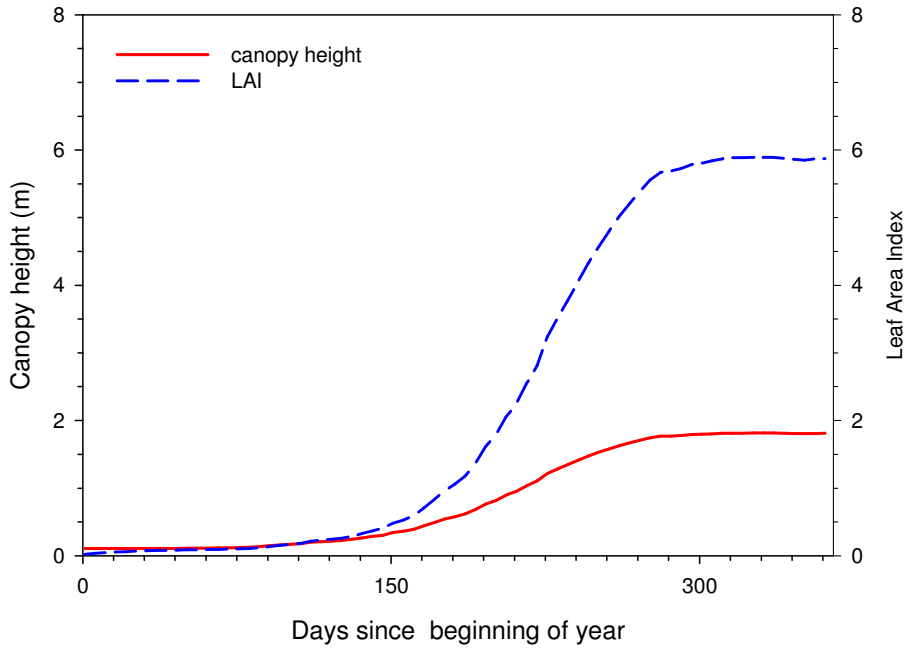

Figure 53 Predicted development of the canopy height and LAI of *Miscanthus*

4.5.4 Switchgrass

The parameter values for switchgrass are derived from the measurements made in this study. The rooting depth is assumed to be represented by the maximum depth at which the measured soil water contents changed, at both the Rothamsted and Woburn sites. The canopy capacity parameter, $\delta C_m/\delta\Lambda$, was determined by dividing the measured canopy capacity, see Section3.3.3.1, by the measured LAI. The parameters for the stomatal conductance model were the values determined from the measurements, see Section 3.3.3.4.

No data were available to test the parameterisation of the energy fluxes. The parameters which mainly affect the growth of the vegetation, were obtained by doing model runs, driven by hourly meteorological data, and manually adjusting the parameter values until the measured maximum LAI and canopy height were reproduced. The time series, for a three year period, of the canopy height and LAI, predicted by the model are shown Figure 54.

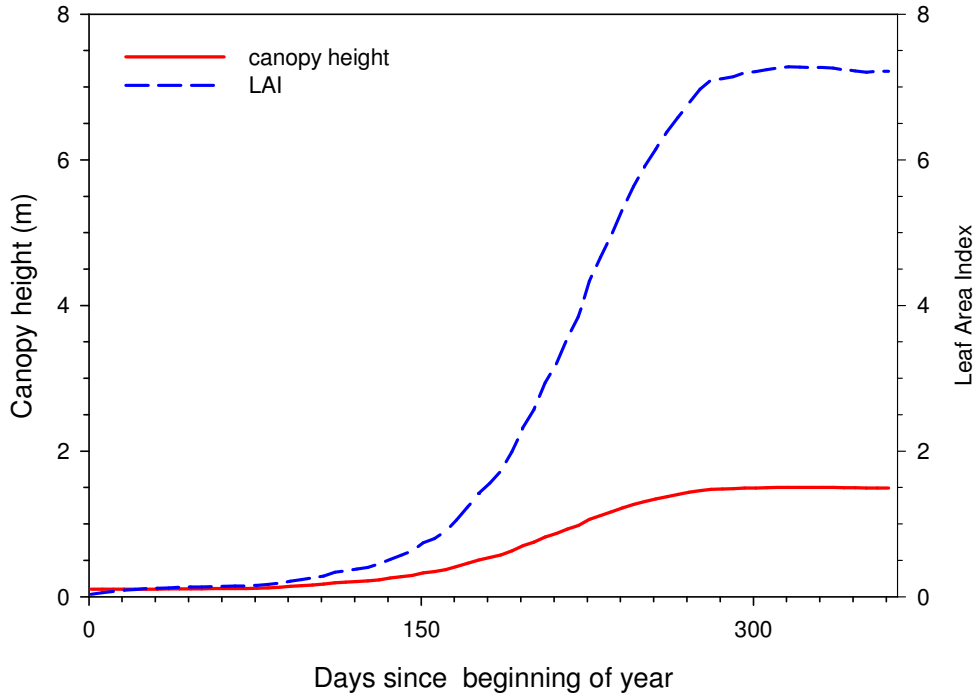

Figure 54 Predicted development of the canopy height and LAI of switch grass

4.6 Uncertainties

The uncertainties in the predicted water use of the vegetation types arise from a three main sources: the simplifications in the numerical model made in representing the physical processes; the need to represent the natural variability by single values for parameters; the uncertainties in the driving data. Each of these is discussed below.

It is not possible to quantify the uncertainties to any degree because the model includes a number of feedbacks so the effects of the uncertainties on the predictions is non-linear. Rather, it is important to be aware that they exist and thus to know when the results are likely to be less reliable.

4.6.1 Representation of the processes by the model

The MOSES model is, inevitably, a simplified representation of the real world. It attempts to include the dominant processes involved in the energy, water and carbon exchanges between the land surface and the atmosphere. A notable omission is that nutrients are not included and so there is an implicit assumption that nutrients do not limit the growth of the vegetation. In practice, this is probably not a real limitation as, agricultural practices will normally be expected to supply sufficient nutrients. The omission is only likely to have an impact where natural conditions apply on nutrient poor soils. The effects of exposure on the growth of the crop is not included.

Some degree of simplification is necessary with most of the processes. An example is the processes involved in the impact of low soil water contents on the stomatal conductance. The detail of these are still not fully understood, see Chavez *et al.* (2003), and, even if they were, the complexity of accurately representing them in a model appropriate to the scale required by this project would not be warranted. Therefore the MOSES model uses a simple relationship between the stomatal conductance and the soil water content. Experience suggests that this simplification does not lead to a level of uncertainty significantly greater than any other.

No consideration is given to the potential effect of the environment on the mortality of any of the energy crops. Examples of possible causes of mortality are late frosts and water logged soils. The possible effects of pests are also not included.

It is assumed that the crops are already well established and that no irrigation occurs, either for the existing land cover or the energy crops. The energy crops are assumed to be harvested on the 31st December; annually in the case of the grasses and every third year for the short rotation coppice. The indicative yield of the SRC is taken as the above ground carbon, excluding the leaves. In the case of the grasses, the indicative yield includes the leaves, which is appropriate for winter harvesting but not necessarily for spring harvesting. In calculating the indicative yield, no allowance is made for losses during harvesting.

4.6.2 Uncertainties about the current land cover and soils

With the exception of tilled land, the existing land cover types are assumed to be fully mature. Thus, recently planted and young plantations of trees are not included. This is likely to result in an over estimate of the water use of these types. However, in practice, the area of immature vegetation is likely to be small compared to the total area and so the uncertainty is likely to be small.

It is difficult to suggest how the assumption that all tilled land is covered by winter wheat will affect the uncertainty of the predicted water use. Other cereal crops probably do not have a water use that is

significantly different. However, other crops, such as potatoes, have a significantly higher water use and so the tendency is probably to underestimate the water use.

The MOSES assumes uniform soil hydraulic and thermodynamic properties with depth and a soil depth of 3 m (although the rooting depth is a property of the vegetation type). It is unlikely that, in most situations, the assumption of uniform properties will lead to major errors as the significant change in properties tends to occur in the top 0.2 m as a result of disturbance and an increased organic carbon content. A greater source of uncertainty is the soil depth of 3 m. (It should be noted that the definition of a soil used here is that of a hydrologist and not a soil scientist; so that the emphasis is on the soil hydraulic properties rather than the mineralogy and degree of weathering.) There are many areas of England and Wales where this assumption does not hold. These are mainly areas where hard bedrock is near the surface, such as Dartmoor and much of the Lake District. These areas tend to occur in the west of the country and coincide with high rainfall rates, thus reducing the dependence of the vegetation on soil water held for any length of time and so reducing the uncertainty arising from this assumption.

An increase in uncertainty occurs where the soil is Chalk. The hydraulic properties of the Chalk are exceptional and, from the perspective of this project, mean that evaporation is rarely limited by soil water availability because water can be drawn up from considerable depth; up to 10 m at times of extreme drought, see Wellings and Cooper *(*1983) and Price *et al*. (1993). This process is not captured by the MOSES. As a result the predicted values will tend to under estimate the water use on this type of soil (which is encountered in HOST class 1).

4.6.3 Uncertainties in the parameter values

The parameter values used to characterise each land cover type give rise to two sources of uncertainty. The first is the uncertainty associated with the determination of the parameter value. The values used have either been determined by field observations or by calibrating the model output against field measurements. In either case the approximations made will lead to a level of uncertainty in the outputs from the model.

A greater degree of uncertainty is using these parameter values, which were determined at a few sites, across the whole of England Wales. There is no way of knowing whether the values used are a good representation of typical conditions or whether they represent unusual conditions. In terms of the energy crops, many of the parameter values were determined on experimental plots and we do not know how typical these are of the conditions that will occur when the crops are grown on farms. However, most of these parameters are scaled by the crop growth, usually by the LAI, and so the impact of the assumptions is likely to be reduced.

4.6.4 Uncertainties in the driving data

Inevitably, there are errors in the measured values of the driving variables arising from approximations in the calibration values for the sensors and the accuracy and precision of the instruments used to make the measurements. These uncertainties are likely to be comparatively low, less than 5%.

The major source of uncertainties arise from the need to spatially interpolate the data. This is especially true of the air temperature, humidity, wind speed and sunshine hours. The uncertainty about the first three of these variables is likely to be low as they tend to be conservative (Met Office 1975a, 1975 b and 1976). However, here is likely to be a greater degree of uncertainty with the sunshine hours because these data are dominated by the cloud fraction and type. As a result, the data is likely to represent the impact of orography on the clouds poorly. This is unlikely to be an issue in lowland areas, but will increase the uncertainty in hilly areas.

5. Predicted water use and indicative yield

It was necessary to “spin up” the model. This involves driving the model with data spanning several years and has the purpose of allowing the various variables that describe the state of the system, e.g. soil moisture content, canopy height etc., to stabilise to values that can be considered as the initial conditions of the model. The time series runs were spun up by running the model for 1971-1978, before the main run over the period of 1971-1999. To produce the spatial outputs, the model was first spun up over 1984 (which was considered "typical" for the period 1971-1999) assuming the current land cover, to produce an initial condition for the soil water content. Subsequent runs were started from this soil moisture state and were spun up for a further year before the model then ran for the three year period of interest, the final year being the selected wet, dry or typical year.

The outputs from the model runs are presented in two forms. The first is as time series, with monthly time intervals, of the water use, change in water use, and the indicative yield. The second is as a series of maps of the water use, change in water use and indicative yield for a wet, a dry and a typical water year. These are presented below together with comments to highlight the major features of the results.

The following discussions of the predictions are necessarily very general. The predicted impacts can only be really evaluated when combined with other information. For example, the yield is only one factor that a farmer will include when deciding whether to grow an energy crop. Other factors, such as crop subsidies and the market price, will also be considered. Therefore, it is not possible, in this report, to comment on which areas of the country it is practical to grow energy crops. Similarly, when considering the issue of water use, factors such as abstractions and river habitats within the catchment will also be relevant.

5.1 Time series

To provide details of the seasonal and inter-annual variability, the model has been used to produce time series, at monthly intervals, for eight of the grid cells. The information on these cells is given in Table 14 and the locations in Figure 55.

Table 14 Locations, soil types and principal land cover of the time series grid cells

Grid cell centre easting	Grid cell centre northing	Location	HOST class	Principal land cover (% of cell)	1971-2000 annual average rainfall (mm)
415500	540500	Durham	24	grass (72%)	750
365500	405500	Lancashire	24	grass (53%)	978
495500	390500	North Lincolnshire	2	crop (62%)	591
280500	300500	West Wales	17	grass (80%)	1644
340500	285500	South Shropshire	4	grass (69%)	830
612500	285500	East Anglia	24	crop (86%)	614
455500	145500	East Hampshire	1	crop (90%)	798
299500	106500	East Devon	3	crop (40%)	883

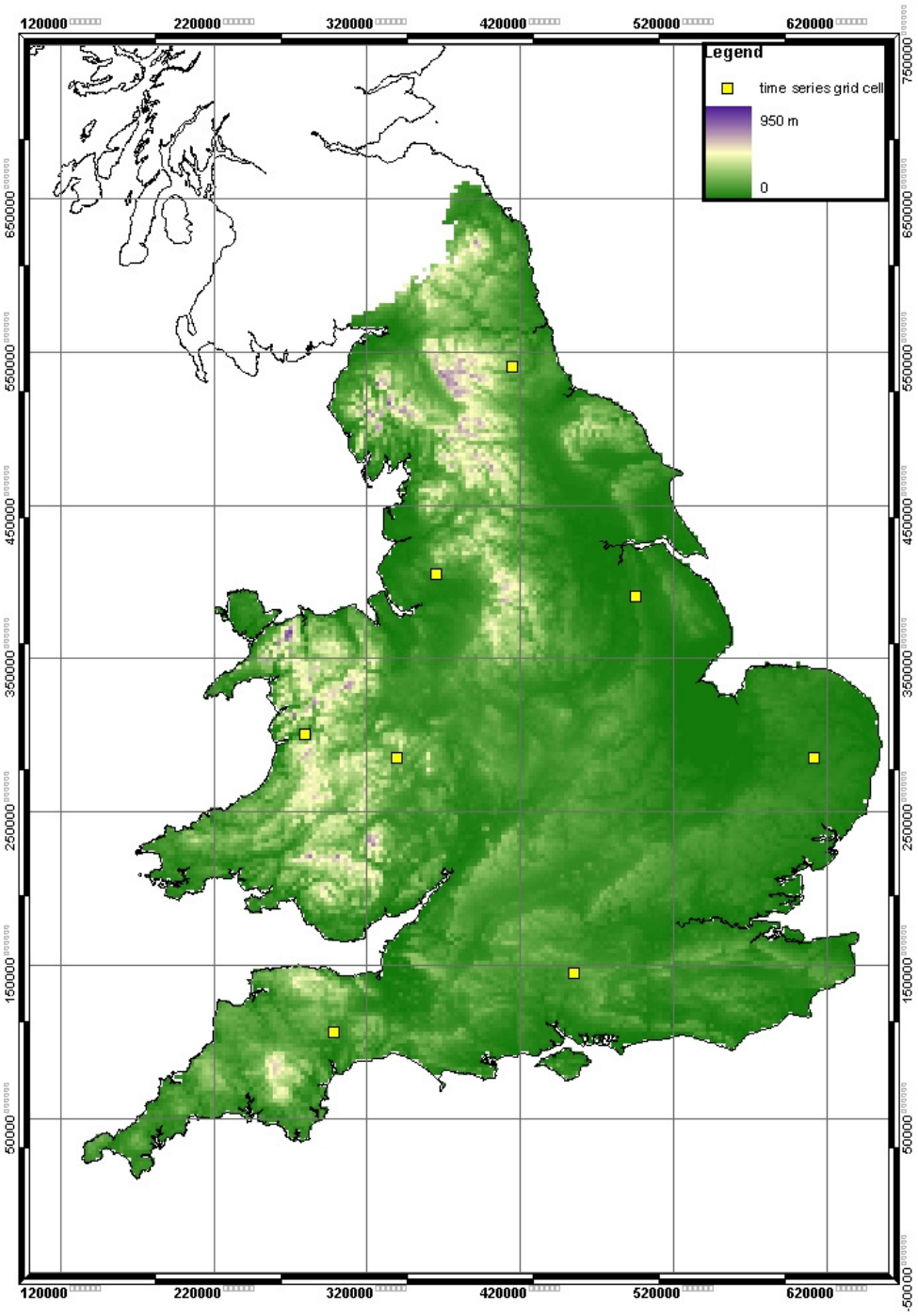

Figure 55 Locations of the model grid cells used in the time series runs

The locations were selected to give a range of soil and climatic conditions. The definitions of the HOST (soil) classes can be found in Table 11. In summary class 1 is Chalk soils, 2 soils on limestones, 3 are soils on permeable sandstone, 4 are the soils on the less permeable sandstones, 17 are soils on hard impermeable rocks and 24 are soils on slowly permeable units.

The resulting predicted water use (taken as the sum of the interception loss and the evaporation and transpiration losses from the soil and snow sublimation) for Miscanthus, switchgrass, poplar SRC and willow SRC are shown in Figures 56 to 59 inclusive. The change in water use, compared to the current land cover are shown in Figures 60 to 63, and the indicative yield, in Figures 64 to 67.

A feature of these graphs is that the poplar SRC is distinctly different to the other energy crops. This is interpreted as being due to the lack of any control on the stomata in response to the atmospheric evaporative demand. As a consequence, when soil water is available, transpiration occurs at a rapid rate which is also reflected in the rapid uptake of carbon. However, when this occurs in a low rainfall location, such as East Anglia or North Lincolnshire, the soil water is rapidly depleted and so growth is restricted. In high rainfall areas, such as west Wales, the poplar is able to exploit the available water and take up significantly more carbon than the other types of energy crop. In practice, factors not included in the model, e.g. nutrients, soil depth and exposure, are likely to limit the indicative yield.

The effect of the differences in the available water content between the soils is apparent in the results. HOST class 24 is described as slowly permeable, whilst class 17 is impermeable, thus these soils have less available water than classes, 1 (Chalk), 2 (limestone) and 3 (weakly consolidated, macroporous). Class 4 is described as strongly consolidates, non or slightly porous. Thus, the greater soil water stored is able to support higher rates of water use during periods when the potential evaporation exceeds the rainfall. This assumes that the rooting depth, up to 3 m in the case of SRC, is not limited by the soil depth. There are areas of England and Wales, notably upland areas composed of ‘hard’ rocks where this might not occur; thus further limiting the available soil water. However, it is difficult to separate the effects of the soil types from those of the rainfall, which tend to dominate the amount of water use. What is clear is that the amount of water available is predicted to have a profound effect on the indicative yield.

For the poplar and willow, the three year cycle of harvesting is discernable in the plots of the change in water use, Figures 62 and 63. The model includes the increasing height and LAI during the three year cycle and differences in the meteorological variables. The small decrease in indicative yield in the autumn is due to the leaves being shed. The range in indicative yields between the sites is greatest for the poplar due to its greater water use. All the energy crops are predicted to use less water than the current land cover in the early part of the year, particularly where grass is the principal existing land cover. This is because the energy crops do not maintain green leaves during the winter period, and thus transpiration is negligible (although interception can still take place, albeit at a reduced rate for the SRC due to the loss of canopy storage via the leaves). However, where crops are present, the effect is less marked because the canopy of winter cereals will be small during the winter, but will show rapid growth in the spring, before the energy grasses begin to develop This is illustrated in Figure 68, which compares the canopy development, indicated by the canopy height, of *Miscanthus* and winter wheat for the grid cell in East Anglia.

It is possible that the poplar and willow will use less water in the first year of the three year growth cycle. This will particularly be the case where the land cover is permanent, such as pastures, woodlands and heathland. This is demonstrated in Figure 69, which shows the predicted monthly water use and the cumulative water use for 1979 to 1981 for the grid cell in Devon. This grid cell was chosen as it has a mid-range annual average rainfall, a fairly porous soil, and has a comparatively high potential evaporation because it is located in the south. In the first five months, the evaporation from the energy crops is initially similar and is then less than the existing land cover, because the canopies of the energy crops is not present. As the canopies begins to develop, the evaporation rates increase so that, for the last five months

of the year the evaporation rates are comparable. After one year the cumulative evaporation for the willow SRC and the energy grasses are similar to each other and slightly less than the current land use. However, the cumulative evaporation from poplar SRC is slightly greater than the existing land cover. This pattern is repeated each year for the energy grasses because these have an annual harvest cycle. For the SRC, the monthly evaporation rates from poplar SRC always exceed that of the existing land cover, whilst that for willow is only less in three months of the year. At the end of the second year, during which the canopy of the SRC develops further, the cumulative evaporation from willow SRC is about the same as from the existing land cover whilst that from poplar SRC is significantly greater. During the third year, these differences are accentuated so that, when the SRC is harvested, the cumulative evaporation of the SRC exceeds that of the current land use; implying a significantly higher evaporation rate during the third year.

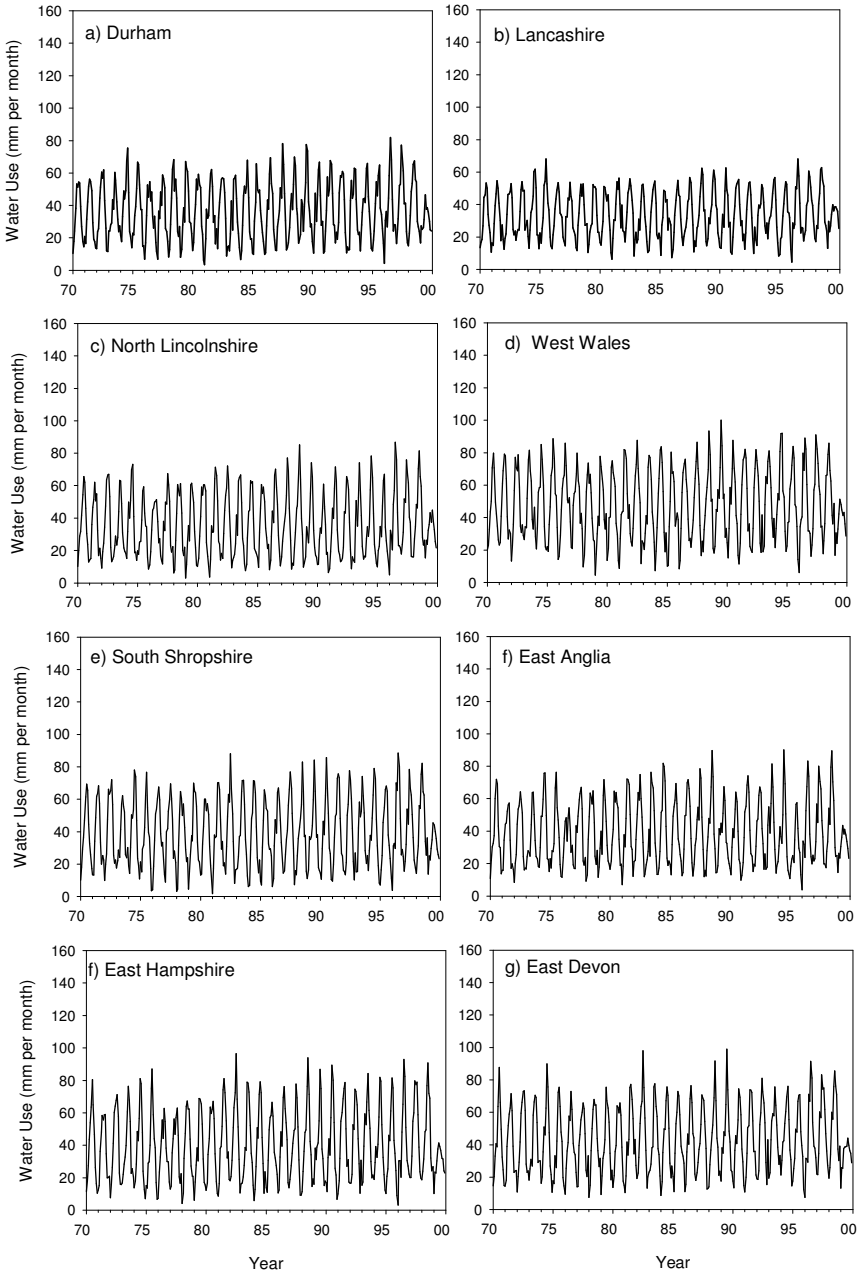

Figure 56 Time series of predicted water use of *Miscanthus* 1971-2000

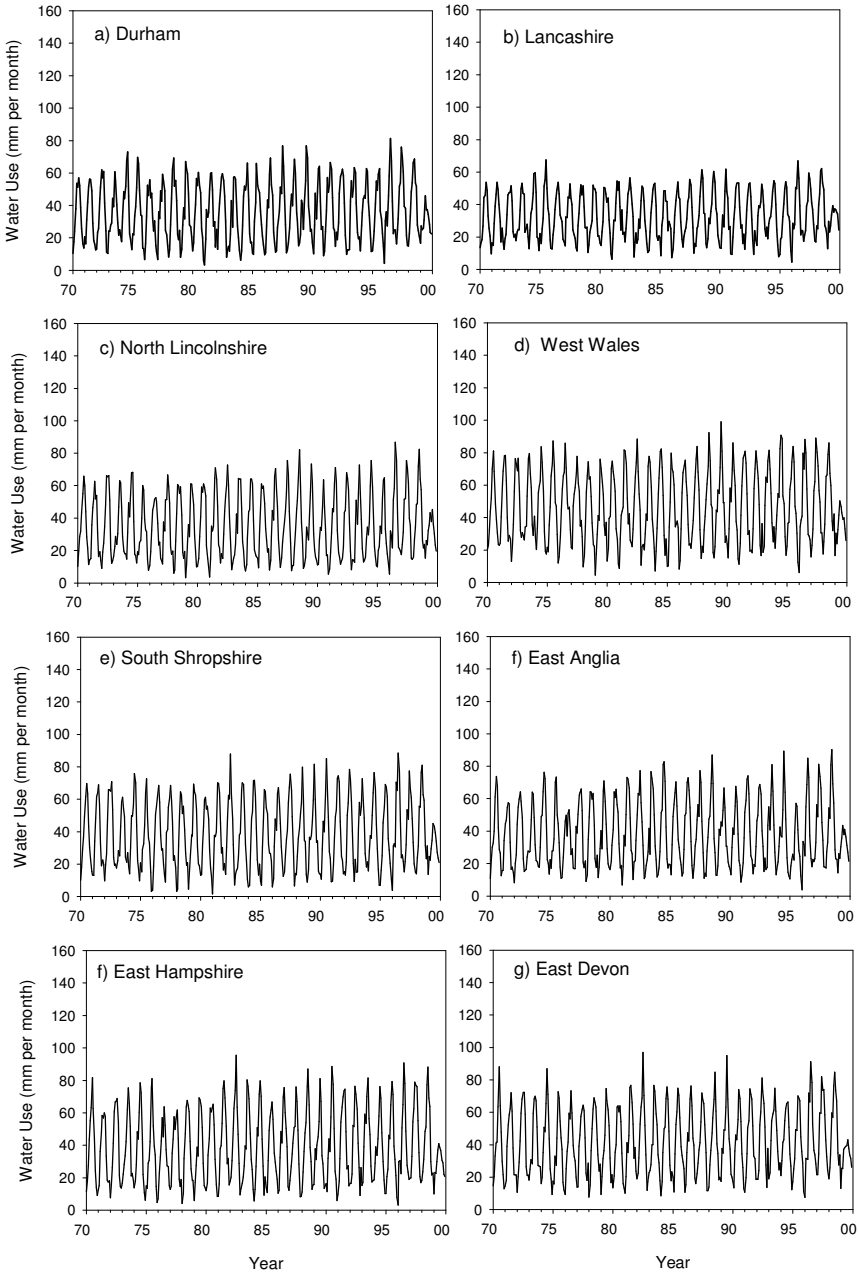

Figure 57 Time series of predicted water use of switchgrass 1971-2000

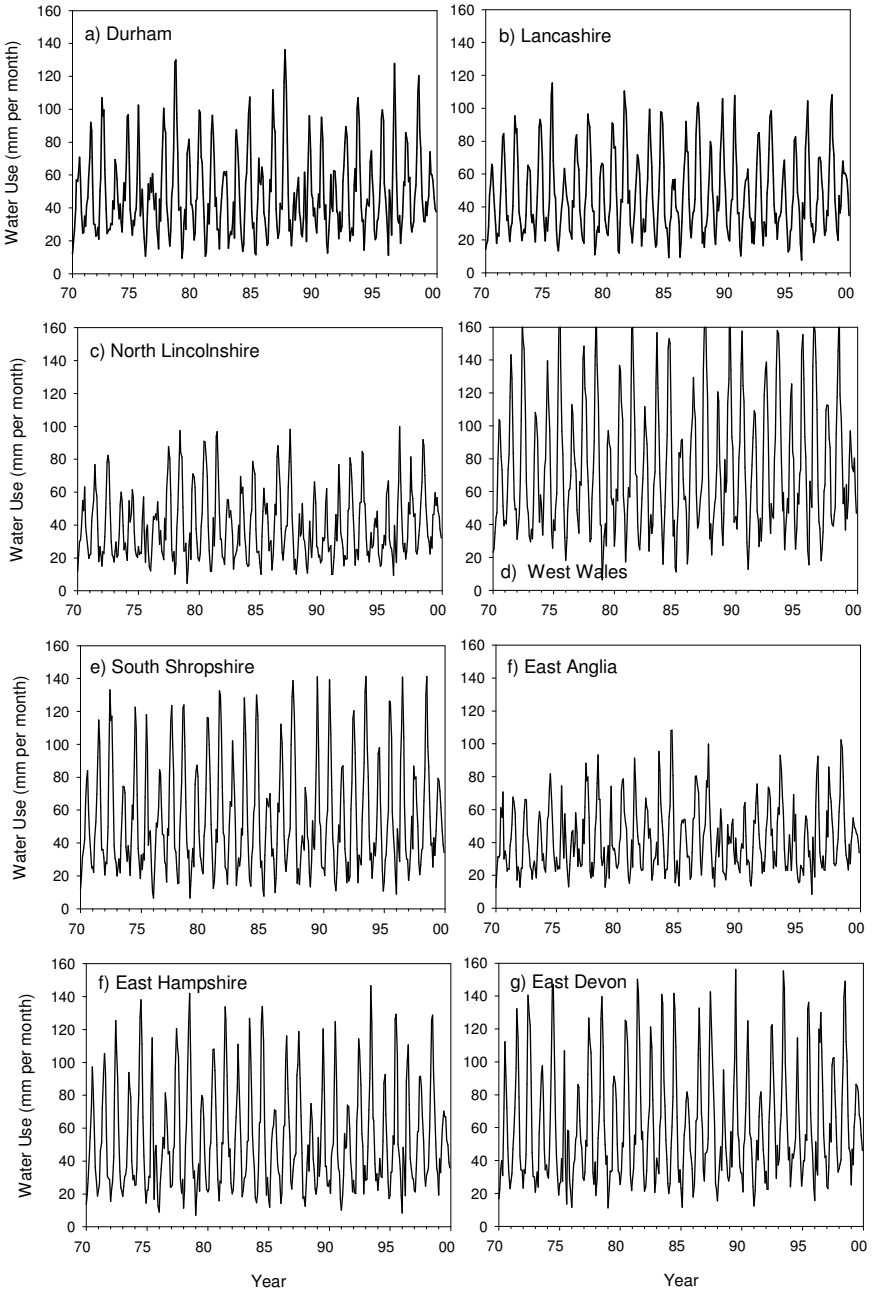

Figure 58 Time series of predicted water use of poplar SRC 1971-2000

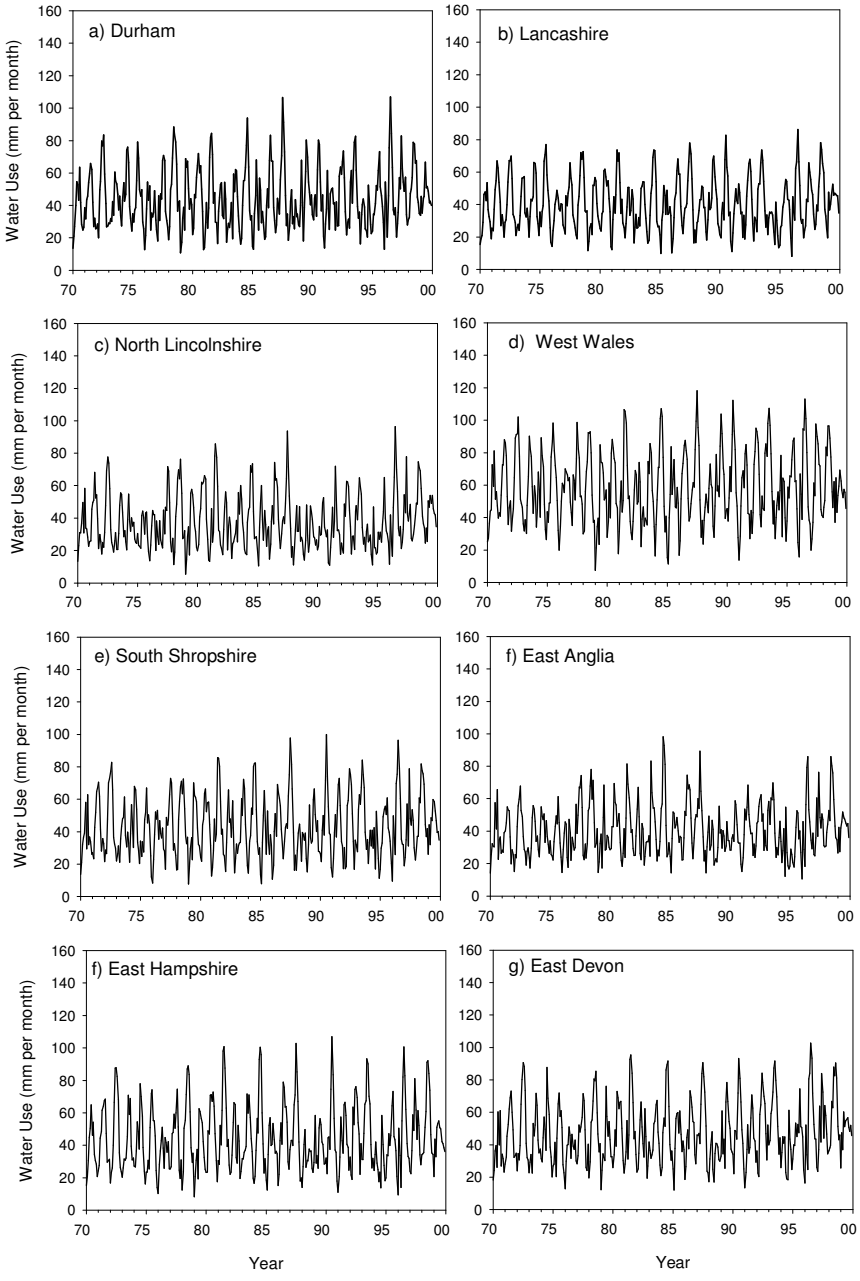

Figure 59 Time series of predicted water use of willow SRC 1971-2000

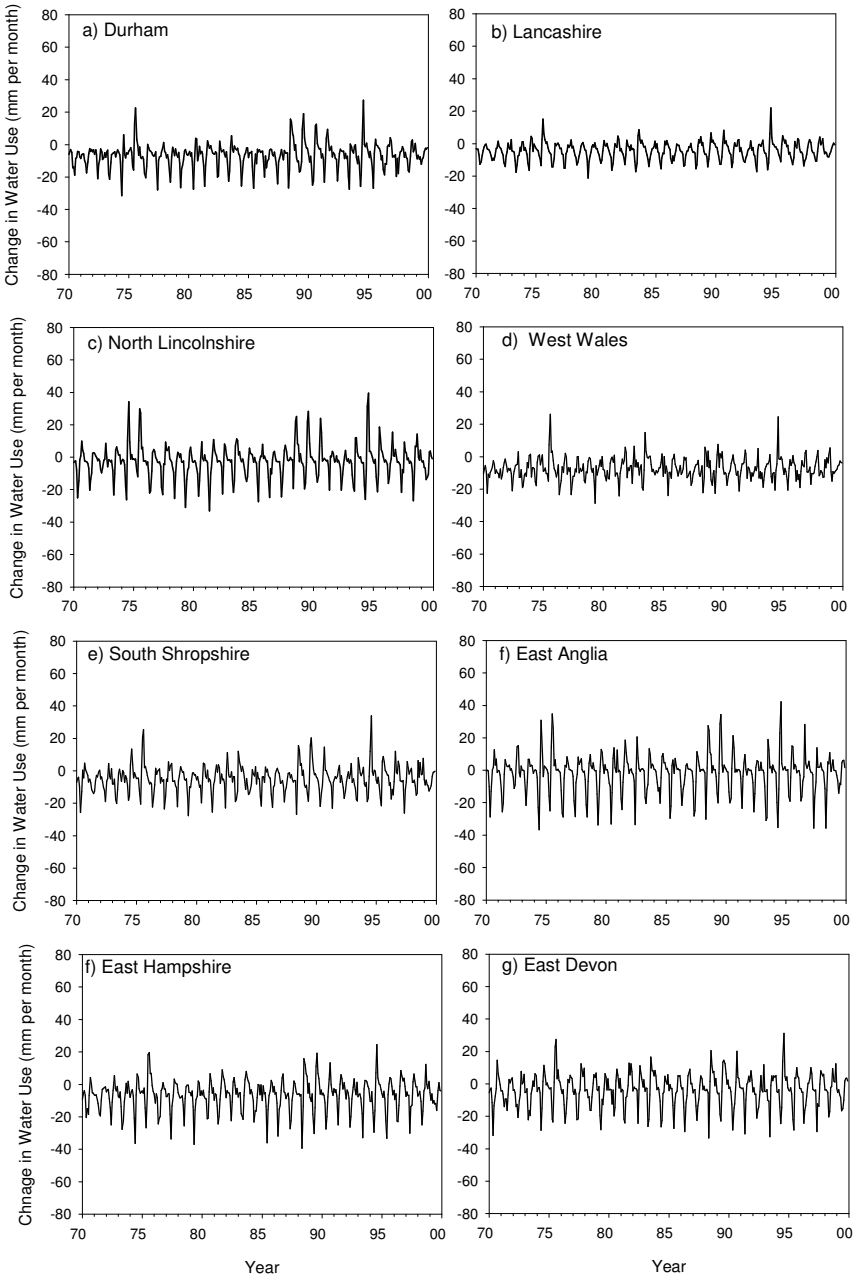

Figure 60 Time series of predicted change in water use of *Miscanthus* compared to the current land use 1971-2000

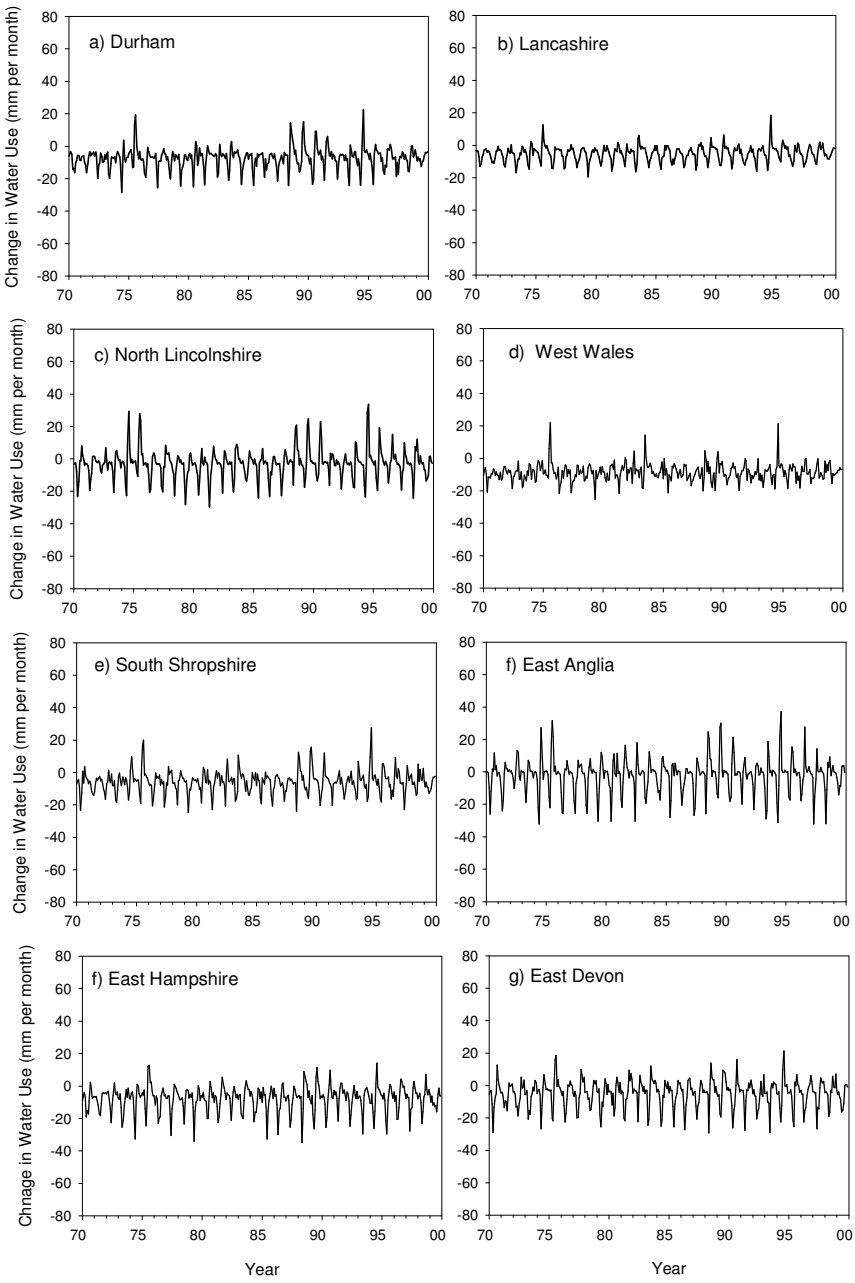

Figure 61 Time series of predicted change in water use of switchgrass compared to the current land use 1971-2000

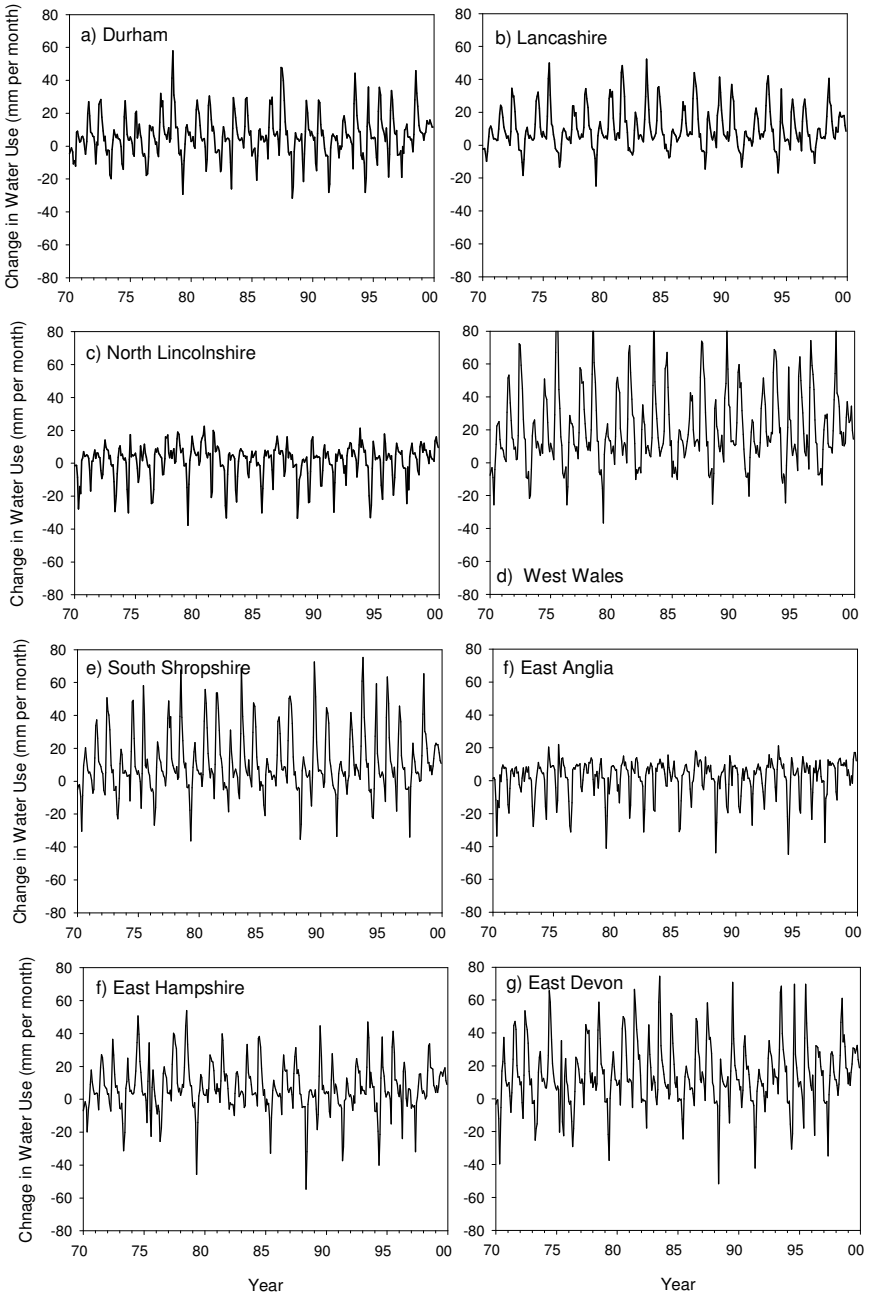

Figure 62 Time series of predicted change in water use of poplar SRC compared to the current land use 1971-2000

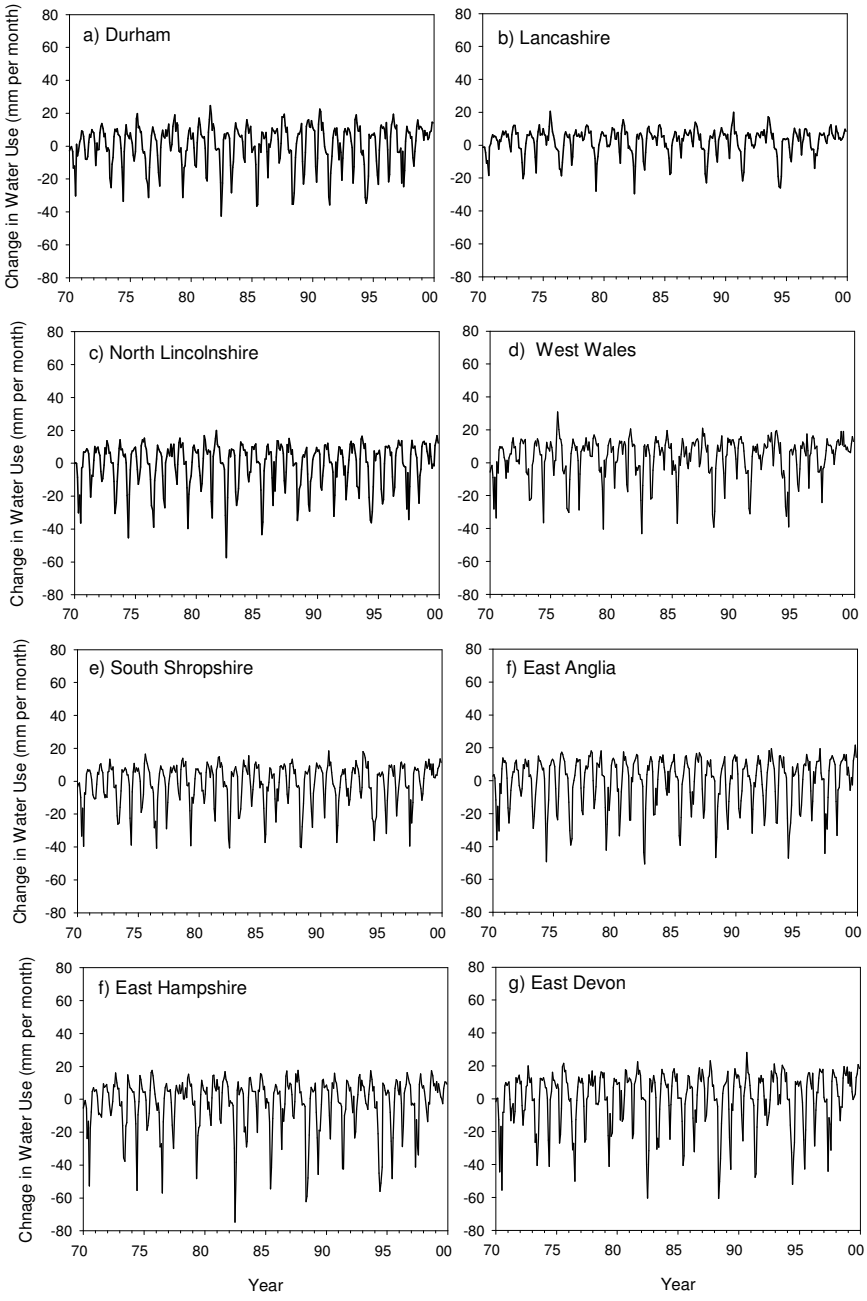

Figure 63 Time series of predicted change in water use of willow SRC compared to the current land use 1971-2000

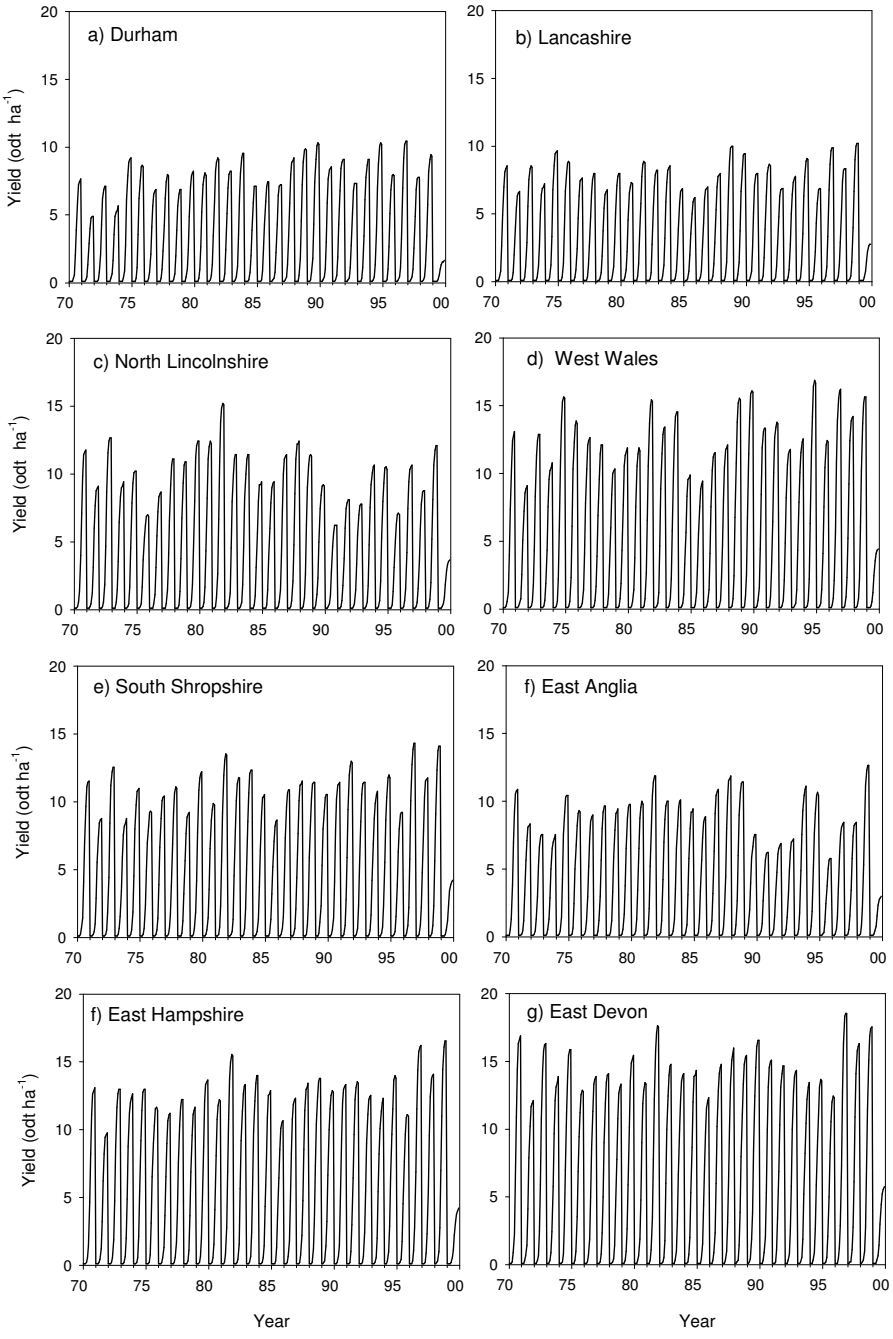

Figure 64 Time series of predicted indicative yield of *Miscanthus* 1971-2000

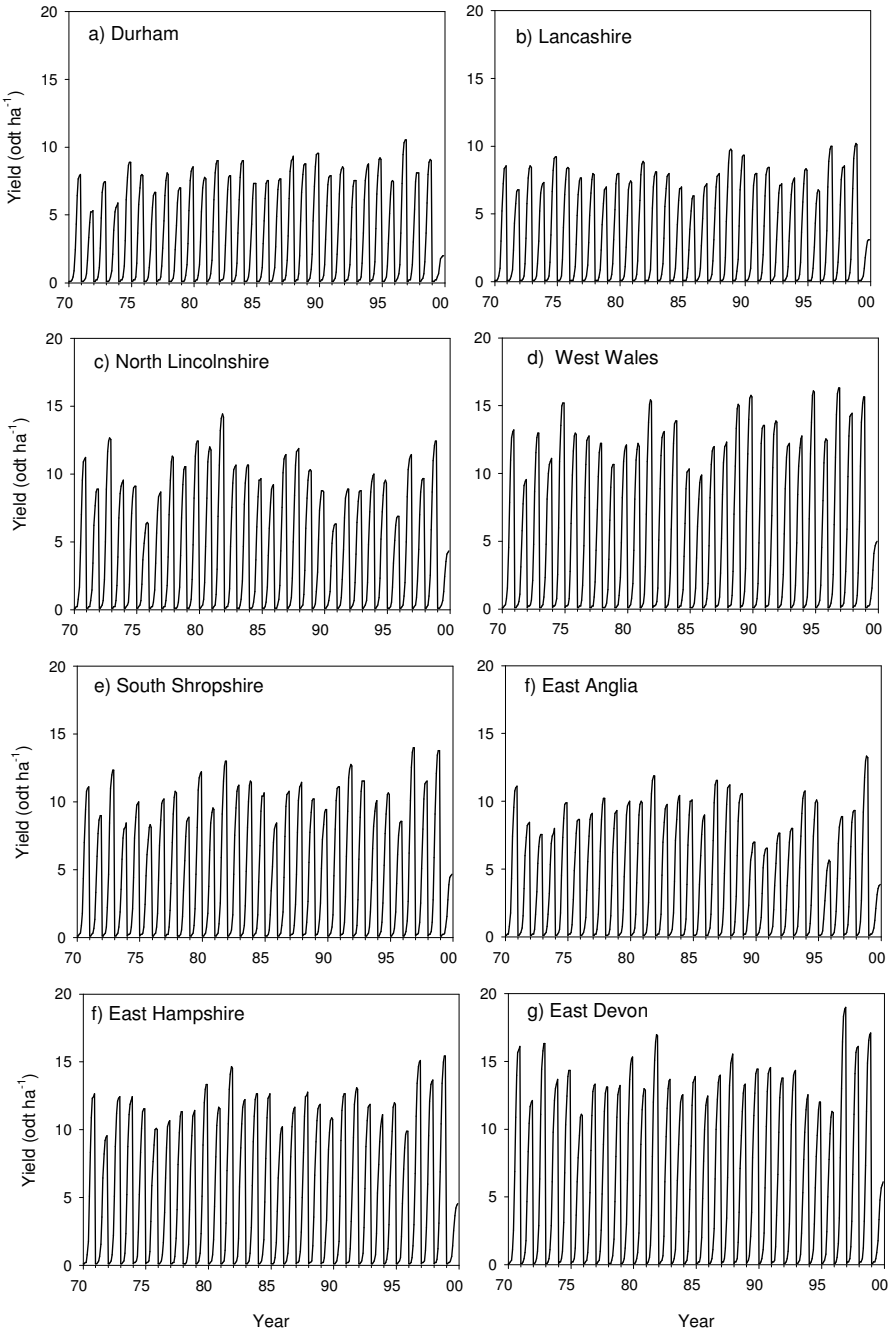

Figure 65 Time series of predicted indicative yield of switchgrass 1971-2000

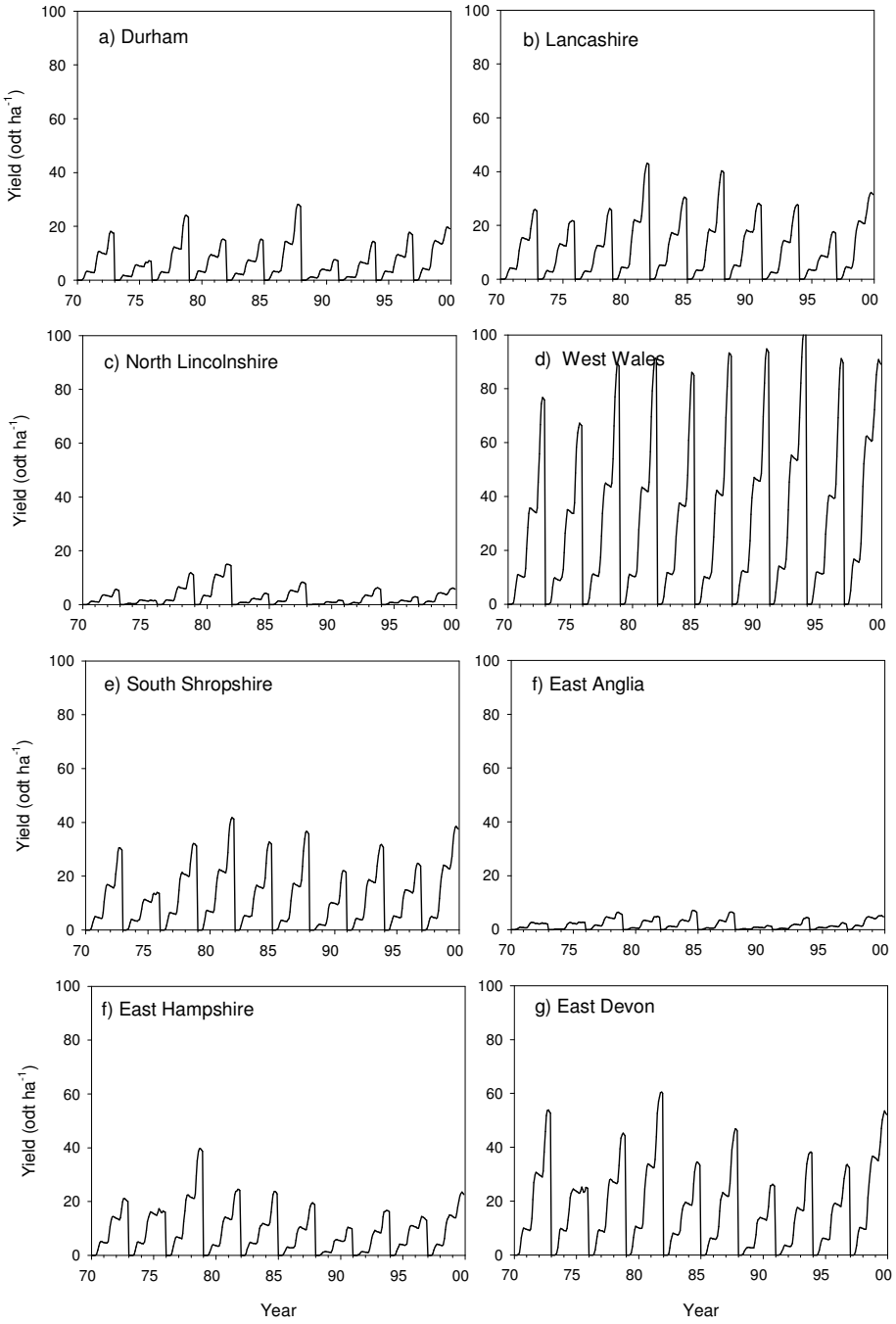

Figure 66 Time series of predicted indicative yield of poplar SRC 1971-2000

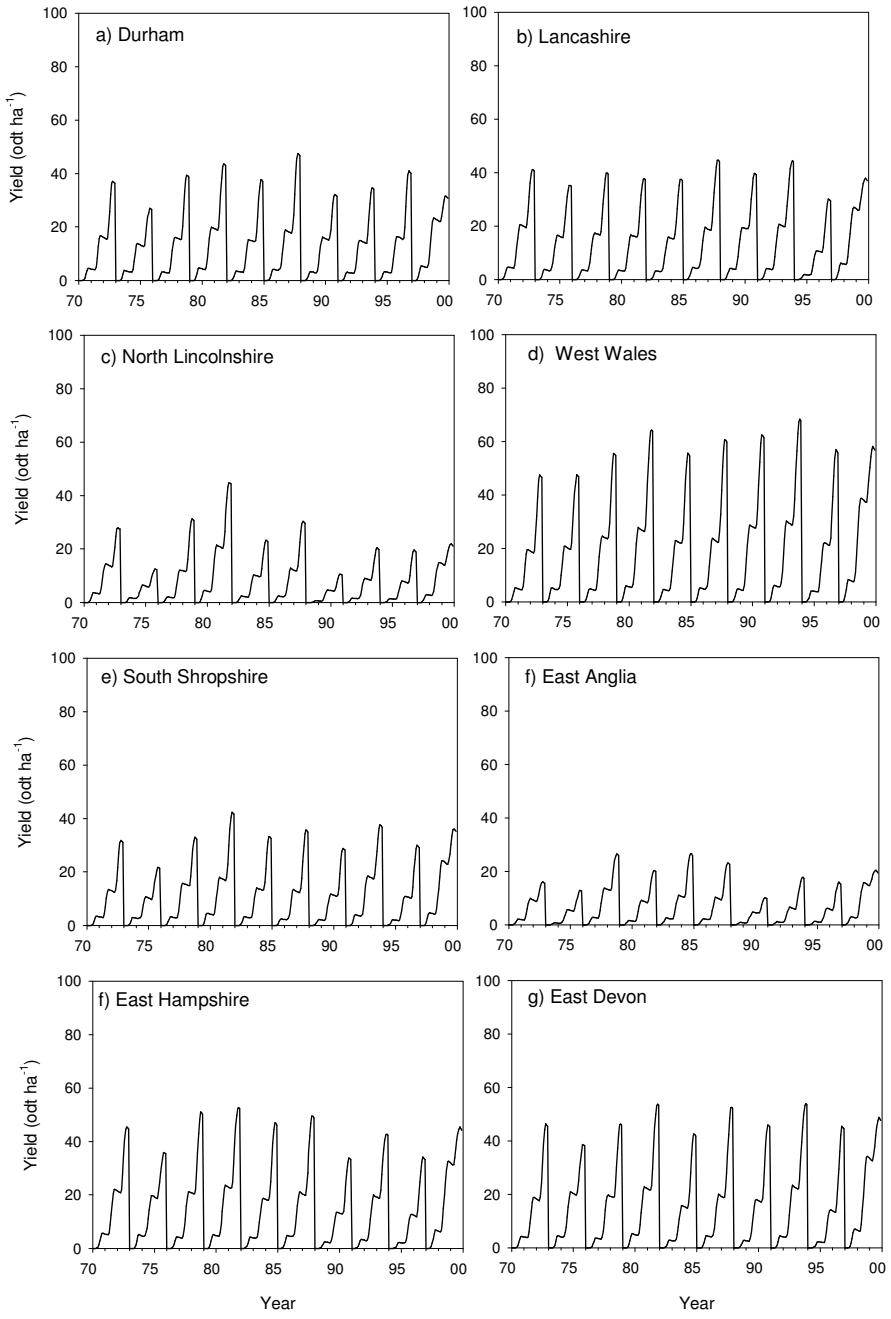

Figure 67 Time series of predicted indicative yield of willow SRC 1971-2000

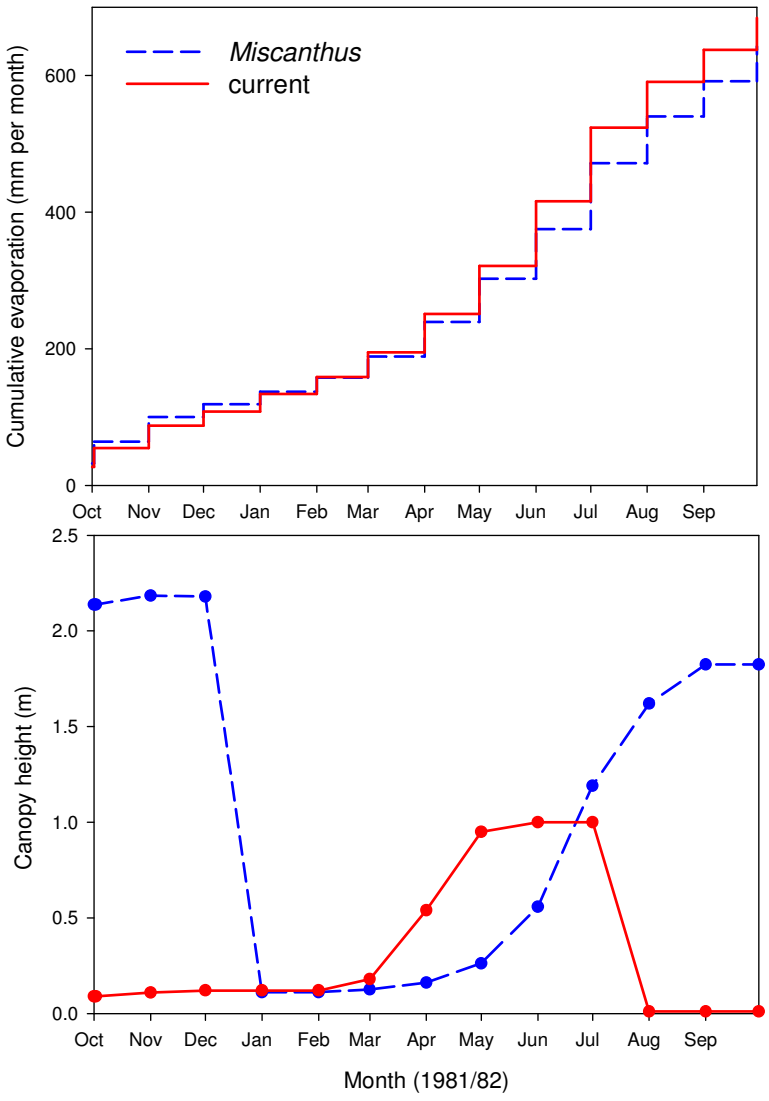

Figure 68 Comparison of the predicted canopy development and evaporation of *Miscanthus* and winter wheat

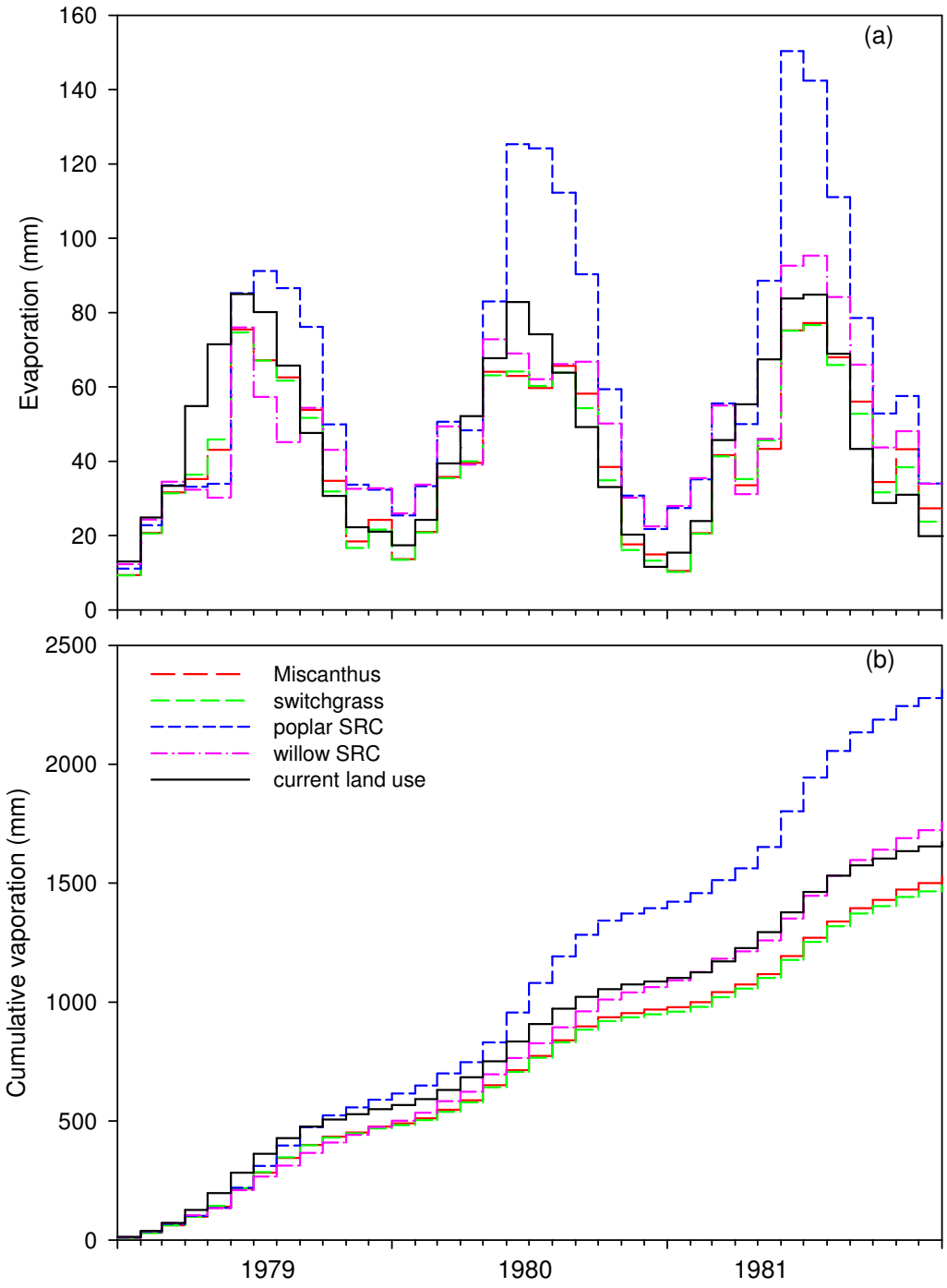

Figure 69 Comparison of the predicted monthly water use of the energy crops and current land use 1979-1981

5.2 Spatial distributions

The predicted spatial distributions of the water use, change in water use and the indicative yield are presented as 39 maps. Figures 70 to 84 give the water use for the current land cover and the four energy crops for water years with typical, high and low rainfall. Figures 85 to 96 give the change in water use if the current land cover were replaced with one of the energy crops, for water years with typical, high and low rainfall. Figures 97 to 109 give the indicative yield for the four energy crops for years with typical, high and low rainfall.

These results should be interpreted with some caution, and the potential impacts of the uncertainties, discussed in Section 4.6, should be considered. Comparing the impact of the variations in annual rainfall on a given energy crop can probably be done with some confidence. Less confidence should be given to comparing one crop with another. This is because the results are dependent on the values of the parameters used for a given crop and thus the uncertainties are higher.

The numerical model is a simplification of the real world in terms of both the processes included in the model, the degree of complexity with which these processes are described and the variation in the model parameters. For example, no variation of the type of hybrids available for a given crop is included. Similarly, the variability of the soils at a scale of less than one kilometre is not included. The sources of uncertainty and the potential impact on the predictions are discussed in Section 4.6

In generating these maps, the energy crops have been excluded from replacing the existing land cover if the latter is in the form of urban or water. The urban areas are apparent in most of the maps, notably because the evaporation (i.e. water use) is low for this land cover type. Water bodies will tend to have high evaporation rates.

5.2.1 Water use

The values predicted by the model for the existing land cover are generally within the range that would be expected. The effect of the hydraulic properties of the different soils on the water use of the vegetation is quite noticeable. In general, the predicted values in some areas, notably in Wales, may be a bit high because the model assumes all soils permit roots to grow to a depth of up to 3 m. This is incorrect on the upland areas, where the soils are almost certainly thinner. However, these are also areas of higher rainfall, see Figure 109, which will tend to reduce the error arising from overestimating the size of the soil water store.

In general the land use of England and Wales has a small proportion of woodland, so the majority of the change will be due to the energy crop replacing grassland or crops.

The water use for the SRC is likely to be a worse case scenario because the annual water use is based on the last year in the cropping cycle, i.e. when the canopy is greatest. It is possible that, during the first year of the cropping cycle, the water use might be less than or comparable to the existing land cover, as discussed in Section 5.1

The results show that, when soil water is plentiful, poplar SRC uses considerably more water than the current land cover. This is mainly due to two properties of the poplar. The first is that it is comparatively deep rooting, up to 3m; a feature it shares with the willow SRC. As a result, replacing crops or grass, which generally root to around 1 and 0.8 m respectively, results in greater water use as the SRC can maintain higher transpiration rates for longer during the summer, before depletion of the soil water store begins to limit transpiration. In the case of the poplar, the lack of any stomatal response to high

atmospheric evaporative demand, as reported by Hall *et al.* (1996), means that the water use is always very high, only being limited by soil water availability. Thus, the model predicts very high transpiration rates, particularly in the spring and early summer. However, where low summer rainfall and/or a limited soil water store occur, then these high transpiration rates cannot be maintained because soil water stress soon limits the transpiration. This then reduces the indicative yield from this crop (Figures 97, 101 and 105). The measurements upon which the stomatal conductance sub-model was parameterised were made at two site in the UK and on five clones at one site and one at the other. Thus the basis on which this prediction is made is sound. It is possible that other varieties of poplar may have, or could be bred to have, stomatal controls that are more sensitive to the atmospheric demand and thus reduce this water use There are indications that this is possible in results reported by Price *et al.* (submitted) who describe measurements, including transpiration and stomatal conductance, which imply that the stomatal conductance was responding to changes in the atmospheric demand. Nevertheless, the conclusion is that, for the varieties on which the measurements were based, poplar SRC plantations will have a much higher water use than the existing land cover, whilst willow SRC will have a higher water use although the difference will not be as great.

The model predicts that the water use of *Miscanthus* and switchgrass is likely to be less than the existing land cover (figures 85, 86 89, 90, 93 and 94). This is probably as a result of the canopy development occurring later in the season than for the current land cover types. The numerical model includes a parameter which is the temperature, below which, photosynthesis ceases. For C_3 grasses, i.e. grassland and crops, this is given the value of 0 °C, whilst for C_4 grasses, i.e. *Miscanthus* and switchgrass, the value is 13 °C. Thus growth, and so transpiration, is initiated later in the year. Similarly with the lower temperatures at the end of the calendar year, photosynthesis and transpiration cease earlier. The presence of the full canopy until it is harvested, which is assumed to occur at the end of the calendar year, means that little downward radiation reaches the soil surface or any understory; nor does the wind. The result is to reduce losses from the soil water store, due to evaporation and transpiration, at this time of year. To a certain extent this might be counterbalanced by the higher interception losses from the canopy.

During the summer months, when the evaporation rate can exceed the rate of rainfall, the greater rooting depth of the energy grasses compared to the existing land cover, with the exception of trees, gives them access to more water stored in the soil with the result that they can maintain a higher rate of transpiration.

The model does not include any understory, although this was present, in the form of native grasses, in the field of *Miscanthus* at Richard's Castle. The presence of an understory would have the effect of increasing the water use from energy grass crops as it would be able to transpire during the first part of the year, before competition from the crop over took it. Unfortunately there are no measurements of the water use of an energy grass through a full year. In this project we have made measurements of soil water and evaporation for a period of several months, focussing on the summer when the transpiration and evaporation rates would be highest. In effect, we have used the numerical model to extrapolate these results to cover the full seasonal cycle. Further measurements are needed to confirm this prediction.

5.2.2 Indicative yield

Price *et al.* (2004) have used a simple model to predict the yield of *Miscanthus* across England and Wales. The resulting predictions are broadly in agreement with those of this study. A notable exception is in terms of the impact of the hydraulic properties of the Chalk on the predicted indicative yield. Price *et al.* (2004) predict that the yield will be reduced whilst this study suggests that they will not. This discrepancy is explained by the different way the two models represent the Chalk. In this study, the parameterisation is such as to permit evaporation to be supported at a higher rate by soil water being drawn up from depths significantly (several metres) below the root zone. This phenomena has been observed in many studies of soil water on the Chalk, e.g. Wellings 1984.

It should be noted that, for the SRC, the indicative yield is determined by the woody biomass as the model has simulated leaf fall, which occurs prior to the assumed harvest date.

The impact of a variety of factors is apparent in the maps of predicted indicative yield. The indicative yield of both *Miscanthus* and switchgrass declines northwards as a consequence of the lower temperatures and less solar radiation, as would be expected as these are quasi-temperate grasses. This trend is less marked for the SRC which are more tolerant of these factors.

The different soil types, mainly because of the differences in the ability of the soils to store water, are also reflected in the predicted indicative yields. This is clearly illustrated in the south east of England (Figures 97 to 100), where the soils of the London basin, dominantly clays, have less ability to store water than those of the surrounding Chalk outcrops of the Downs. This strongly indicates that soils with a high soil water storage will produce the higher indicative yields. It can be inferred from these predictions that indicative yields in the areas of England and Wales with low rainfall, see Figure 109, may be limited by water availability.

Poplar SRC is predicted to have low indicative yields in much of the midlands and east of England. This is as a result of its lack of any mechanism to limit transpiration when the atmospheric demand is high. As a consequence it uses up the stored soil water very rapidly which restricts growth for much of the year. It is only in areas of high rainfall, see Figure 109, that poplar SRC are likely to be viable.

All the energy crops are vulnerable to drought, Figures 105 to 108. Despite their deeper rooting, the willow and poplar SRC are predicted to be more affected. This is probably as a result of the *Miscanthus* and switchgrass being quasi-temperate grasses and thus more tolerant of drought through a higher water efficiency.

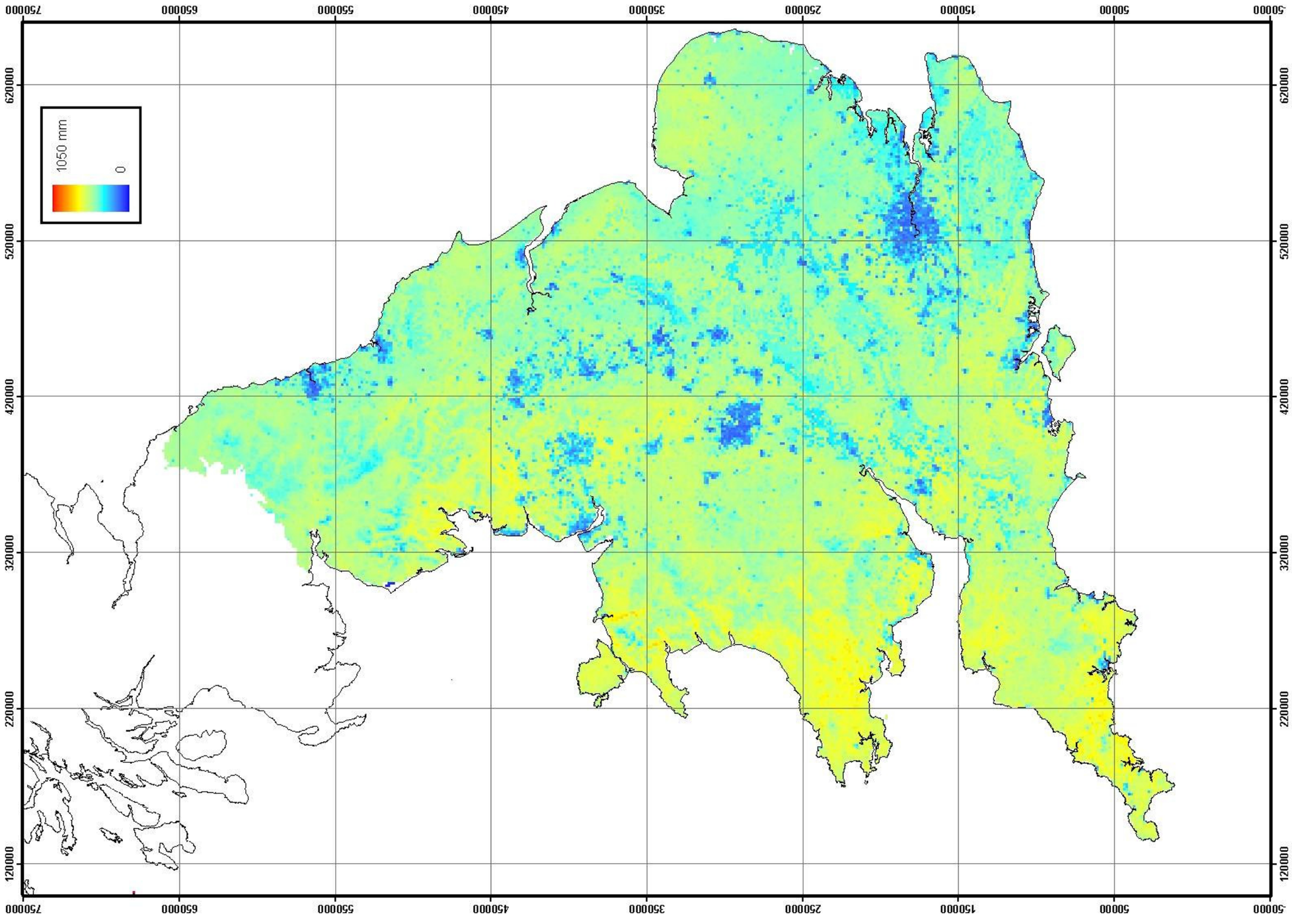

Figure 70 Predicted spatial distribution of the annual water use of the current land cover during a water year with typical rainfall (1981/82)

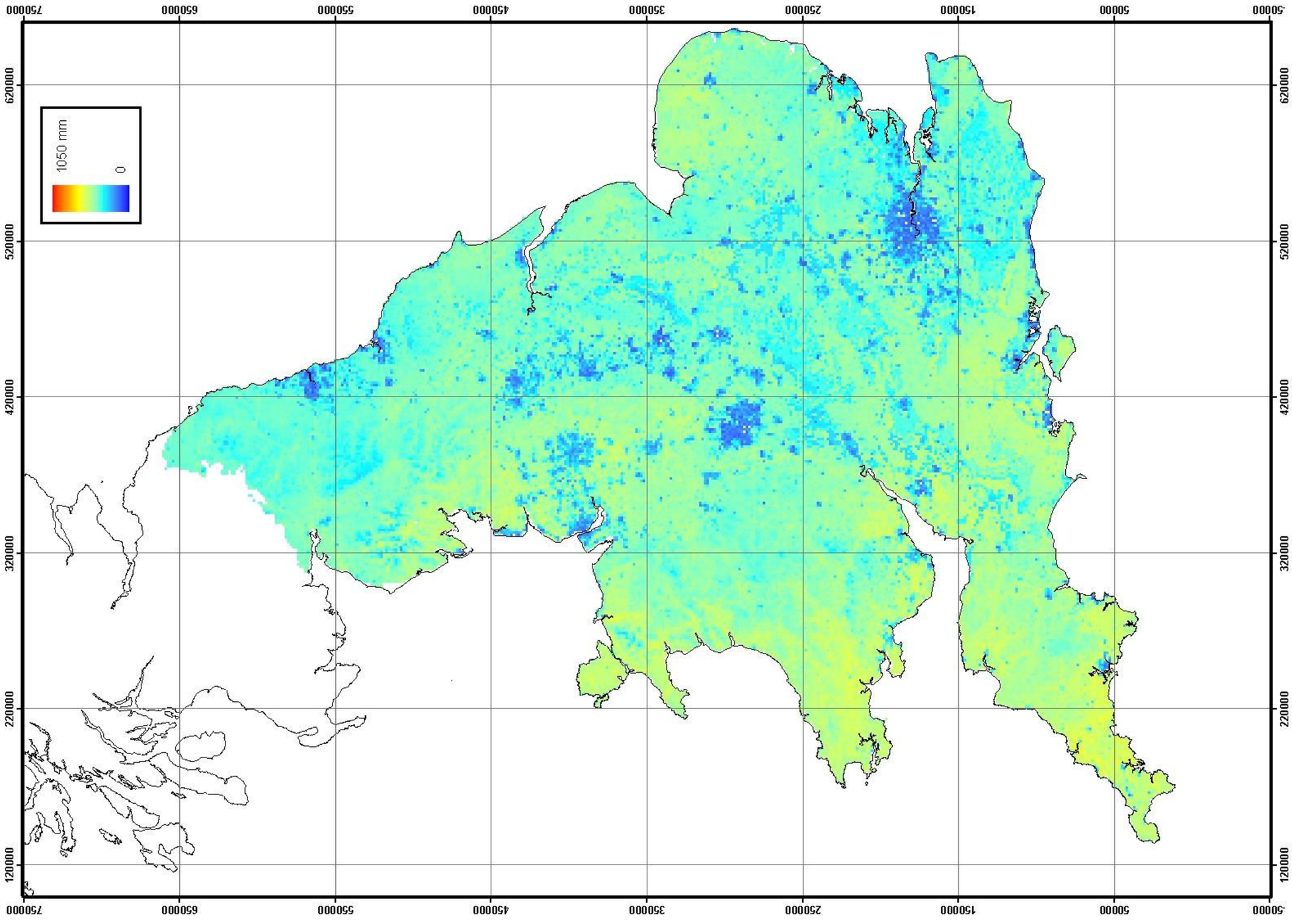

Figure 71 Predicted spatial distribution of the annual water use of *Miscanthus* during a water year with typical rainfall (1981/82)

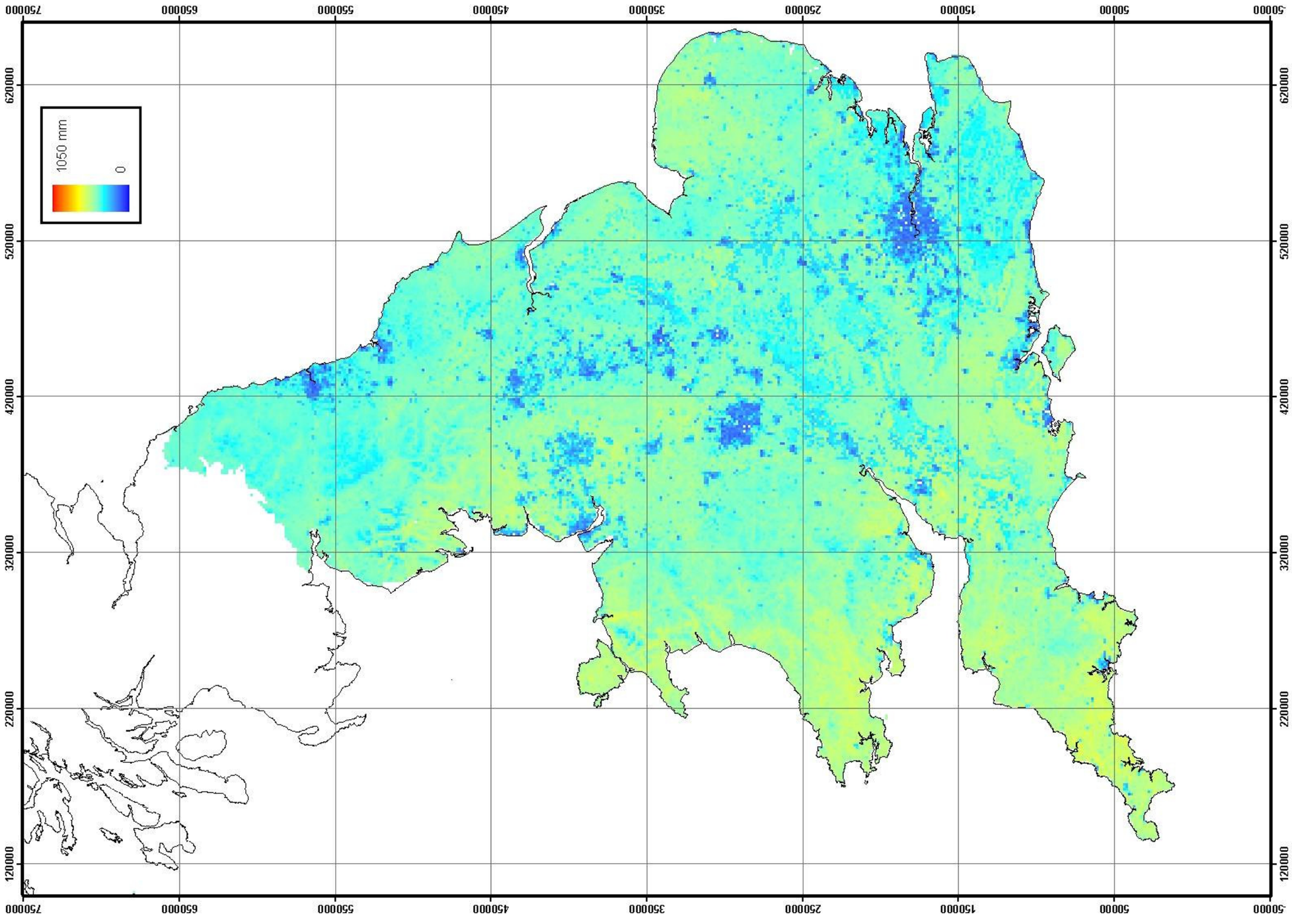

Figure 72 Predicted spatial distribution of the annual water use of switchgrass during a water year with typical rainfall (1981/82)

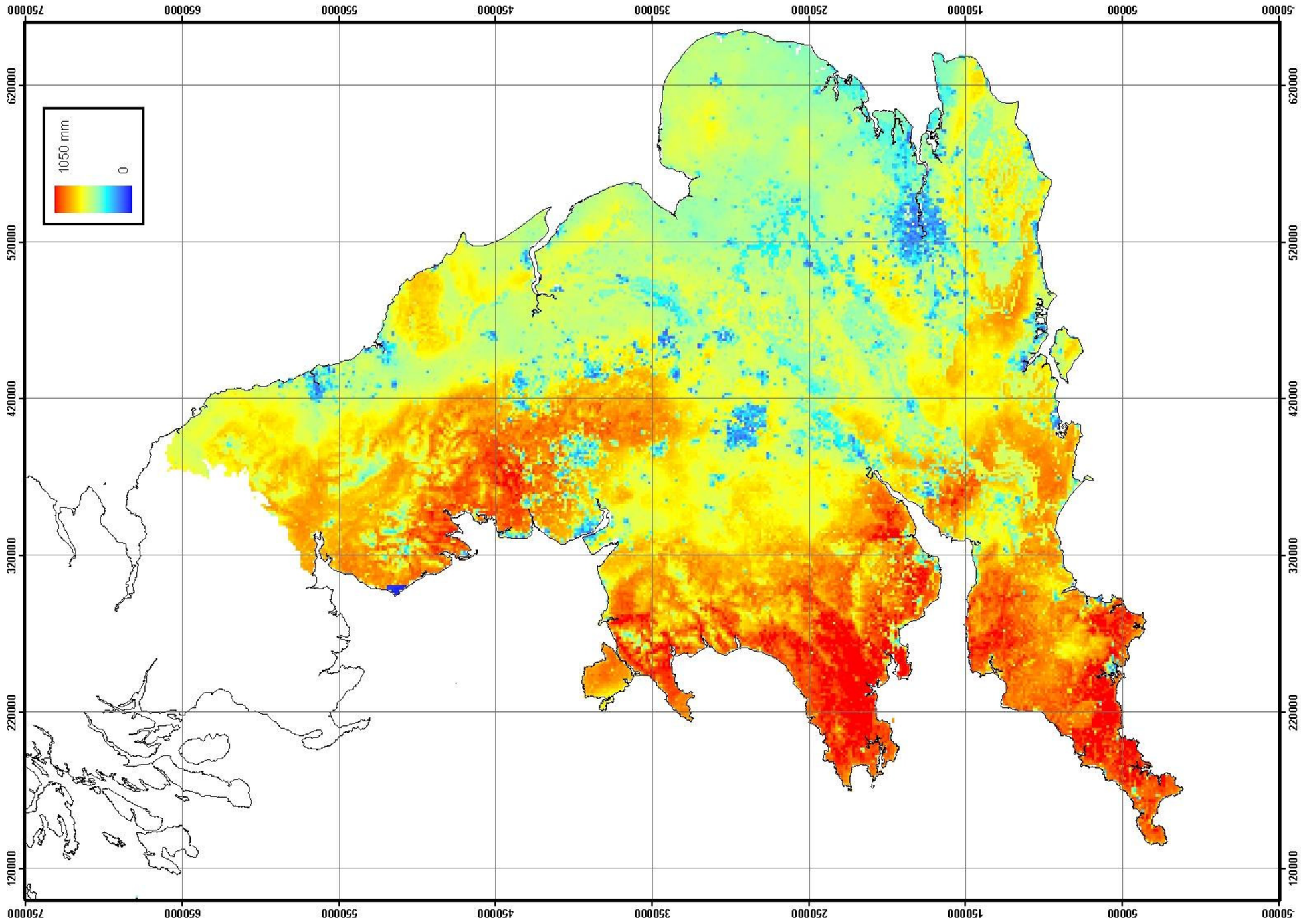

Figure 73 Predicted spatial distribution of the annual water use of poplar SRC during a water year with typical rainfall (1981/82)

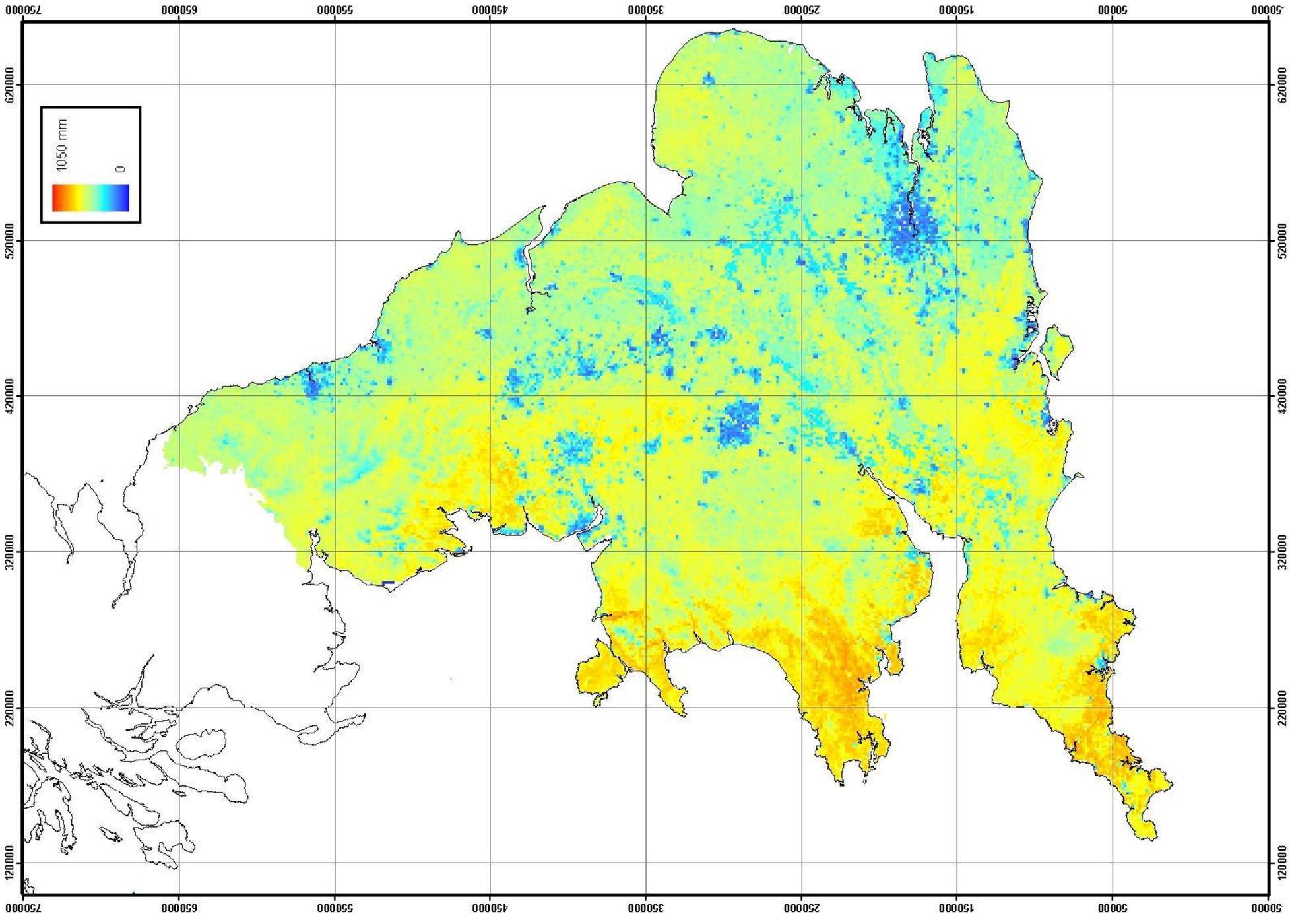

Figure 74 Predicted spatial distribution of the annual water use of willow SRC during a water year with typical rainfall (1981/82)

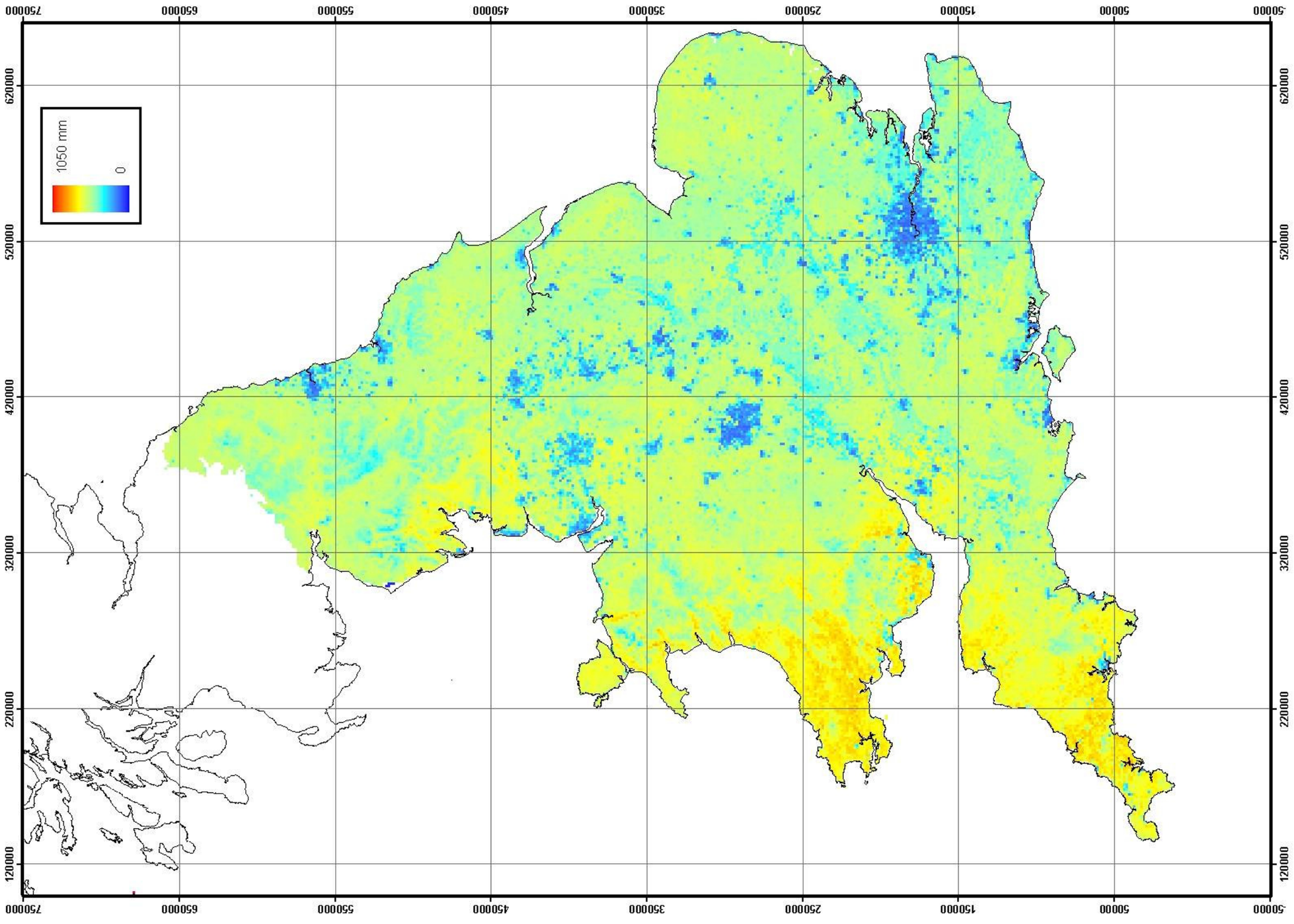

Figure 75 Predicted spatial distribution of the annual water use of the current land cover during a water year with high rainfall (1987/88)

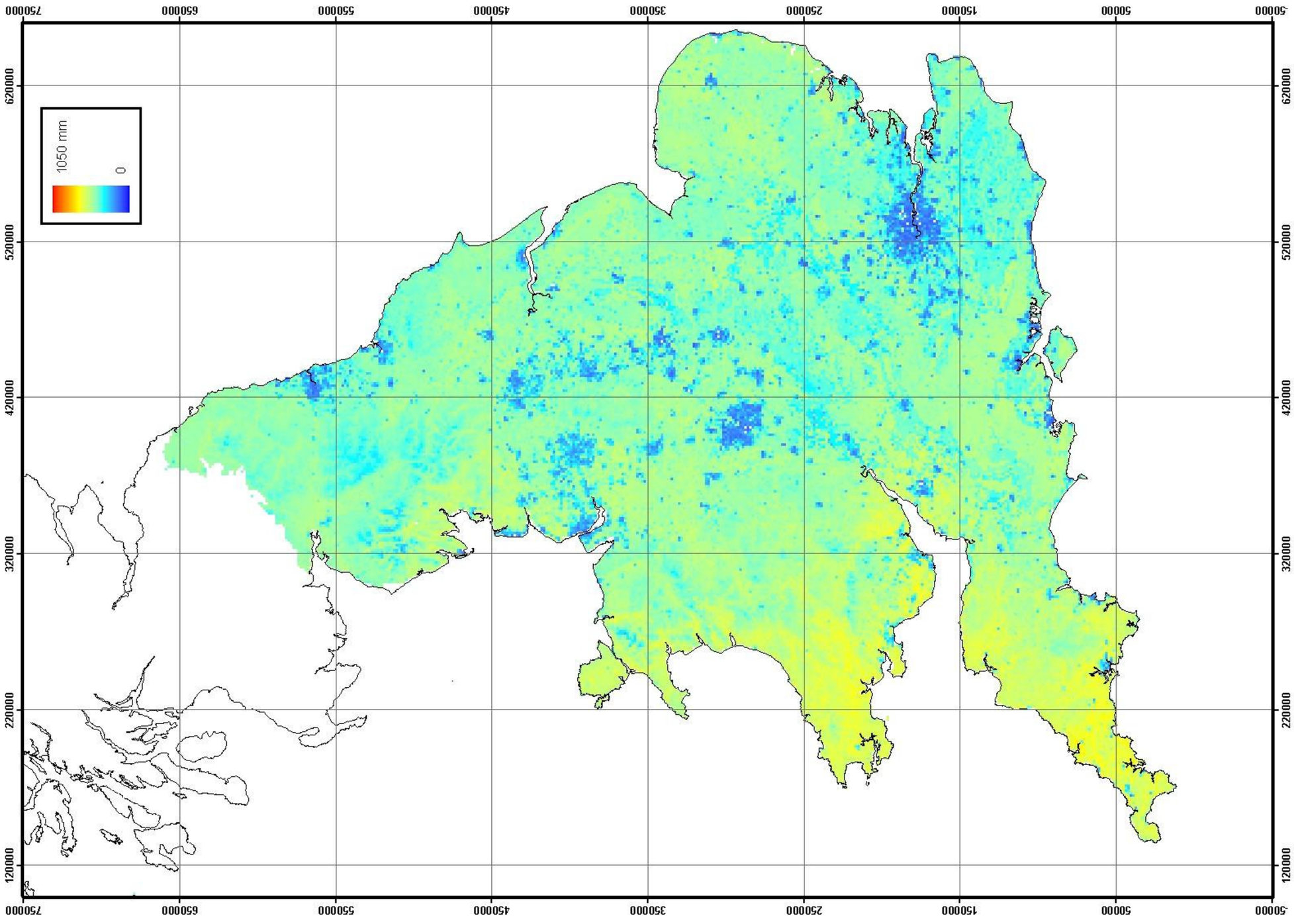

Figure 76 Predicted spatial distribution of the annual water use of *Miscanthus* during a water year with high rainfall (1987/88)

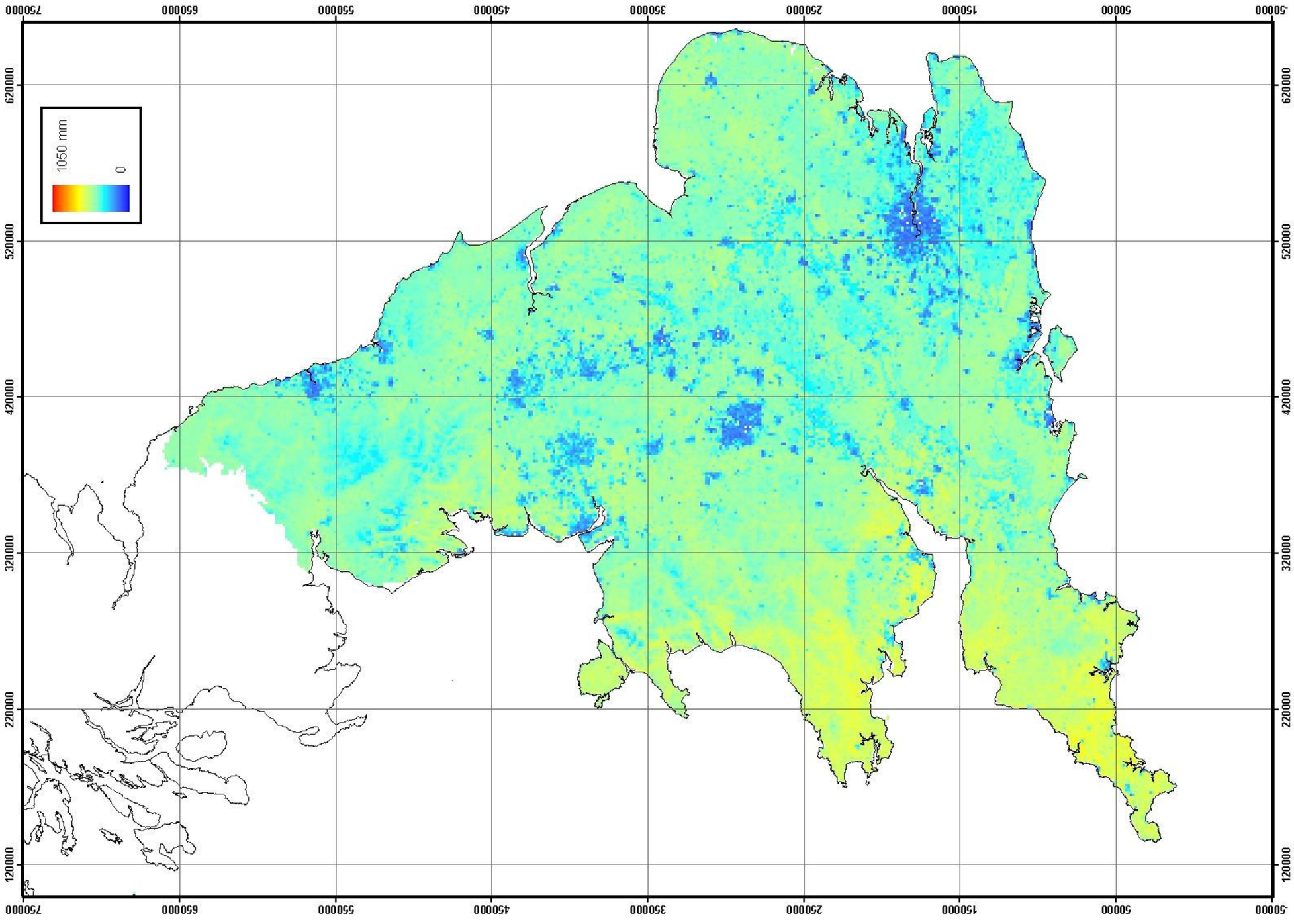

Figure 77 Predicted spatial distribution of the annual water use of switchgrass during a water year with high rainfall (1987/88)

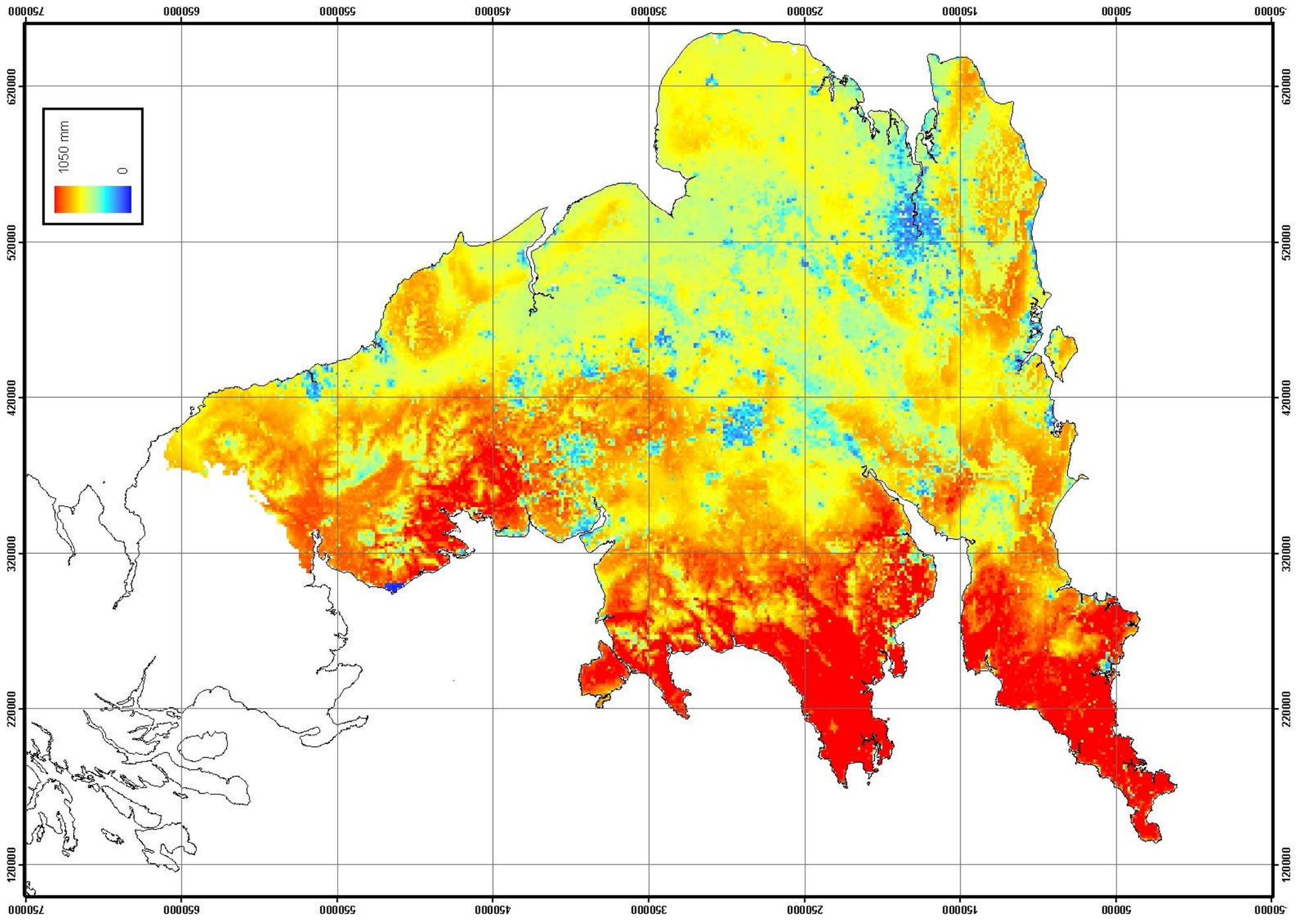

Figure 78 Predicted spatial distribution of the annual water use of poplar SRC during a water year with high rainfall (1987/88)

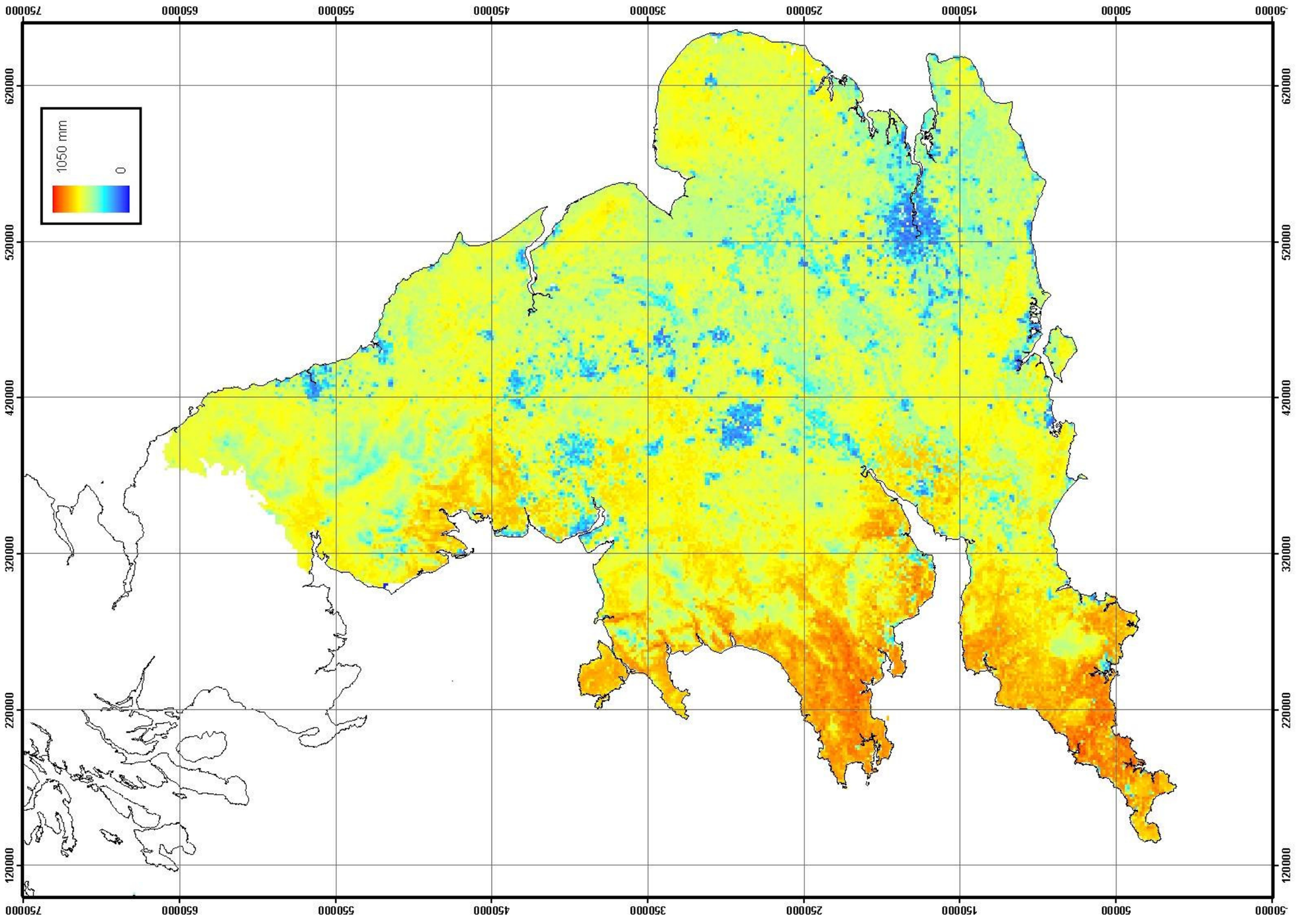

Figure 79 Predicted spatial distribution of the annual water use of the willow SRC during a water year with high rainfall (1987/88)

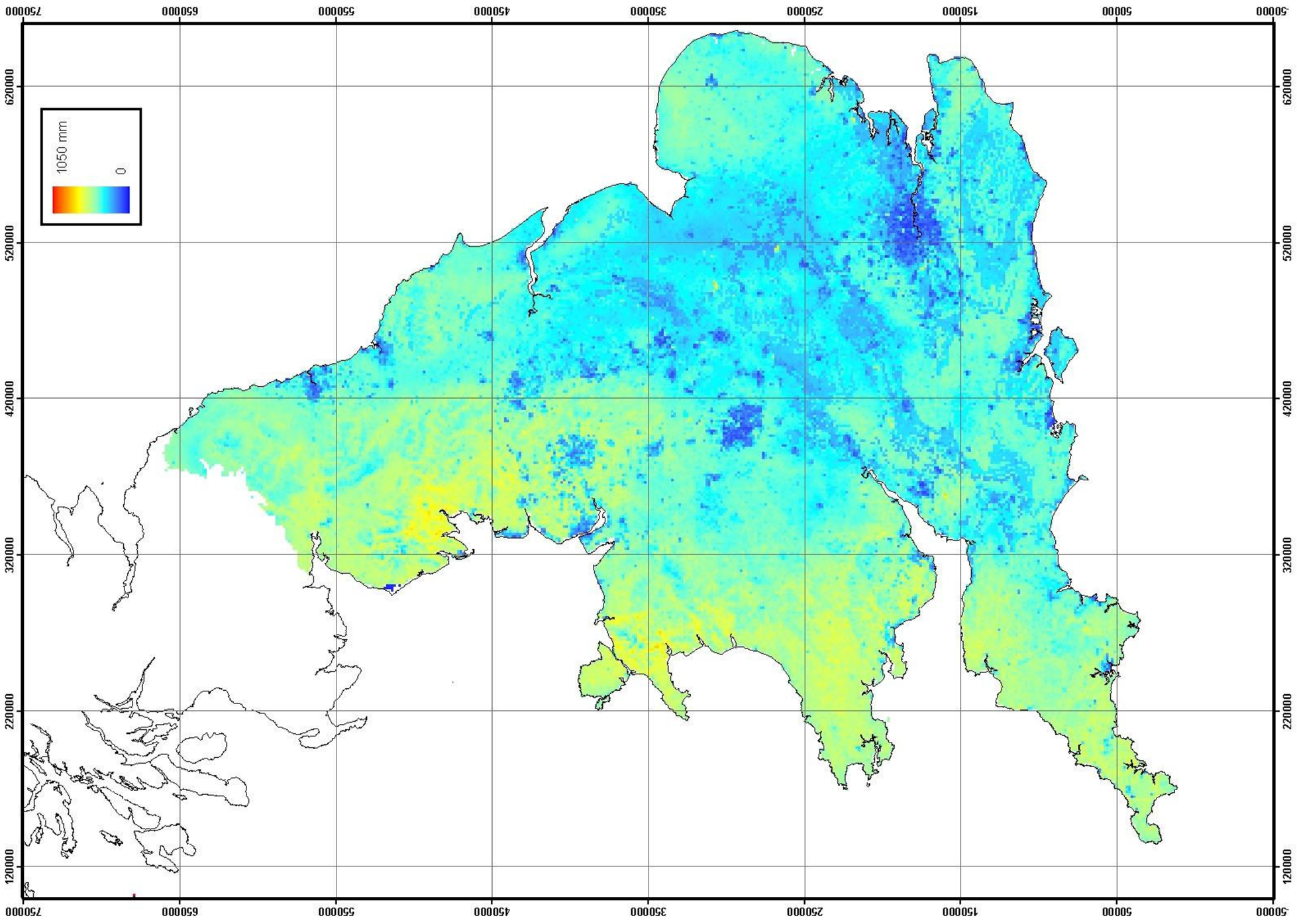

Figure 80 Predicted spatial distribution of the annual water use of the current land cover during a water year with low rainfall (1975/76)

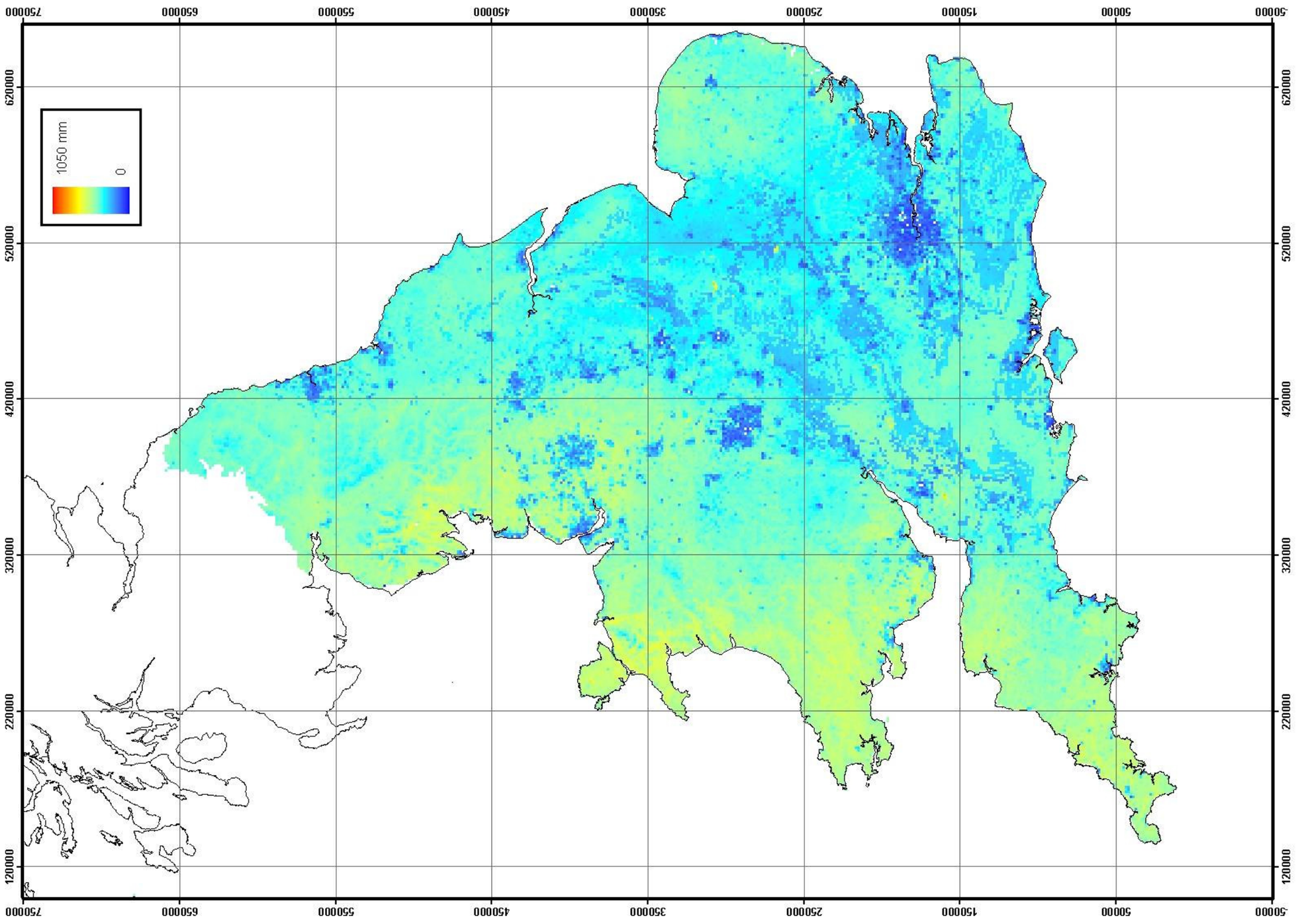

Figure 81 Predicted spatial distribution of the annual water use of *Miscanthus* during a water year with low rainfall (1975/76)

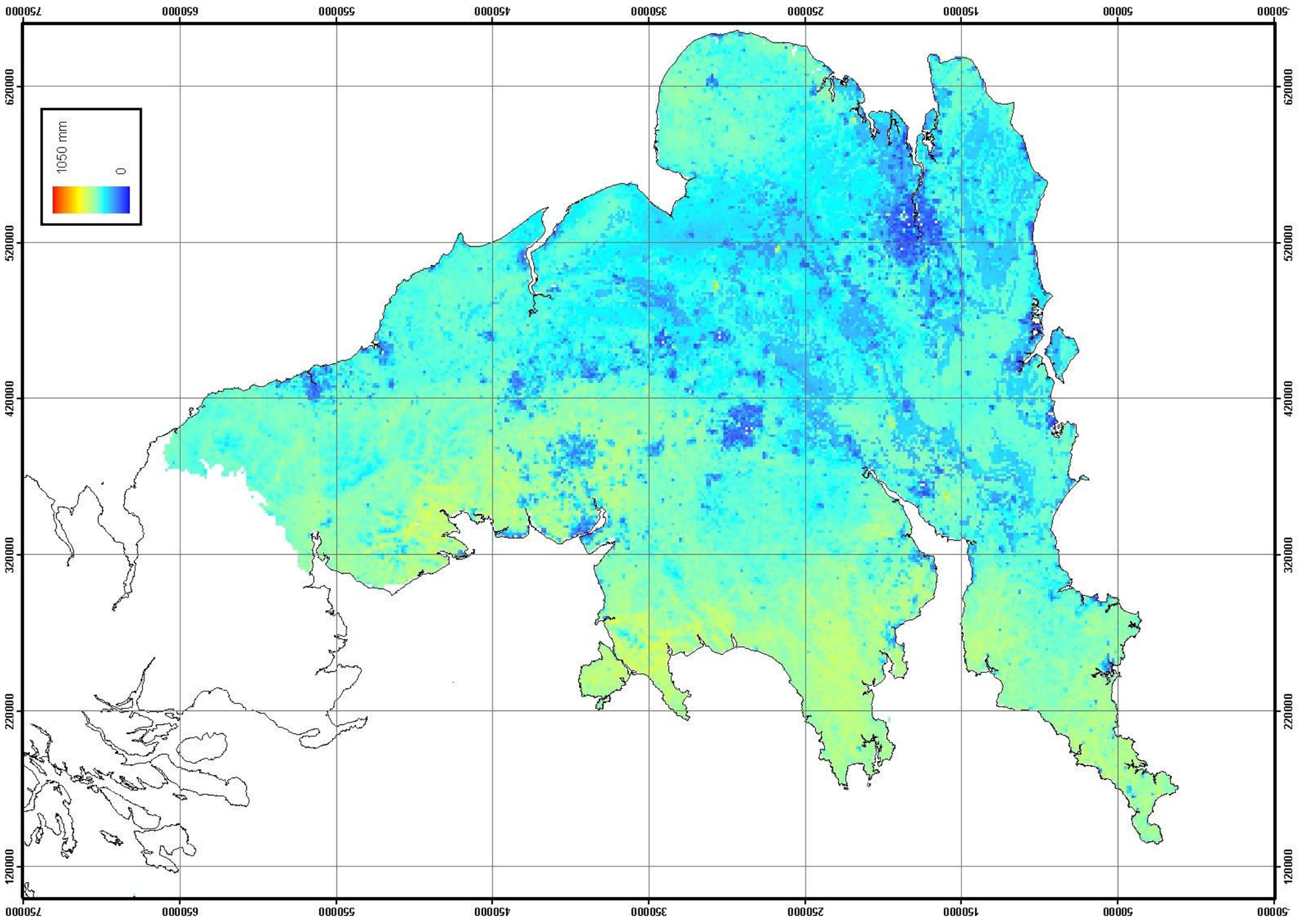

Figure 82 Predicted spatial distribution of the annual water use of switchgrass during a water year with low rainfall (1975/76)

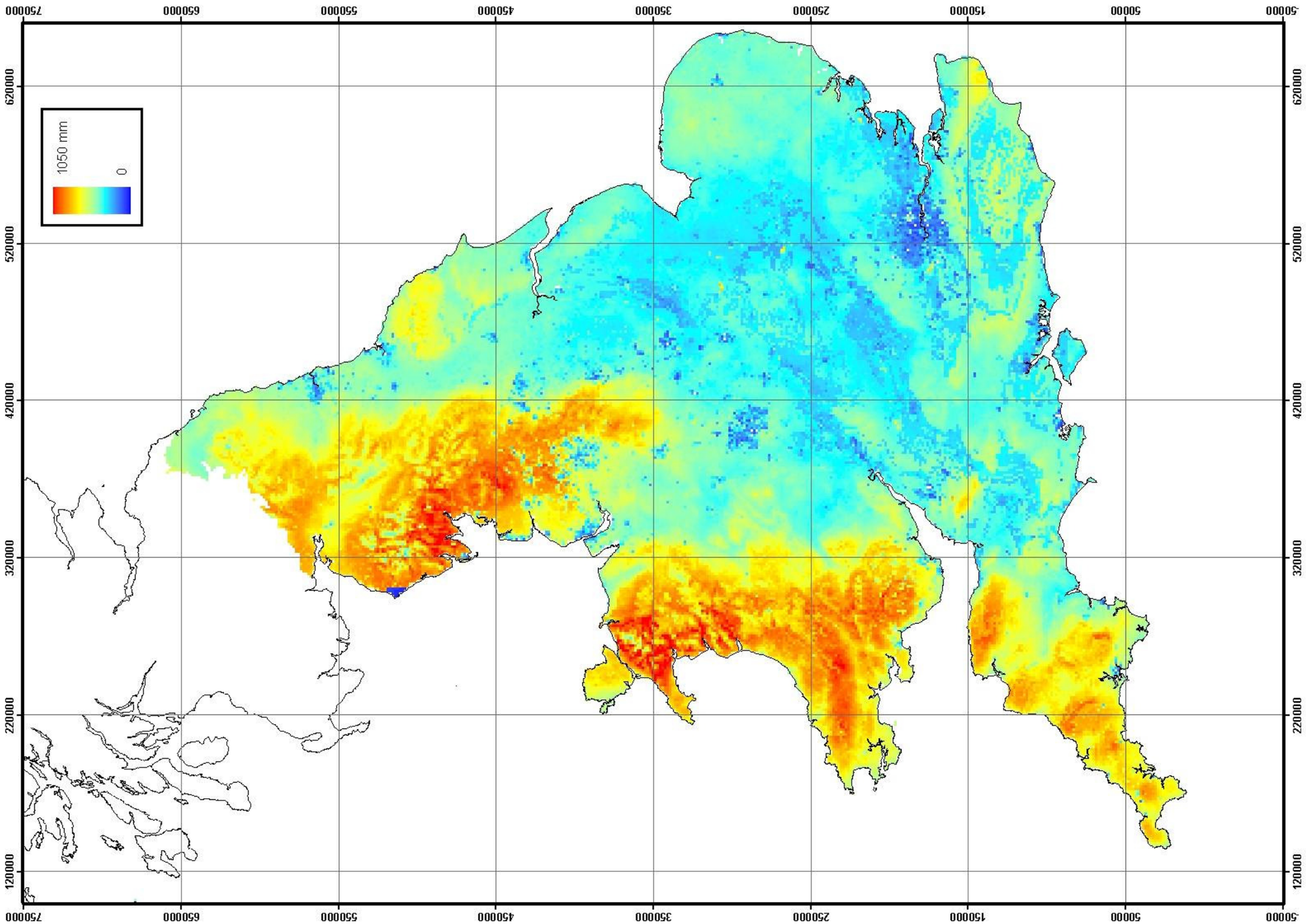

Figure 83 Predicted spatial distribution of the annual water use of poplar SRC during a water year with low rainfall (1975/76)

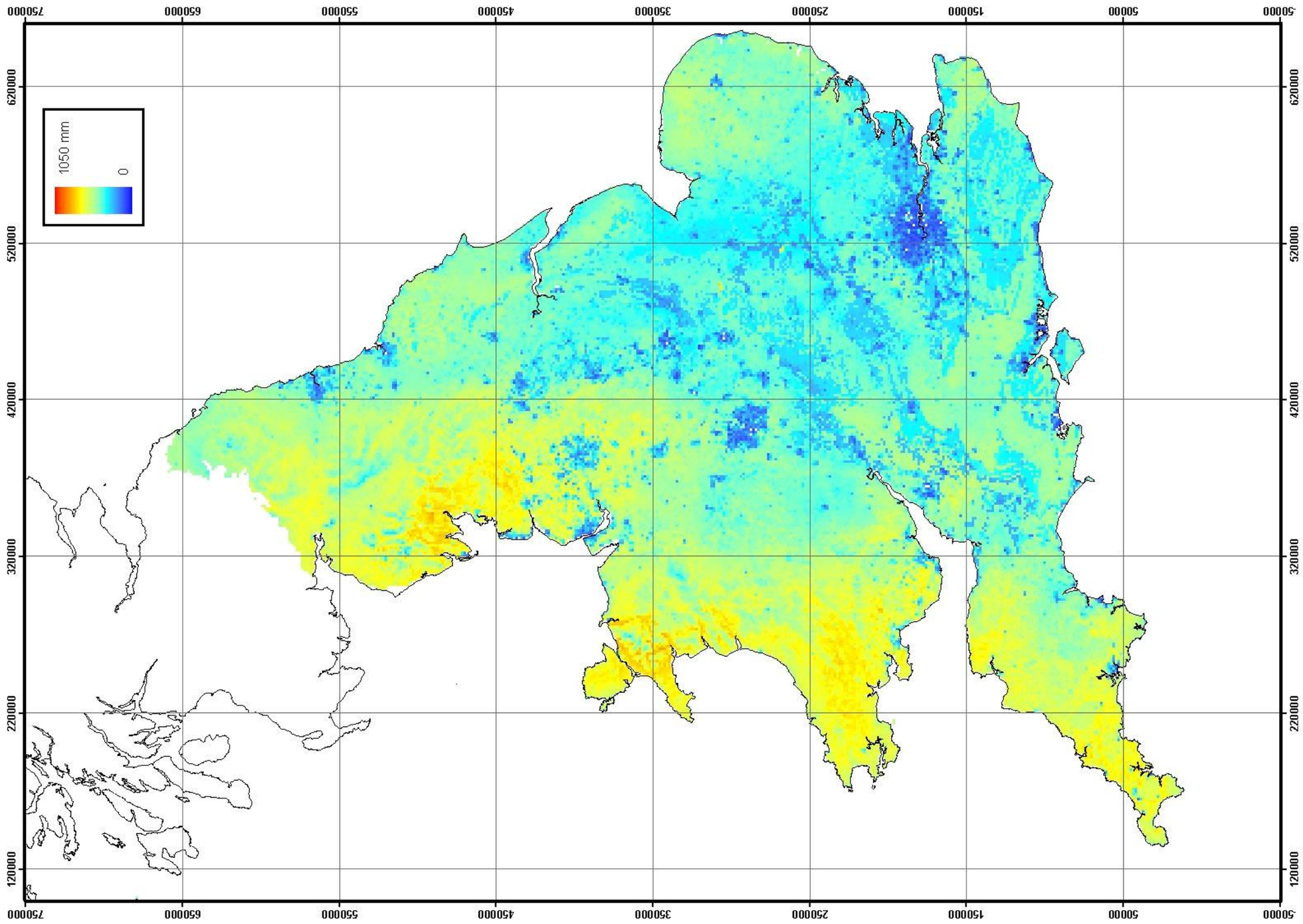

Figure 84 Predicted spatial distribution of the annual water use of willow SRC during a water year with low rainfall (1975/76)

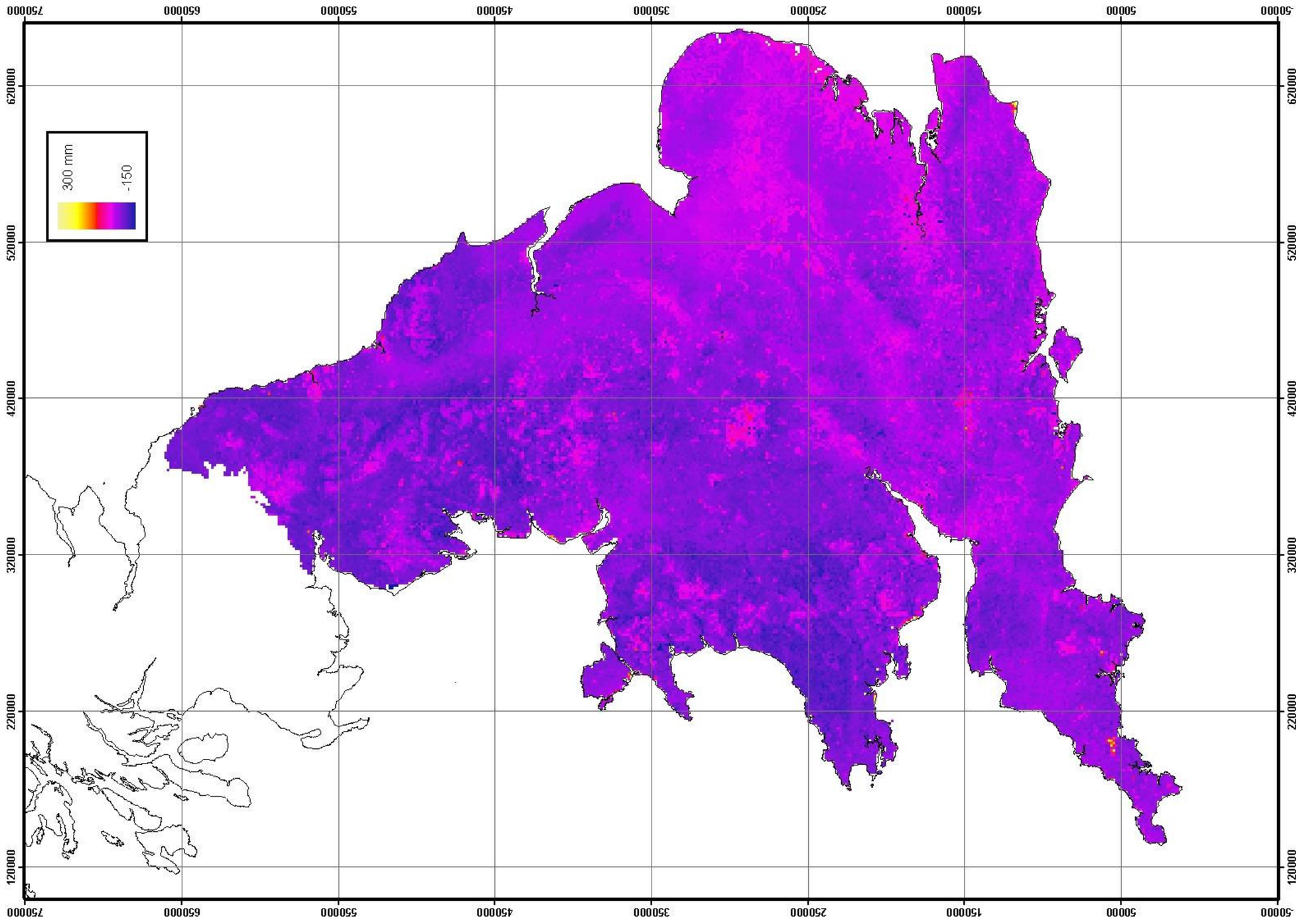

Figure 85 Predicted spatial distribution of the change in annual water use due to *Miscanthus* during a water year with typical rainfall (1981/82)

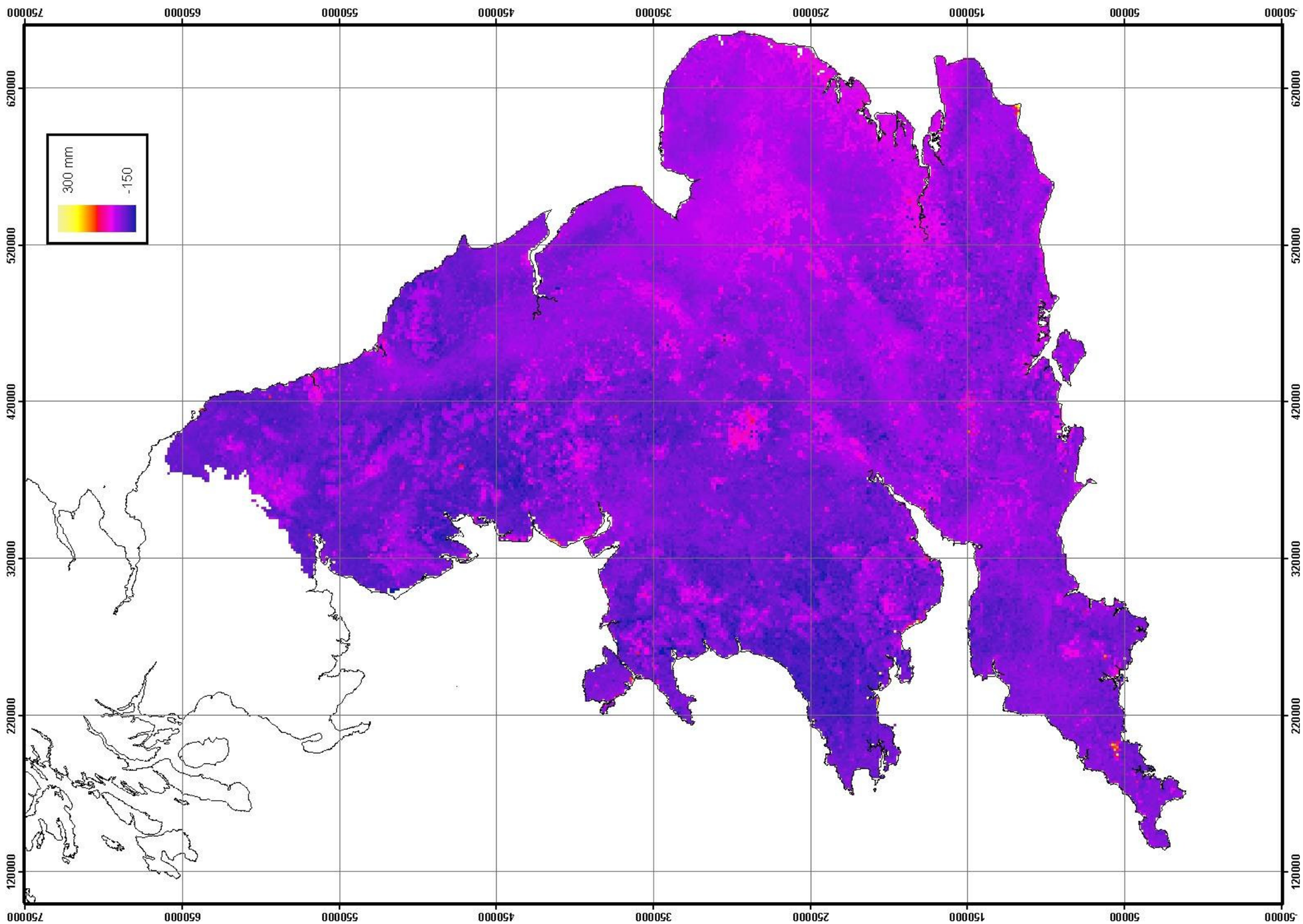

Figure 86 Predicted spatial distribution of the change in annual water use due to switchgrass during a water year with typical rainfall (1981/82)

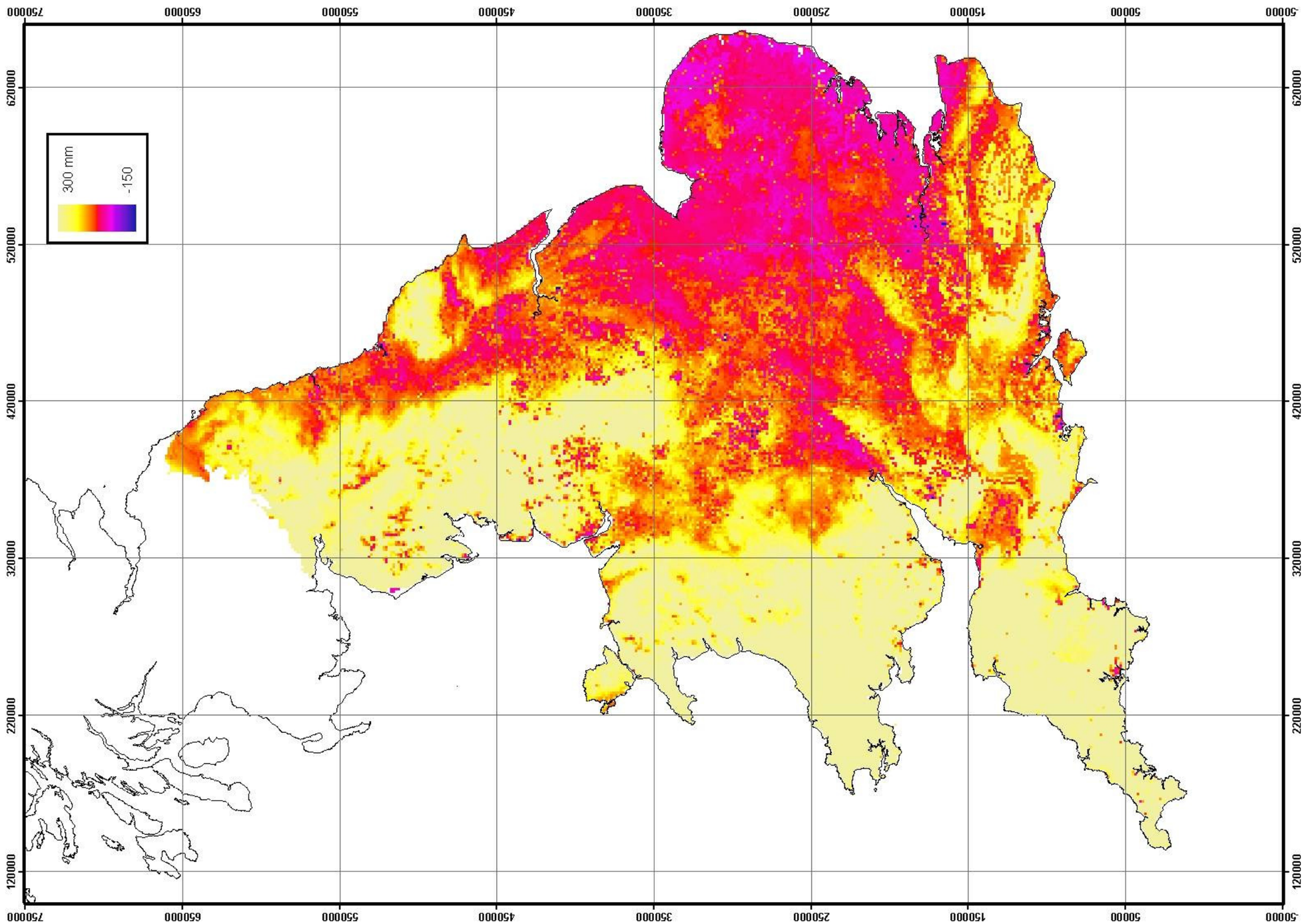

Figure 87 Predicted spatial distribution of the change in annual water use due to poplar SRC during a water year with typical rainfall (1981/82)

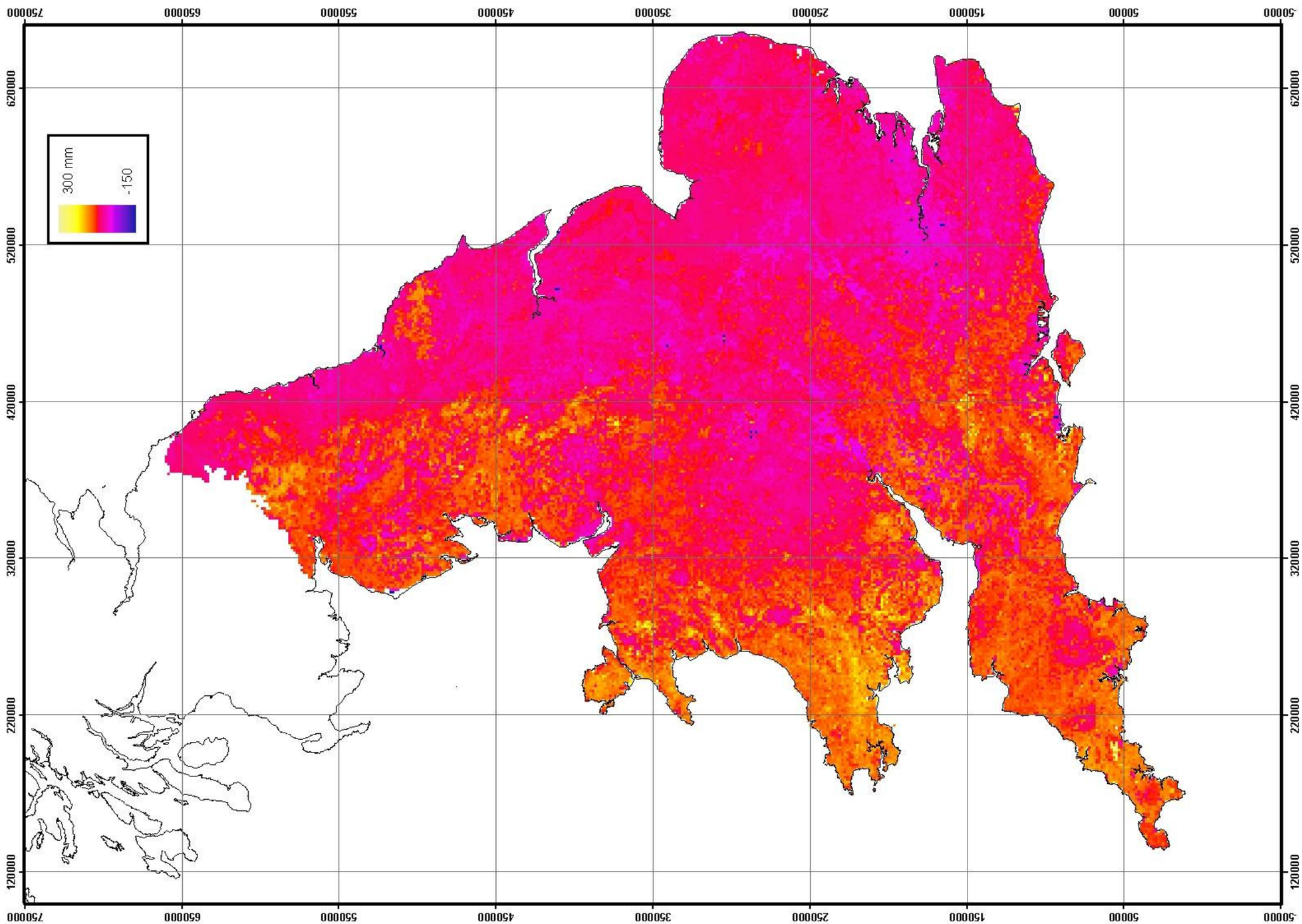

Figure 88 Predicted spatial distribution of the change in annual water use due to willow SRC during a water year with typical rainfall (1981/82)

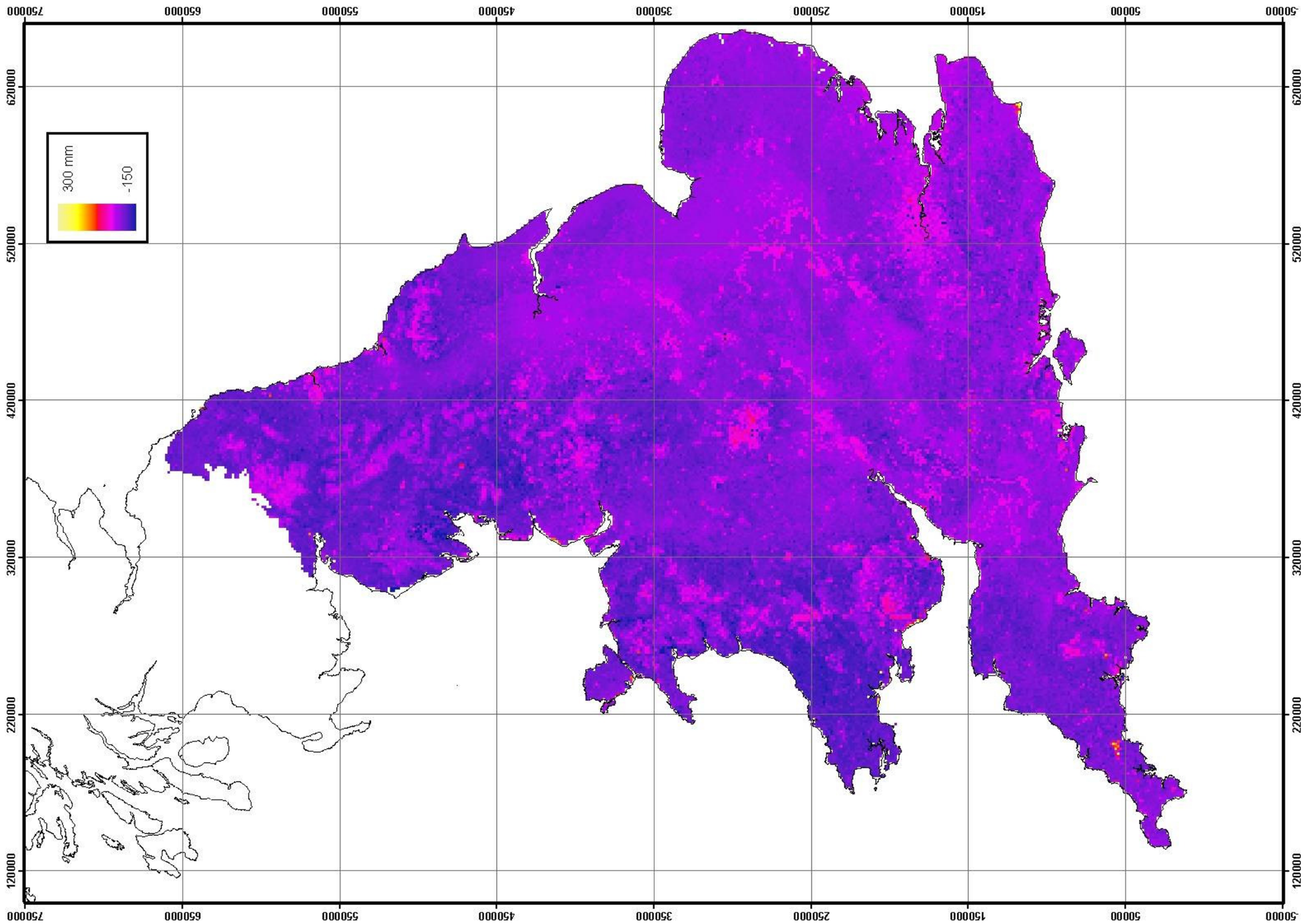

Figure 89 Predicted spatial distribution of the change in annual water use due to *Miscanthus* during a water year with high rainfall (1987/88)

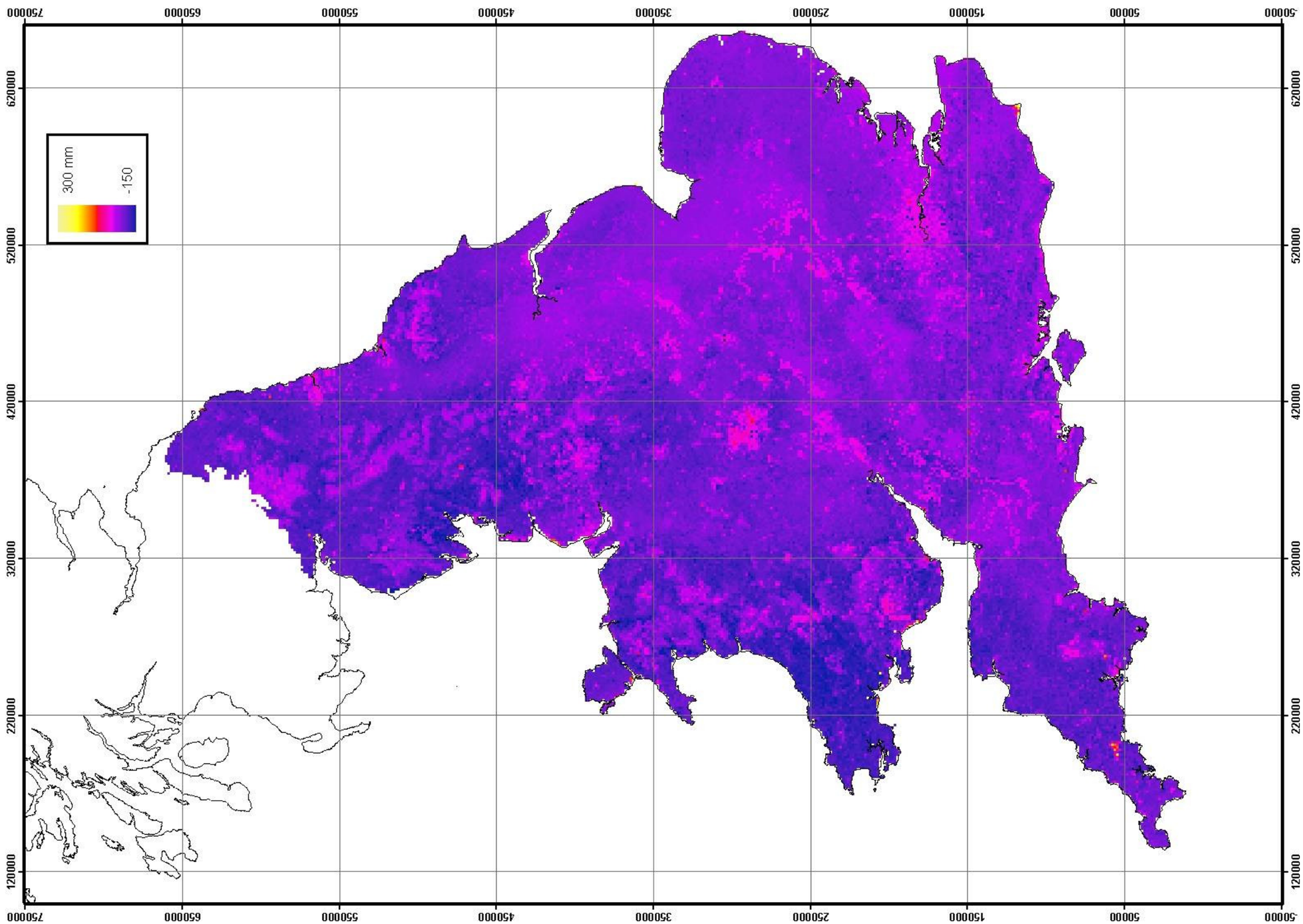

Figure 90 Predicted spatial distribution of the change in annual water use due to switchgrass during a water year with high rainfall (1987/88)

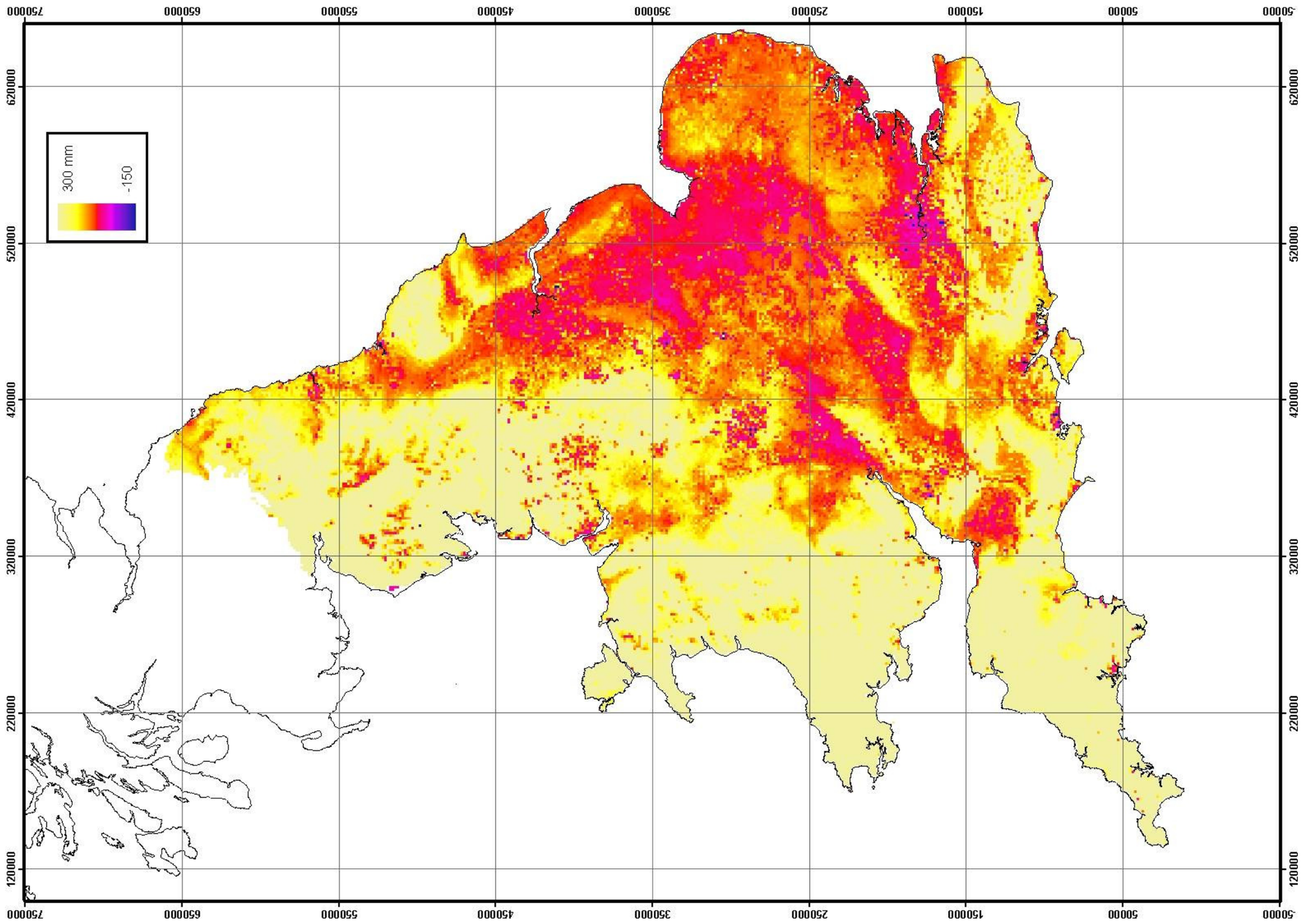

Figure 91 Predicted spatial distribution of the change in annual water use due to poplar SRC during a water year with high rainfall (1987/88)

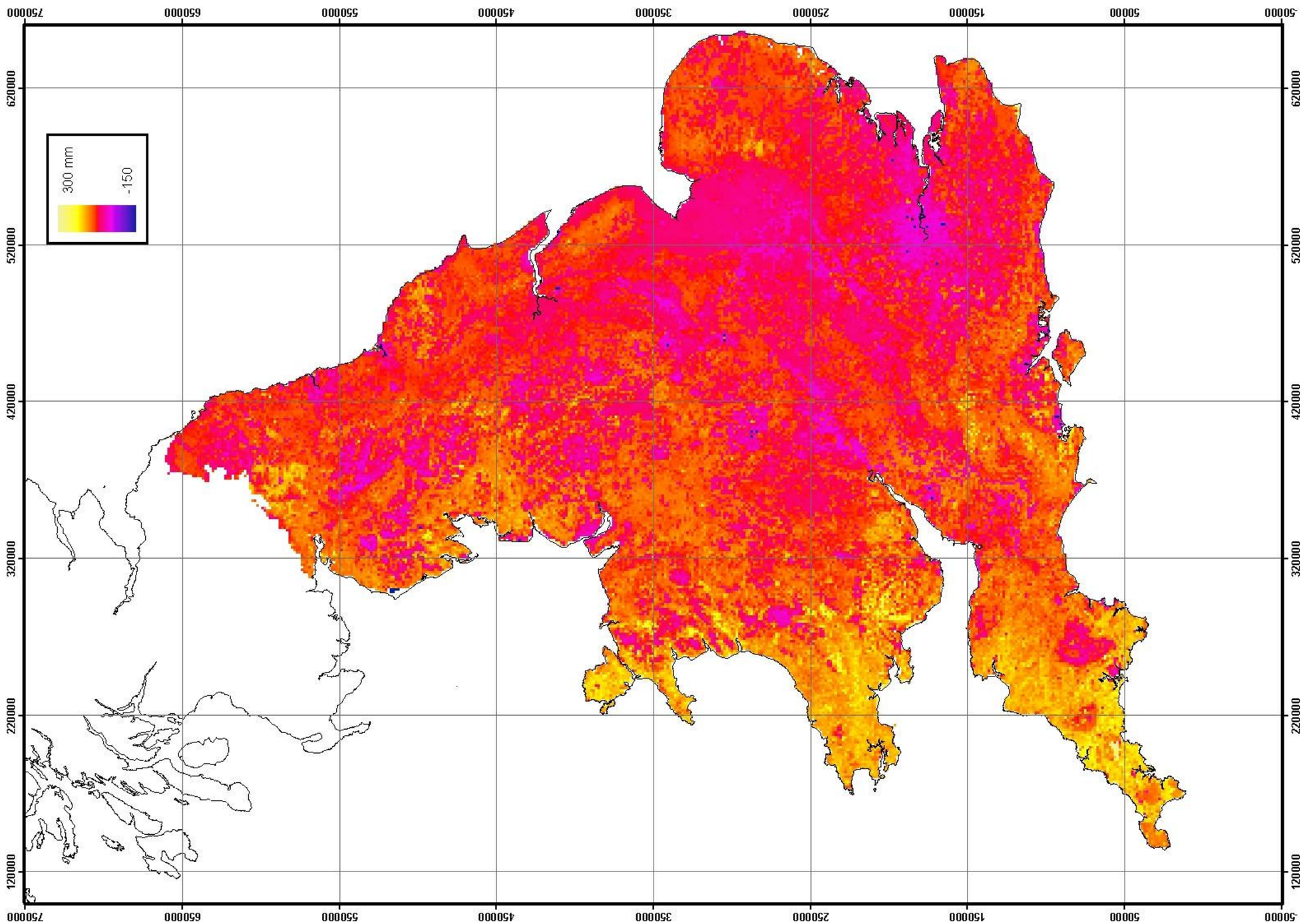

Figure 92 Predicted spatial distribution of the change in annual water use due to willow SRC during a water year with high rainfall (1987/88)

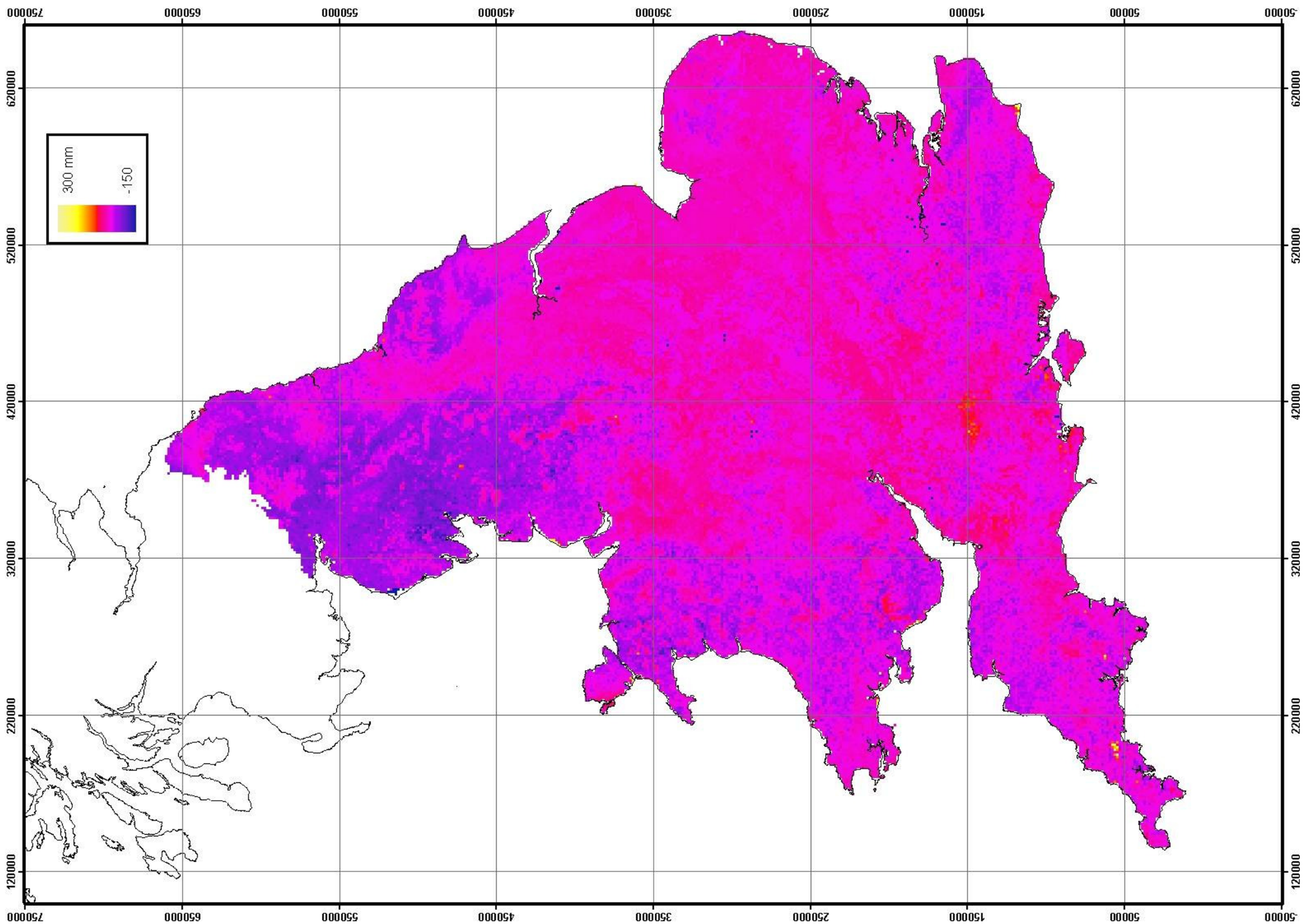

Figure 93 Predicted spatial distribution of the change in annual water use due to *Miscanthus* during a water year with low rainfall (1975/76)

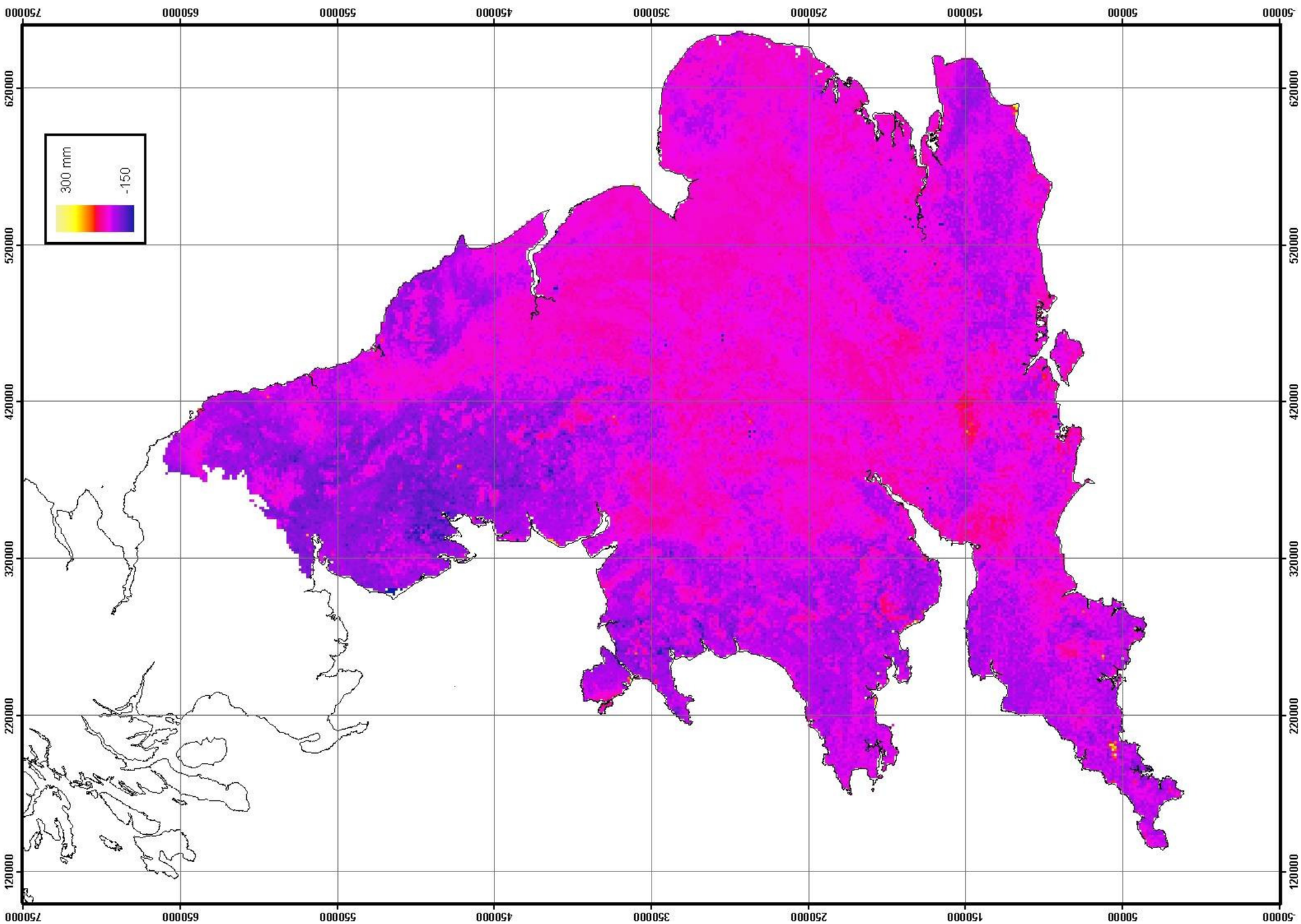

Figure 94 Predicted spatial distribution of the change in annual water use due to switchgrass during a water year with low rainfall (1975/76)

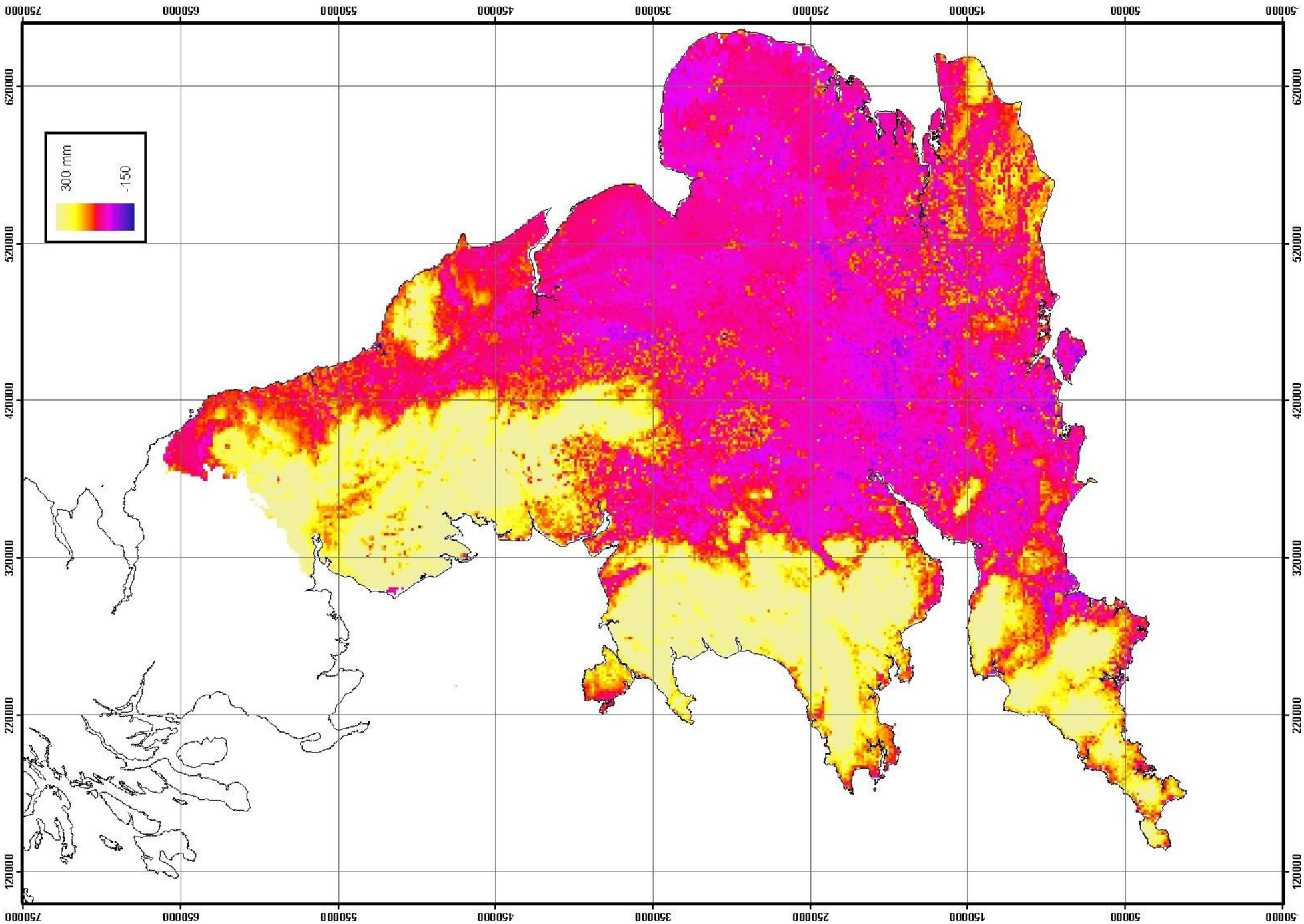

Figure 95 Predicted spatial distribution of the change in annual water use due to poplar SRC during a water year with low rainfall (1975/76)

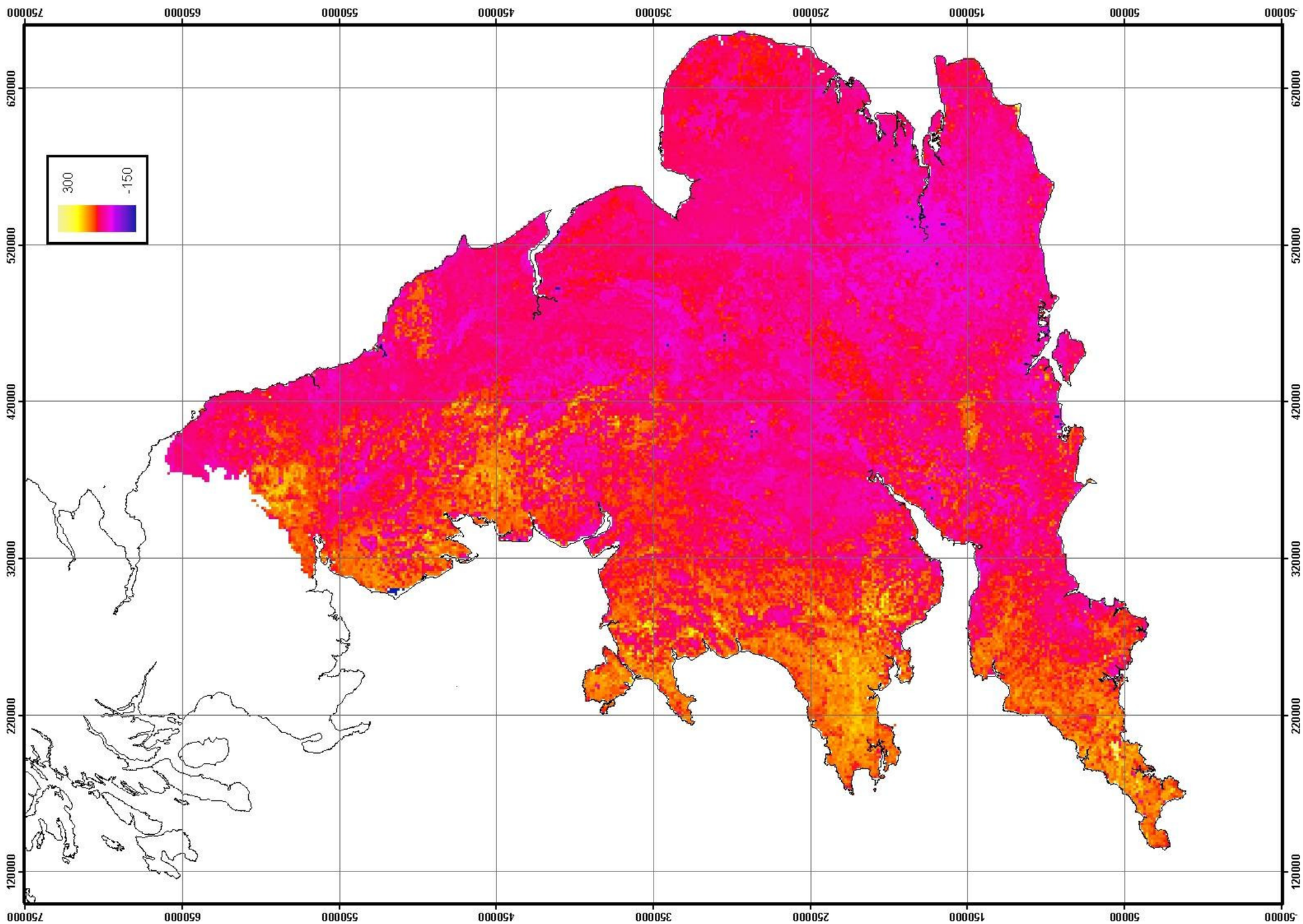

Figure 96 Predicted spatial distribution of the change in annual water use due to willow SRC during a water year with low rainfall (1975/76)

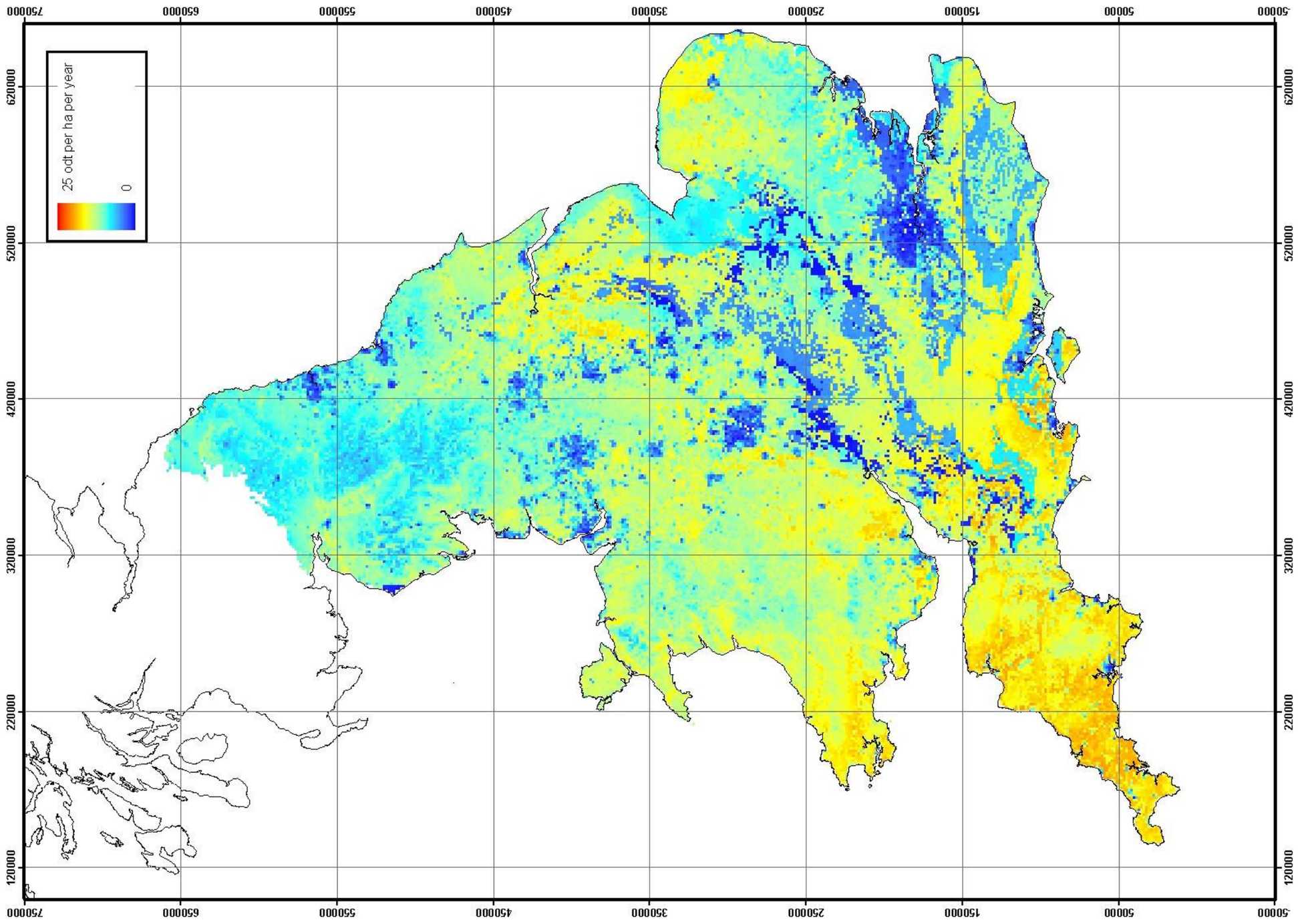

Figure 97 Predicted spatial distribution of the indicative yield of *Miscanthus* during a water year with typical rainfall (1981/82)

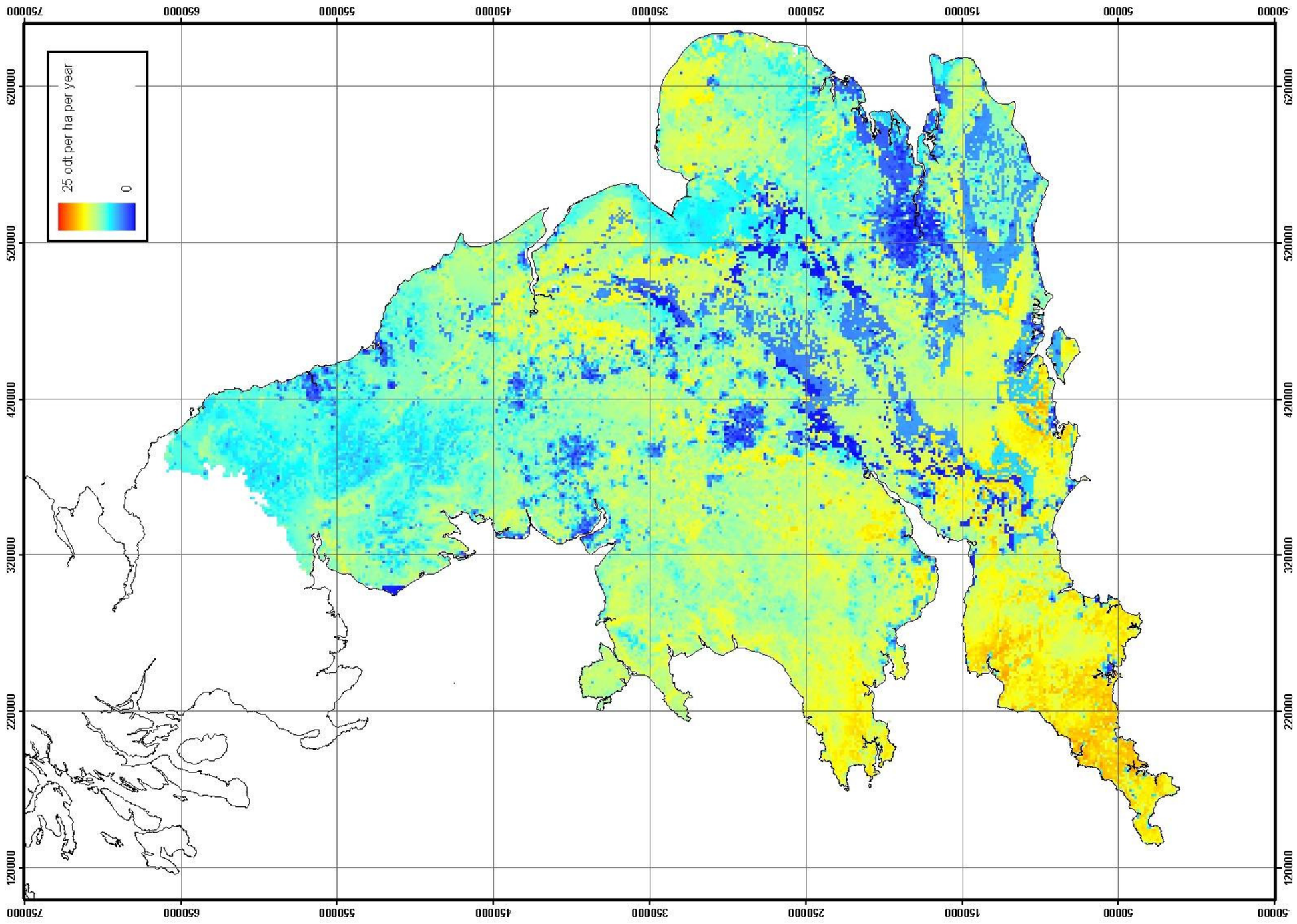

Figure 98 Predicted spatial distribution of the indicative yield of switchgrass during a water year with typical rainfall (1981/82)

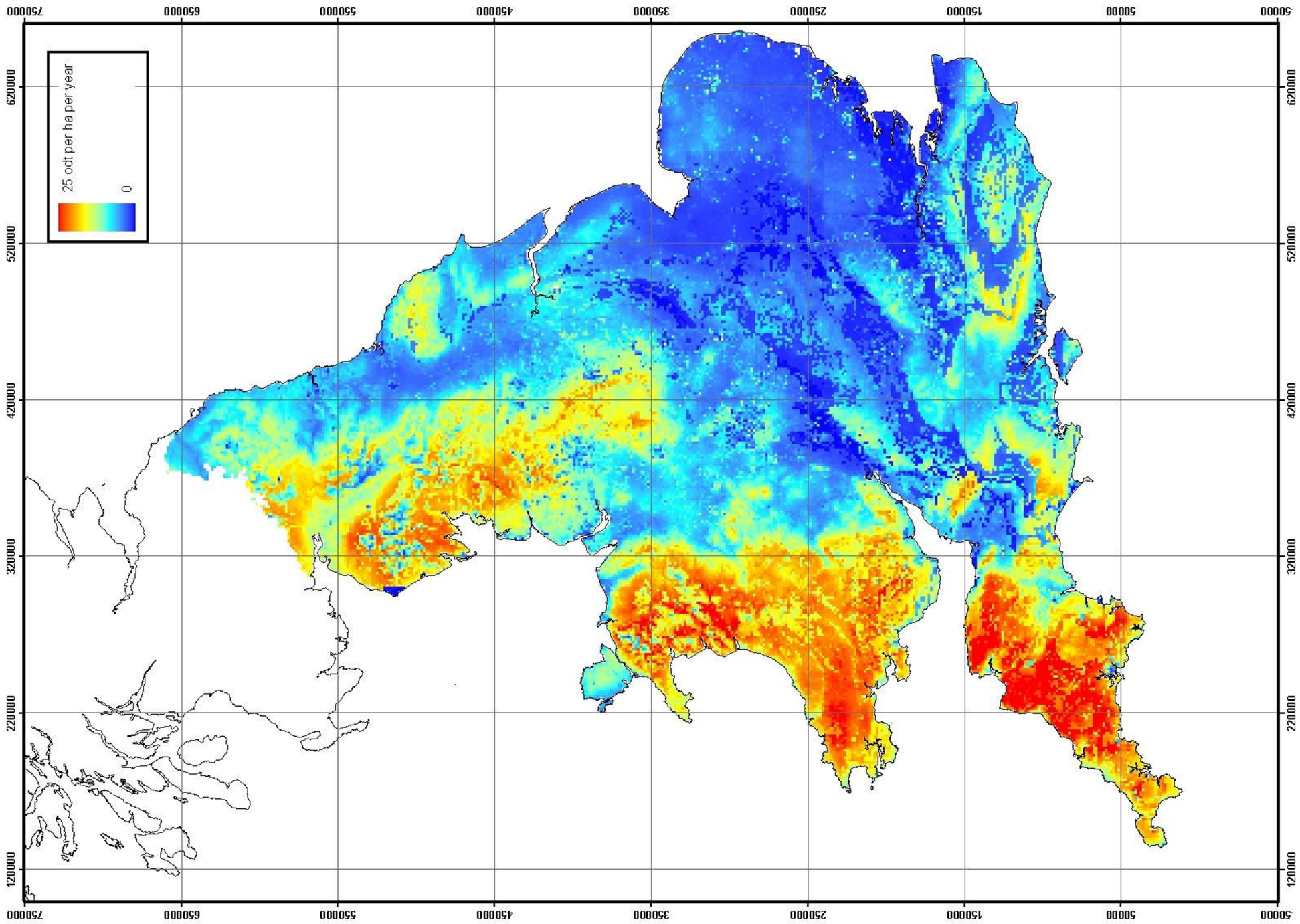

Figure 99 Predicted spatial distribution of the indicative yield of poplar SRC during a water year with typical rainfall (1981/82)

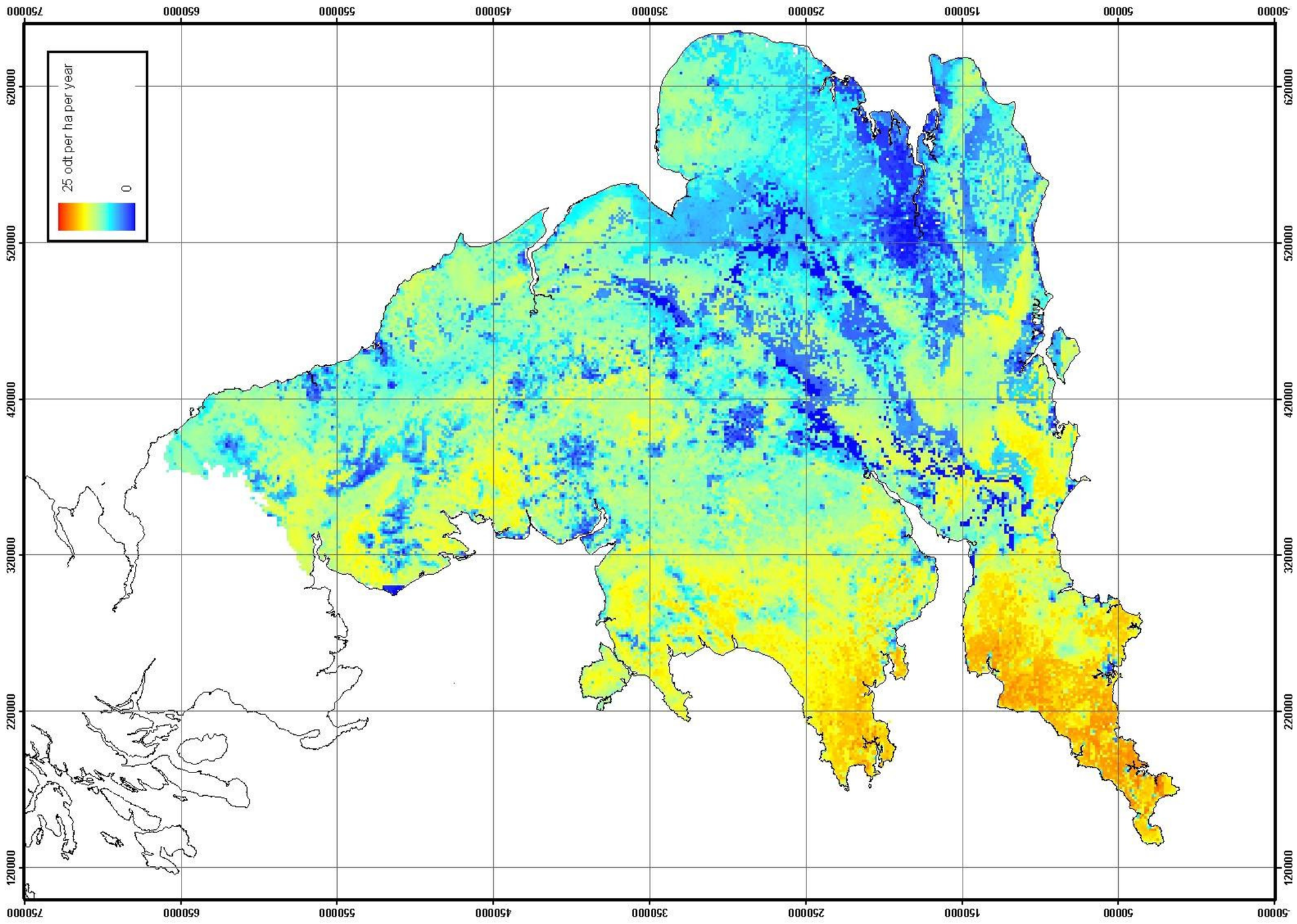

Figure 100 Predicted spatial distribution of the indicative yield of willow SRC during a water year with typical rainfall (1981/82)

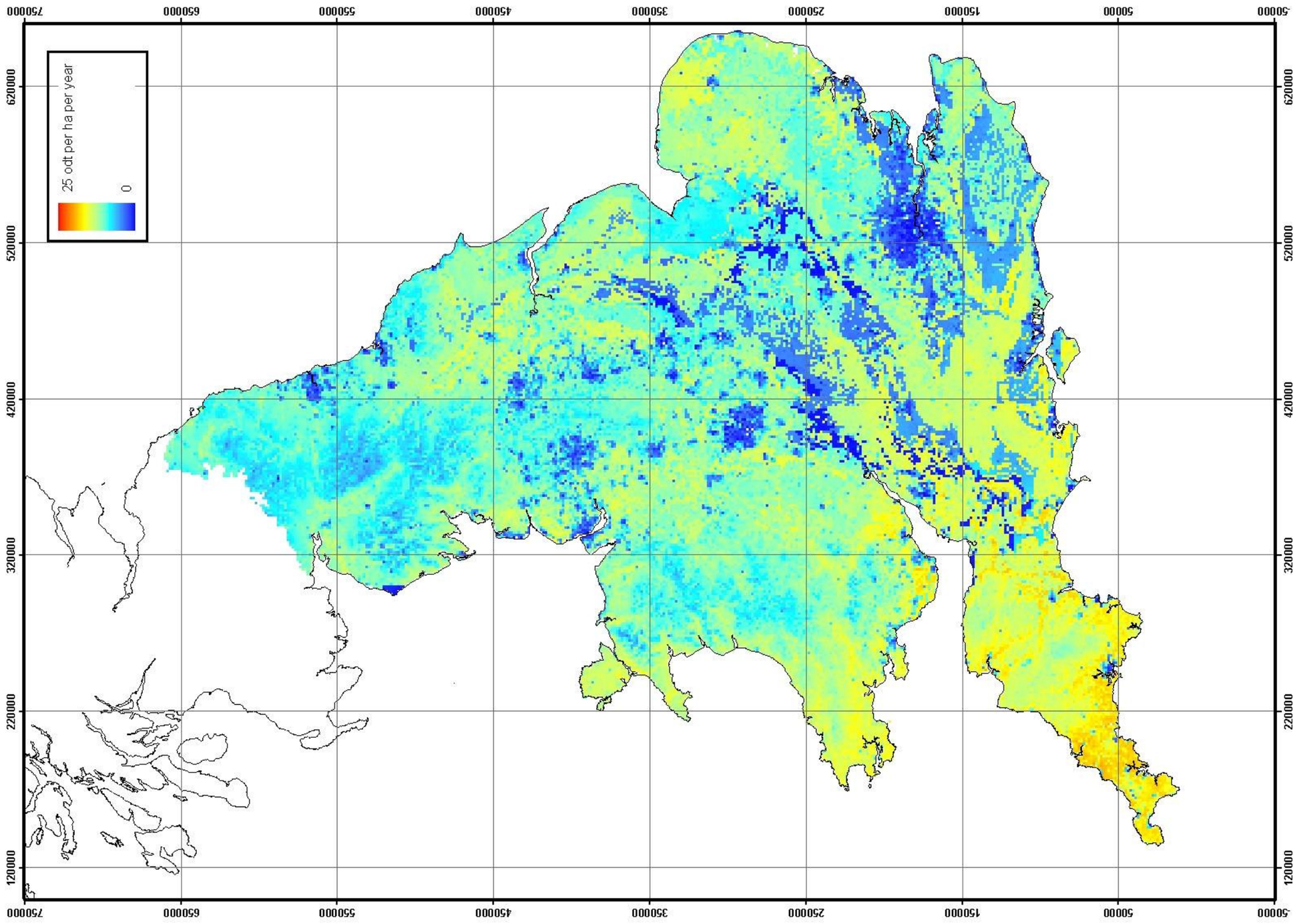

Figure 101 Predicted spatial distribution of the indicative yield of *Miscanthus* during a water year with high rainfall (1987/88)

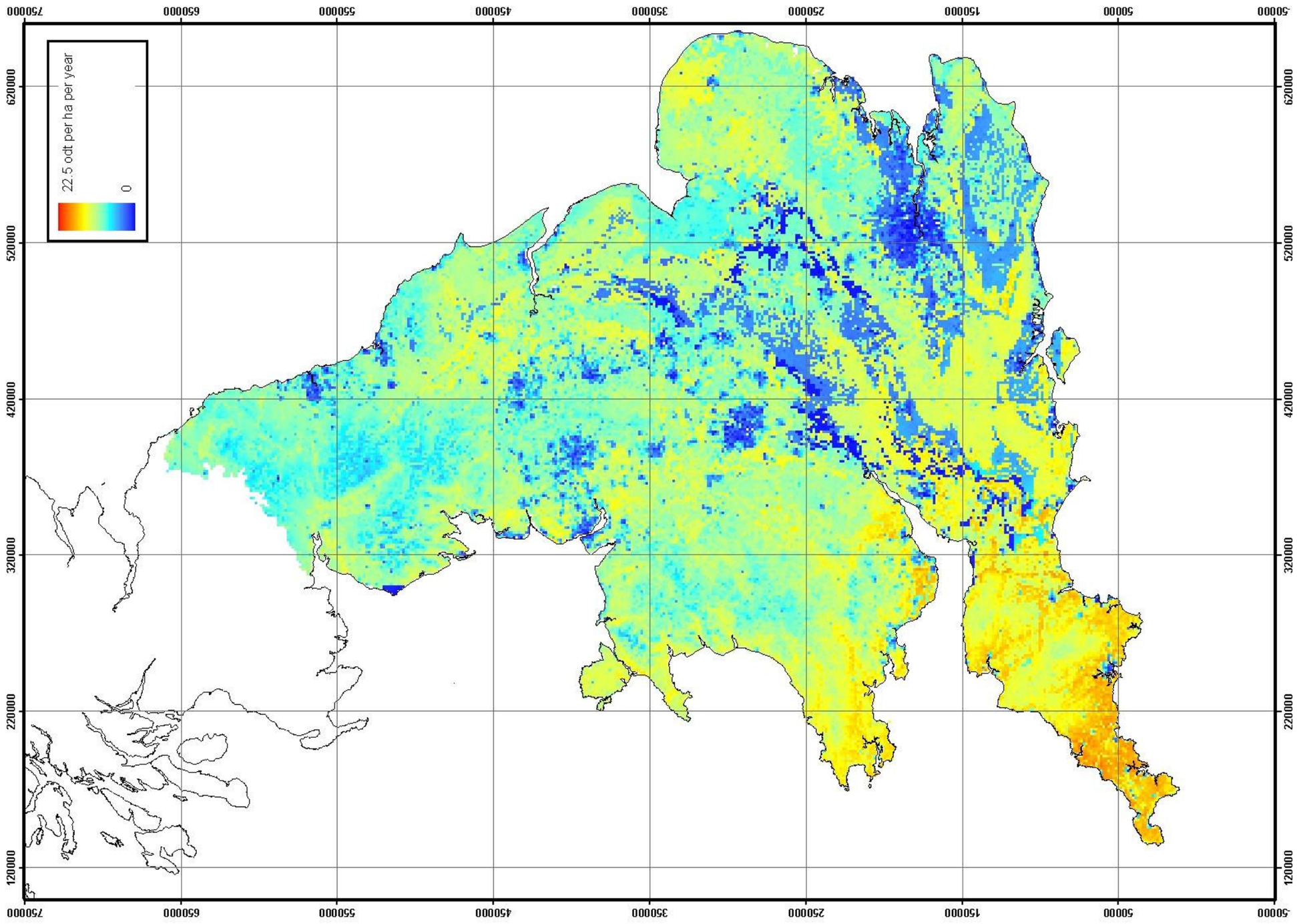

Figure 102 Predicted spatial distribution of the indicative yield of switchgrass during a water year with high rainfall (1987/88)

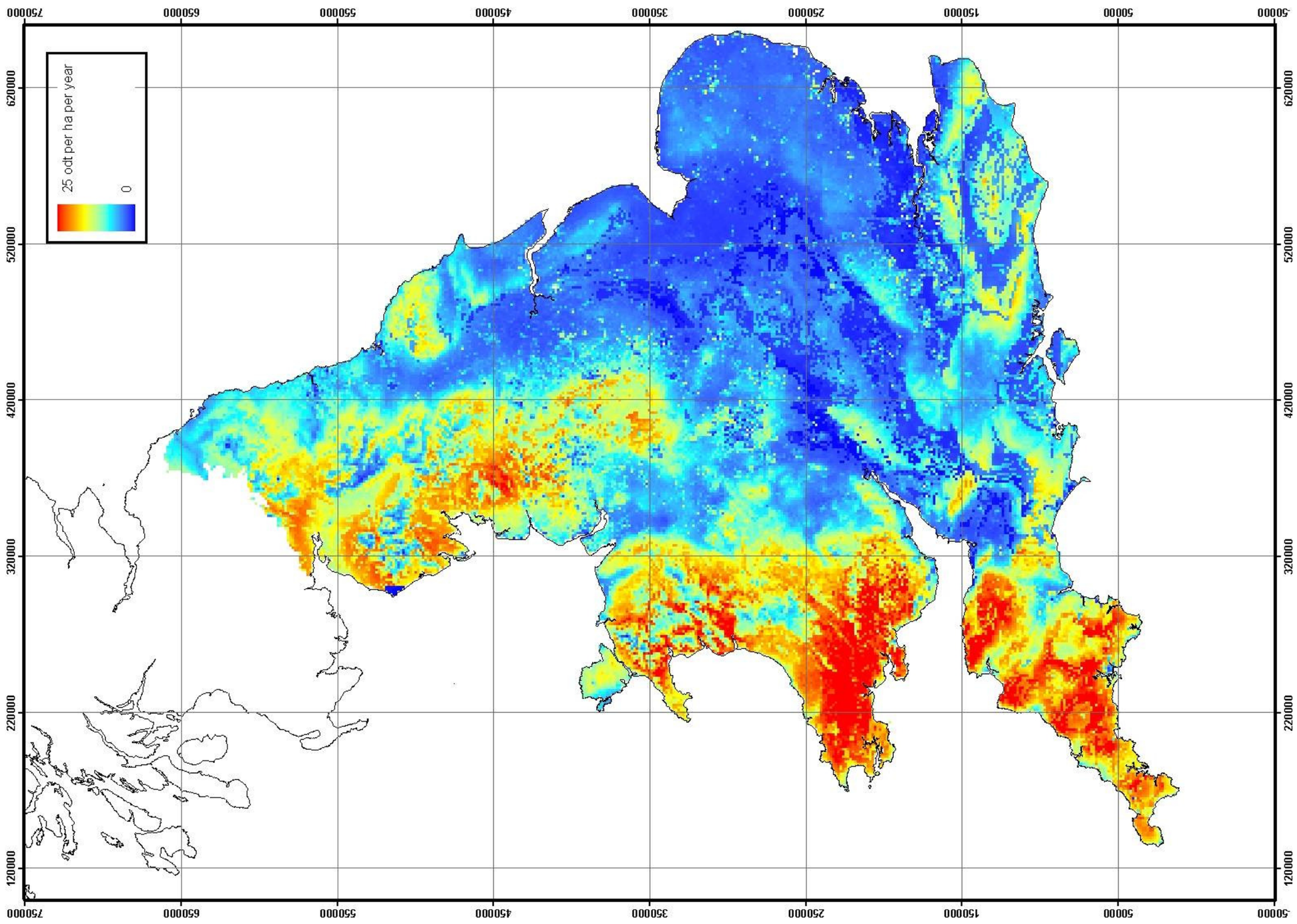

Figure 103 Predicted spatial distribution of the indicative yield of poplar SRC during a water year with high rainfall (1987/88)

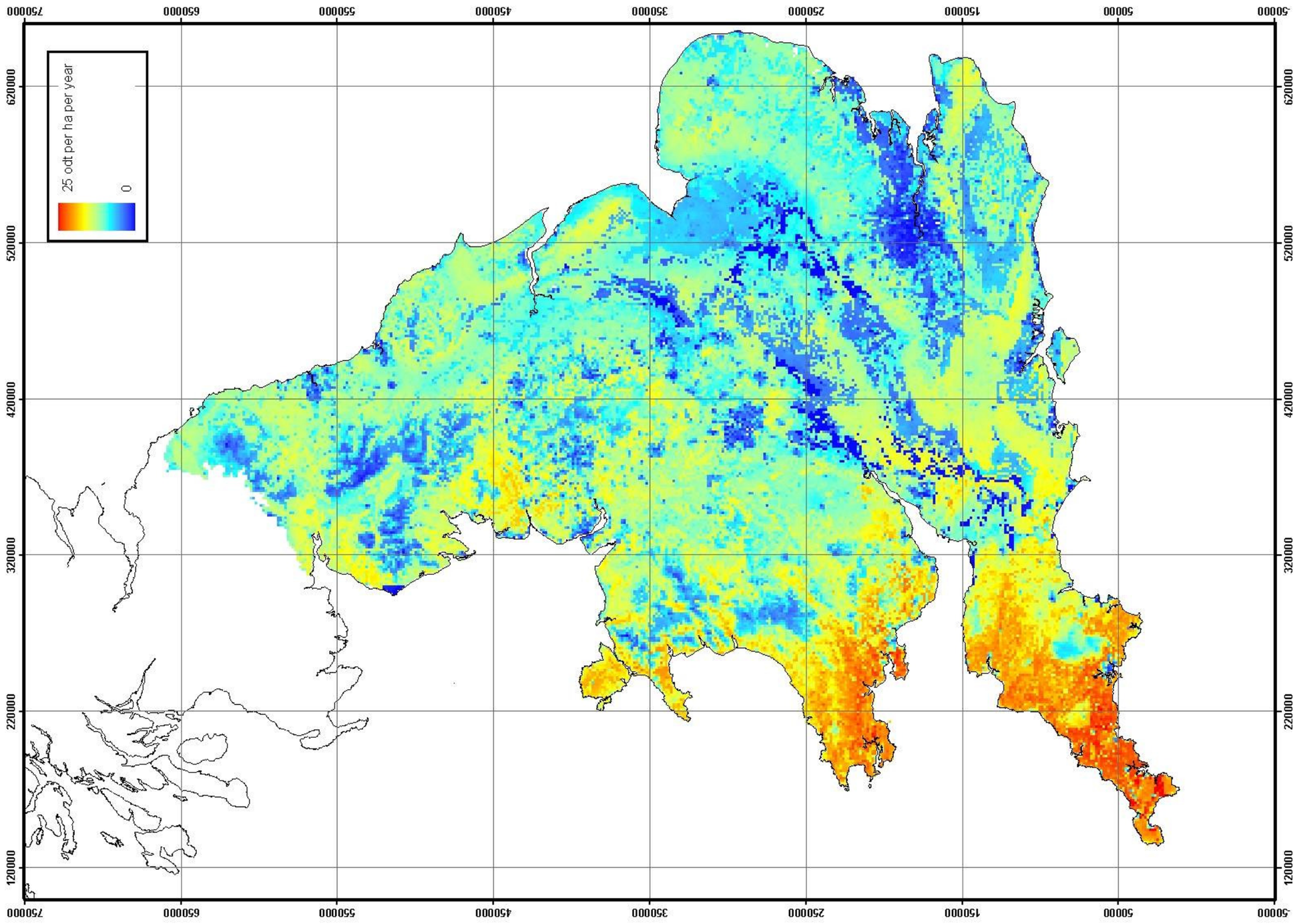

Figure 104 Predicted spatial distribution of the indicative yield of willow SRC during a water year with high rainfall (1987/88)

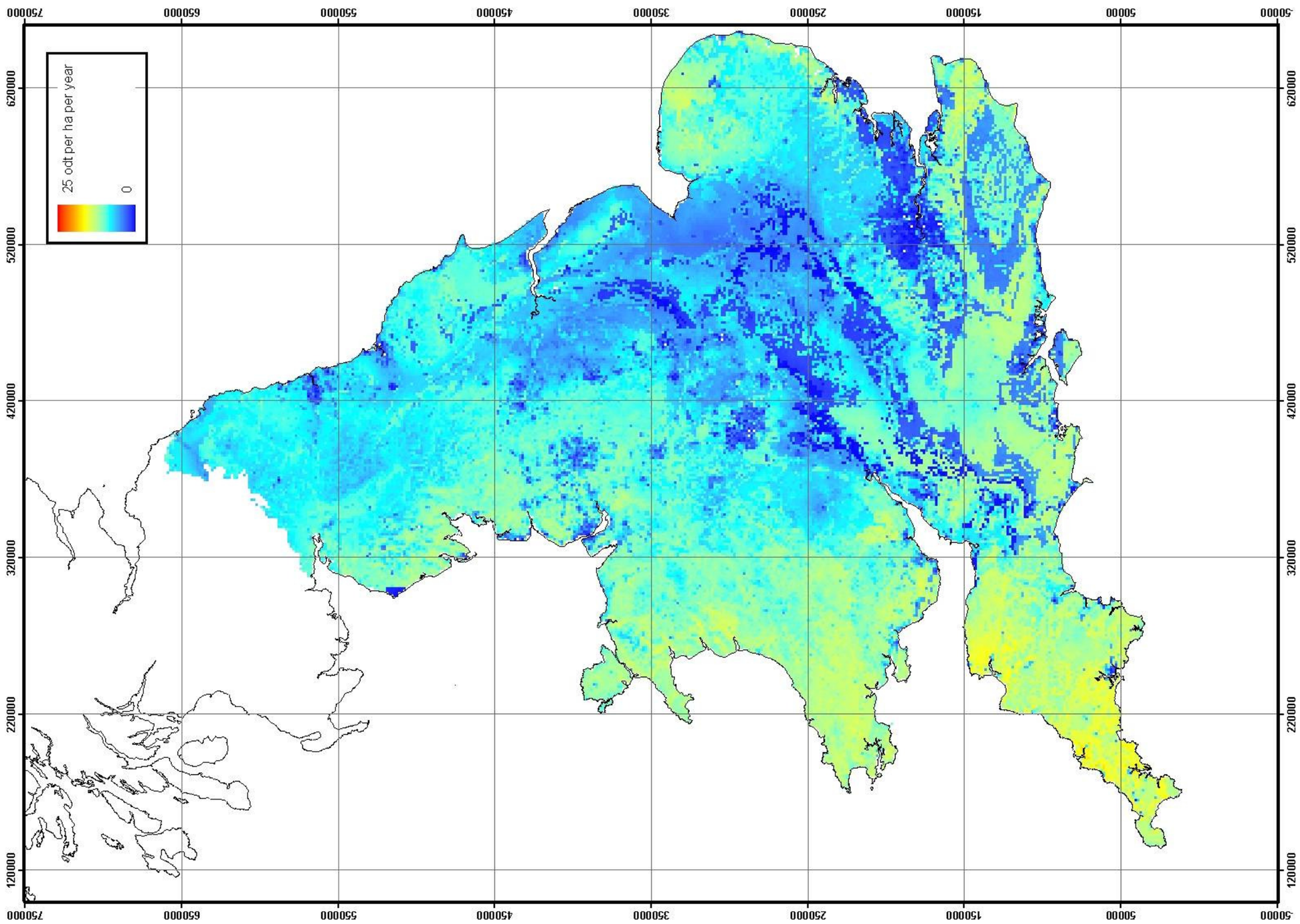

Figure 105 Predicted spatial distribution of the indicative yield of *Miscanthus* during a water year with low rainfall (1975/76)

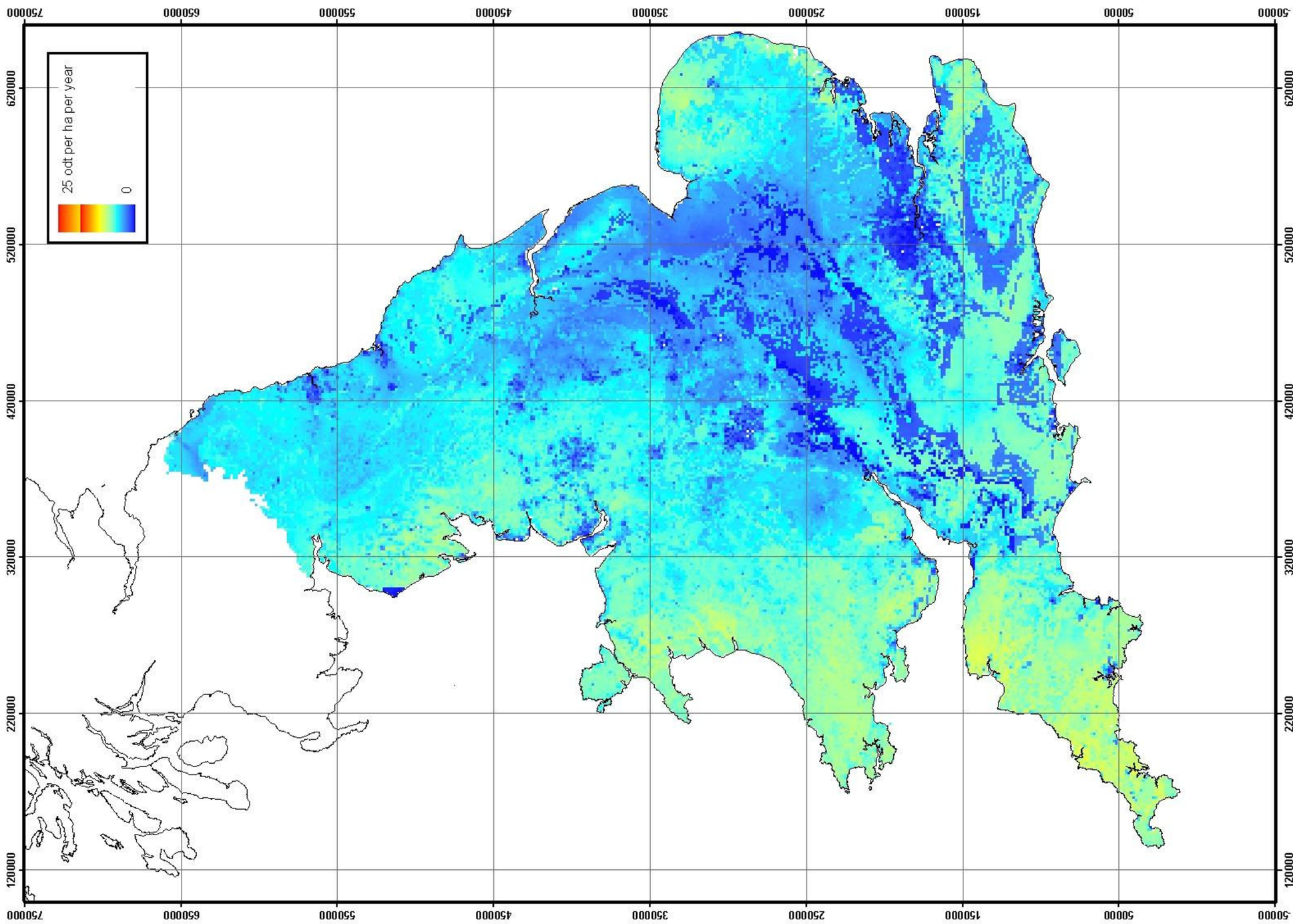

Figure 106 Predicted spatial distribution of the indicative yield of switchgrass during a water year with low rainfall (1975/76)

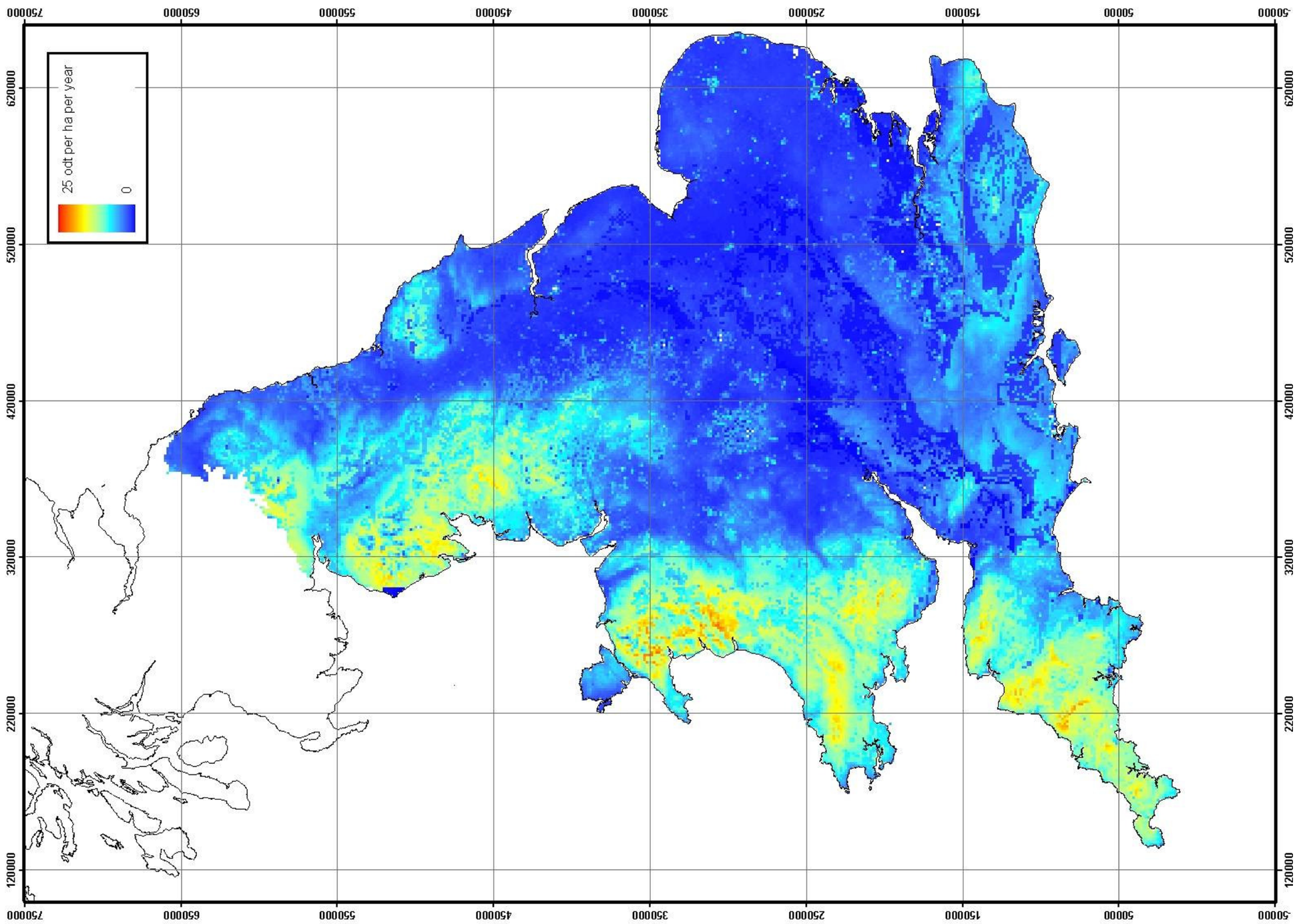

Figure 107 Predicted spatial distribution of the indicative yield of poplar SRC during a water year with low rainfall (1975/76)

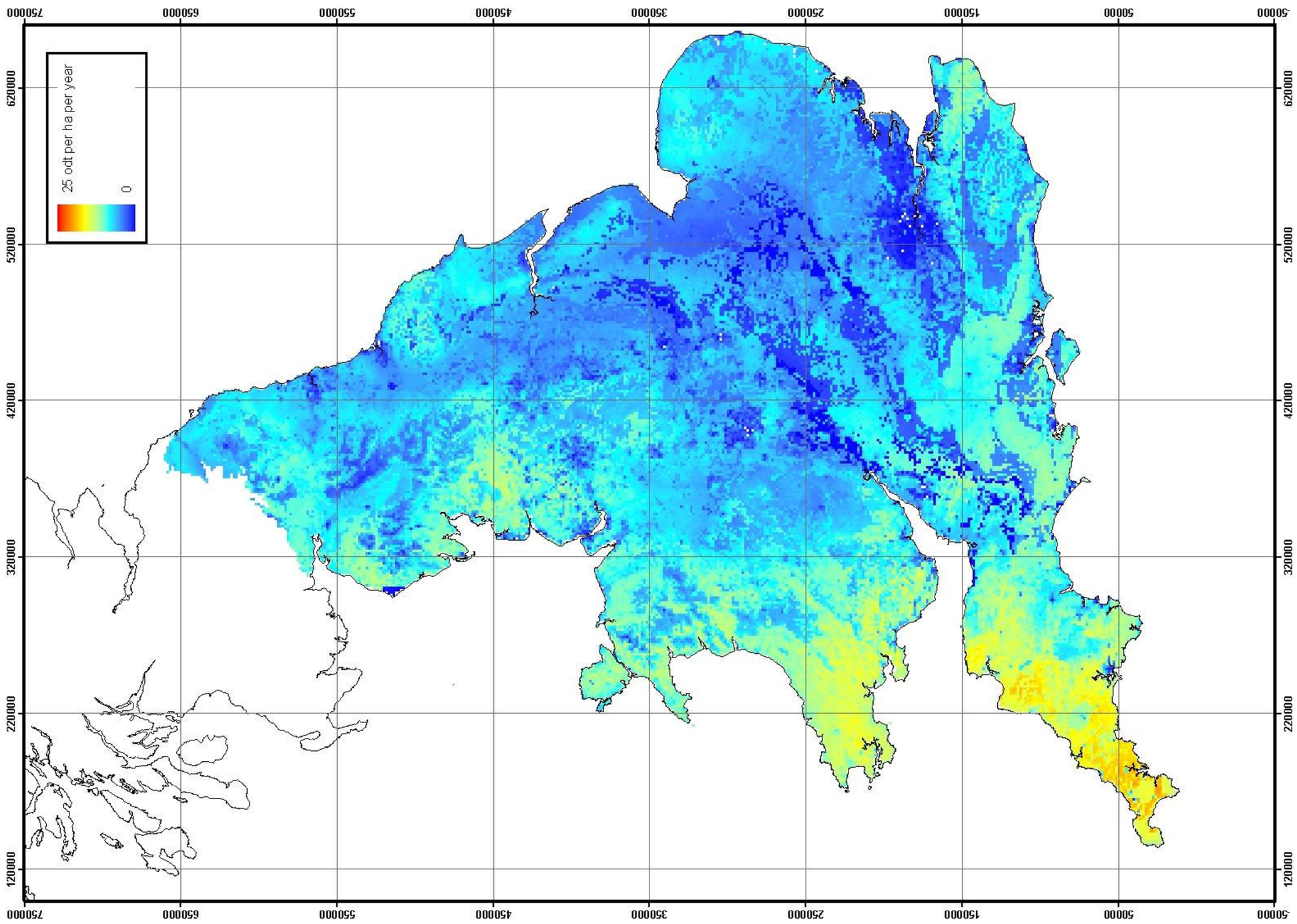

Figure 108 Predicted spatial distribution of the indicative yield of willow SRC during a water year with low rainfall (1975/76)

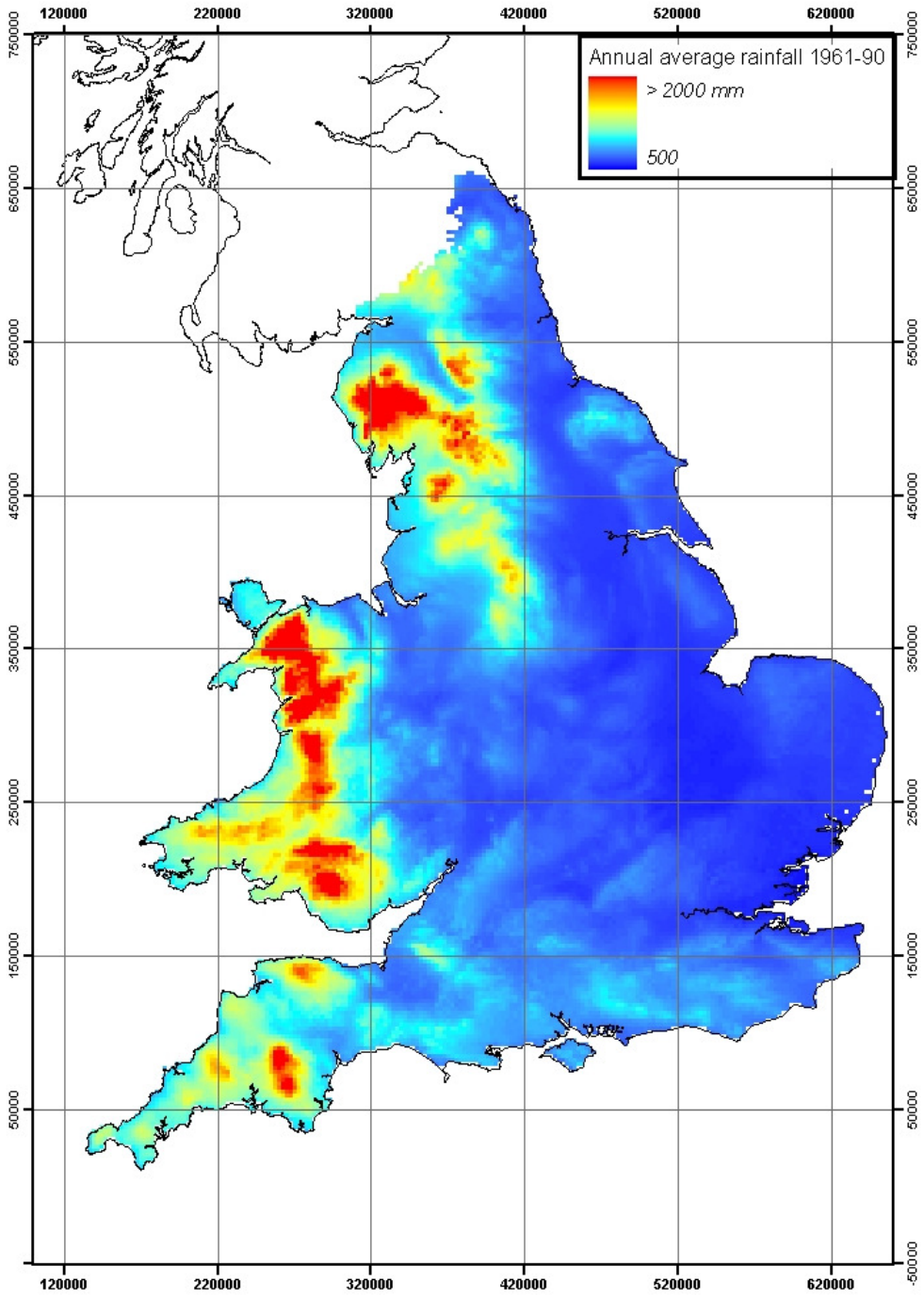

Figure 109 The average annual rainfall of England and Wales, 1961-1990

6. Demonstration GIS

Software, written in Visual Basic, has been developed to allow the model results to be interrogated for a demonstration area of 60 × 60 km, covering the upper part of the river Severn (the OSGB coordinates of the lower left corner are 280000 280000). It allows the user to determine the additional annual water use, in the form of a virtual abstraction, of a future energy crop plantation and the annual evaporative losses of the catchment that the plantation is located in. The files must be installed on a device which allows writing, e.g. a hard disk.

The user interface, Figure 110, allows the user to select one of four energy crops (willow SRC, poplar SRC, *Miscanthus* or switchgrass) and the type of rainfall year (typical, wet or dry). The location of the centre of the planned plantation is entered as the OSGB grid reference easting and northing, in metres, and the total area of the plantation (in ha). The system assumes that the plantation shape is a square. The catchment that will be affected by the energy crop is specified by entering the OSGB grid reference easting and northing, in metres, of the outflow point or it can be given as an input file by selecting the click button. This file should be a floating point binary file, covering the of 60 × 60 km area, such as can be produced by ARC-GIS. The catchment cells should be coded as 1. The file must have the name "demo_wshed" and be in the same folder/directory as the software.

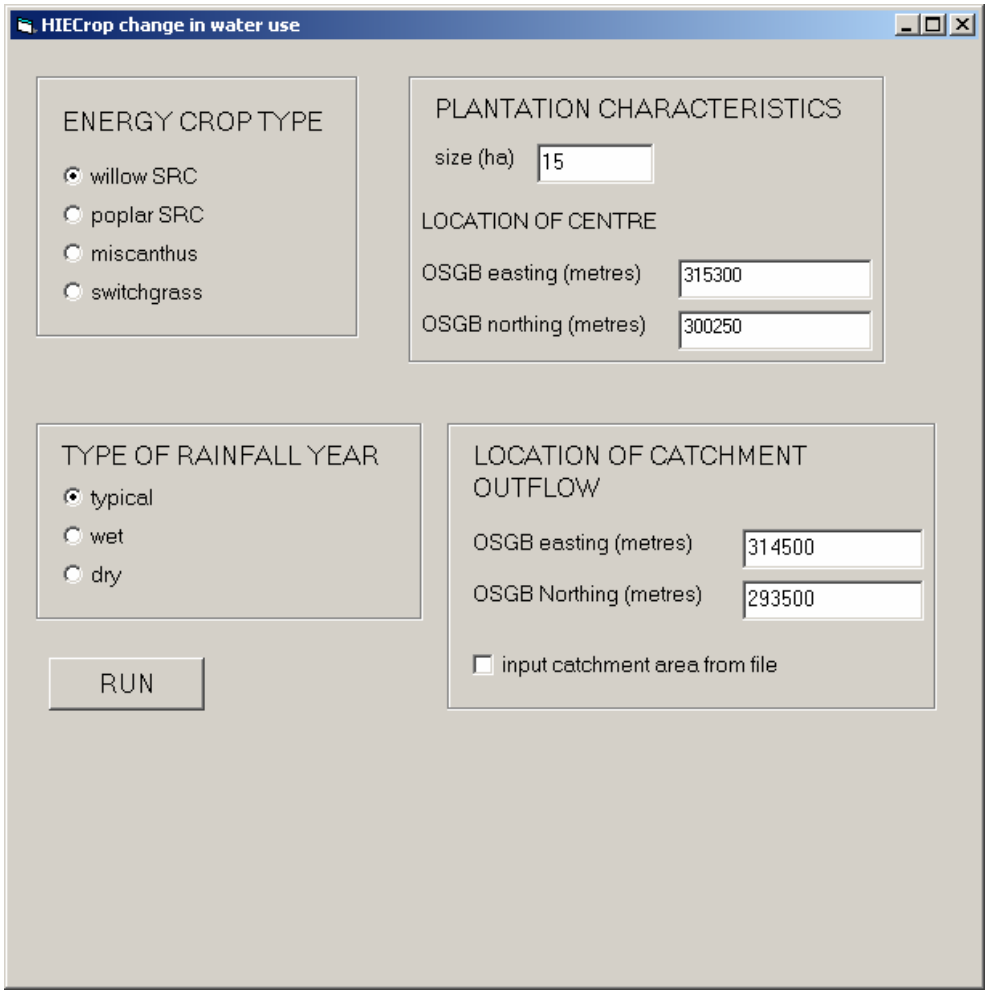

Figure 110 The user interface for the demonstration GIS

When the user is satisfied with the selection, he/she clicks on the "RUN" button. The software calculates the catchment boundary, using a data set of the flow direction that has been previously derived from a digital terrain model, and creates a mask that corresponds to the area covered by the catchment. The additional virtual abstraction is calculated by summing the predicted water use of the existing land cover, held in a data set, in the plantation area and subtracts the predicted water use of the energy crop. If the energy crop type is either willow SRC or poplar SRC, then the software calculates the enhancement factor and includes this in the estimated water use. The value is presented on the screen, see Figure 111 for an example. The total evaporation of the catchment is then calculated and also presented on the screen.

The catchment area is calculated from data based on a 1 km resolution DTM. As a consequence, it is not possible to resolve small catchments with any accuracy. A much more reliable result would be possible if a higher resolution DTM, 100 m or better, were available. It is also recommended that, if the system were used operationally, the catchment outlines should be input to ensure consistency with other catchment management systems.

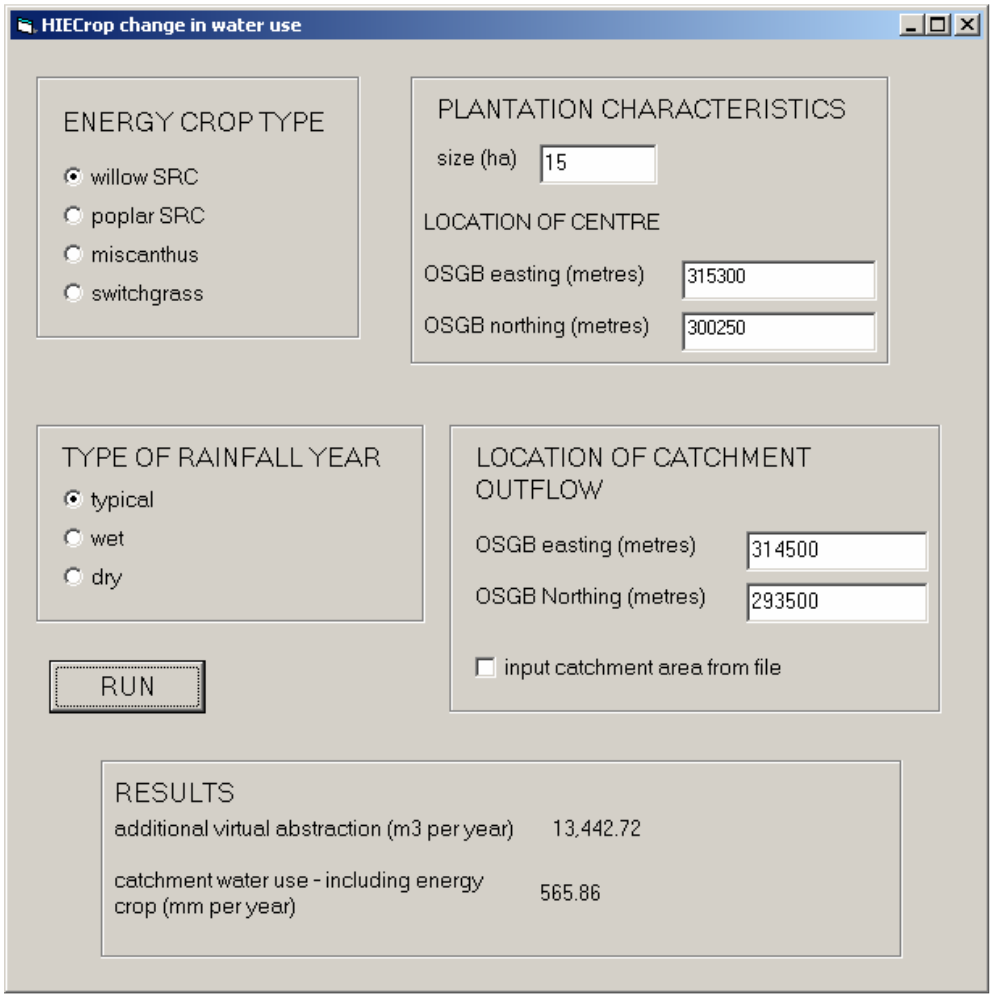

Figure 111 An example of the results returned by the demonstration GIS

7. Discussion and conclusions

The development and testing of the numerical model has been the key thread that has run throughout this project because it is the model that is used to extrapolate, in time and space, the measurements so as to predict the water use and indicative yield of the four energy crops across England and Wales for different rainfall conditions. Thus, the prime effort of the field measurements has been to provide the information to give values for the model parameters and to provide data to test the model's predictions against. It has been shown that the model's predictions are in reasonable agreement with the measurements.

The numerical model is an approximation to the real world and a full discussion of the assumptions and uncertainties can be found in Section 4.6. The conclusions that follow should be considered with these in mind.

7.1 SRC plantation edge effect

The issue of the enhanced evaporation at the edge of SRC plantations has been studied and it has been shown that there is a measurable increase in the evaporation, which is dominantly due to increased leaf area at the edge. From this understanding it is possible to state that the effect is very localised, only affecting the two outermost rows to any significance. This has allowed a simple function to be designed, which encapsulates this knowledge, so that the enhanced evaporation can be quantified as a function of the area of a contiguous plantation. The enhancement factor, F, is, for a plantation of area A m^2:

$$F = \frac{A + 9.6(A^{0.5} - 0.8) + 6.4(A^{0.5} - 2.4) - 6.4(A^{0.5} - 1.6)}{A}$$

Because the enhanced evaporation is limited to the perimeter of the plantation, it decreases rapidly as the area of the plantation increases; for a plantation of 1 ha, the factor is predicted to be about 9.5 % whilst for one of 2 ha it is 6.7 % and for one of 10 ha it is 4.3 %. In the case of the latter, the effect is well within the range that can be expected from other factors, e.g. soil type, slope and aspect of the site etc.

7.2 Water Use

Unsurprisingly, there is no simple answer to the question of whether energy crops use more water than the existing land cover. This is because a number of factors are involved: the type of energy crop, the type of existing land cover, the nature of the soil and the climatology.

For the purposes of this study, it has been assumed that, with the exception of the tilled land, the land cover is mature, i.e. there is no growth, with the obvious exception of leaf up and leaf fall. In the case of needliferous woodland and grass the physical characteristics (canopy height, leaf area index and rooting depth) do not change. For broadleaf woodland and heath, the leaf area index (LAI) changes seasonally but the height and rooting depth are constant. It is only for the tilled land, represented by winter wheat, that all three change both seasonally and annually, in response to the climate. In addition, the rooting depth of the woodland is greater than for the other vegetation types so that they are able to make use of more water stored in the soils during dry periods. As a consequence the annual water use, i.e. evaporative losses, tends to be highest for needliferous woodland; broadleaf woodland and heathland tend to be next with grass only slightly less. The water use from tilled land tends to be least, partly because of the shallow rooting depth, comparable to the existing grass, but dominantly because of the period of the year without vegetation cover.

By comparison, the energy crops, which are assumed to be fully established, all have dynamic physical characteristics, except for the rooting depth. In the case of the energy grasses, which have an annual

cropping cycle, the height and LAI change through the season and inter-annually, in response to climate, and have a period in the first part of the calendar year when there is no above ground biomass with the consequence that evaporation is limited to the bare soil. The SRC have a three year cropping cycle so there is a trend of increasing height over this period, with change concentrated into the summer months. The LAI shows both a seasonal cycle and a trend of the maximum value increasing in subsequent years. The energy grasses have a seasonal cycle in both height and LAI. The rooting depth of the SRC is deep, assumed to be 3 m, and so is comparable with existing woodlands. The rooting depth of the energy grasses is greater than the existing grass or tilled land, but less than the SRC or existing woodland, in the range of 1.7 to 1.9 m. Thus they have access to an intermediate amount of water stored in the soil. Additionally, they are taller and have a higher LAI than the existing grass or crop and so will tend to have higher evaporation rates

An additional factor to consider is the water use efficiency which differs between species and even varieties. A major factor in determining this is the photosynthetic pathway. All the vegetation considered have the C_3 pathway, with the exceptions of the two energy grasses, *Miscanthus* and switchgrass, which are C_4. C_4 plants are generally about twice as efficient as C_3 plants (Jones, 1992).

Without considering either the soils or climatology, were the energy grasses to replace the existing land cover types then the plus factors of the higher water efficiency and seasonal canopy and the negative factors of rooting depth and height and LAI lead to the conclusion that they are likely to have a water use that is comparable to winter wheat, comparable or lower than grass and lower than woodland and heathland. Examples of these conditions can be found in the maps of the change in water use during a typical rainfall year, Figures 85 and 86, although these maps are dominated by the variations in soils and rainfall. Notably, there is trend of less water use, compared to the existing land cover, in the west where the energy crops would dominantly replace grass. Thus, across the whole of England and Wales, there is unlikely to be a major increase in the water use. This is illustrated if the annual average water use for the eight model grid cells, Table 14 and Figure 55, are compared, see Table 15.

Table 15 The average annual water use (mm) predicted for eight grid cells , 1971-2000

	Existing land cover	Miscanthus	Switchgrass	SRC poplar	SRC willow
Durham	520	440	432	595	533
Lancashire	455	403	393	574	484
North Lincolnshire	549	428	423	475	451
West Wales	660	572	557	829	701
South Shropshire	529	470	460	661	515
East Anglia	483	463	460	508	485
East Hampshire	560	481	467	641	534
East Devon	560	516	502	735	568

Comparing the water use of SRC is more complex because of its three year cropping cycle, which results in the highest water use in the third year, so that the simple comparison on the basis of a single year, as presented in the maps, does not tell the whole story. Nevertheless, the water use is generally going to be comparable or greater than the existing woodlands and heathland and higher than grass or winter wheat. In the case of poplar SRC, the water use is particularly high. Thus the water use is likely to increase were SRC to replace the existing land cover, as illustrated in Table 15.

A note of caution must be sounded here. The model predictions for poplar SRC show a very high water use compared to the existing land cover and the other energy crops. This is because the model is based on the results of a previous study that made measurements on a number of varieties of poplar SRC at two sites in England. These results consistently showed that the poplar had a very high water use, primarily because the plants had little control on the stomata in response to high atmospheric evaporative demand or soil water stress. Thus these predictions are only valid for these varieties of poplar or similar types. There are indications that varieties of poplar which have stronger stomatal controls could be bred or may already exist. Of course, the converse also applies and other varieties of the other energy crops may have lower water efficiencies than those on which the model is based and so transferring the conclusions of this study to other varieties must be done with caution and knowledge of the specific characteristics of those varieties.

In areas of low annual rainfall, i.e. the east and south of England, see Figure 109, the hydraulic properties of the soils are having an effect on the water use of all the land cover types, principally through the amount of water that the soil s can store and is available to the plants for transpiration, the available water content. The effect is particularly noticeable where soils of very different properties are in proximity, i.e. HOST classes 1 and 25 west of London. The model predicts that the energy crops tend to use less water on the soils with the smaller available water, implying that they are more susceptible to drought. The higher evaporation rates deplete the soil water faster so that, over the whole year, they use less water. The energy grasses require a higher average temperature for photosynthesis than the other vegetation types. As a consequence, they are particularly active during the summer, when the potential evaporation rate exceeds the rainfall rate, and so are more reliant on soil water to maintain transpiration and thus growth.

In particularly dry years, there is the potential that the large soil moisture deficits that develop during the summer, under the SRC in particular but also the energy grasses to a lesser extent, will not necessarily be replenished by rainfall during the following winter. This will result in reduced recharge and runoff with consequent impacts on water resources and the ecology of water courses and riparian areas.

In the areas of higher rainfall, i.e. the west in general and upland areas in particular, see Figure 109, the vegetation is less dependent on soil water to maintain transpiration in the summer and so the effect of the soils is diminished. As a consequence, the patterns of differing soils is not readily discerned in the maps of predicted water use in these areas. Also the predicted water use tends to be higher in these areas because it is not reduced by soil water stress.

The differences in water use in years between typical and low rainfall are more marked for the SRC than the energy grasses. This is because of the greater rooting depth of the SRC, which allows the plants to maintain higher transpiration rates through the summer and so results in the change in water use being higher in a dry than a typical rainfall year. Nevertheless the energy grasses also tend to show an increase in water use, compared to the existing land cover, in a dry rainfall year compared to one with typical rainfall., again as a result of the ability to utilise more soil water.

During a year with high rainfall, there is a tendency for all four energy crops to use more water than in a typical year, compared to the existing land cover. Soil water is no longer an important factor so it is the height and leaf area that are the dominant factors and both the interception and transpiration are higher.

The effect of differences in the climate are apparent in the predictions. Water use tends to be less in the upland areas, primarily due to lower air temperatures and greater amounts of cloud reducing the amount of sunshine. There is also a trend of decreasing water use northwards which is a result of the progressively lower solar elevations. However, these effects also apply to the current land cover and so there is little impact on the change in water use.

7.3 Indicative yield

The indicative yields follow essentially the same trends as the water use since these are linked. There are trends which generally are the inverse of the topography, so that growth is restricted by lower average air temperatures and less sunshine. There is also a trend of decreasing indicative yield with increasing latitude, which reflects decreasing average air temperatures and amounts of sunshine. The results suggest that the indicative yields from the energy grasses are more likely to be affected by this latitudinal effect than those of the SRC, Table 16. This is because the threshold temperature, below which photosynthesis cannot occur, is higher. This table also shows the wide variation in the predicted indicative yields for poplar. This is a consequence of the lack of any control on the stomata in response to either atmospheric demand or soil water stress. Again, it should be emphasised that this is based on the particular hybrids used in the previous study and does not necessarily apply to other hybrids already available or those that could be developed. Further measurements on such varieties would be needed and the model re-run.

Table 16 The average annual indicative yield (odt ha^{-1}) predicted for eight grid cells, 1971-2000

	Miscanthus	Switchgrass	SRC poplar	SRC willow
Durham	7.4	7.3	4.9	10.9
Lancashire	7.3	7.3	8.7	11.5
North Lincolnshire	9.3	9.1	1.8	7.1
West Wales	11.7	11.8	26.3	17.1
South Shropshire	10.0	9.7	8.9	9.7
East Anglia	8.4	8.5	1.2	5.5
East Hampshire	11.7	10.9	6.1	12.9
East Devon	13.3	12.7	12.3	14

As discussed in the preceding section, in the areas of low rainfall, see Figure 109, the patterns of the different soil classes can be identified in the predicted indicative yields. This strongly suggests that, in these areas, the ability of the soil to store water that can be used by the plants for transpiration is an important factor in limiting the indicative yield of the crops. In a dry year, the indicative yields will be severely affected. There is not necessarily much of an increase in indicative yield in a year with high rainfall because the increase in rainfall tends to be during winter months and so there is less scope for it to be exploited by the vegetation because the soil water stores will be full anyway.

The impact of low rainfall is likely to be more complex in the case of SRC, compared to the energy grasses, because of the three year cropping cycle. It is unclear whether, if the drought occurs during the first year of the cycle, the indicative yield will be made up by faster growth during the two subsequent years. If the drought occurs in the third year then the impact may be greater because it is during this year that more biomass is accumulated.

7.4 Demonstration GIS

The demonstration GIS software shows how it would be possible to use the information produced by this project in catchment management. However, the capability of the demonstration system is limited. This is particularly true of the procedure for automatically deriving catchment boundaries, which makes use of a data set with 1 km resolution. This spatial resolution is insufficient for the size of catchment in the UK. The real strength of the information will become apparent if it is integrated with operational systems so that the potential impacts of the energy crops can be assessed in concert with other information.

7.5 Reducing the uncertainties

The uncertainties in the predictions made by this study could be reduced in a number of ways:

- Measurements on the energy crops to determine the threshold temperature below which photosynthesis stops. This parameter is important in determining the period during the year during which transpiration occurs but there is mo information on what value is appropriate.
- Measurements of the stomatal conductance of *Miscanthus* to allow the effect of atmospheric demand and soil water to be described with confidence.
- Measurements on additional poplar varieties to determine whether the high water use is a consistent feature.
- Time series measurements of soil water, evaporation, leaf area, and height to be made at other sites with different soils and climatology to allow the model predictions to be tested further.
- Including a limit to the rooting depth, when the geology/soils dictate this, in the model and a data set to inform this.
- Field measurements and model runs for varieties of the energy crops whose characteristics differ significantly from those which were used in this study.
- Including other forms of tilled land in the model.
- Running the model with a changed climate.

7.6 Summary of Conclusions

- The effect of enhanced evaporation at the edges of SRC plantations is localised and so will have the greatest impact on small plantations. For plantation greater than 10 ha the effect is certainly comparable or less than other factors, e.g. the nature of the soil.
- More measurements are needed on poplar SRC varieties to determine whether the high water use is a consistent feature and, if not, the model should be run using the new information.
- Additional measurements are needed on the energy grasses in order to reduce the uncertainty arising from the model parameter values.
- For the same rainfall and soils, the water use of the energy grasses is likely to be less or comparable to that of the existing land cover where it is grass or tilled land and less if the existing land cover is woodland or heathland.
- In the final year of the three year cropping cycle, the water use of SRC is likely to be greater than the existing land cover if it is grass or tilled land and comparable or greater if it is woodland or heathland. However, in the first year it is likely to be less than existing land cover types.
- The results for poplar SRC show a very high water use. These results should be interpreted with caution as it is likely that varieties could be or are available that would have lower water use. In which case the water use is likely to be comparable to that of willow SRC.
- In areas of high annual average rainfall (greater than around 800 mm), the nature of the soil has little impact on the water use of the energy crops, or the existing land cover. However, in other areas, the soil hydraulic properties, particularly the ability to store water that can then be used by the plants for transpiration, can be important because of the higher transpiration rates of the energy crops.
- When the rooting depth of the energy crop is deeper than the existing land cover, there is the possibility that, after a period of drought, the soil water deficits will be greater resulting in a reduction in recharge and/or runoff in the following winter.
- During years with above average rainfall, when transpiration rates are not constrained by soil water, the energy crops tend to use more water than the existing land cover, mainly due to the higher interception losses.

- The predicted indicative yield from the energy crops is a function of air temperature and the amount of sunshine. The energy grasses are predicted to be more sensitive to these factors than the SRC and so show a more marked trend of decreasing indicative yield with increasing latitude and altitude.
- There are strong indications that, in areas of low annual average rainfall (less than about 700 mm), the indicative yields of all the energy crops are reduced by soil water stress.

8. References

Beale, C. V., Morison, J. I. L. and Long, S. P. (1999) Water use efficiency of C-4 perennial grasses in a temperate climate *Agricultural and Forest Meteorology,* **96,** 103-115.

Boorman, D.B., Hollis, J.M. and Lilly, A. (1995) *Hydrology of soil types: a hydrologically based classification of the soils of the United Kingdom,* Institute of Hydrology, 126 pp. 137.

British Standards Institute (1996) BS 7843: *Guide to the acquisition and management of meteorological precipitation data*.

Brooks, R. H. and Corey, A. T. (1964) Hydraulic properties of porous media, Colorado State University, Hydrology Paper 3 pp. 27.

Bullard, M. (1999) *Miscanthus agronomy (for fuel and industrial uses),* Ministry of Agriculture, Fisheries and Food, NF0403 pp. 60.

Cain, J. D. (1998) *Modelling evaporation from plant canopies,* Institute of Hydrology, Report 132

Chaves, M. M., Maroco, J. P. and Pereira, J. S. (2003) Understanding plant responses to drought - from genes to the whole plant *Funct. Plant Biol.*, **30**, 239-264.

Cienciala, E. and Lindroth, A. (1995a) Gas-exchange and sap flow measurements of *Salix-viminalis* trees in short-rotation forest .1. transpiration and sap flow *Trees-Structure and Function,* **9,** 289-294.

Cienciala, E. and Lindroth, A. (1995b) Gas-exchange and sap flow measurements of *Salix-viminalis* trees in short-rotation forest .2. diurnal and seasonal-variations of stomatal response and water-use efficiency *Trees-Structure and Function,* **9,** 295-301.

Cox, P. M. (2001) *Description of the TRIFFID dynamic global vegetation model,* Met Office, Hadley Centre technical note 24 pp. 16.

Essery, R., Best, M. J. and Cox, P. M. (2001) *MOSES 2.2 Technical Documentation,* Met Office, Hadley Centre technical note 30 pp. 30.

Hall, R. L., Allen, S. J., Rosier, P. T. W., Smith, D. M., Hodnett, M. G., Hopkins, R., Davies, H. N., Kinniburgh, D. G. and Goody, D. C. (1996) *Hydrological effects of short rotation energy coppice,* Institute of Hydrology and British Geological Survey, Wallingford, ETSU B/W5/00275/REP

Harding, R. J., Huntingford, C. and Cox, P. M. (2000) Modelling long-term transpiration measurements from grassland in southern England *Agr.Forest.Meteorol.,* **100,** 309-322.

Hough, M. N. and Jones, R. J. A. (1998) The United Kingdom Meteorological Office rainfall and evaporation calculation system: MORECS version 2.0 - an overview *Hydrol. Earth Syst. Sc.,* **1,** 227-239.

Iritz, Z., Tourula, T., Lindroth, A. and Heikinheimo, M. (2001) Simulation of willow short-rotation forest evaporation using a modified Shuttleworth-Wallace approach *Hydrol. Process.,* **15,** 97-113.

Jones, H.G. (1992) *Plants and microclimate,* Cambridge University Press, Cambridge, 428 pp.

Lindroth, A. (1993) Aerodynamic and canopy resistance of short-rotation forest in relation to leaf area index and climate *Boundary-Layer Meteorology,* **66,** 265-279.

Met.Office (1975a) *Maps of mean and extreme temperature over the United Kingdom 1941-1970,* The Meteorological Office, Climatological Memorandum No 73 pp. 53.

Met.Office (1975) *Maps of mean vapour pressure and of frequencies of high relative humidity over the United Kingdom,* The Meteorological Office, Climatological Memorandum No 75 pp. 21.

Met.Office (1976b) *Maps of hourly mean wind speed over the United Kingdom, 1965-1973,* The Meteorological Office, Climatological Memorandum No 79 pp. 11.

Monteith, J. L. (1965) Evaporation and environment, In *19th Symposium of the Society of Experimental Biology*, Cambridge University Press, Cambridge, UK, pp. 205-234.

Monteith, J. L. and Unsworth, M. (1990) *Principles of environmental physics,* Edward Arnold, London.

Moore, R. J. (1985) The probability-distributed principle and runoff production at point and basin scales *Hydrolog. Sci. J.*, 30, 273-297.

Price, L, Bullard, M, Lyons, H, Anthony, S and Nixon, P (2004) Identifying the yield potential of *Miscanthus x giganteus*: an assessment of the spatial and temporal variability of *M-x giganteus* biomass productivity across England and Wales *Biomass Bioenerg.,* **26,** 3-13.

Riche, A. B. and Christian, D. G. (2001) Rainfall interception by mature *Miscanthus* grass in SE England *Aspects of Applied Biology,* **65,** 143-146.

Ward, R. C. and Robinson, M. (1990) *Principles of Hydrology,* McGraw-Hill Book Co., London, 363 pp.

Wellings, S.R. (1984) Recharge of the upper Chalk aquifer at a site in Hampshire, England 1. Water balance and unsaturated flow *J. Hydrol.,* **69,** 259-273.

Wellings, S. R. and Cooper, J. D. (1983) The variability of recharge of the English Chalk aquifer *Agric.Wat.Man.,* **6,** 243-253.

9. Appendices

9.1 Weather variables collected at Roves Farm

The data collected by the automatic weather station at Roves Farm are presented in the following figures.

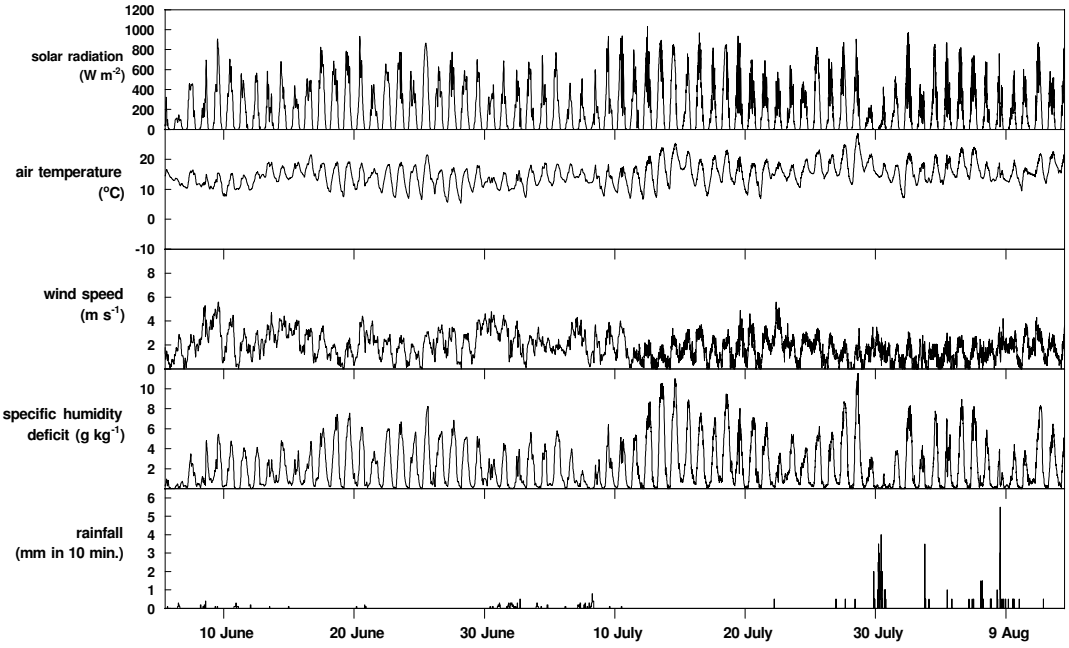

Figure 112 Key weather variables recorded by the automatic weather station over the willow SRC at about 10 m above the ground at Roves Farm during the early summer 2002.

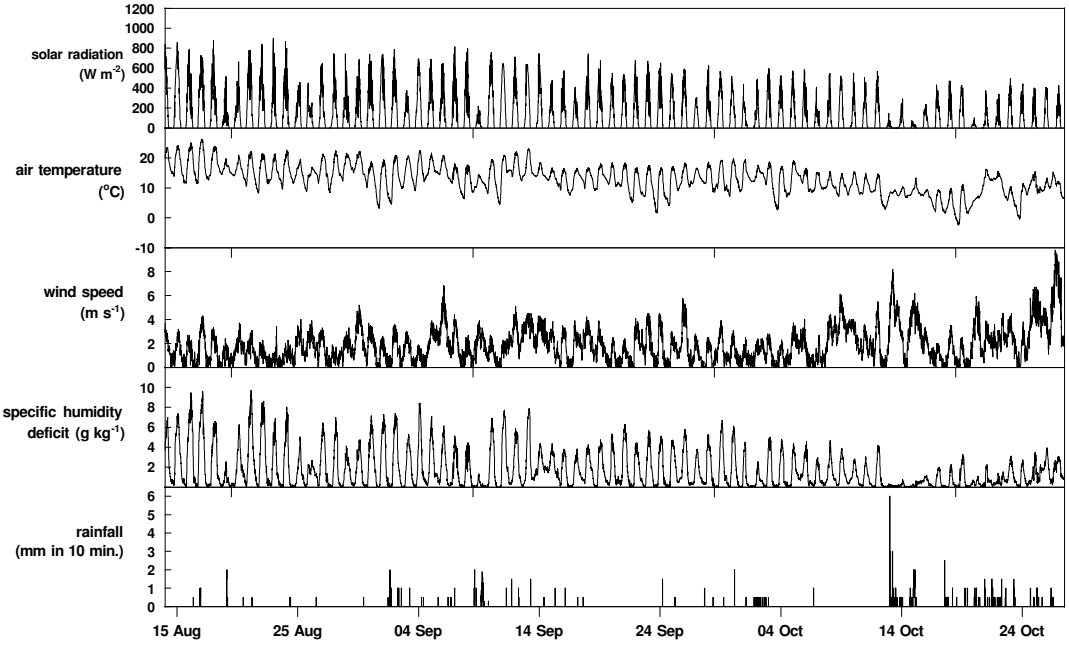

Figure 113 Key weather variables recorded by the automatic weather station over the willow SRC at about 10 m above the ground at Roves Farm during the late summer early autumn 2002.

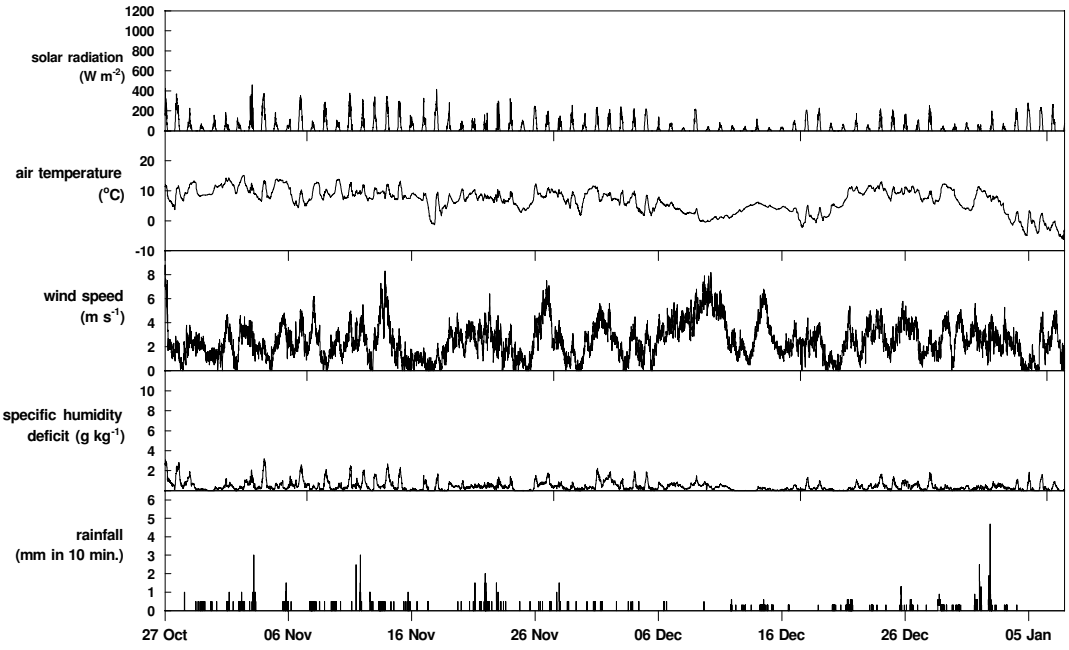

Figure 114 Key weather variables recorded by the automatic weather station over the willow SRC at about 10 m above the ground at Roves Farm during the late autumn and winter 2002.

9.2 Stem data

The results of the survey of stem diameters made on 25 April are presented in the following figures. Diameters were measured at one metre above the ground (d_{100}) from 467 stools in a block of 21 rows by about 22 at the western edge of the plantation. Within this block there were eight varieties of willow.

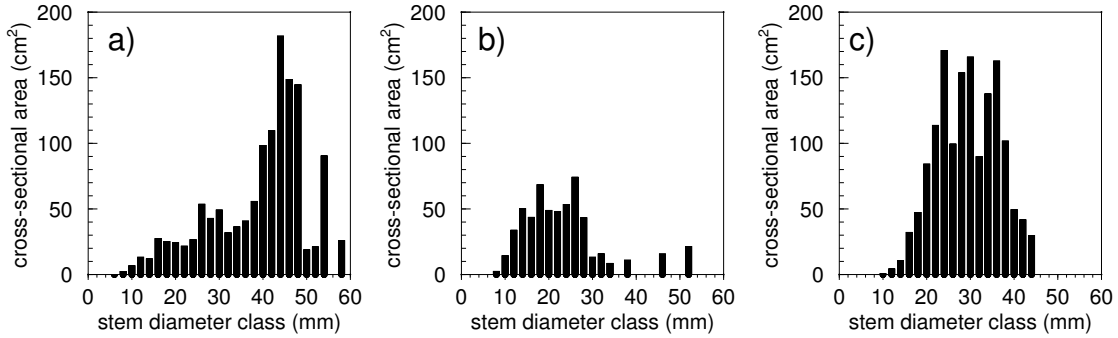

Figure 115 The distribution of stem cross-sectional area by diameter class for a) Dasyclados, b) Bowles Hybrid and c) Orm

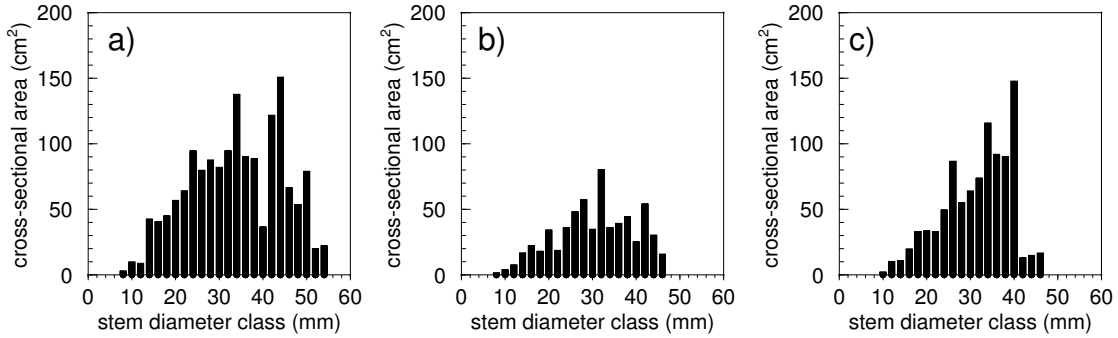

Figure 116 The distribution of stem cross-sectional area by diameter class for a) Q83, b) Germany and c) Ulv

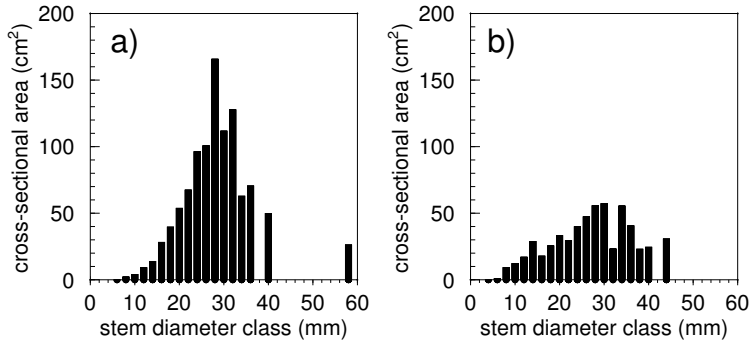

Figure 117 The distribution of stem cross-sectional area by diameter class for a) Jorunn and b) ST2481/55